AD-A164 919 OPTO-ACOUSTIC TELEPHONE STUDY(U) HARRIS CORP MELBOURNE 1/2
FL GOVERNMENT COMMUNICATION SYSTEMS DIV
S R ADHAV ET AL. 01 JAN 83 JA-1023 DAAB77-82-C-J011
UNCLASSIFIED F/G 20/6 NL

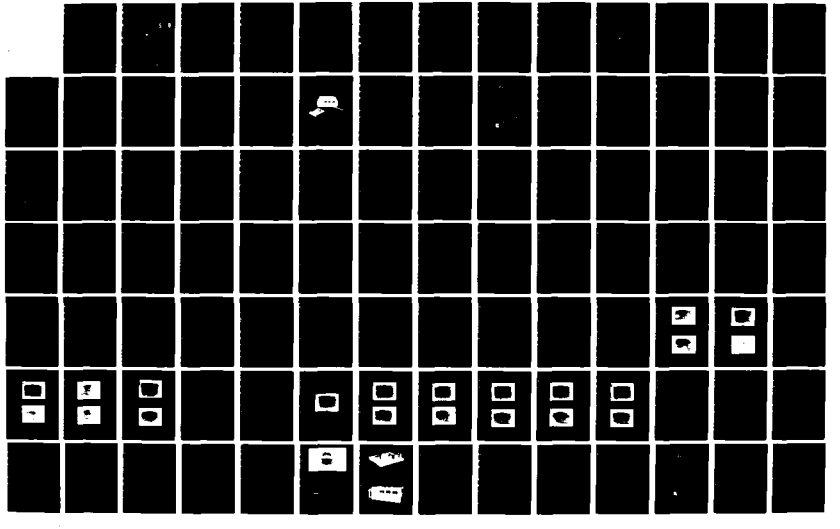

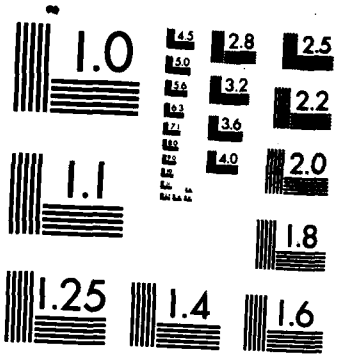

OPTO-ACOUSTIC TELEPHONE STUDY

FINAL TECHNICAL REPORT

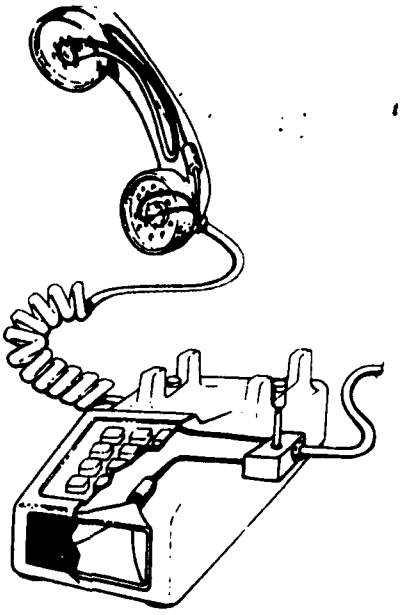

PREPARED FOR

UNITED STATES ARMY CECOM

FT. MONMOUTH, NEW JERSEY

CONTRACT NO. DAABO7-82-C-JO11

JANUARY 1, 1983

PREPARED BY

OPTICAL SYSTEMS DEPARTMENT

HARRIS

HARRIS CORPORATION GOVERNMENT COMMUNICATIONS SYSTEMS DIVISION
P.O. BOX 92000, MELBOURNE, FLORIDA 32901, (305) 727-4000

DISCLAIMER NOTICE

THIS DOCUMENT IS BEST QUALITY PRACTICABLE. THE COPY FURNISHED TO DTIC CONTAINED A SIGNIFICANT NUMBER OF PAGES WHICH DO NOT REPRODUCE LEGIBLY.

people spoke into the mechanism and the resulting light modulation was converted back into sound by the EIU. The response of the cell was such that the individual voices were easily understandable and identifiable. Tonal quality was similar to that of the conventional telephone set.

The HEAR mechanism was fabricated and initially tested by placing the absorption cell near the ear and detecting the output. The laser diode, biased at 10 mW, was 100% modulated by the audio generator and the light signal was applied to the Hear cell. The tone was easily audible. Final HEAR horn testing its continuing.

The Ring mechanism described in Section 4 was fabricated and tested with the EIU. After four seconds of a 16 mW cw light signal, the ring signal began and continued until the light pulse turned off. The ring produced an audio output of 75 dB at a distance of 1 meter from the mechanism, as required.

6. CONCLUSIONS/FUTURE OF THE CONCEPT

The results of the current study indicate that an all optical telephone set is technical feasible. The implementation methods and subsequent designs were chosen after an intensive literature survey of past research and brainstorming sessions for new ideas. The techniques selected were determined primarily on a risk/performance basis where the lowest risk approach having the greatest chance of success was chosen. It is obvious that much work still needs to be done both in optimizing the performance and manufacturing cost parameters of those functions investigated in this study as well as other functions such as hook switch, sidetone and dialing. The associated technologies required already exist with low loss optical fibers and high power laser diodes commercially available. The authors are hopeful that the all optical telephone first envisioned by Alexander Graham Bell over 100 years ago, will soon become a reality.

ACKNOWLEDGEMENT

The authors wish to thank Mr. Rollie McCollum and Mr. Thomas Conroy for their work on the mechanical and electronic interface designs and Mr. Scott Stewart for his assistance in the fabrication and testing. The funding for the program was from the U.S. Army, CECOM at Fort Monmouth, New Jersey.

REFERENCES AND FOOTNOTES:

1. S. Edelman, U.S. Patent Pending.
2. D. Kleinman and D. Nelson, The Photophone - An Optical Telephone Receiver, J. Acoust. Soc. Am., Vol. 59, No. 6., June 1976.
3. S. Edelman, Private Communications, Acoustic-Optic Workshop, Ft. Monmouth, March 31, 1982.
4. D. Nelson, K. Wecht and D. Kleinman, Photophone Performance, J. Acoust. Soc. Am., Vol. 60, No. 1., July 1976.

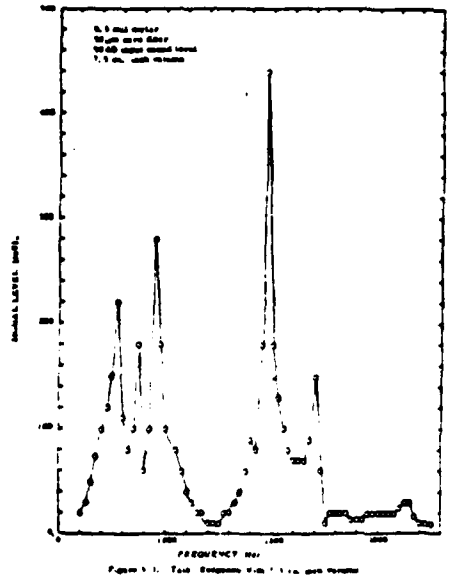

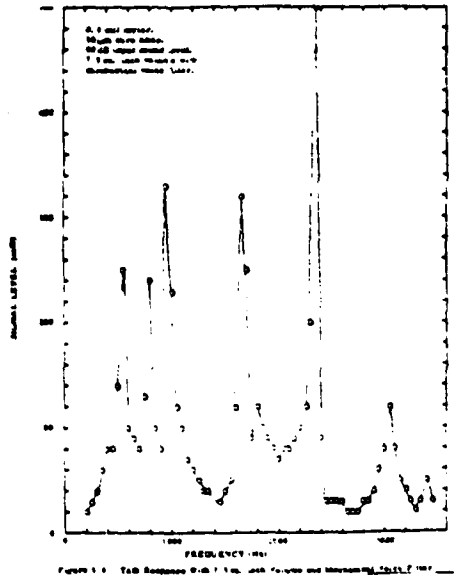

case, bandwidth was not a major concern and was traded off for increased response over a narrow band. The RING horn is similar in design to the HEAR horn but the larger diameters are due to the different load impedance. The input radius is 0.05 cm and the output radius is 15.0 cm. The overall length is 17 cm. The cell volume is 5.0×10^{-4} cm^3 and the equalizer tube diameter and lengths are 0.02 cm and 20 cm respectively. The predicted acoustic output is shown in Figure 4.1. The predicted peak response 1 meter from the horn is 75 dB with 2.5 mW of light and increases to 92 dB with 18 mW of light.

The second approach investigated utilized the optical ring signal to trigger the release of mechanically stored energy which was then converted into acoustic energy to alert the user of an incoming call. The released mechanical energy is restored at the conclusion of the call through the action of the hook switch which, when depressed, can be used to compress a spring, twist a torsion bar, or displace a weight, etc. The actual production of sound can be accomplished with a bell type device, a bellows/vibrating reed, etc.

The initial investigation concentrated on the trigger mechanism. When irradiated, the trigger released a predetermined amount of mechanical energy into the sound producing device. The designed mechanism incorporated a bimetallic strip; when heated by optical energy, the strip bends from its normal position releasing the mechanical energy. After the light pulse ends, only a few seconds is required for the strip to cool to ambient and return to its initial latching position. Thus, each light pulse can trigger a ring cycle.

The Harris RING mechanism, incorporating the bimetallic trigger, is shown in Figure 4.2. Mechanical energy is stored by means of a spring geared to a low torque governor. The bimetallic trigger in its normal off position latches the governor. When a ring signal is sent, the light output from the fiber is focused by two lenses onto a blackened bimetal strip which deflects as it heats up, releasing the governor. The drum rotates, causing a set of bells to be struck, producing a sound much like that of a conventional phone. Although the feasibility design implemented was constructed of metal, ringers can be fabricated of plastics and ceramics. For this program, it was decided to build and test the ringer shown in Figure 4.2, primarily because it was easier and faster to build, as well as lower risk than the RING horn described previously. The experimental results are described in the following section.

5. EXPERIMENTAL RESULTS

An electronic interface unit (EIU) was constructed to test the three components. Three Optical Information Systems, 20 mW laser diodes were incorporated in the EIU along with their associated signal circuitry and power supplies. The laser diodes were biased at 20 mW for the RING and 10 mW for the TALK and HEAR. The optical telephone side tone feedback signal was generated electronically. A 3000 cm, 4 fiber optical link was used for interconnection in testing the components.

The TALK signal levels were measured as a function of input frequency. The measurement breadboard is shown in Figure 5.1. A helium neon laser was coupled to the input fiber through a 20X microscope objective. An optical power meter was used to detect the light variations; the output of the meter was fed to an oscilloscope for measurement. An audio oscillator provided the sound frequency input which was normalized to 90 dB at each frequency. Data was taken under three conditions: the cell placed flat on the bench, placed over a 7 cubic inch volume, and finally a mechanical voice filter (a standard telephone mouthpiece) was placed over the membrane. The measured voltage as a function of input sound frequency is shown in Figures 5.2, 5.3, and 5.4 for these three cases. These experimental results are of the same form as the theoretical prediction shown in Figure 2.1. The response, observed when the diaphragm was backed by a reasonable volume, has a series of resonances with the primary peak at about 2375 Hz. Tests were then run in which different

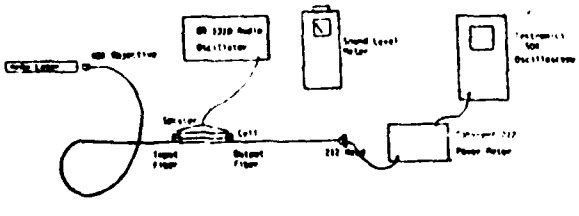

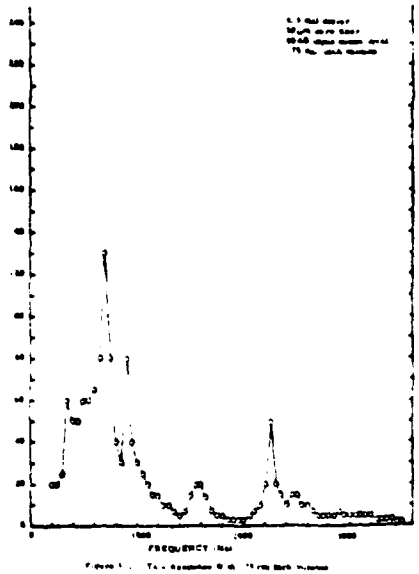

Further manipulation yields the transfer function, H_ω:

$$H_\omega = G_m^2 \left(\frac{9.1 \times 10^{-4}\ cm^4}{r_1^2 r_2^2}\right) \cdot \left(\frac{a}{k}\right)^2 \frac{\exp[(-r_o/r_1)\xi]\,|G_\omega|^2}{|g(k)|^2 (1 - 2e^{-\Delta}\cos\phi + e^{-2\Delta})} \quad (3)$$

where: G_m, figure of merit for the gas; air = 1.

G_ω, dispersion function for a sphere volume approximation of the cell.

$\phi = 2n\ell + \dot{\Delta} - 2\varphi$

$\varphi = g(k)$

Integration of $1 - 2e^{-\Delta}\cos\phi + e^{-2\Delta}$ over 2π in equation 3 (the term of which arises from oscillations due to resonances of travelling waves in the tube) results in an average or a smoothed response, $< H_\omega >$:

$$<H_\omega> = G_m^2 \left(\frac{9.1 \times 10^{-4}\ cm^4}{r_1^2 r_2^2}\right) \cdot \left(\frac{a}{k}\right)^2 \frac{\exp[(-r_o/r_1)\xi]\,|G_\omega|^2}{|g(k)|^2 [1 - e^{-2\Delta}]}$$

The output intensity is the product of H_ω with the following function, D_ω.

$$D_\omega = \frac{R_o^2 (\gamma - 1)^2 (P_{opt} \times 10^4)^2}{2 (\gamma_o P_o I_o)^2}$$

where:

R_o, 880 gm/sec cm^4, a constant to normalize H_ω.

γ_o, specific heat ratio of gas.

P_{opt}, RMS optical power, mW.

P_o, atmospheric pressure, dynes/cm^2.

I_o, 2×10^{-4} dynes/cm^2.

A computer predicted plot of the Harris HEAR mechanism response compared to the K-N photophone appears in Figure 3.4.

4. RING FUNCTION

As in the case of the HEAR function, the technical challenge of the RING implementation lies in the need to obtain a noticeable acoustic output from the telephone set at a level of approximately 75 dB sound pressure level (SPL) at 1 meter with only an optical input from the fiber link. However, the RING function, unlike the HEAR, does not convey detailed communications, but serves only to alert the telephone user to an incoming call. There are two possible means for producing the required sound; direct conversion of the optical RING signal to acoustical energy as in the HEAR function and the use of the optical ring signal to trigger the release of stored mechanical energy into a predetermined acoustic signal, loud and noticeable enough to attract the attention of the telephone user. Both approaches were investigated.

The direct conversion of optical to acoustical energy can be obtained, as in the HEAR function, by the photo-acoustic effect. The problem is the same as that of the HEAR function, except for the value of the load impedence. The HEAR couples into a fixed volume load, whereas, to be useable in a manner comparable to existing systems, the RING must couple into free space. Using the HEAR computer programs, a design for a RING horn which optimized the sound output for a load impedance of a massless air piston was derived. In this

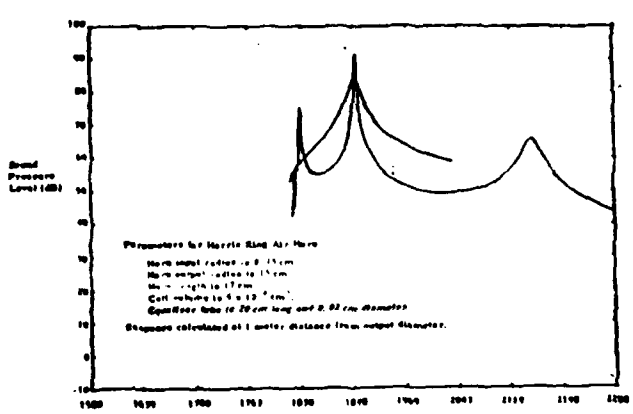

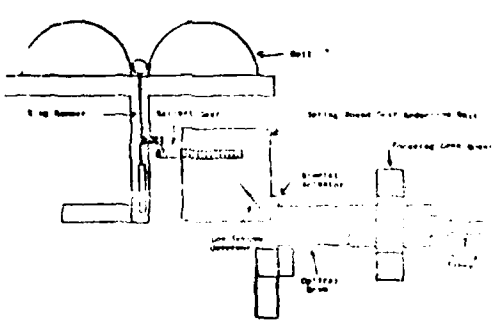

expected performance of the Edelman[3] and the Kleinman-Nelson[4] approaches indicated that the latter approach had a 10 dB higher conversion efficiency. Because of this and the proven nature of the Kleinman-Nelson approach, it was decided to incorporate this technique in the Harris design.

The Harris HEAR mechanism design consists of an exponential horn similar to that of Kleinman-Nelson approach. The Harris design was computer optimized and resulted in a mechanism with 10% less overall length and an increase of approximately 3 dB in output over the desired bandwidth as compared to the Kleinman-Nelson approach. Air was chosen as the internal gaseous medium for ease of fabrication, although it has been shown[3] that other internal gases can increase sensitivity. However, this requires added complexity of a diaphragm for gas confinement.

It was decided to fabricate the horn by machining a two piece aluminum mandril on a lathe, electroplating copper on the outside of the mandril and, subsequently, etching the aluminum in a hot sulphuric acid bath. The resulting form is a rigid copper horn whose inside dimensions are the same as the outside dimensions of the aluminum mandril. Inertance tube equalizers, photo-acoustic cell and ear-piece coupler can then be attached.

Following the nomenclature of Kleinman-Nelson (K-N)[3], the equivalent circuit of the photophone is shown in Figure 3.3. The solution of the circuit shown reduces to:

$$\left|\frac{P_E}{S_L}\right|^2 = \left(\frac{2}{\pi}\,\frac{\delta c n}{r_1^2 r_2^2 k}\right)^2 \cdot \frac{\exp\{|(-r_0/r_1)\xi|}{|g(k) + h(k)\exp(2jnl + j\Delta - \delta)|}^2$$

where: $g(k) - h(k) = \left(1 + \frac{Z_1}{z_c} + \frac{z_1}{z_c}\right) \cdot \left(\frac{z_2}{z_e} - \frac{Z_2}{z_e} - 1\right)$

$z_{1,2} = \frac{j\omega\delta}{m \pm \pi r_{1,2}^2}$, characteristic impedance of a lossless tube.

$m \pm = \alpha \pm jn$, lossless solutions.

$\alpha = (\ln(r_2/r_1))/l$, exponential taper constant.

l, length of horn, cm.

P_E, pressure at ear-piece coupler, dynes/cm^2.

z_e, acoustic impedance of ear coupler, gm/sec cm^4.

z_c, acoustic impedance of source volume, gm/sec cm^4.

S_L, velocity flow of photo-acoustic source, cc/sec.

$Z_{1,2}$, equalizer impedances, gm/sec cm^4.

TVD, thermoviscous damping, gm/sec cm^4.

δ, density of medium, gm/cc.

c, velocity of sound, cm/sec.

$r_{1,2}$, input and output radii of the horn, cm.

r_o, boundary layer radius, cm.

n, complex term of propagation constant.

$k = \omega/c$, rad/cm.

ξ, Δ, frequency dependent functions for boundary layer approximation.

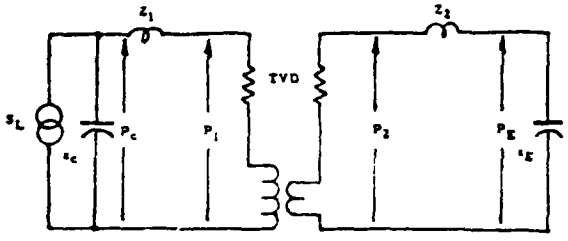

Figure 3.3. Kleinman-Nelson Equivalent Circuit

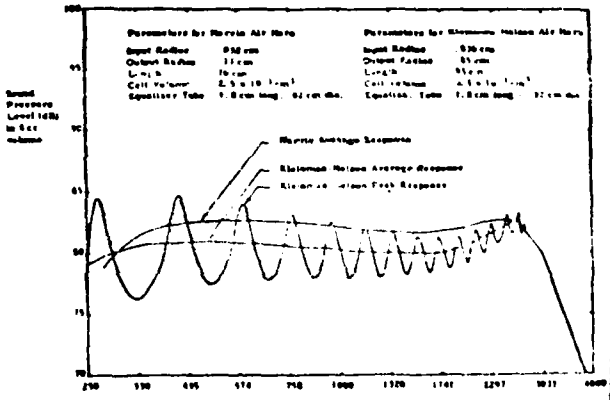

Figure 3.4. Kleinman Nelson Versus Harris Predictions

waves incident on the membrane cause it to vibrate resulting in changes in the coupling efficiency between the two fibers. The amount of coupling, and therefore the magnitude of the intensity variations, depends on the amplitude of the diaphragm vibrations.

The TALK mechanism model is a homogeneous circular membrane driven by a constant pressure across the surface with no damping forces. Solution of the wave equation of this system for the amplitude of the membrane displacement, y, results in:

$$y = \frac{P}{kT}\left(\frac{Jo(kr)}{Jo(ka)} - 1\right)$$

where:

Jo(kr), Bessel function of order zero.
P, drive pressure, dynes/cm^2.
T, membrane tension, dynes/cm^2
$k = \omega\sqrt{s/T}$, rad/cm.
s, area density, gm/cm^2.
a, cell radius, cm^2.
ω, frequency, rad/sec.
r, the radius at which the displacement is measured, cm

This equation was used to generate plots of membrane displacement at the center of the cell, where the fiber ends were placed, as a function of frequency. Since the fiber ends, one fixed and one moving with the membrane, are at the center, the plots represent instantaneous fiber coupling and thus, light amplitude. A typical plot is shown in Figure 2.1. As mentioned previously, in order to reproduce ideally the individual voice characteristics of the user, the response of the TALK mechanism should be flat across the voice band from 300 to 3300 Hz. One way to accomplish this is to set the membrane parameters such that the first resonance is above the band of interest. The other option is to generate resonances across the frequency band, especially at the high frequency end where overtones typically give voices their individuality.

The Harris design for the talk mechanism is shown in Figure 2.2. A disk of 12.7 micron thick mylar was stretched across a 4 cm ring and fixed at the edges. The input fiber was attached to the mounting ring and to the center of the membrane by a small drop of epoxy. The output fiber was mounted inside a hypodermic needle cut and polished flat at both ends. The 50μm core input and output fibers were aligned to maximize the coupling efficiency of the light in the static mode, and then the needle attached to the ring mount by epoxy to hold the fiber stationary.

3. HEAR FUNCTION

The passive HEAR mechanism must convert light into sound with a bandwidth of 300-3300 Hz and a sound pressure level at the ear of at least 81 dB. Two design approaches were considered. In the first, the Edelman[1] approach shown in Figure 3.1, the optical energy is absorbed as heat in optical fibers having a high Youngs modulus, low specific heat and a large coefficient of thermal expansion. The fibers expand and contract under tension as a function of the modulated optical input and drive a diaphragm element which is impedanced matched for the desired voice bandwidth. Input modulated light is thus converted into sound pressure waves by the moving diaphragm.

The second approach, the Kleinman-Nelson[2] approach shown in Figure 3.2, consists of a small photo-acoustic cell, which converts the light modulation into sound waves, and an acoustic impedance matching system. The last impedance matching element is an exponentially tapered horn which couples sound to the ear. The photo-acoustic interaction occurs between the light and a small quantity of suspended carbonized cotton. As the input light intensity varies with the HEAR signal, the cotton and surrounding gas heat and cool and thus expand and contract producing an acoustic pressure wave. The impedance matching system maximizes the acoustic energy transmitted to the ear. Calculations made of the

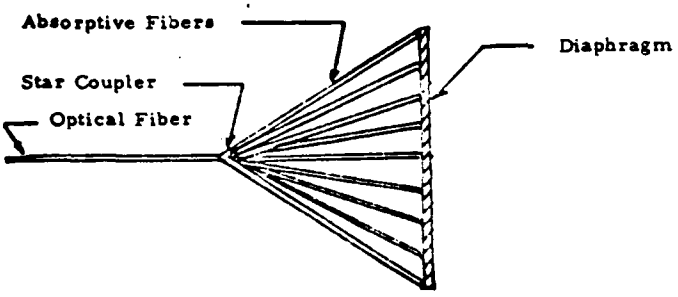

Figure 3.1. Edelman Approach

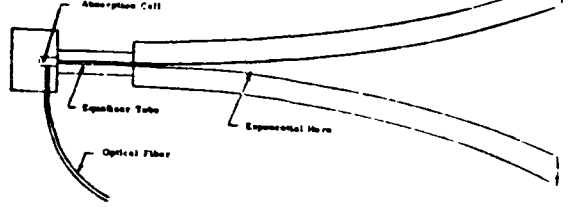

ALL OPTICAL TELEPHONE DEVELOPMENT

FOC-82 - Sep 15, 1982 -- Los Angeles CA

B.G. Grossman, S.R. Adhav, L.M. Ralston, and R.K. Morse,
Harris Corporation, N. Feldman, CECOM

1. INTRODUCTION

The optical fiber, as a medium for communications, has been successfully replacing metallic cable trunks. It is presently serving the communication industry in both high capacity and low capacity links. Thus far, with few exceptions, the highest volume users of transmissions lines, subscribers, have been neglected.

When Mr. Feldman discussed his "All Optical Telephone" at ICC-81 in Denver, Colorado in June 1981, it was a step toward correcting this neglect. He described an instrument served by optical fibers, simple, and inexpensive, requiring no electrical power. His conceptual system contained six components, two of which, earphone and ringer, seemed to present some measure of barrier to successful implementation. A government contract was awarded to Harris Corporation, Melbourne, Florida, in November 1981, to demonstrate the feasibility of the concept. The barrier items would get special attention in the execution of this contract.

In this paper, we will describe the work pursued and accomplished by Harris. Three of the six components, hear (earphone), talk, and ring, will be addressed. The expended effort has consisted of a judicious mix of computer modeling, brainstorming, engineering, and model shop work. Our efforts will be described, our results documented, and our designs discussed.

It should be noted that one barrier component, the optical to sound converter, was addressed 100 years ago by Alexander Graham Bell. Though several experimenters have worked on it since, we believe that this is the first work directed at its use in a complete telephone instrument. What is reported here is a first cut effort to demonstrate feasibility. We realize these efforts are primitive, but, fully expect that the refinement process and optimization will follow rapidly.

2. TALK FUNCTION

The function of the TALK mechanism is to convert spoken words into modulated light. This light is coupled by optical fiber to an electronic switchboard and then reconverted into sound at a HEAR mechanism. The frequency response of the TALK mechanism must be reasonably flat over the voice band, 300 to 3300 Hz, and typical voice levels must generate sufficient optical modulation to be detected and reconverted to sound with a sufficient signal to noise ratio, as in a conventional telephone set.

Two basic modulation methods, phase modulation and amplitude modulation, were considered for the talk mechanism. Phase modulation of light by pressure waves recently has been explored and optimized using optical fibers for underwater sensor applications. The major disadvantage of this method is that complicated interferometric techniques are usually required to demodulate the phase encoded information. It was decided, therefore, because of their easier implementation, to concentrate on amplitude modulation techniques. There are numerous passive amplitude modulation techniques, including sound dependent fiber misalignment, frustrated total internal reflection, microbending loss modulation, etc. The approach selected by Harris for the TALK function was the first represented as loss modulation by variable optical coupling between two end-to-end coaxially aligned fibers. In this technique, one of the fibers is fixed in position, while the other is attached to the center of a thin membrane diaphragm. Sound

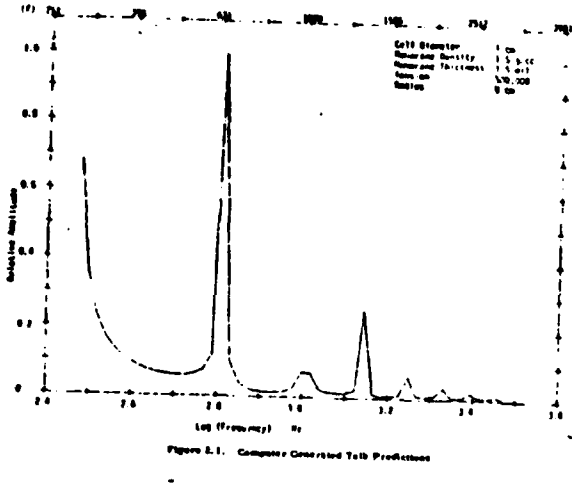

Figure 2.1. Computer Generated Talk Predictions

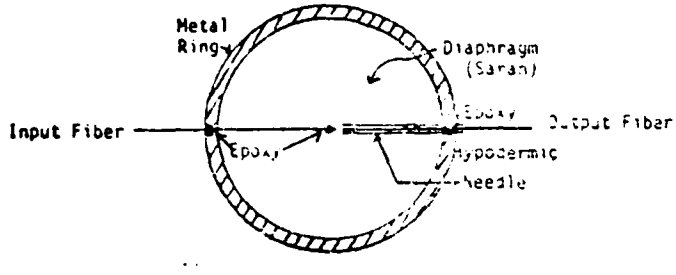

Figure 2.2. Talk Design

OPTO-ACOUSTIC TELEPHONE STUDY

FINAL TECHNICAL REPORT

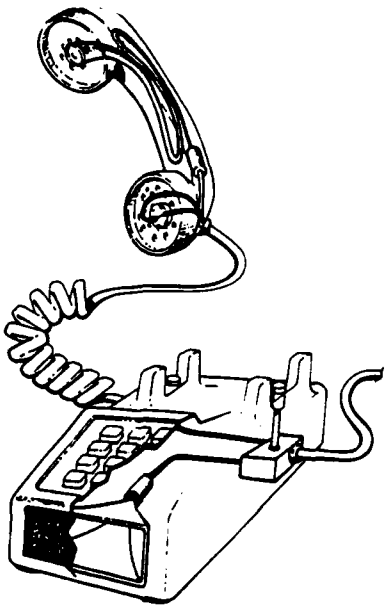

PREPARED FOR

UNITED STATES ARMY CECOM

FT. MONMOUTH, NEW JERSEY

CONTRACT NO. DAAB07-82-C-J011

JANUARY 1, 1983

PREPARED BY

OPTICAL SYSTEMS DEPARTMENT

HARRIS CORPORATION

Unclassified

SECURITY CLASSIFICATION OF THIS PAGE (When Data Entered)

REPORT DOCUMENTATION PAGE		READ INSTRUCTIONS BEFORE COMPLETING FORM
1. REPORT NUMBER	2. GOVT ACCESSION NO. AD-A164919	3. RECIPIENT'S CATALOG NUMBER
4. TITLE (and Subtitle) OPTICAL TELEPHONE STUDY		5. TYPE OF REPORT & PERIOD COVERED Final Report December 1981 to Jan. 1983
		6. PERFORMING ORG. REPORT NUMBER JA 1023
7. AUTHOR(s) S. R. Adhav, A. M. Bardos, B. G. Grossman, L. M. Ralston		8. CONTRACT OR GRANT NUMBER(s) DAAB07-82-C-J011
9. PERFORMING ORGANIZATION NAME AND ADDRESS Harris Corporation G.C.S.D. P. O. Box 92000 Melbourne, FL 32901		10. PROGRAM ELEMENT, PROJECT, TASK AREA & WORK UNIT NUMBERS
11. CONTROLLING OFFICE NAME AND ADDRESS CECOM Ft. Monmouth, N.J. 07703		12. REPORT DATE January 1, 1983
		13. NUMBER OF PAGES
14. MONITORING AGENCY NAME & ADDRESS(if different from Controlling Office)		15. SECURITY CLASS. (of this report) Unclassified
		15a. DECLASSIFICATION/DOWNGRADING SCHEDULE

16. DISTRIBUTION STATEMENT (of this Report)

17. DISTRIBUTION STATEMENT (of the abstract entered in Block 20, if different from Report)

18. SUPPLEMENTARY NOTES

19. KEY WORDS (Continue on reverse side if necessary and identify by block number)

Fiber Optics
Fiber Optic Sensors
Optical Telephone
Photoacoustics

20. ABSTRACT (Continue on reverse side if necessary and identify by block number)

This report documents the results of an optical telephone feasibility study and resultant demonstration and includes the detailed design and fabrication of a remote optical telephone experimental subset with Talk, Hear and Ring functions. All conversions within the subset go directly between optical and acoustical energy; there are no electrical circuits to effect the process. The optical telephone has potential in military communication links where security and resistance to radiation of all forms is desired.

DD FORM 1 JAN 73 1473 EDITION OF 1 NOV 65 IS OBSOLETE

Unclassified

SECURITY CLASSIFICATION OF THIS PAGE (When Data Entered)

TABLE OF CONTENTS

← 3-12

LIST OF ILLUSTRATIONS

ACKNOWLEDGEMENTS

During the course of the program, we received technical advice and cooperation from several people. We wish to acknowledge in particular the assistance of the following:

Donald F. Nelson, Bell Laboratories, Murray Hill, New Jersey

Seymour Edelman, formerly of the National Bureau of Standards, Washington, District of Columbia

Bob Lucas, Optical Information Systems, Elmsford, New Jersey

It is also a pleasure of acknowledge the encouragement, interest and guidance of Nat Feldman and Harold Bock of CENCOMS.

SECTION I

INTRODUCTION AND MANAGEMENT SUMMARY

1.0 INTRODUCTION AND MANAGEMENT SUMMARY

This Final Technical Report for the Opto-Acoustic Telephone Study details work performed by the Optical Systems Department of Harris Corporation, GCSD, under contract No. DAAB07-82-C-J011 for U. S. Army CECOM, Ft. Monmouth, New Jersey. The objective of the study was to determine the technical feasibility of developing and producing a telephone subset for voice, in which all conversions at and within the subset are directly between optic and acoustic energy. An additional objective was that the subset contain no electronic or electrical interface circuits. The scope included demonstration of the feasibility of three telephone set functions; Hear, Talk and Ring. Harris has met these objectives.

Key program tasks were:

1. Conduct a complete literature survey of applicable technology.
2. Perform engineering feasibility tradeoff and systems analyses for possible Talk, Hear and Ring concepts.
3. Design, breadboard and fabricate an experimental feasibility system with full duplex capability.
4. Test, optimize and characterize the resultant system.
5. Demonstrate the experimental breadboard system at CECOM.
6. Deliver final Engineering Report, including recommendations for future work.

Deliverable items included:

1. Eight monthly technical and financial progress reports and one engineering final report.
2. Residual breadboard components purchased on the program.

Following an intensive literature survey and performance analysis tradeoff, a conceptual implementation was chosen for each of the Hear, Talk and Ring functions. This was followed by analytical modeling which culminated in computer programs written to predict the theoretical performance of the experimental breadboard hardware. The devices were designed and fabricated and an Electronic Interface Unit (EIU) was built for evaluating the devices together with a full duplex fiber optic voice link. The link and Electronic Interface Unit were designed and built specifically to interconnect a standard electrical telephone set with its all-optical counterpart.

A link distance of one hundred feet was chosen for convenience and to demonstrate the concept. The breadboard components developed are shown in Figure 1.1. Table 1.1 summarizes their measured performance and capabilities, and compares them with a standard electrical telephone set.

The breadboard system provided adequate voice communication over the test link with the standard electrical telephone set. As shown in Table 1.1, however, the Hear and Talk performances were lower than those of a standard telephone set. Analysis

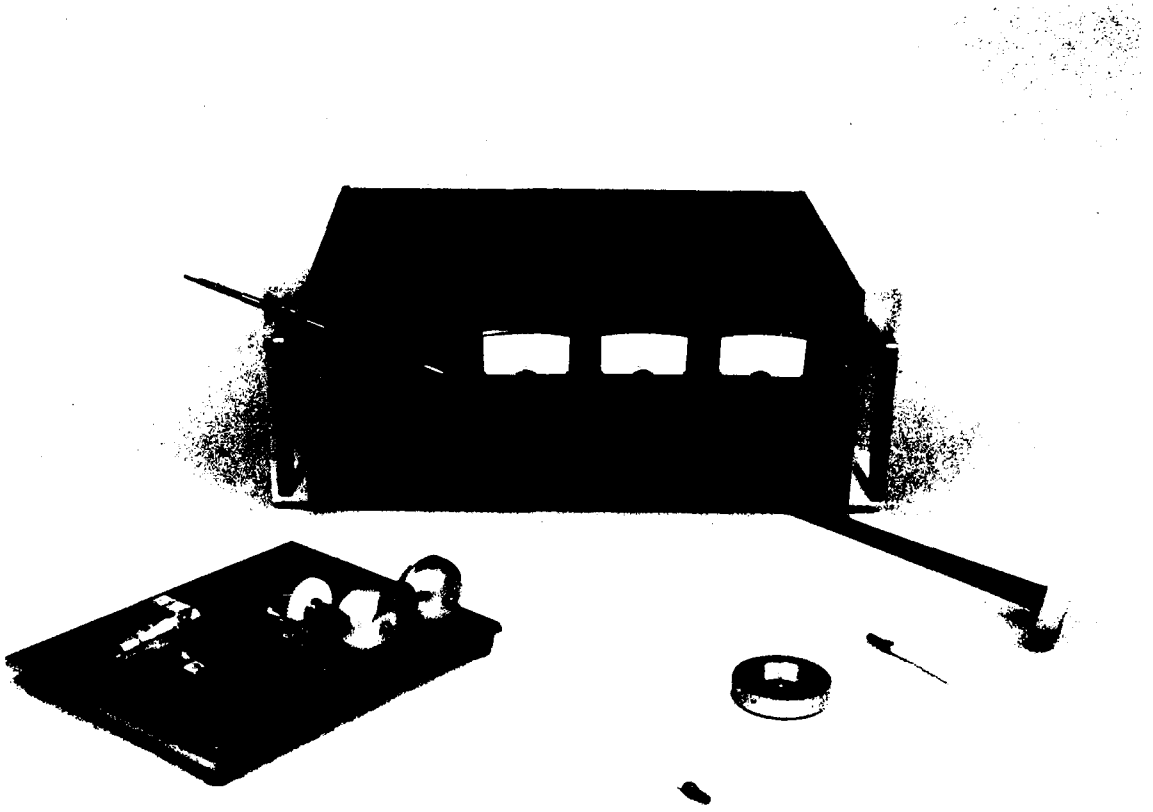

FIGURE 1.1 Photograph of Harris Optical Telephone Experimental Breadboard

Table 1.1. COMPARISON BETWEEEN HARRIS BREADBOARD OPTICAL TELEPHONE SET AND STANDARD TELEPHONE SET

PARAMETER	HARRIS BREADBOARD OPTICAL TELEPHONE SET	STANDARD TELEPHONE SET
Transducer types	Acoustic/Optical Conversions	Acoustic/electrical conversions
Required electrical power at telephone set	None required, completely passive	Requires electrical power for all functions
Construction Materials	Although breadboard contains some metal parts, plastics and ceramics can easily be substituted.	Requires metal parts particularly since electrical conductors are needed.
Compatibility with Optical Links	Can connect directly with fiber optic links, no interface unit required.	Requires optoelectronic interface for fiberoptic useage
Hea Response	Measured 300-1500 Hz with 75 dB output. Output level and frequency response sufficient for understandability. Requires optimization.	Measured 300-3300Hz with 81 dB output. Exceeds requirements for average user.
Talk Response	Measured 300-2000 Hz, sufficient modulation for acceptable signal to noise ratio, requires optimization for better quality	Measured 300-3300Hz with sufficient modulation for acceptable signal to noise ratio. Good quality.
Ring Response	Measured 80 dB output at 1 meter distance with mechanical ring/horn implementation feasible	Measured 75 dB at 1 meter distance.

shows that performance levels comparable to a standard set are achievable with further device optimization. This optimization was not possible on the current study but could be accomplished on future development efforts. The work done by Harris demonstrates feasibility of the all-optical telephone and provides a baseline for future work. A conceptual drawing of a complete all-optical telephone set is shown in Figure 1.2.

The remainder of this report is organized in the following manner. Section 2, Design Analysis, discusses basic theory behind the design of each of the various telephone mechanisms, technical tradeoffs involved between different concepts, theoretical/computer analyses of each function, and Electronic Interface Unit (EIU) and system design. Experimental results are presented in Section 3.0. Section 4.0 includes conclusions and recommendations. Appendices A through E detail the results of the literature survey, and contain the electronic interface unit schematics, computer programs, and pertinent papers.

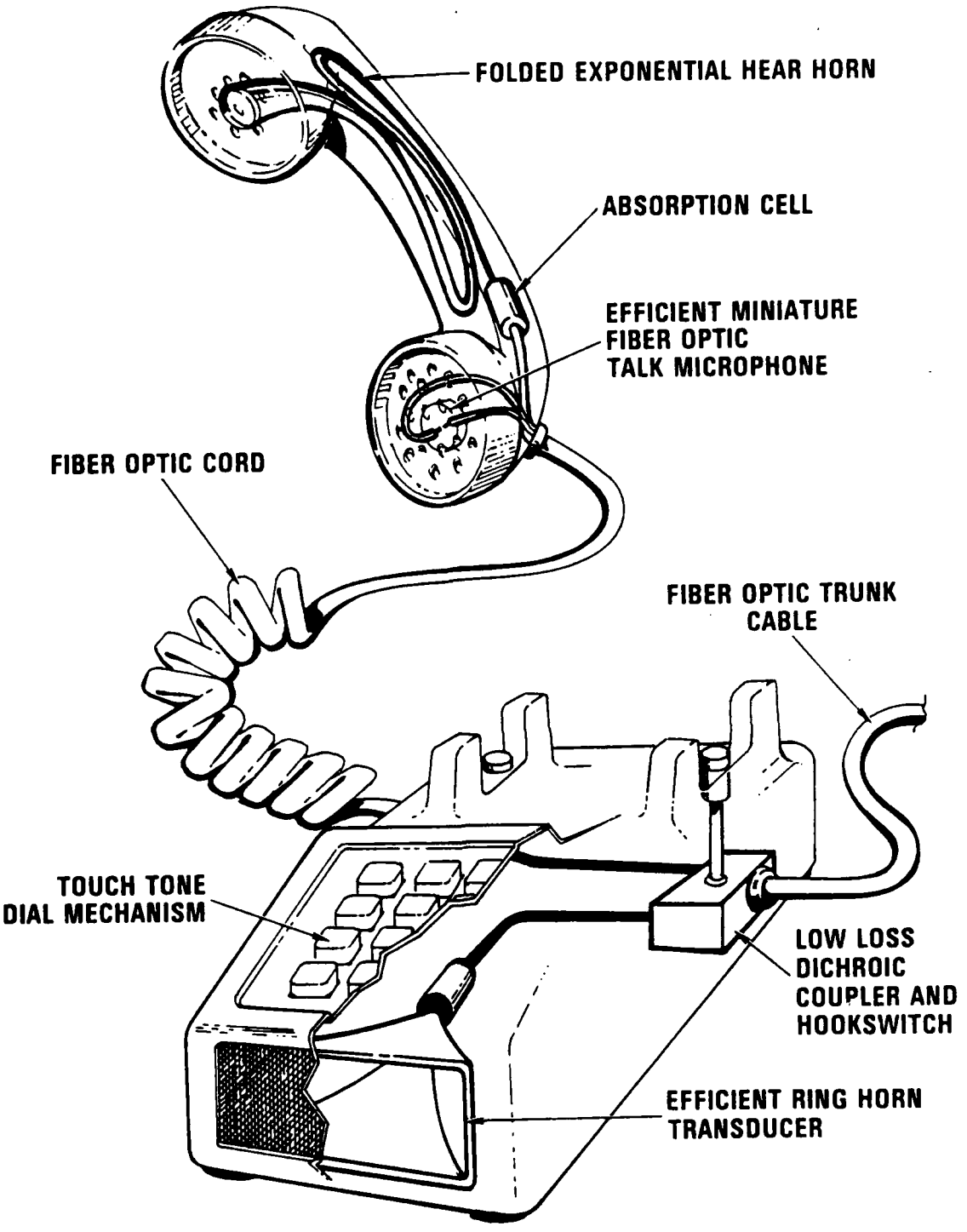

Figure 1.2 Engineering concept of the optical telephone of the future. Cutaway view shows all plastic-ceramic construction with no metal parts. Improvements include dichroic coupler and hook switch utilizing two trunk fibers and a completely passive Ring - feasible with present day technology.

SECTION II

DESIGN ANALYSIS

2.0 DESIGN ANALYSIS

In this section we discuss the component and system design tradeoffs and analyses.

2.1 BASELINE APPROACH

During the design phase of this study, a literature survey was conducted and engineering tradeoffs made to select, for each functional element to be demonstrated, the approach with the highest likelihood of success. The results of the literature search are listed in Appendix A.

Talk Function - The Talk function was the most straight forward to implement, since there are a number of potential methods for modulating light in a fiber link. As discussed in the introduction, a prime design consideration was that the system be passive, (i.e., contain no electronics). Two fundamental alternatives, phase modulation and amplitude modulation, were considered. Phase modulation has greater sensitivity, but is more complex, since it involves an interferometric fiber configuration. Amplitude modulation, although less sensitive, is sufficient and easily implemented in several ways. Some of these are outlined below:

1) Microbending loss modulation - light rays are directed by microbending of the fiber from the core to the lossier cladding where they are attenuated.
2) Fustrated Internal Reflection (FIR) - transmission loss

is modulated by varying the evanescent field coupling across a gap with a pressure wave.

3) Fiber coupling modulation - modulation is achieved by varying the lateral, longitudinal or angular alignment of the fiber link. Optical elements, such as lenses, graded neutral density filters or gratings may be used to enhance sensitivity, linearity or other performance parameters.

The following table summarizes the various Talk function amplitude modulation schemes.

TABLE 2.1 TALK FUNCTION TRADEOFFS

MODULATION TYPE	SENSITIVITY	COMPLEXITY	TECHNICAL RISK
Microbending loss	low	moderate	moderate
Fiber Coupling	low/medium	low	low
Frustrated Internal Reflection	high	medium/high	medium/high

Fiber coupling loss modulation was chosen as the baseline approach because it has lower risk and, within the scope and effort allowed on this program, it represented the surest way to demonstrate feasibility. To further reduce complexity and increase reliability, a diaphragm coupled fiber sensor was selected for implementation with no additional optical elements. Sensitivity is determined by parametric characteristics of the diaphragm, such as tension, density and diameter, and by fiber diameter, numerical aperture and fiber gap.

Hear Function - The literature survey and the initial investigation identified two probable alternatives for the Hear function, both using the same fundamental energy conversion process. In a concept developed by Edelman[1], light from an optical fiber is coupled to an absorptive fiber network that expands and contracts efficiently at audio frequencies in proportion to the energy absorbed. These absorptive fibers are acoustically matched to a diaphragm to produce sound output and must have a large Young's modulus, high coefficent of thermal expansion and low specific heat. This enables modulated light to be absorbed in the fibers and converted to heat, causing the fiber-diaphragm structure to expand and contract at audio frequencies. Figure 2.1 shows a representative implementation of this approach.

The second method, shown in Figure 2.2, first presented by Kleinman and Nelson of Bell Labs[2], utilizes a small optically absorptive chamber filled with carbonized fiber in which sound is generated by the local gas/fiber expansion and contraction. Sound is coupled from the small absorptive chamber to the ear by an exponentially tapered horn acting as an impedance matching transformer. Harris selected the Kleinman-Nelson approach, because it is theoretically and experimentally more developed[3].

Ring Function - For the Ring function two approaches were considered. The first involves coupling of a small absorptive

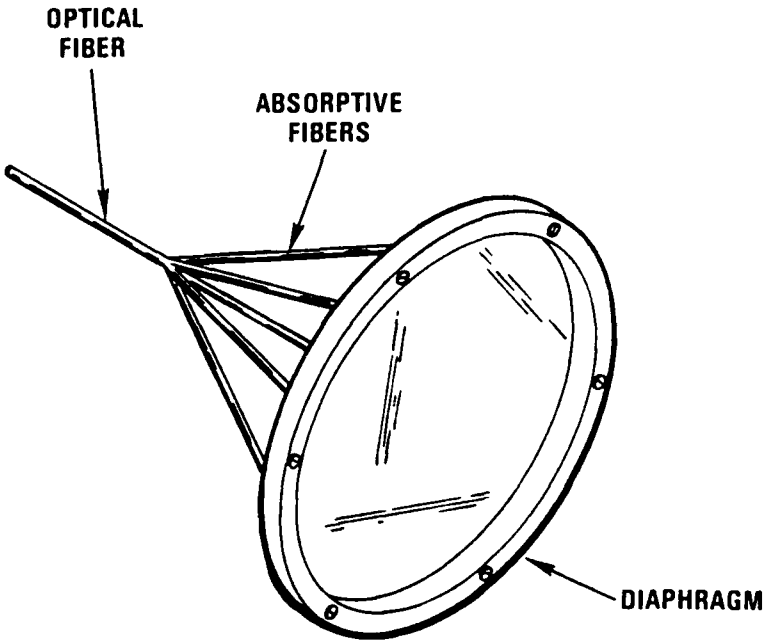

Figure 2.1 Edelman Hear Design

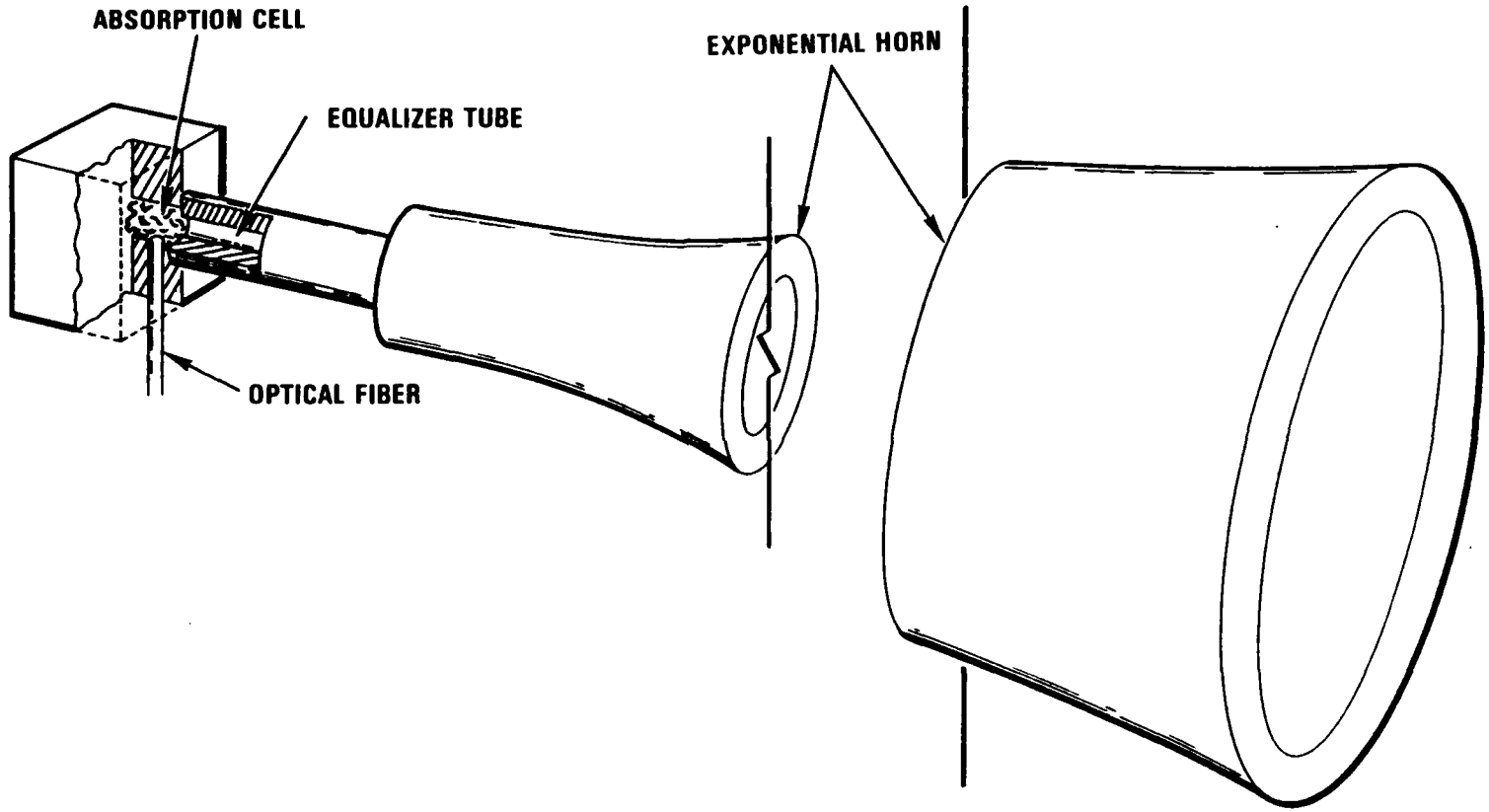

Figure 2.2 Kleinman-Nelson Hear design

resonant chamber to an impedance matched horn to produce the required sound output of 75 dB at a 1 meter distance.

The second approach involves the release of stored mechanical energy by a optically triggered bimetallic latch which then couples the mechanical energy to a sound producing device. The energy storage can be effected by depressing the switch hook to compress a spring, twist a torsion bar, displace a weight, or some other mechanism, and could be released to strike a bell, blow air by a bellows to vibrate a reed, etc.

The latter ring approach was chosen because the required design and fabrication effort was better accommodated within the program cost and schedule constraints. The resonant horn approach however, was analyzed and designed for future evaluation and possible implementation.

System Configuration - The overall system configuration was chosen for ease of layout, low complexity, operational simplicity and functionality. It used a laser diode for each of the three functional elements and incorporated a 100 foot, four fiber link. A fiber was used for each functional element with the extra fiber for the Talk return signal to the photodiode electronics. The Electronic Interface Unit (EIU), which serves the function of the switchboard, generated an audio sidetone from the photodiode and directed the signal to the Hear mechanism via the optical link. The EIU also incorporated circuitry for laser diode protection against electrical power transients. Injection

Laser Diode (ILD) vendors were surveyed and the highest available CW output power ILD's were used.

2.2 TALK DESIGN

The approach chosen by Harris for the Talk mechanism was loss modulation by variable optical coupling between two end-to-end axially aligned fibers. In this technique, one fiber is attached to the center of a thin, taut diaphragm while another fiber is mechanically fixed. Sound waves striking the diaphragm cause it to vibrate, changing the optical coupling between the two fiber ends. The degree of coupling, hence the light intensity variations, is a function of acoustic pressure variations.

Free Membrane - For a thin stretched membrane the equation of motion without driving forces is:

$$\frac{\partial^2 y}{\partial t^2} = c^2 \nabla_r^2 y \qquad (2.1)$$

where:

$c = \sqrt{\frac{T}{\sigma}}$ is the velocity of wave propagation in the membrane, cm/s

T = tension, dynes/cm^2

σ = area density, grams/cm^2

$$\nabla_r^2 = \frac{\partial^2}{\partial r^2} + \frac{1}{r}\frac{\partial}{\partial r} + \frac{1}{r^2}\frac{\partial^2}{\partial \theta^2}$$

∇_r^2, Laplacian operator in polar coordinates.

The circularly symmetric solutions for a membrane rigidly

constrained at its diameter are of the general form:

(2.2) $y = AJ_o(kr)$, where:

A = amplitude determined by initial conditions

J_o = Bessel function of the first kind and zero order

w = frequency, radians/sec

k = w/c, propogation constant, rad/cm.

r, radial coordinate, cm.

At the radius of the membrane (at r=a), the deflection is zero, therefore only those discrete k values offer solutions for which ka is a null of the Bessel function.

Forced Vibrations - For a membrane driven by a sinusoidally varying pressure, Pe^{jwt}, the particular part of the equation must be included, namely:

(2.3) $$\frac{\partial^2 y}{\partial t^2} = c^2 \nabla_r^2 y + \frac{P}{\sigma} e^{jwt}$$

If we assume the steady state solution of the form

(2.4) $y = Ye^{jwt}$

then

(2.5) $$\nabla_r^2 Y + k^2 Y = \frac{-P}{\sigma c^2} = \frac{-P}{T}$$

The solution then becomes the sum of the general and the particular solutions:

(2.6) $Y = AJ_o(kr) - P/(k^2 T)$

Applying the boundary condition that Y=0 when r=a gives:

(2.7) $A = P/(k^2 TJ_o(ka))$

The amplitude of the vibrations, Y, becomes:

$$(2.8)\quad Y = \frac{P}{kT}\left(\frac{Jo(kr)}{Jo(ka)} - 1\right)$$

While the time varying solution is

$$(2.9)\quad y = Ye^{jwt}$$

The frequency response of the fiber microphone was evaluated using a Bessel function approximation algorithm to solve the problem of a diaphragm driven by pressure waves. The amplitude at the center (r=o) was calculated by a computer program listed in Appendix B using Equation 2.8. To generate a broadband response from 300 to 3300 Hz, two alternatives were investigated. In one, the fundamental resonance of the diaphragm was increased to above 3000 Hz; this resulted in reduced sensitivity. In the other technique, selected for our breadboard, a number of inband resonances were allowed for an overall high average response across the bandwidth as shown in the computed response in Figure 2.3.

Coupling Loss Modulation - Critical alignment was necessary to achieve optimum coupling loss and optical bias for AM modulation. Proper optical biasing occurs when the modulation response is maximized by the appropriate vertical offset, while low distortion is maintained. A large vertical offset will induce too much loss, while insufficient offset will cause distortion in the mechanical to optical modulation transfer function. Figure 2.4, a curve of the coupling efficiency vs. fiber displacement, illustrates this tradeoff. In this idealized model, uniform light distribution is assumed inside the 50 micrometerdiameter of the fiber. The curve shows a sharp break

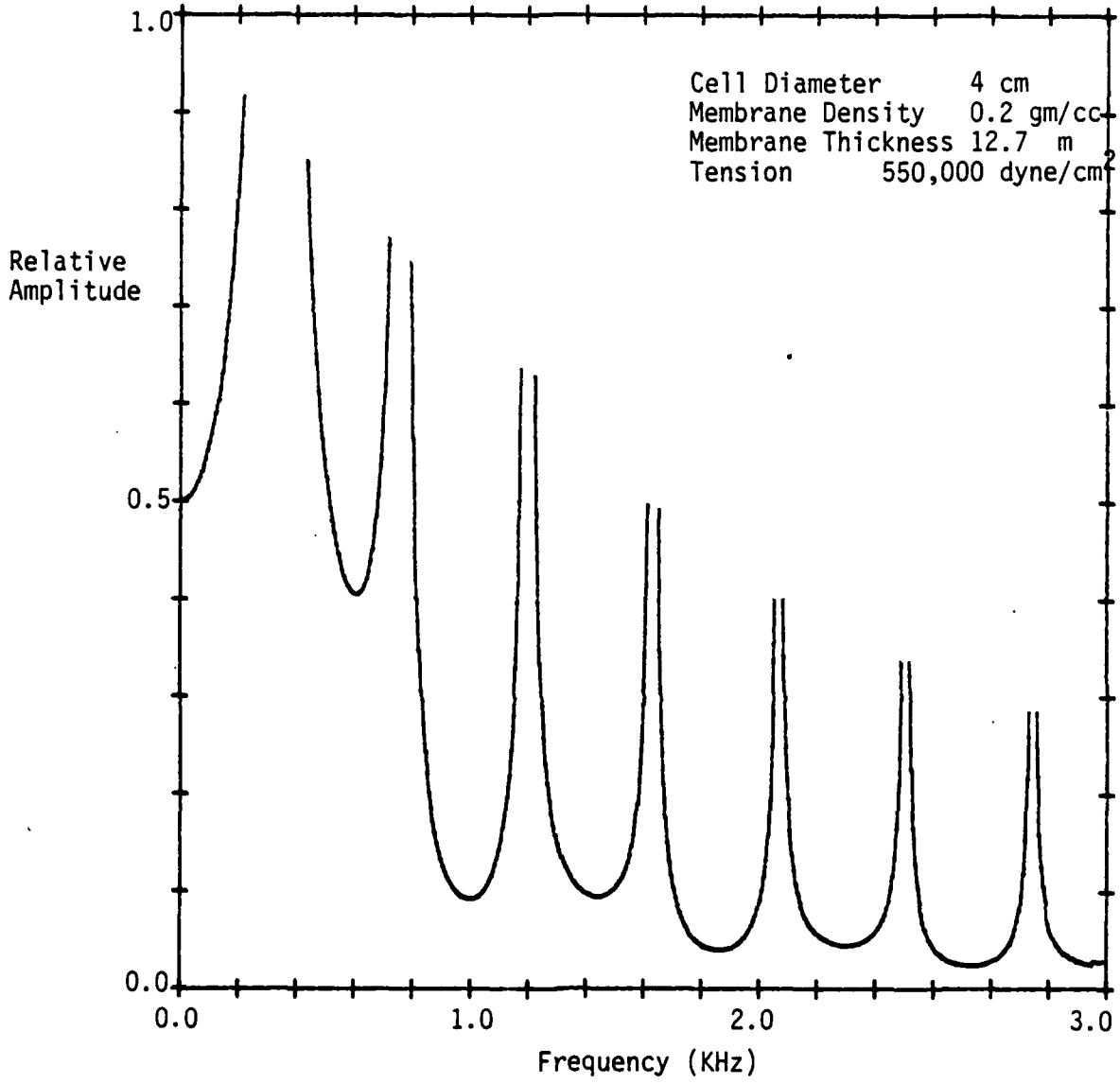

Figure 2.3 Computed response of the Talk mechanism

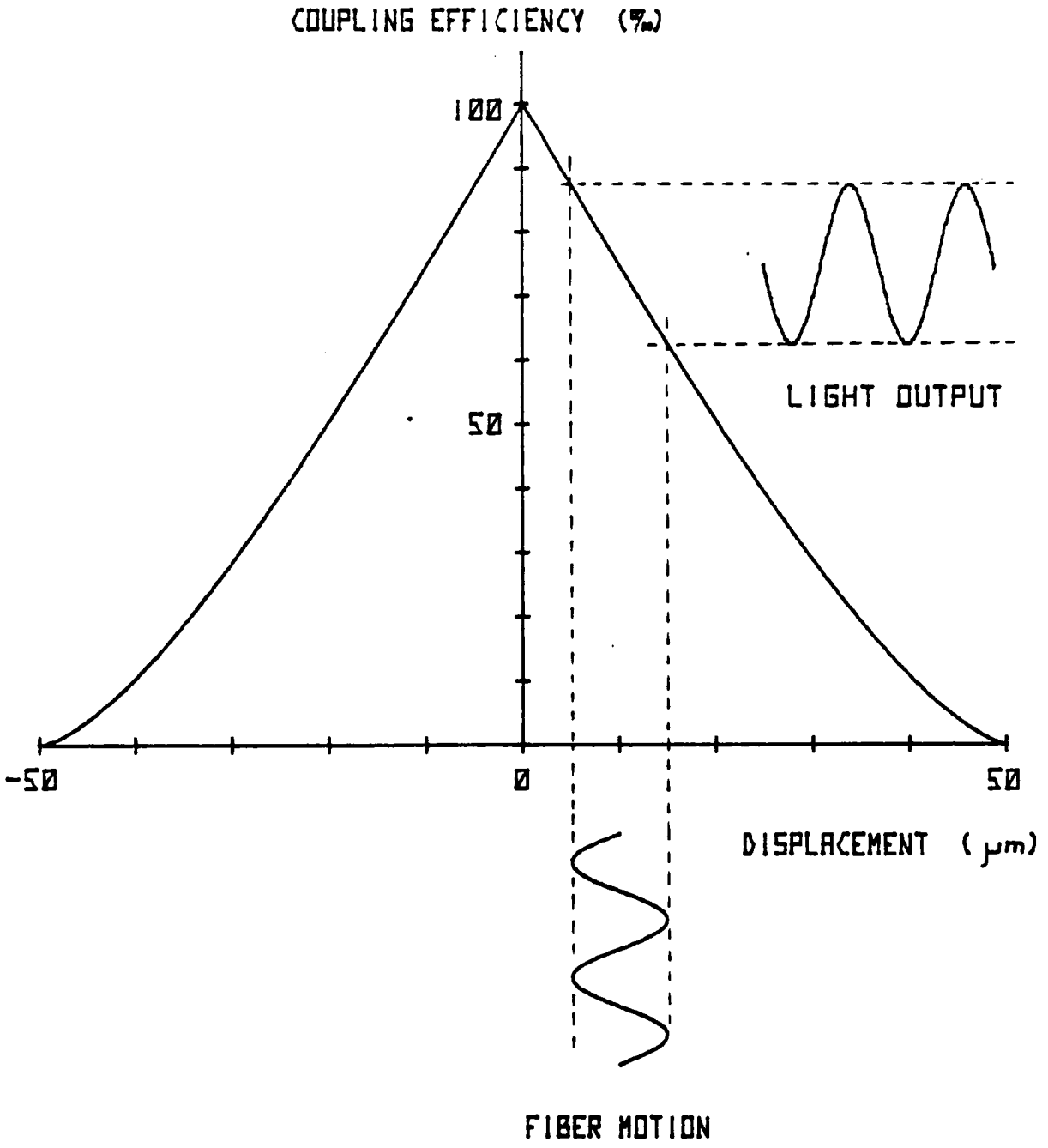

Figure 2.4 Fiber coupling efficiency versus fiber placement for the Talk mechanism.

well as maximum slope near the center. Optimum bias, therefore is as close to the centered position as possible without causing the signal to cross the slope discontinuity at zero, and thus creating undesirable distortions. A possible operating point is shown at 10 microns offset, with a 10 micron peak to peak fiber oscillation resulting in a coupling efficiency modulation from 62 to 87%.

Offsets in the lateral and horizontal directions were optimized carefully. Small shifts due to epoxy or diaphragm aging made an occasional readjustment necessary. Initial tests were performed with a 100 micron diameter fiber, but enhanced sensitivity was achieved by reducing the Talk sensor fiber core diameter to 50 microns.

2.3 HEAR DESIGN

The Hear Design is a refinement of the photoacoustic technique first conceived by Alexander Graham Bell in 1881. Practical theoretical development of the technique, however, was done nearly 100 years later by Kleinman and Nelson of Bell Labs in 1977. Their concept was further optimized in the Harris design and their predicted response will be compared with the Harris Hear Design.

The photoacoustic effect originates when light interacts with matter in an acoustically active medium. Light illuminating a material is absorbed to some degree and raises the temperature of the substance to a level which depends on its absorption coefficient, and the thermal conduction, convection and radiation processes present. In our case, the absorber was a matrix of carbonized cotton fibers suspended in air. This combination may be regarded as a "pseudo gas." To model the photo acoustic effect in the pseudogas, several essential simplifying assumptions were made:

1) Under optical powers of 4 to 5 milliwatts, the average temperatures of the gas and the solid absorber are equivalent.
2) Gas absorption and desorption processes have higher time constants compared to the highest frequency of interest.
3) The solid absorber and gas vibrate in phase.

The cotton absorber is housed in a cell whose dimensions are

small compared to the smallest acoustic wavelength of interest so that the acoustic pressure is constant throughout the volume (approximately 10^{-3} cc). The sound output of the cell is coupled to the small end of a long tapered acoustic tube. The output of the tube is then connected to the chamber formed by the human ear and the telephone earpiece. The tube converts sound from a high pressure, low flow condition to a low pressure, high flow condition. The tube, therefore, acts as an acoustic impedance transformer converting the high impedance of the small absorber volume to the low impedance of the larger ear volume. The Kleinman-Nelson schematic representation is shown in Figure 2.5. Inertance equalizers are necessary to resonate with the capacitive nature of the volumes for a broadband response.

The following variables are used in the design equations:

S_L	Sound Flow Source, cc/sec
P_E	Sound Pressure in the ear, dynes/cm^2
$z_{1,2,C,E}$	Acoustic impedance, see equations 2.25 and 2.32 gm/cm^{4}sec
$Z_{1,2}$	Acoustic impedance of equalizers, see equation 2.33 gm/cm^{4}sec
T	Transfer matrix or temperature
I	Intensity, W/cm^2
R_o	Normalizing constant for H_w, 880 gm/sec cm^4
G_a	Utilization factor for light absorption
G_m	Figure of merit for gas; air = 1, xenon = 2
G_w	Dispersion function of cell
P_w	Optical power input, ergs/sec
L	Length of horn, cm
$L_{1,2}$	Equalizer inertance, gm/cm^4
r_1	Input radius of horn, cm
r_2	Output radius of horn, cm
α	Horn flare constant
δ	Density, gm/cc
c	Velocity of sound, cm/sec
n	Complex propagation constant
w	Angular frequency, rad/sec
k	Wave propagation constant, w/c, rad/cm
$\xi(k)$	Frequency dependent solutions. See Equation 2.30

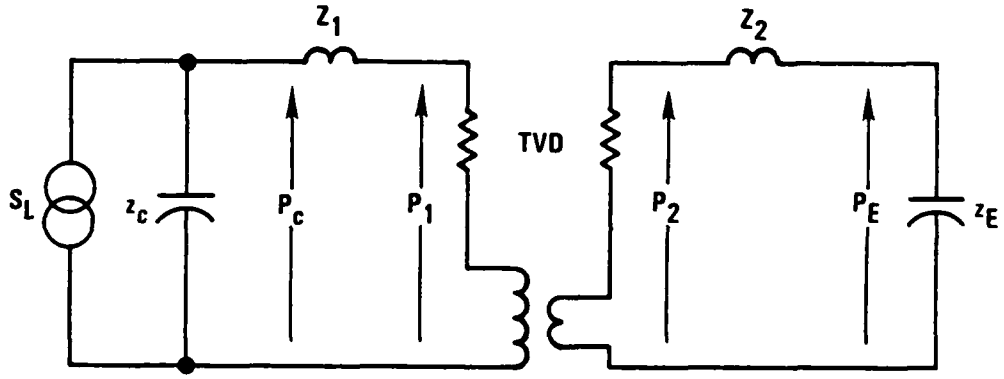

Figure 2.5 Schematic representation of Hear equivalent circuit

$\Delta(k)$ Frequency dependent solutions. See Equation 2.31.
Φ Phase Term. See Equation 2.39.
φ Phase of $h(k)/g(k)$
γ Specific heat ratio
$V_{C,E}$ Volume. cc
r_o Boundary layer radius of lossless tube. cm.

The matrix equation of the two port network may be written as:

(2.10) $$P_1 = T_{11} P_2 + T_{12} S_2$$

(2.11) $$S_1 = T_{21} P_2 + T_{22} S_2$$

If we denote the equalizers by matrices [EQ1] and [EQ2], the overall coupling matrix, [C] is:

(2.12) $$C = [EQ1] \cdot [T] \cdot [EQ2]$$

The solution of the circuit is

(2.13) $$\frac{S_1}{P_E} = C_{21} + \frac{C_{11}}{z_C} + \frac{C_{22}}{z_E} + \frac{C_{12}}{z_C z_E}$$

Using the equalizer matrices of the form

(2.14) $$[EQ] = \begin{bmatrix} 1 & Z \\ 0 & 1 \end{bmatrix}$$

The solution of the circuit reduces to:

(2.15) $$\frac{S_L}{P_E} = \frac{T_{11}}{z_C}\left(1 + \frac{Z_2}{z_E}\right) + \frac{T_{12}}{z_E z_C} + T_{21}\left(1 + \frac{Z_1}{z_C}\right)\left(1 + \frac{Z_1}{z_E}\right) + \frac{T_{22}}{z_E}\left(1 + \frac{Z_1}{z_C}\right)$$

The intensity, I, has the general form

(2.16) $$I = (R_o^2 G_a^2 (\gamma-1)^2 / 2(\gamma_o P_o)^2) |P_w|^2 H_w$$

where

(2.17) $$H_w = \left|\frac{P_E}{S_L}\right|^2 \cdot \left(\frac{G_m 2}{R_o 2}\right) \cdot |G_w|^2$$

H_w contains all the acoustic properties of the absorbing

medium, the volume V_c, the coupling matrix (C) and all dependence on frequency. Therefore, I reduces to

(2.18) $I = 3.13 \times 10^{-8} G_a^2 P_w^2 H_w$

and

(2.19) $$H_w = 1.29 \times 10^{-6} G_m^2 \left| G_w \right|^2 \left| \frac{P_c}{S_L} \right|^2$$

Now the sound pressure level (SPL) can be expressed as

(2.20) $SPL(dB) = 10\log(I/P_{ref}^2)$

$$= -1.065 + 10\log P_w^2 + 10\log H_w$$

assuming the light utilization factor, $G_a = 1$

and P_{ref} is 2×10^{-4} dynes/cm^2.

Figure 2.6 shows the variation in the resistive and reactive components of the input impedance for conical, hyperbolic and exponential flare horns with the same cutoff frequency[4]. The conical flare has the lowest distortion but the lowest cutoff slope indicating insufficient band limiting. The hyperbolic horn has the fastest slope for the best slope cutoff but the highest distortion due to nonlinearities when the air is moving in the region of lowest flare growth. For these reasons, an exponential taper is used widely in musical instruments and was used in the Harris optical telephone Hear mechanism as the impedance matching transformer.

Utilizing the exponential horn solution which assumes the boundary layer approximation for sound propagation (equivalent tube radius for a lossless tube), and neglects thermoviscous damping except in the exponents, results in

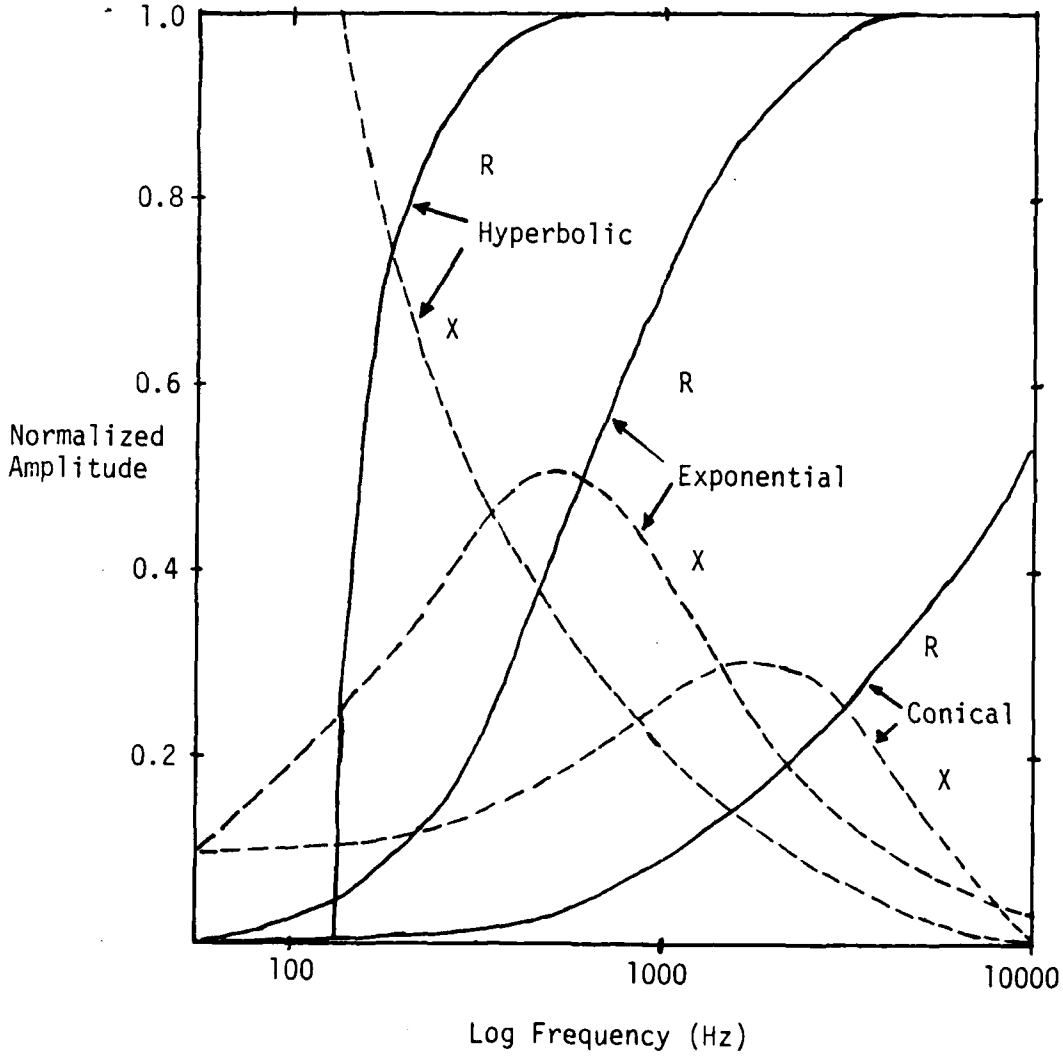

Figure 2.6 Comparison of resistive and reactive components for conical, exponential and hyperbolic horns of the same cut off frequency.

$$(2.21)\quad \left|\frac{P_E}{S_L}\right|^2 = \left(\frac{2}{\pi}\,\frac{\delta cn}{r_1^2 r_2^2 k}\right)^2 \frac{\exp\{(-r_o/r_1)\xi\}}{\left|g(k) + h(k)\exp(2jnL + j\Delta - \Delta)\right|^2}$$

where

$$(2.22)\quad \left|\frac{P_E}{S_L}\right|^2 = \left(\frac{2}{\pi}\,\frac{\delta cn}{r_1^2 r_2^2 k}\right)^2 \frac{\exp\{(-r_o/r_1)\xi\}}{|g(k)|^2\left|1+(h(k)/g(k))\exp(2jnL+j\Delta-\Delta)\right|^2}$$

$$(2.23)\quad g(k)=\left(1+\frac{Z_1}{z_C}+\frac{z_1}{z_C}\right)\left(\frac{z_2}{z_E}-\frac{Z_2}{z_E}-1\right)$$

and

$$h(k)=\left(1+\frac{Z_1}{z_C}+\frac{z_1}{z_C}\right)\left(1+\frac{Z_2}{z_E}-\frac{z_2}{z_E}\right)$$

$$(2.24)\quad g(k)=-h(k)^*$$

$$(2.25)\quad z_{1,2} = \frac{j\omega\delta}{m \pm \pi r^2_{1,2}}$$

$$(2.26)\quad m \pm = \alpha \pm jn$$

$$(2.27)\quad n = \left(k^2 - \alpha^2\right)^{1/2}$$

$$(2.28)\quad \alpha = \ln(r_2/r_1)/L$$

$$(2.29)\quad r_o = 2\,\gamma'(\alpha c)^{1/2},\ \gamma',\ \text{Kirchhoff constant for air, } 0.565\ \text{cm/sec}^{1/2}$$

$$(2.30)\quad \xi(k) = \left(\frac{2\alpha}{k}\right)^{1/2}\left(\frac{2nk^2 - \alpha k^2 - 2q\alpha(\alpha n - \alpha^2 - 2n^2)}{\alpha(k^2+3n^2)}\right)$$

$$(2.31)\quad \Delta(k) = \left(\frac{r_o}{r_1}\right)\left(\frac{8n^2}{\alpha k}\right)^{1/2}\left[\frac{k^2 - \alpha^2 q}{k^2+3n^2}\right]$$

The impedances z_E and z_C are given as:

$$(2.32)\quad z_E = \frac{j\gamma P_o}{wV_E}\ ,\quad z_C = \frac{j\gamma P_o}{wV_C}$$

The ideal equalization inertances have an impedance of

$$(2.33)\quad Z_1 = -jwL_1\ ,\quad Z_2 = -jwL_2$$

where L_1 and L_2 are the inertances of a lossless tube radius, a, of.

$$(2.34)\quad L_{1,2} = \frac{\delta L}{\pi a^2} + \frac{2\delta}{4a}$$

where the second term describes end effects.

The dispersion function, G_w, gives the frequency dependence due to thermal conduction in the pseudogas. G_w is a function that depends on the size and shape of the volume, V_c.

$$(2.35)\quad Gw = 1 - 3\left(\frac{\psi \coth \psi - 1}{2}\right)$$

where

$$(2.36)\quad \psi = (1-j)\left(\frac{15\, w\tau}{2}\right)^{1/2}$$

and

$$(2.37)\quad \tau = \frac{\gamma a^2}{15\upsilon}$$

where τ is the thermal relaxation time for a sphere of volume V_c and radius a.

Existance of g(k) gives rise to oscillations due to resonances of waves travelling back and forth in the horn. Since the only damping in the horn model is the thermoviscous damping in the tube, it follows that the reflection coefficient, h(k)/g(k), must have a magnitude of unity and that the oscillations must have the maximum possible peak to peak variations. The following term describes the oscillations in Hw,

(2.38)

$$\left| 1 + \frac{h(k)}{g(k)} \exp\left(2\,jnL + j\Delta - \Delta\right) \right|^{-2} = \left(1 - 2e^{-\Delta}\cos\Phi + e^{-2\Delta}\right)^{-1}$$

where

(2.39) $\Phi = 2n\ell + \Delta - 2\varphi$

(2.40) $\varphi =$ [illegible]

Now the frequency response, H_w, can be expressed as:

(2.41)

$$H\omega = G_m^2 \left(\frac{\delta}{\delta_0 c_0}\right)^2 \frac{\left[\left(\frac{2}{\pi}\right)^2 1.29\times10^{-6}(\delta_0 c_0)^2\right]}{r_1^2 r_2^2} \left(\frac{n}{k}\right)^2 \frac{\exp\left\{(-r_0/r_1)\xi\right\} |G\omega|^2}{|g(k)|^2 (1-2e^{-\Delta}\cos\Phi+e^{-2\Delta})}$$

where the factor $(\delta c/\delta_0 c_0)^2$ is a convenient term used when two different gases are in the horn.

Averaging the term $1-2e^{-\Delta}\cos\Phi + e^{-2\Delta}$ over 2π as follows results in the "smoothed" or average frequency response.

(2.42)

$$\frac{1}{2\pi}\int_0^{2\pi} \left(1-2e^{-\Delta}\cos\Phi + e^{-2\Delta}\right)^{-1} d\Phi = \left(1 - e^{-2\Delta}\right)^{-1}$$

The outcome is the smoothed response, $\langle H_w \rangle$

(2.43)

$$\langle H\omega \rangle = G_m^2 \left(\frac{9.1 \times 10^{-4}\ \text{cm}^4}{r_1^2 r_2^2}\right) \left(\frac{n}{k}\right)^2 \frac{\exp\left\{(-r_0/r_1)\xi\right\} |G\omega|^2}{|g(k)|^2 \left\{1 - e^{-2\Delta}\right\}}$$

A BASIC computer program was written to calculate and plot these functions. Full documentation is given in Appendix C. The plot of $\langle H_w \rangle$ does not show the peak-to-peak variations in the response but it significantly reduces the computation time. Air was chosen as the gas medium in the horn although other gases potentially have better output response efficiency. Gases other than air, however, require a more complicated horn design incorporating a diaphragm to prevent their leakage to the

atmosphere. Their use, therefore would reduce the simplicity and reliability of the horn, although possibly would increase the output level. Horn design was optimized with the computer by varying the horn parametrically to obtain the relative responses shown in Figure 2.7 Comparative equalized horn parameters are shown in Table 2.2.

Utilizing another gas such as xenon could theoretically give 10 dB improvement mainly due to an increased figure of merit, Gm, for the absorbing medium and enhanced acoustic coupling of the sound wave at the gas-air interface. The figure of merit, Gm may be written as:

$$G_m = \left(\frac{1 - \gamma^{-1}}{1 - \gamma_o^{-1}}\right) \cdot \left(\frac{\partial \ln T}{\partial \ln p}\right)_v \qquad (2.44)$$

where the partial derivative is unity for an ideal gas and γ is the specific heat ratio for the gas and γ_o is that of air. A diaphragm is required for gas confinement. The term $(\delta c / \delta_o c_o)^2$ in equation 2.41 further enhances H_w by effecting a better acoustic match when using a gas such as xenon with a higher acoustic impedance, δc, to that compared to air, $\delta_o c_o$. The comparison between the computed xenon horn response and air horn response is shown in Figure 2.8.

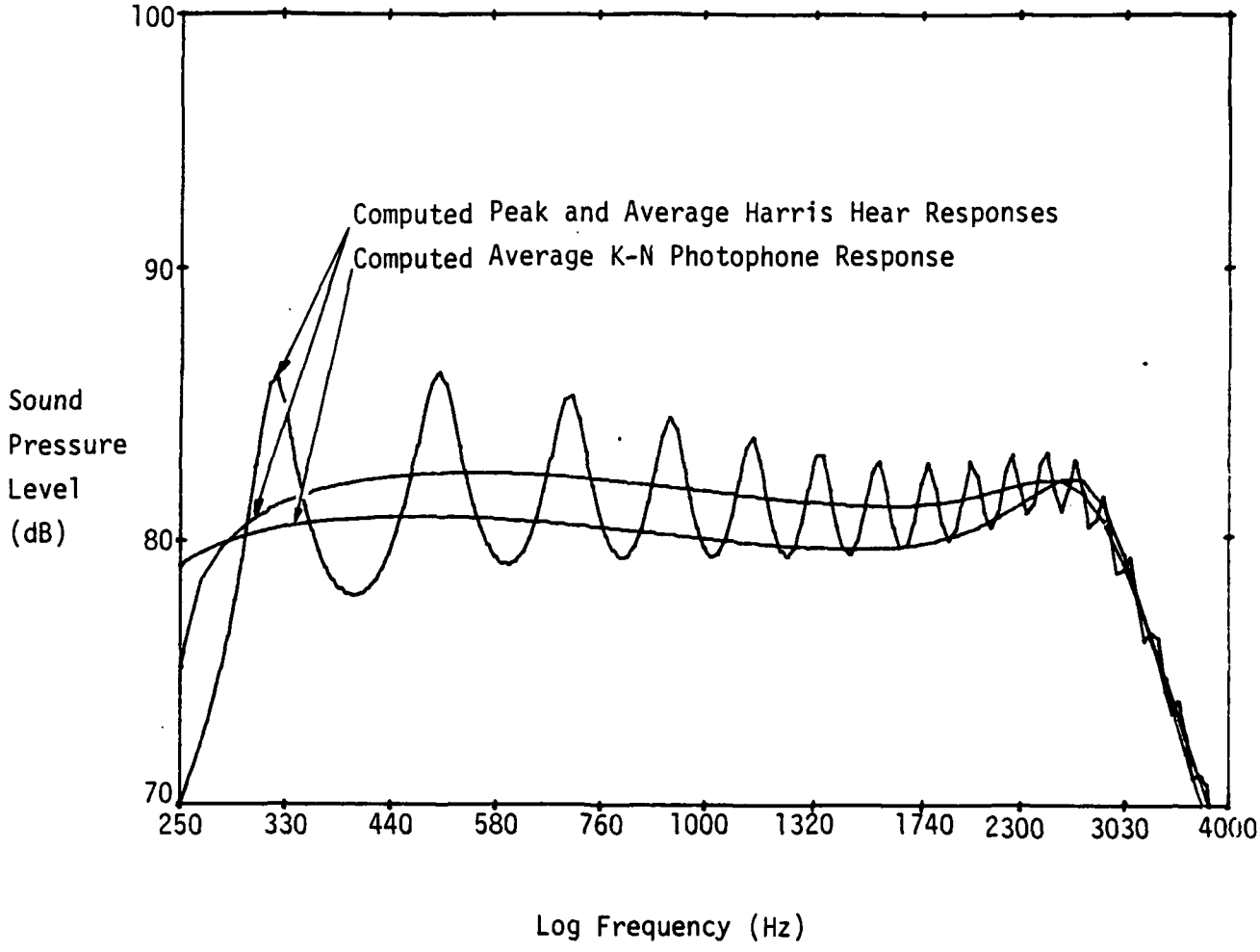

Figure 2.7 Comparison of computer generated plots showing the average response of the Kleinman-Nelson Photophone and average and peak responses of the Harris Hear horn with parameters shown in Table 2.2.

TABLE 2.2

COMPARITIVE HORN PARAMETERS

	Harris Design Air Horn	Kleinman-Nelson Air Horn	Kleinman-Nelson Xenon Horn
gas density (gm/cc)	1.23×10^{-3}	1.23×10^{-3}	5.4×10^{-3}
c (cm/sec)	3.4×10^{4}	3.4×10^{4}	1.77×10^{4}
G_m	1	1	2
L (cm)	70	85	56
r_1 (cm)	0.032	0.036	0.024
r_2 (cm)	0.77	0.85	1.27
V_E (cc)	6	6	6
V_C (cc)	2.5×10^{-3}	2.5×10^{-3}	6×10^{-4}
Predicted Sound Pressure Level with 2.8mW (dB)	84	81	91
Bandwidth (Hz)	300 - 3300	200 - 3300	200 - 3300

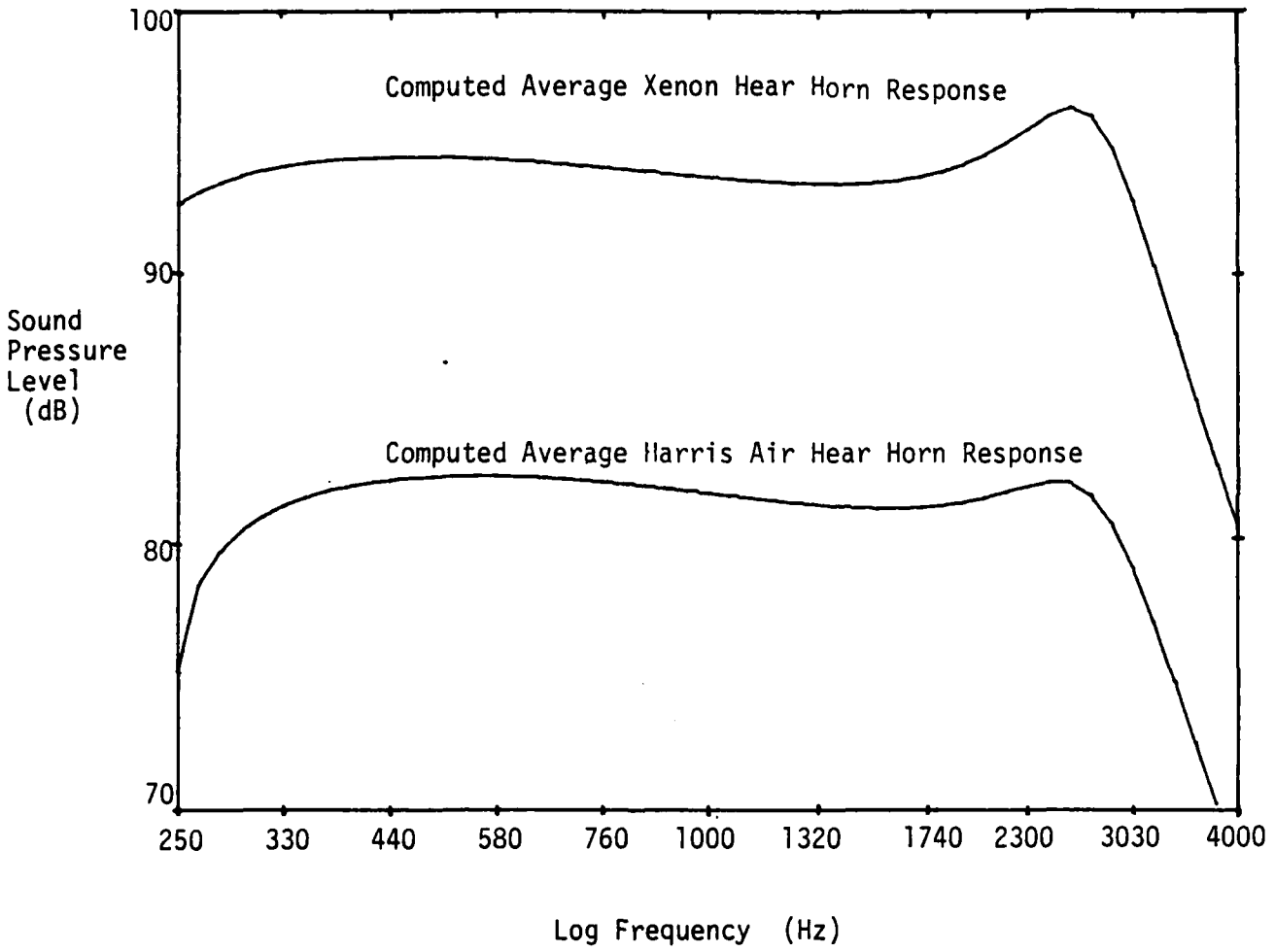

Figure 2.8 Graph of predicted average responses of Xenon Hear horn compared to Harris Air Hear horn with parameters shown in Table 2.2.

2.4 RING DESIGN

Two different design concepts were analyzed: a resonant Ring horn coupled to an absorption cell, and a Ring mechanism consisting of an optically triggered bimetal latch releasing stored mechanical energy.

The first concept, the resonant horn, utilized an approach similar to the Hear horn except that the acoustic coupling was into a free space load rather than into the 6cc volume of the ear. For free space coupling, the mouth of the horn was considered to be an ideal massless air piston mounted in an infinite baffle. This analogy is accurate, assuming neglible phase variations across the air piston. The acoustic impedance of a rigid air piston is:

(2.45) $Z_A = R_1(2kr_2) + j\, X_2(2kr_2)$

where

(2.46) $R = \frac{\delta c}{\pi r_2^2} \cdot R_1(2kr_2)$ and $X = \frac{\delta c}{\pi r_2^2} K_1(2kr_2)$

Impedance functions, $R_1(2kr_2)$ and $K_1(2kr_2)$, have been tabulated in tables[5]. By replacing the acoustic impedance z_E by Z_A in equation 2.21, the SPL at the air piston load is calculated for the horn by following the computation discussed in Section 2.3 to its completion.

RMS pressure can be expressed as

(2.47) $P_{load} = P_{ref}\, 10^{SPL/20}$

Surface velocity amplitude at the mouth of the horn is given as:

(2.48) $U_o = P_{load}/\delta c$

being analogous to I = V/R amps.

Pressure, as a function of distance, varies as

(2.49) $$P(Z) = \frac{kr_2^2 P_{Load}}{2\sqrt{2}\, Z}$$

At a distance of 1 meter, the ring output level of an average telephone is 75 dB. Taking z, the distance, as 100 cm, the SPL is then

(2.50) $SPL = 10\log(P(100)^2/P_{ref}^2)$

These equations were added to the Hear Horn computer program, and a horn was optimized with an ideal, lossless equalizer tube. A representative plot of a horn capable of producing 88 dB at 1900 Hz appears in Figure 2.9.

The second ring concept analyzed was the optically triggered bimetal latch. The bimetal latch operates on the principle that light illuminating a bimetal strip (two metals of dissimilar thermal expansion coefficient bonded together) is absorbed causing a temperature rise that generates a differential expansion causing the strip to deflect.

There are several heat loss processes that must be considered in any analysis: losses by radiation, conduction, convection and energy/work processes. The radiation and conduction losses were calculated for the following assumed parameters.

A surface area, 0.1 cm^2
T_1 steady state surface temperature, 310 K^o
T_2 air temperature, 300 K^o,

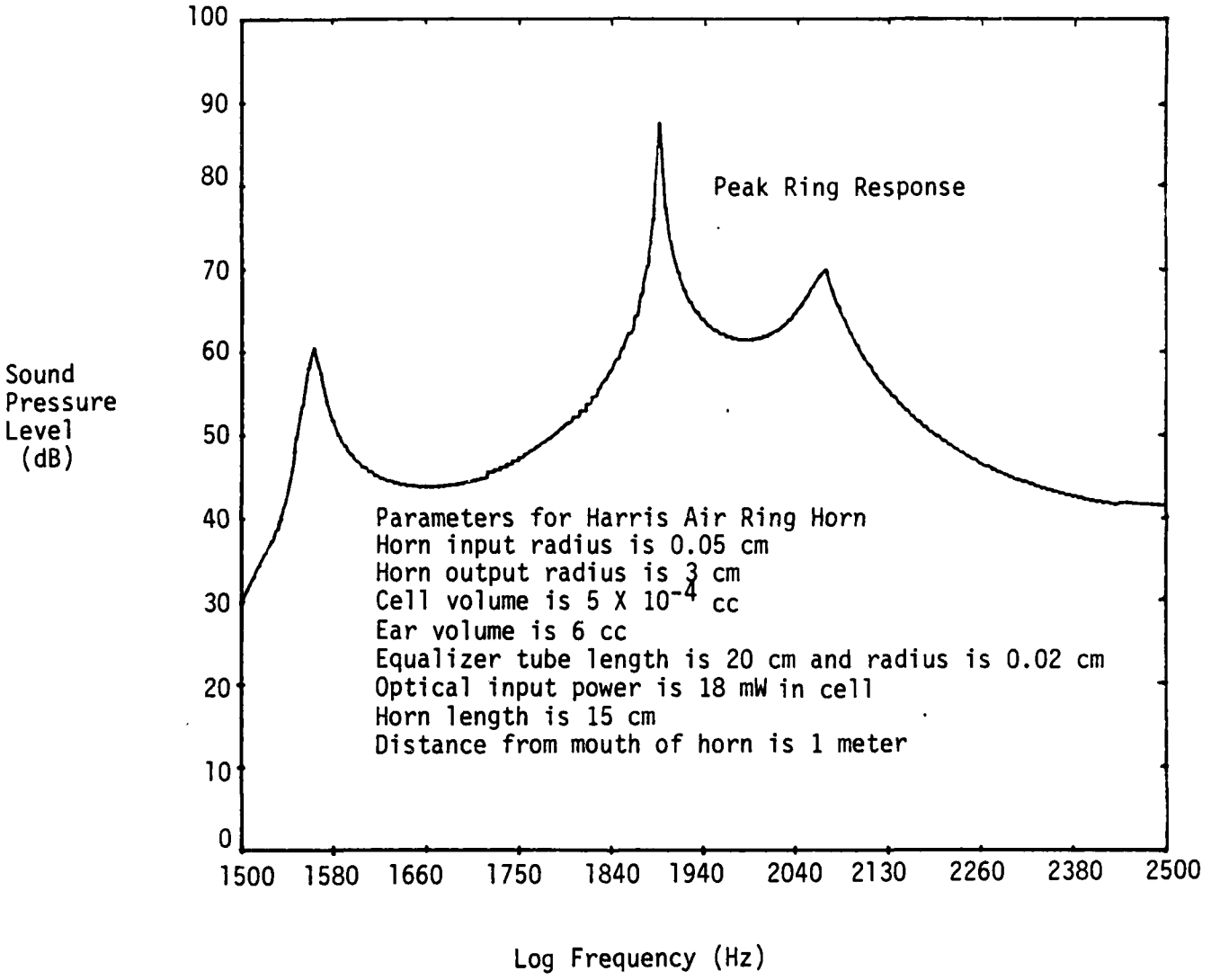

Figure 2.9 Predicted Harris Ring horn response

ϵ surface emissivity of approximately 1
light absorption coefficient of 1
incident optical power of 20 mW

The equation for radiative losses is:

(2.51) $Q/t = \sigma(T_1^4 - T_2^4)A$

where Q/t is the watts of heat lost/sec

σ = Stephan-Boltzman constant, 5.669×10^{-8} W/m^2-^oK

The radiative heat loss is then 0.64 mW which is small compared to the 20 mW expected input optical power.

Heat loss due to conduction of heat at the boundaries was calculated using equation 2.52. We assumed the strip of bimetal to be in a volume with the distance from the strip to the walls being 1 cm and the parameters shown for equation 2.51

(2.52) $Q = KA(T_1 - T_2)/X$

where

K, thermal conductivity for air, 2.35×10^{-4} Joule/s-cm-^oK

X, bimetal to wall distance, 1 cm.

Heat loss for one side of the surface, Q, was calculated to be 0.24 mW. We assumed negligible heat loss through the thin edges and through a well designed support; the heat lost by conduction from both sides was then 0.48 mW. Total heat lost by conduction and radiation was approximately 1.1 mW. The remaining power of 18.9 mW (assuming nearly all the 20 mW incident power is absorbed) is directed into energy/work conversion processes and convection losses.

The majority of the losses occur in air convection which is difficult to calculate. Therefore the experimental set-up, shown in Figure 2.10, was used to determine the characteristics of an optically triggered bimetallic latch. A 50 mW helium neon laser, with adjustable output power, supplied the optical energy. A laser beam expander and cylindrical lens were used to provide a line illumination on the bimetallic strip. The strip, 0.125 x 0.625 x 0.006 inch of Polymetallurgical Corporation PMC 721-575 bimetal (surveyed to have the highest Flexitivity constant, i.e. most sensitive), was painted with a very thin coat of Kodak Photo Black paint on the high expansion side of the bimetal for greatest response speed. When the bimetal was illuminated with 20 mW of light, a deflection of 0.006 inches was reached in 20 seconds. A deflection of 0.004 inches was considered to be the minimum distance to reliably trip a sensitive latch.

Because 20 seconds is a relatively long time to activate a ring, a thinner bimetal was tested with dimensions of 0.040 x 0.625 x 0.006 inch. An optical system was designed using a 10 mm plano-convex lens and a 22.2 mm cylinder lens to illuminate the thinner bimetal with light from a 0.25 numerical aperture, 100 micrometer core fiber. The system was integrated with the bimetal strip and a sensitive spring wound latch to drive a pair of standard phone ring elements. The optical raytrace is shown in Figure 2.11. The speed of response was improved to 5 seconds for 0.006 inch deflections.

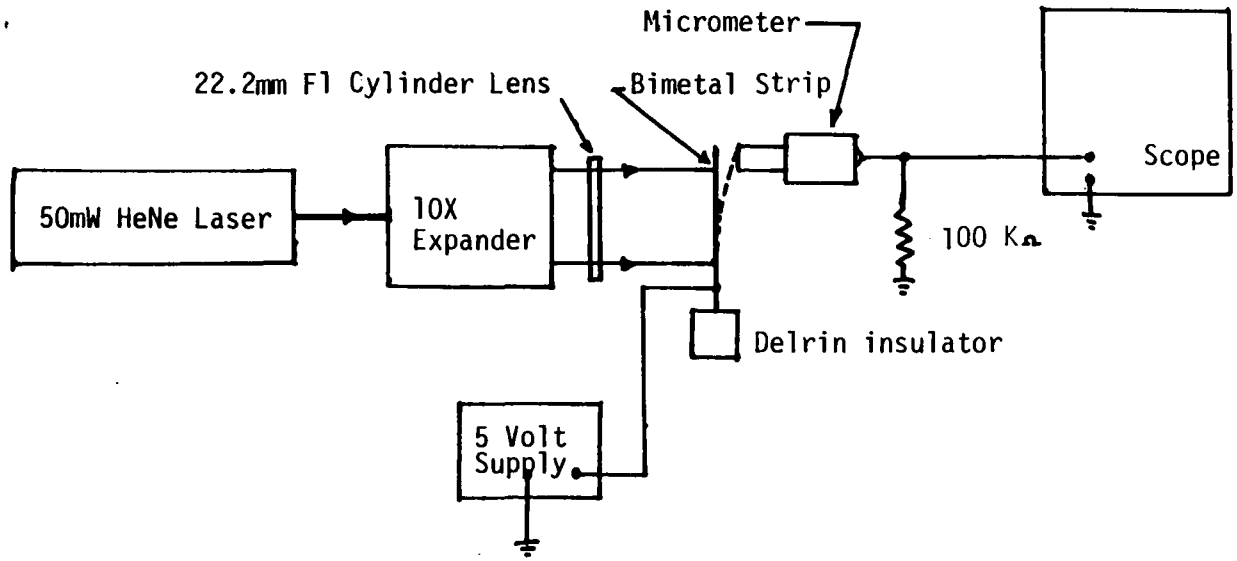

Figure 2.10 Experimental breadboard for bimetal testing

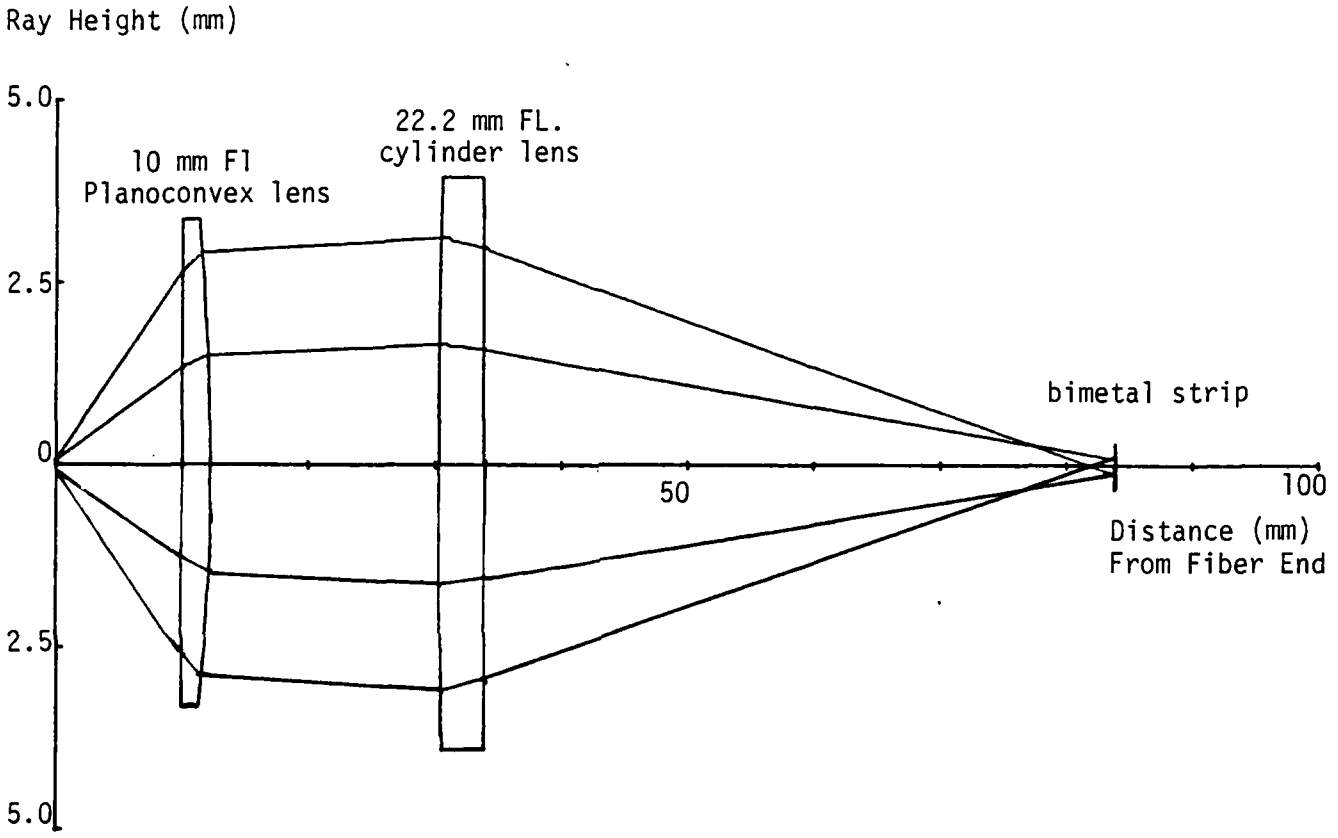

Figure 2.11 Computer ray trace of Ring optics. Light eminates from 50μm cone. Fiber source at origin with a numerical aperture of 0.25 ($\pm$ 14.5^{o}). The vertical cross section of the amorphic system focusing light 50 mm from the final lens resulting in line illumination on the bimetal.

2.5 SYSTEM AND ELECTRONIC INTERFACE UNIT DESIGN

The system for testing the optical telephone components was chosen for optimum simplicity and functionality. The link used four fibers in the configuration shown in Figure 2.12. One fiber was used for each of the functions, Hear, Talk and Ring with the fourth fiber used for the Talk return signal. The fiber initially chosen was a Corning SDF-100 graded index fiber with a 0.33 numerical aperture (N.A.) and a 100 micrometer core diameter with a 140 micrometer cladding diameter to mate with a similar fiber pigtail supplied with the Injection Laser Diodes. However, due to a long lead time of the Corning fiber, a similar Seicor fiber with a 0.25 NA was used. Because most laser diode manufacturers terminate their devices into large NA fibers to increase the power captured by the fiber, a similar or larger NA fiber used in the link will introduce negligible coupling loss from the ILD fiber pigtail to the trunk. The specified loss of the Siecor fiber was 4.5 dB/Km at 830 nm, the ILD wavelength.

Laser diodes selected for the link were Optical Information Systems OSP-562 capable of 20 mW cw out of a 100 micrometer 0.33 NA, one meter long fiber pigtail. The laser diode wavelength is 830 nm and the typical current threshold is 250 mA; operation at 350 mA yields 20 mW optical output. Of the commercially available devices, these had the highest power out of the fiber pigtail. The ILD's had an internal photodiode which can be used

for output power stabilization. Amp connectors, FOC Series model numbers 906-110-5012 (male) and 905-120-5000 (female) were selected because of their low cost and low loss (1.5-2.0 dB).

Serving as the electronic switchboard, the Electronic Interface Unit (EIU) enabled a standard electrical telephone to interconnect to the optical telephone via optical fibers. The EIU housed the laser diodes and associated circuits providing the optical power for the system. Three laser diode control circuits supplied power for each of the individual functions. Additional circuitry was developed to receive the Talk modulated signal. The amplitude modulated Talk return light signal was detected and amplified by a photodiode circuit and the signal then routed to the electrical earpiece at the switchboard phone set. A fraction of the signal also was used to drive the ILD control to electrically generate the sidetone for the Hear mechanism as shown in the block diagram of Figure 2.12

The Ring electronic circuit was designed to produce a 20 mW cw optical level from the Ring laser diode. The Talk circuit was biased such that the Talk ILD operated at 10 mW to enable transmission of a maximum optical ac component to the Talk photodetector without clipping. The Hear circuit was biased such that the Hear ILD output power swung from threshold to 20 mW when the ILD was modulated by an audio signal. The electrical microphone signal of the EIU telephone is summed with the received Talk signal and a portion was sent to the electrical

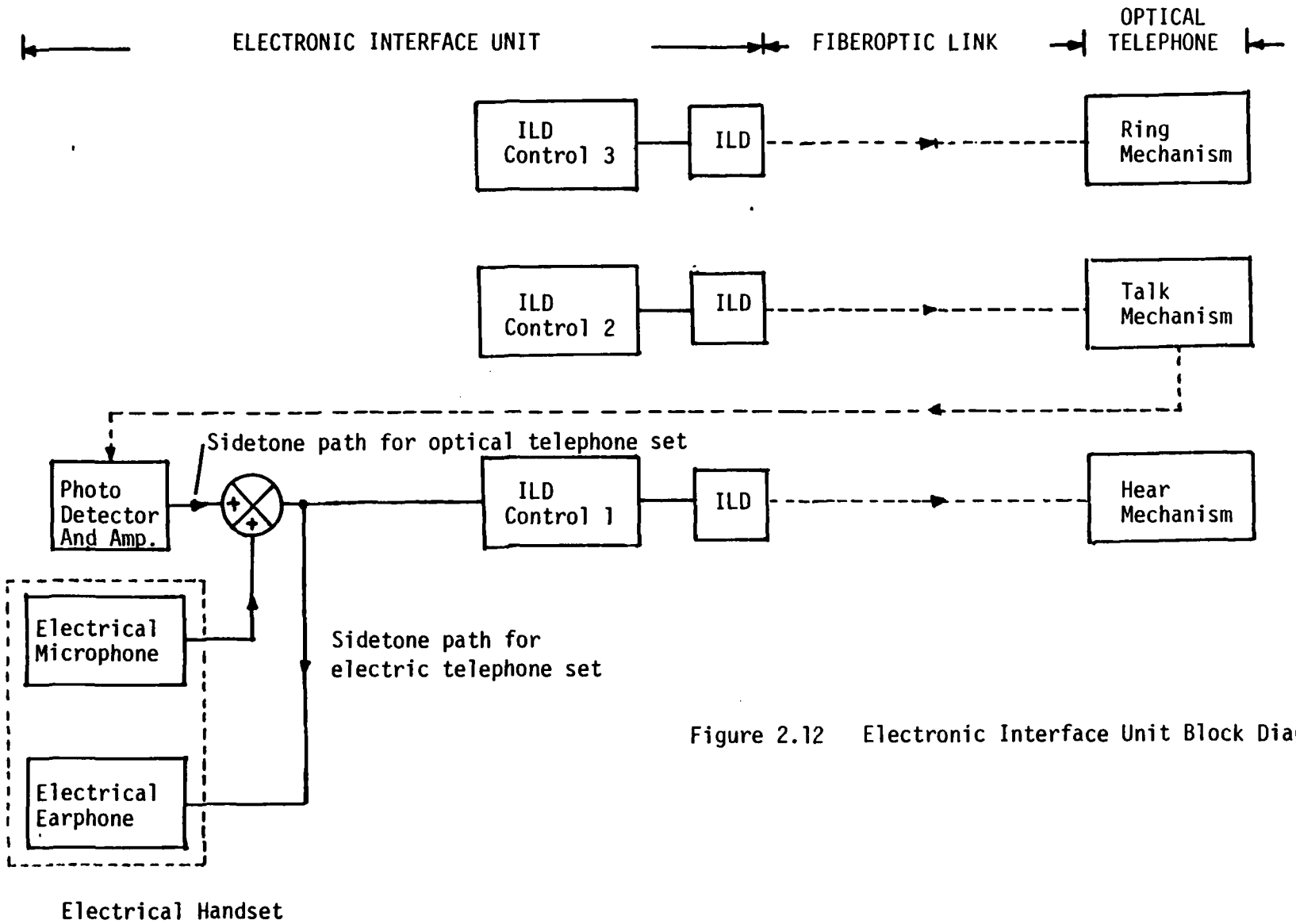

Figure 2.12 Electronic Interface Unit Block Diagram

earpiece.

The ILD control circuitry block diagram is shown in Figure 2.13. The ILD audio input signal was applied to a summing amplifier which controlled a current source. The output of the amplifier directed current to or away from the ILD as demanded by the audio input signal. A current source limited the maximum allowable ILD current. The ILD's integral feedback photodiode monitored the output power and applied a subtractive voltage to the summing amplifier. The output from the feedback amplifier sensed any optical power overload and a temperature sensor detected any temperature overload. These signals were sent to the overload current source which incorporated a sensor to monitor the ILD current for any over current conditions. The overload current source shuts down the ILD by shunting current away from the ILD and directing it to the limiting current sink. A parts list and schematic appears in Appendix D. The EIU was aligned by adjusting the bias on the ILD's such that the modulated light output would clip symmetrically when driven by a sinusoidal current. A graph of ILD output power versus drive current in Figure 2.14 shows that the slope of the output power above threshold is slightly curved which increases the effective gain of the current to light transfer at higher optical powers. As a result, the bias point was aligned for 14 mW output rather than 10 mW as would be expected for a device with 20 mW power output and low spontaneous emission.

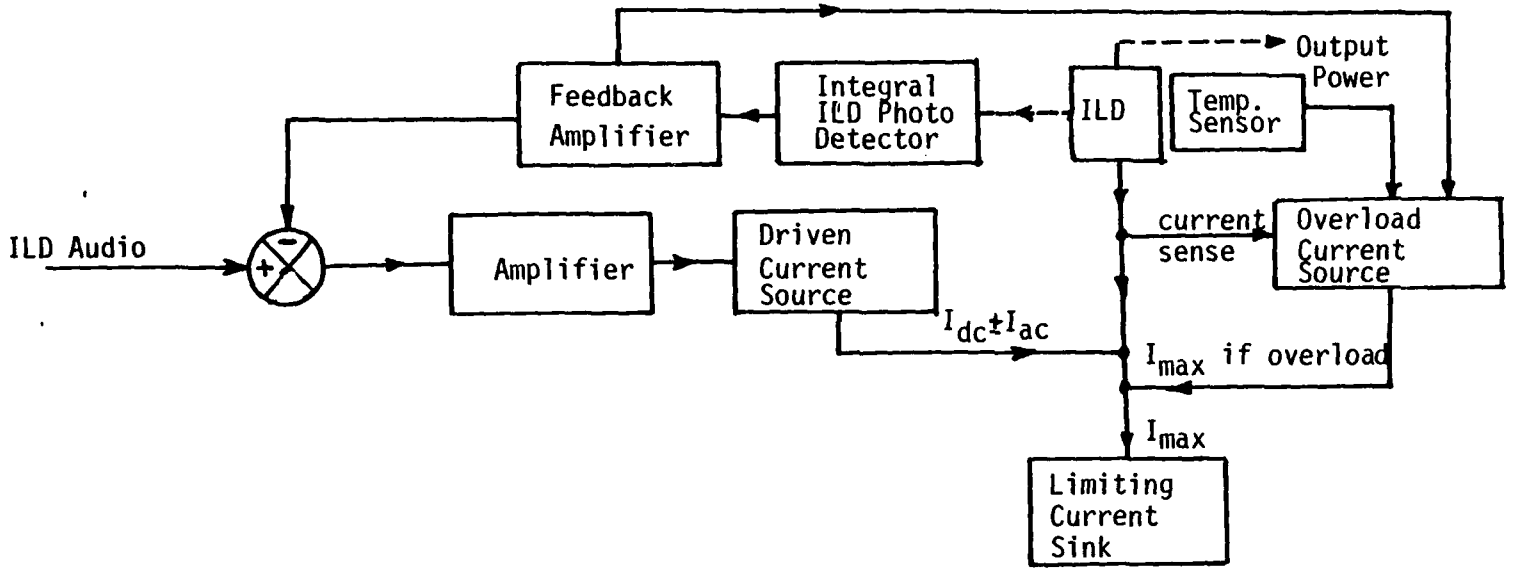

Figure 2.13 Injection Laser Diode (ILD) Control Block Diagram

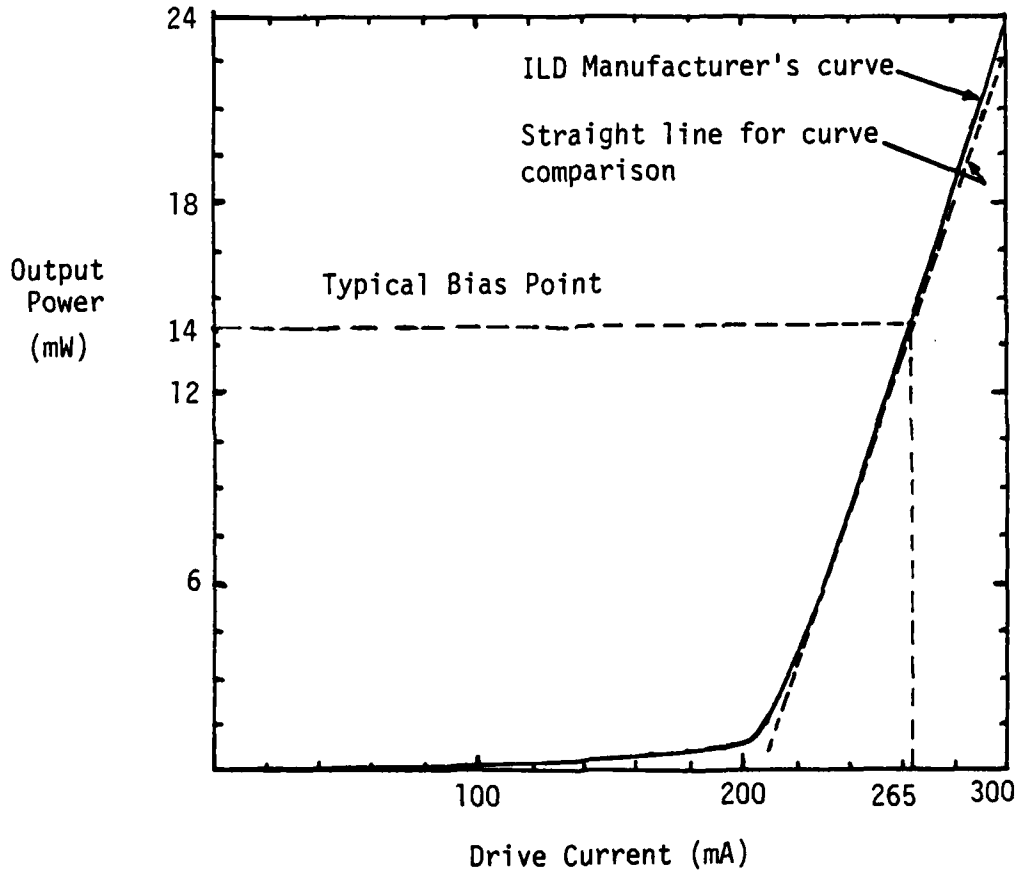

Figure 2.14 ILD manufacturer's supplied data on output power versus drive current for Optical Information Systems laser diode Model No. OSP-562

SECTION III

EXPERIMENTAL RESULTS

3.0 EXPERIMENTAL RESULTS

A breadboard was constructed to prove the feasibility of the all-optical telephone. In this section we describe the construction of the key subsystem, and experimental results, including the Talk, Hear and Ring mechanisms. The experimental results were obtained by directly interfacing the mechanisms to the Electronic Interface Unit (EIU); the fiber optic link was included only in system testing.

3.1 TALK MECHANISM

The Harris Talk mechanism is shown in Figure 3.1. The diaphragm was made of 0.5 mil mylar held under tension by a pair of aluminum rings. A rubber "O" ring was used as the contact surface between the mylar and one aluminum ring to maintain tension in the mylar. The structure was then clamped together by screws on the side of the aluminum rings. Two fiber access holes were provided in the top ring. One 50 micrometer core fiber (with cleaved end) was inserted through one of the holes and epoxied to the diaphragm about a millimeter above the surface of the diaphragm. Another 50 micrometer core fiber was inserted and epoxied into a small diameter, 1 inch long stainless steel tube. The tube holds the sensing fiber rigid preventing unwanted modulation of the fiber due to air currents. The tube assembly was then mounted on a XYZ translation stage, inserted into the remaining hole in the aluminum rings and the position was aligned for optical coupling. As shown in the Talk experimental setup of

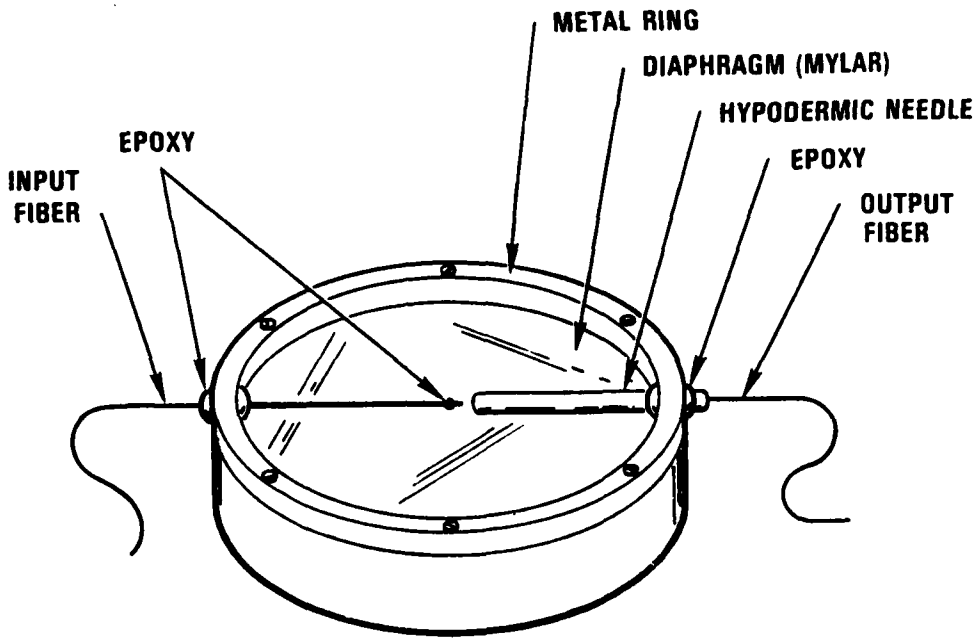

Figure 3.1 Harris Talk mechanism

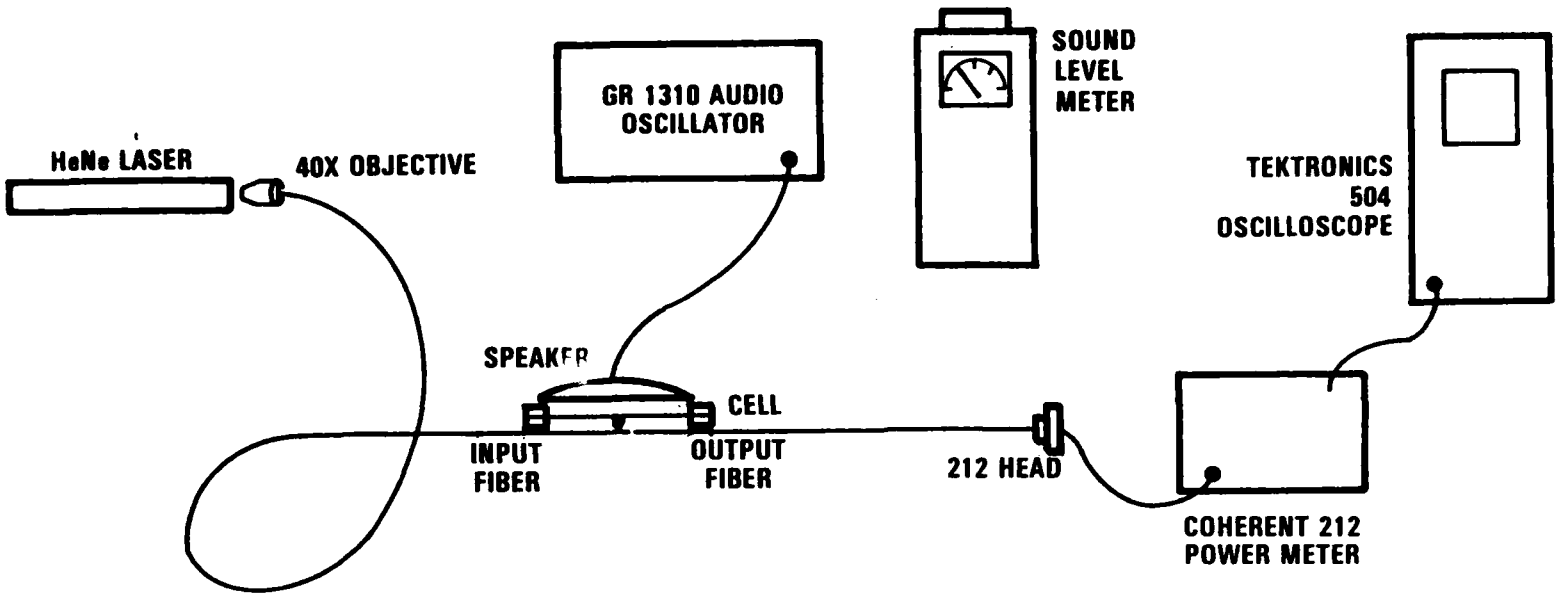

Figure 3.2 Talk experimental breadboard for frequency response measurement.

Figure 3.2, coupling was monitored by focussing a 1 mW HeNe laser into the modulating fiber and detecting the sensing fiber output on a Coherent 212 power meter. Upon optimization, the two sensing fiber ends were fusion spliced to 100 micrometer core fibers.

The response of a standard telephone earpiece, driven by a swept tracking oscillator, was recorded on a Hewlett Packard audio spectrum analyzer using a sound pressure level meter with a 6cc coupling volume. As shown in Figure 3.3, the response is flat within 2 dB from 400 to 3300 Hz and is 3 dB lower at 300 Hz. The earpiece was then used to drive the optical microphone at low signal levels. A coupling volume of 6cc ensured that the earpiece driving response would remain unchanged. The response of the Talk mechanism driven by the electrical earpiece, is shown is Figure 3.4. Figure 3.5 shows low frequency improvement of 2 dB when a 7.5 cu in. volume was coupled below the mechanism. Optimum response, as shown in Figure 3.6, was produced when a mouthpiece filter of a standard telephone mouthpiece was added. The fundamental resonance of the diaphragm generated a 15 dB peak at 1200 Hz. Average response extended from 300 Hz to 2 KHz with a small 5dB peak at 300 Hz due to the low frequency resonance added by the 7.5 cu inch volume. The fundamental resonance can be attenuated by making the diaphragm lossier. This can be accomplished by constructing the diaphragm with other materials or a composite material such as mylar with a film of rubber for damping. Other materials were tried, such as Cronar, which had

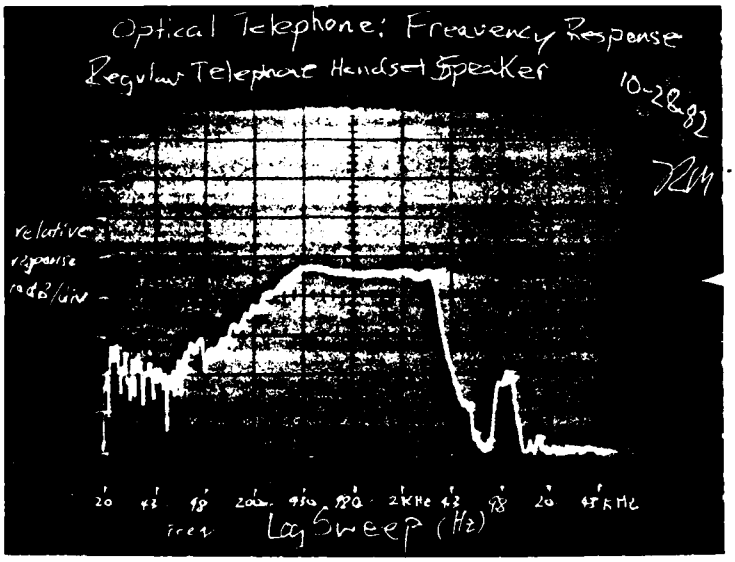

Figure 3.3 Frequency response of standard electrical earpiece in a 6cc volume as used in experiments to drive Talk mechanism.

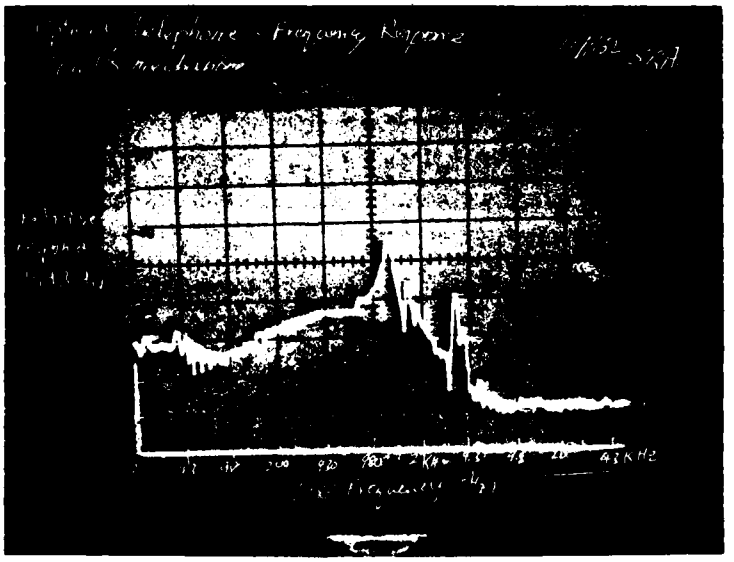

Figure 3.4 Frequency response of Talk mechanism driven by electrical earpiece.

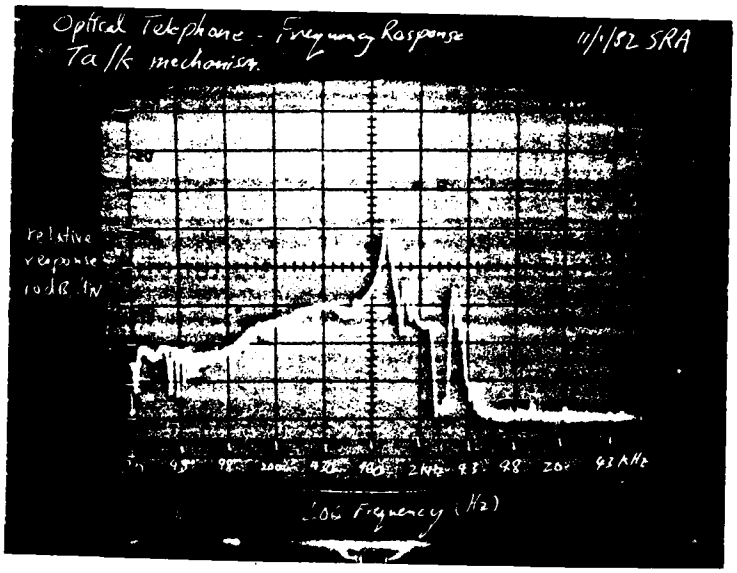

Figure 3.5 Frequency response of Talk mechanism with a 7.5 cu in. volume coupled below.

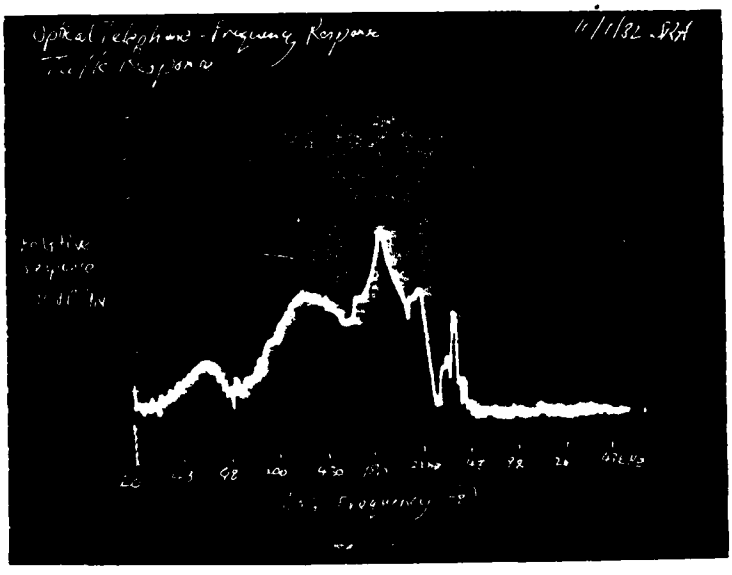

Figure 3.6 Frequency response of Harris Talk function with a standard handset mouthpiece filter and a 7.5 cu in. volume coupled below.

much lower sensitivity and Saran Wrap which had a temperature dependent performance and poor dimensional stability.

Low level distortion measurements of the microphone were taken at 500 Hz, 1000 Hz and 2000 Hz. Figures 3.7 through 3.9 compare the distortion produced by the Talk mechanism to the input residual distortion of earpiece speaker (predominant) and the SPL meter and GR oscillator (secondary). Distortion measurements are summarized in Table 3.1. Total harmonic distortion measured is the square root of the sum of the squares of the harmonic amplitudes.

TABLE 3.1

TOTAL HARMONIC DISTORTION

PRODUCED BY TALK MECHANISM

Frequency (Hz)	Input Residual Distortion (%)	Talk Output Distortion (%)	Actual Distortion (%)
500	0.013	0.06	0.047
1000	0.013	0.3	0.29
2000	0.0025	0.10	0.10

The data shows that the output has very low distortion if driven at levels below clipping, which is the average voice level that most people would talk with into the mouthpiece.

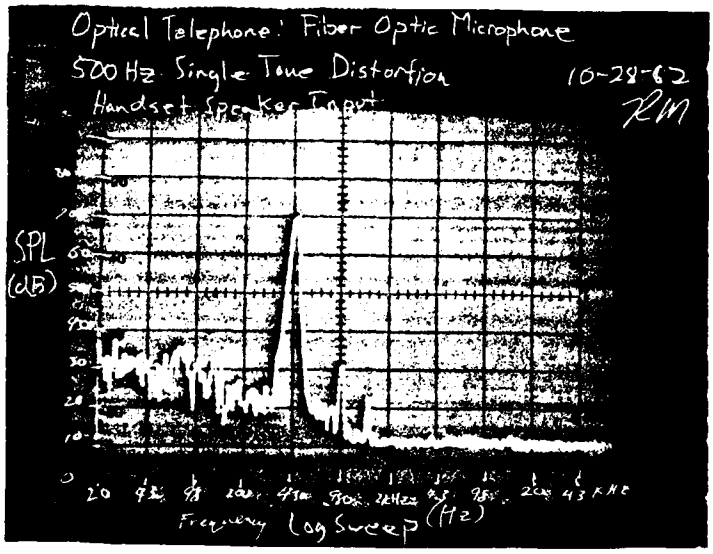

Distortion of Electrical Earpiece Speaker Driven at 500 Hz.

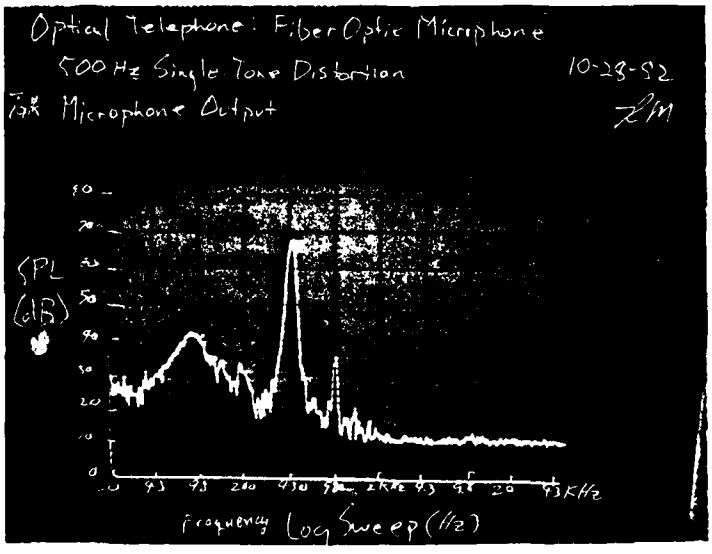

Combined Distortion of Talk Mechanism and Earpiece Speaker with Speaker Driven at 500 Hz.

Figure 3.7 Single tone distortion measurements at 500 Hz

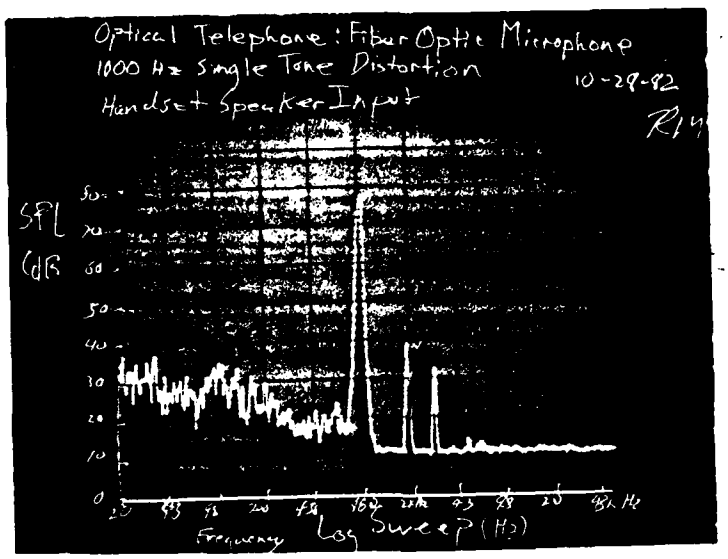

Distortion of Electrical Earpiece Speaker Driven at 1000 Hz.

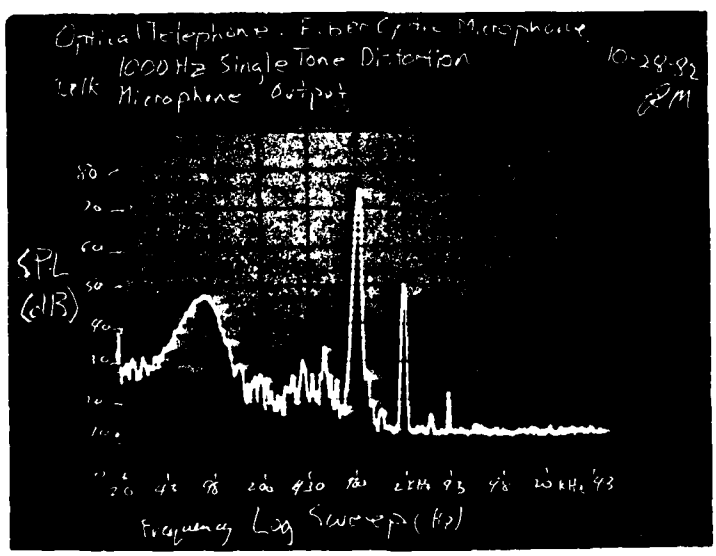

Combined Distortion of Talk Mechanism and Earpiece Speaker with Speaker Driven at 1000 Hz.

Figure 3.8 Single tone distortion of measurements at 1000 Hz

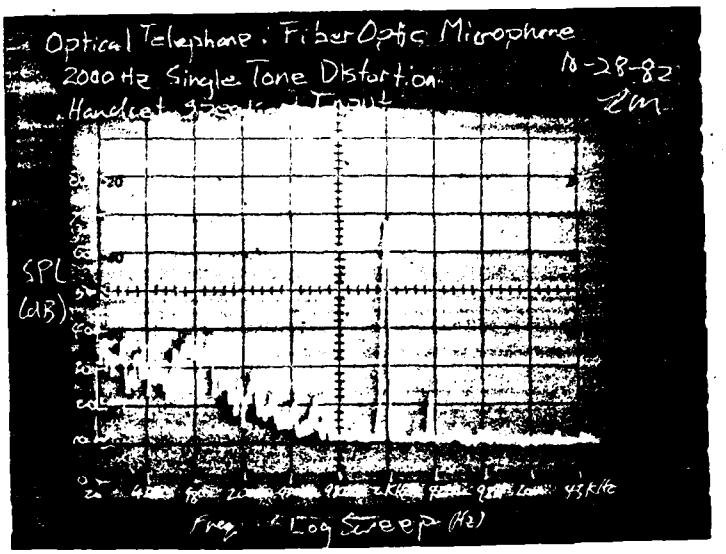

Distortion of Electrical Earpiece Speaker Driven at 2000 Hz

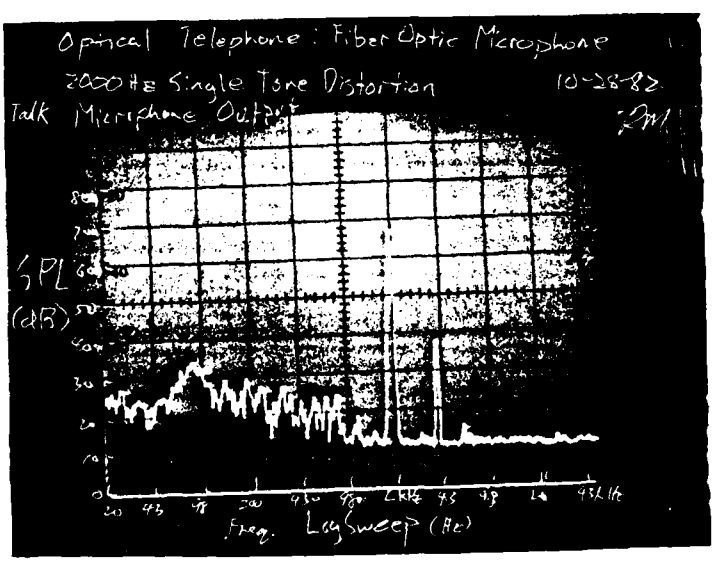

Combined Distortion of Talk Mechanism and Earpiece Speaker with Speaker Driven at 2000 Hz

Figure 3.9 Single tone distortion measurements at 2000 Hz

3.2 HEAR MECHANISM

The Harris Hear mechanism was fabricated by machining an aluminum mandril with a circular cross-section and the prescribed exponential taper discussed in Section 2.3. The aluminum mandril was chemically cleaned and 0.125 inch thick copper was electroformed over the surface of the aluminum. The aluminum was then etched away to form the horn cavity. Due to the very slow etching rate experienced, the horn was cut into several pieces near the source end. The finished horn pieces had slightly flared ends internally because of the nature of the etching process. When the horn was assembled, therefore, there were small discontinuities in the exponential curve at the joints which may affect the ideal horn performance.

Cotton fiber was carbonized in a ceramic crucible in a 500°C oven in an atmosphere of flowing nitrogen for 5 minutes. The cotton was placed in absorption cells with volumes ranging from 0.5 to 2.5 x 10^{-3} cc. The cleaved end of a 100 micrometer core optical fiber was inserted into a small diameter stainless steel tube and placed into the fiber access hole in the absorption chamber. Position of the fiber/tube assembly was optimized with the horn in place and epoxied to an inertance equalizer tube and cell. The equalizer tube increases the horn response at high frequencies and thereby flattens the band response. Optimization was necessary to obtain the best light utilization factor. Because of the high cell impedance, epoxy was used to prevent

minute leaks in the assembly which could produce shunt acoustic capacitance across the source and diminish the output.

The cell/equalizer tube combination which gave the best response was a 5×10^{-4} cc cell coupled to a 0.035cm diameter, 1.6cm long input equalizer tube. As seen in Figure 3.10, the peak response of the horn was 78 to 79 dB at 500 and 700 Hz while the average response is 75 dB from 300 to 1500 Hz for an input optical signal level of 4.77 mW rms. Design calculations indicate that a drive level of 2.8 mW would give an average output of 83 dB. This suggests that an improvement of 8 dB may be possible. The notch response at 7 KHz is probably an anomaly of the exponential horn fabrication. Such a response could result from a volume in series with a tube (series capacitance and inductance) in series with the sound path. The small enclosed volume coupled between the first and second horn segments due to flared ends of the segments may form such a series network. The notch has sufficient depth and amplitude to degrade the response near the 3300 Hz cutoff by rapid roll off. With further effort and experience, we are confident that the experimental response can be improved to nearly the same output as the theoretical calculations predict.

Single tone low and high level harmonic distortion was measured for the EIU and horn combination at several frequencies. Results are shown in Figures 3.11 to 3.15. Total harmonic distortion, shown in Table 3.2, includes distortion products generated by the oscillator and the SPL meter nonlinearity.

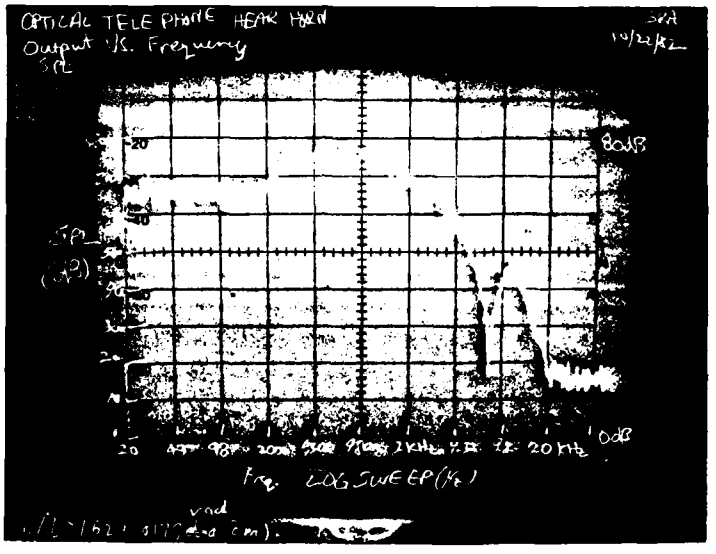

Figure 3.10 Frequency response of Hear function with 1.6 cm long and 0.035 cm diameter equalizer tube and 5 X 10^{-4} cc cell volume

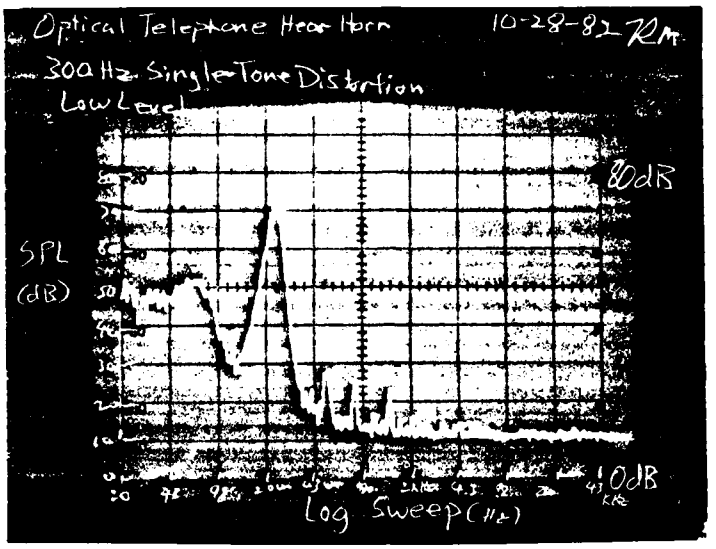

Low Level Hear Horn Distortion at 300 Hz

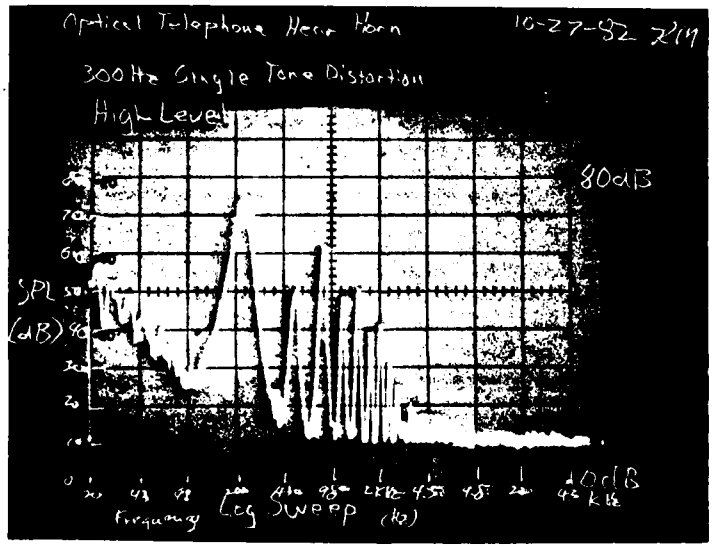

High Level Hear Horn Distortion at 300 Hz

Figure 3.11 Low and high level Hear horn single tone distortion measurements at 300 Hz

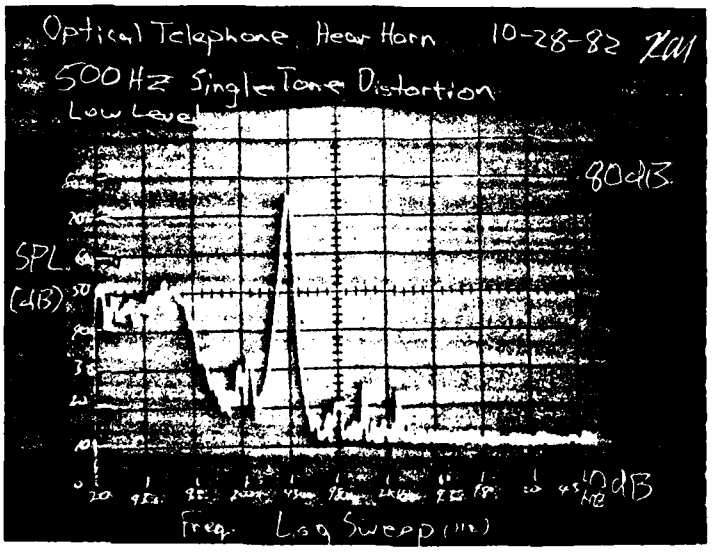

Low Level Hear Horn Distortion at 500 Hz

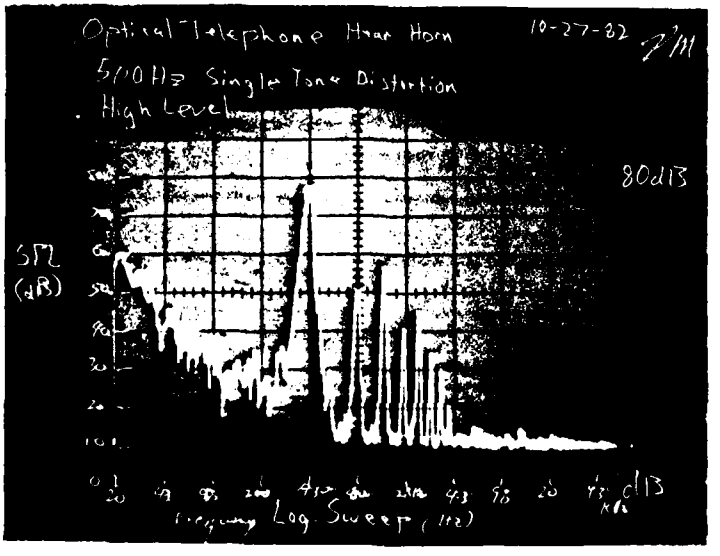

High Level Hear Horn Distortion at 500 Hz

Figure 3.12 Low and high level Hear horn single tone distortion measurements at 500 Hz.

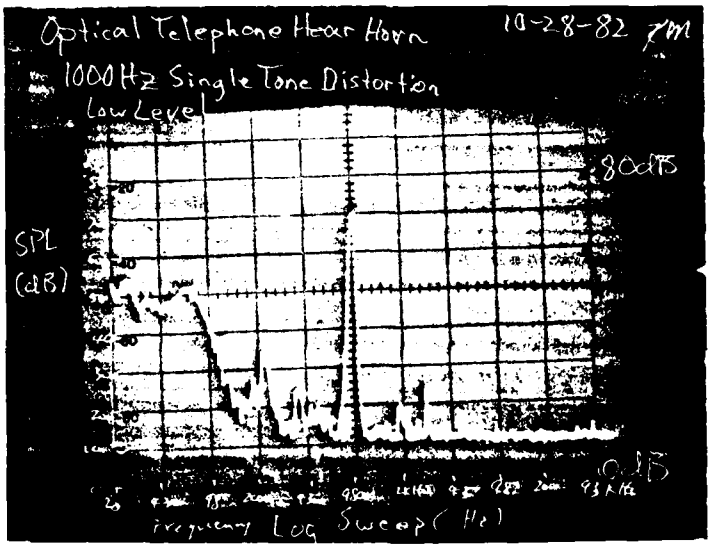

Low Level Hear Horn Distortion at 1000 Hz

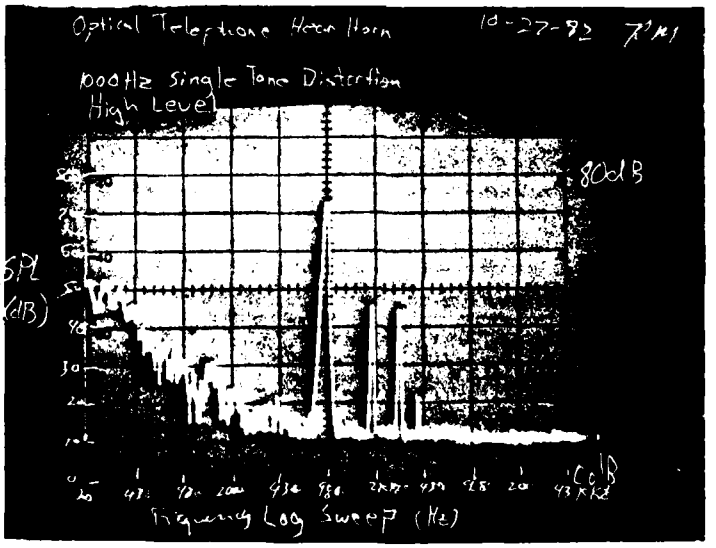

High Level Hear Horn Distortion at 1000 Hz

Figure 3.13 Low and high level Hear horn single tone distortion measurements at 1000 Hz

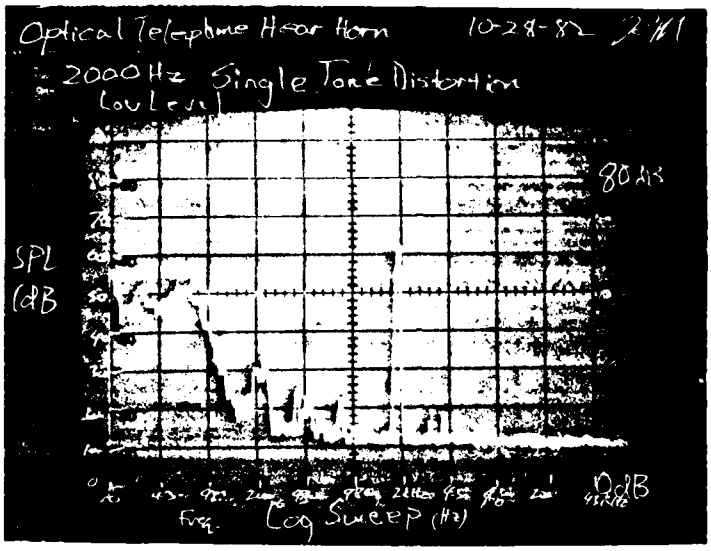

Low Level Hear Horn Distortion at 2000 Hz

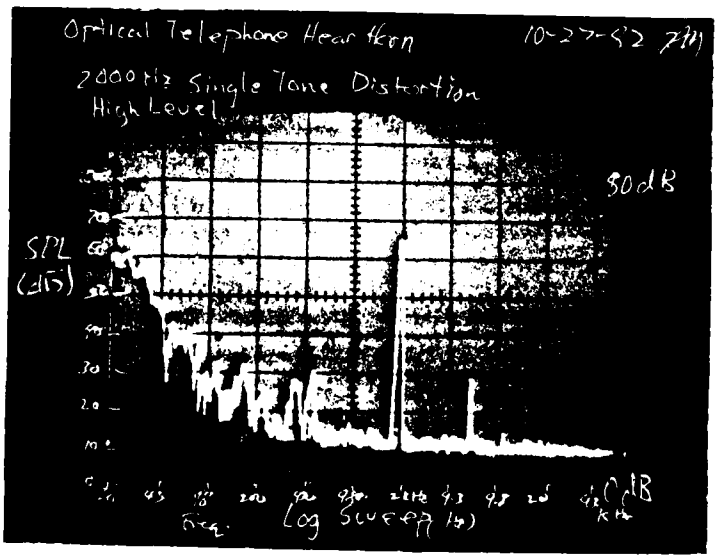

High Level Hear Horn Distortion at 2000 Hz

Figure 3.14 Low and high level Hear horn single tone distortion measurements at 2000 Hz

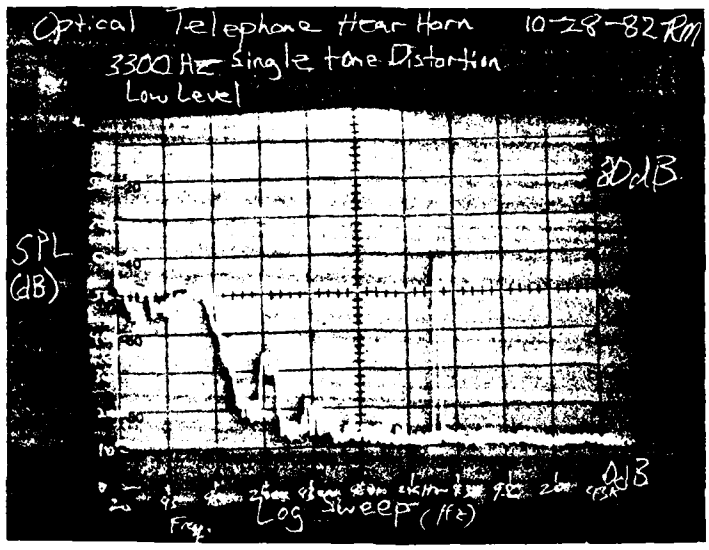

Low Level Hear Horn Distortion at 3300 Hz

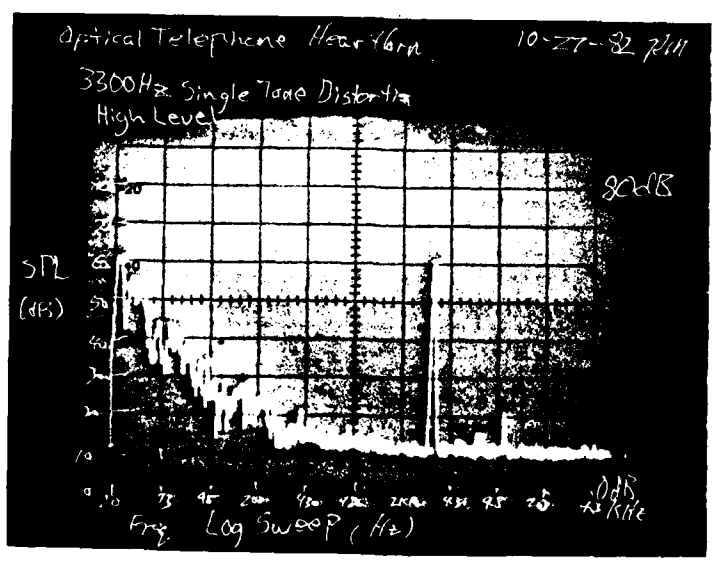

High Level Hear Horn Distortion at 3300 Hz

Figure 3.15 Low and high level Hear horn single tone distortion measurements at 3300 Hz

TABLE 3.2

TOTAL HARMONIC DISTORTION

PRODUCED BY HEAR MECHANISM

Frequency (Hz)	High Level Distortion (%)	Low Level Distortion (%)
300	5.04	0.007
500	1.00	0.001
1000	0.3	0.003
2000	0.02	0.006
3300	0.01	0.003

A computer generated horn response using a cell volume of 0.5×10^{-3} cc, and equalizer of 0.035cm diameter and 1.6cm long, as used in the experiment, is shown in Figure 3.16. The graph shows that the output with the breadboard components would be 2 dB lower than the ideal response at low frequencies and has a 3 dB bandwidth of 300 to 1700 Hz. While the predicted response with the breadboard components is poorer than the predicted response with the optimum components as in the Harris design, the experimental frequency response, was increased by 2 dB at 3000 Hz over the response produced with the optimum components.

Comparative efficiencies between the opto-acoustic horn output and that of a standard military phone were made. MIL

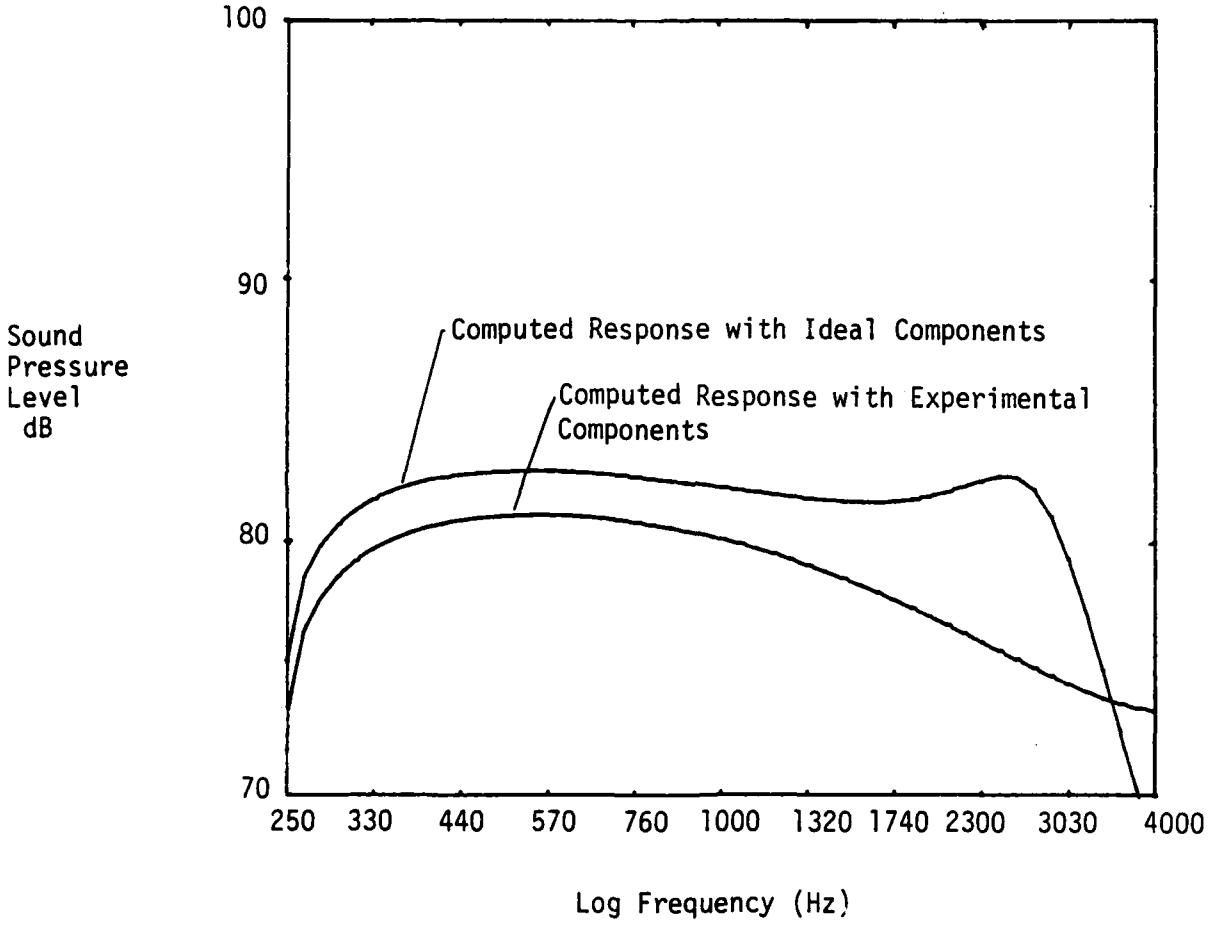

Figure 3.16 Computed response with experimental components compared with computed response with ideal design components for the Hear horn.

Standard 188 indicates that a military earpiece coupled to a 6cc ear volume with an electrical input level of -32 dEm produces an output level of 80 dB. The optical telephone produces 75 dB acoustic power output with 6 8 dBm input optical power. The total difference in efficiency of 43.8 dB means that the optical Hear is 24,000 times less efficient than the standard electrical/acoustic conversion. Another comparison can be made to a photodiode transformer coupled speaker approach by Kleinman-Nelson[6]. This generated an 80 dB output from -16.7 dBm optical input (17 microwatts for 81 dB) which is 31.6 times less efficient than the military phone.

The absolute efficiency (to a good approximation) may be calculated by finding the intensity of sound at 75 dB as:

$$(3.1) \quad I = P(75\ dB)^2/(\delta c)$$

$$= 3.036\ nW/cm^2$$

where

$$\delta = 1.225 \times 10^{-3}\ gm/cc$$

$$c = 3.403 \times 10^{4}\ cm/sec$$

$$P(75\ dB) = 0.0002 \times 10^{75/20}$$

$$= 1.125\ dynes/cm^2$$

Multiplying the intensity by πr_2^2, ($r_2 = 0.77$ cm), results in a source strength of 5.6 nW or -52.5 dBm, indicating an efficiency of 1.17×10^{-6} with an input of 6.8 dBm.

The Hear and Talk mechanisms were tested with the EIU/link for subjective listening response. The Hear horn had a low, but

adequate output level when the listener placed his or her ear close to the output of the horn. The sound quality of the voice output was good but slightly nasal, possibly due to the resonances in the horn. The oscillating response of the horn did not seem to degrade vocal transmission. The Talk microphone with EIU was highly sensitive. The sound quality had a slight bass character due to the low frequency peaks at 300 Hz and 1200 Hz. Despite the peaks, both male and female voices were recognizable and intelligible.

3.3 RING MECHANISM

A diagram of the assembled Ring mechanism is shown in Figure 3.17. A bimetal latch triggered ringer was designed, fabricated and tested for sound output level at 1 meter distance from the ringer. Average sound output was 80 dB. This was greater than the 75 dB output level for a standard dial telephone set although the bells employed were the same. This difference was due to the lack of an enclosure covering the bells as there is in the standard phone set. Optical power required for activating the bimetal latch was 15 mW with a response time of 4 seconds. The mechanical energy storage required 4.5 turns of the spring windup to allow the mechanism to ring down in 150 seconds. The sustaining force required to latch the mechanism was measured to be less than 0.1 gm, below the resolution of the spring testing gauge used.

The present Ring mechanism requires mechanical energy to be stored by actions of the user of the phone such as depressing the hookswitch when the telephone is raised or lowered on its cradle. A more desirable concept for the Ring would be the photo-acoustically generated ring as described in Section 2.4 of this report.

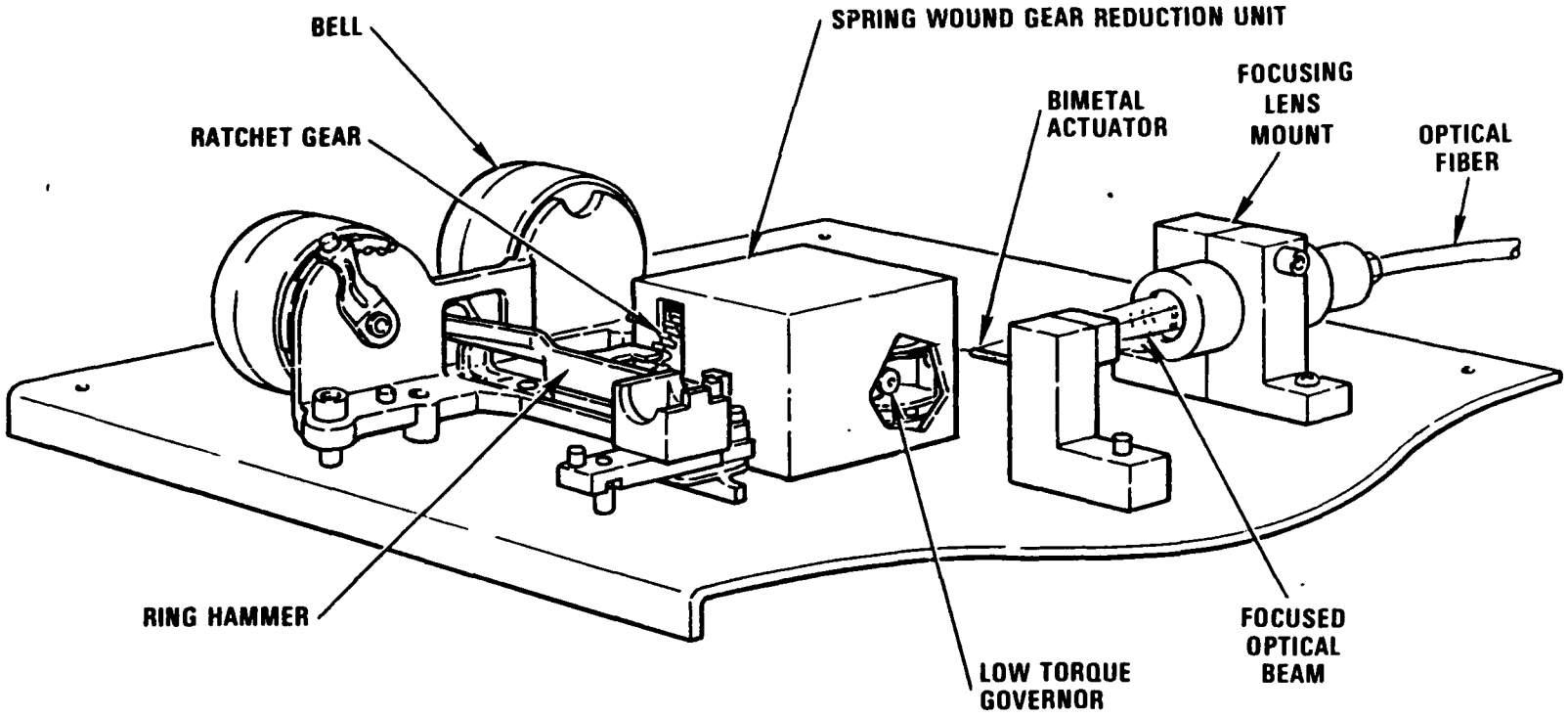

Figure 3.17 Diagram of Harris Ring Mechanism

3.4 SYSTEM TESTING

System layout and power budget is shown in Figure 3.18. photographs of the individual components in Figures 3.19 to 3.21. The system was integrated with the 100 foot optical link and tested. Losses averaged 1.6 dB per connector and 6 dB at the Talk mechanism due to 50 vs. 100 micrometer fiber mismatch. The fusion splices introduced negligible loss (approximately 0.1 dB). The available power was 15.2 mW at the Ringer, 0.95 mW at the input to the photodiode and 3.2 mW rms into the absorption cell.

The system is operated by turning the EIU on, connecting the 100 meter link, if necessary, plugging in the EIU phone set, raising the phone receiver and depressing the Ring ILD button. When the receiving user answers, the Ring ILD is shut off by depressing the EIU phone set hookswitch once. Next, the Talk and Hear ILD's should be turned on by depressing the ILD buttons. Conversation is terminated by placing the phone receiver on its hookswitch.

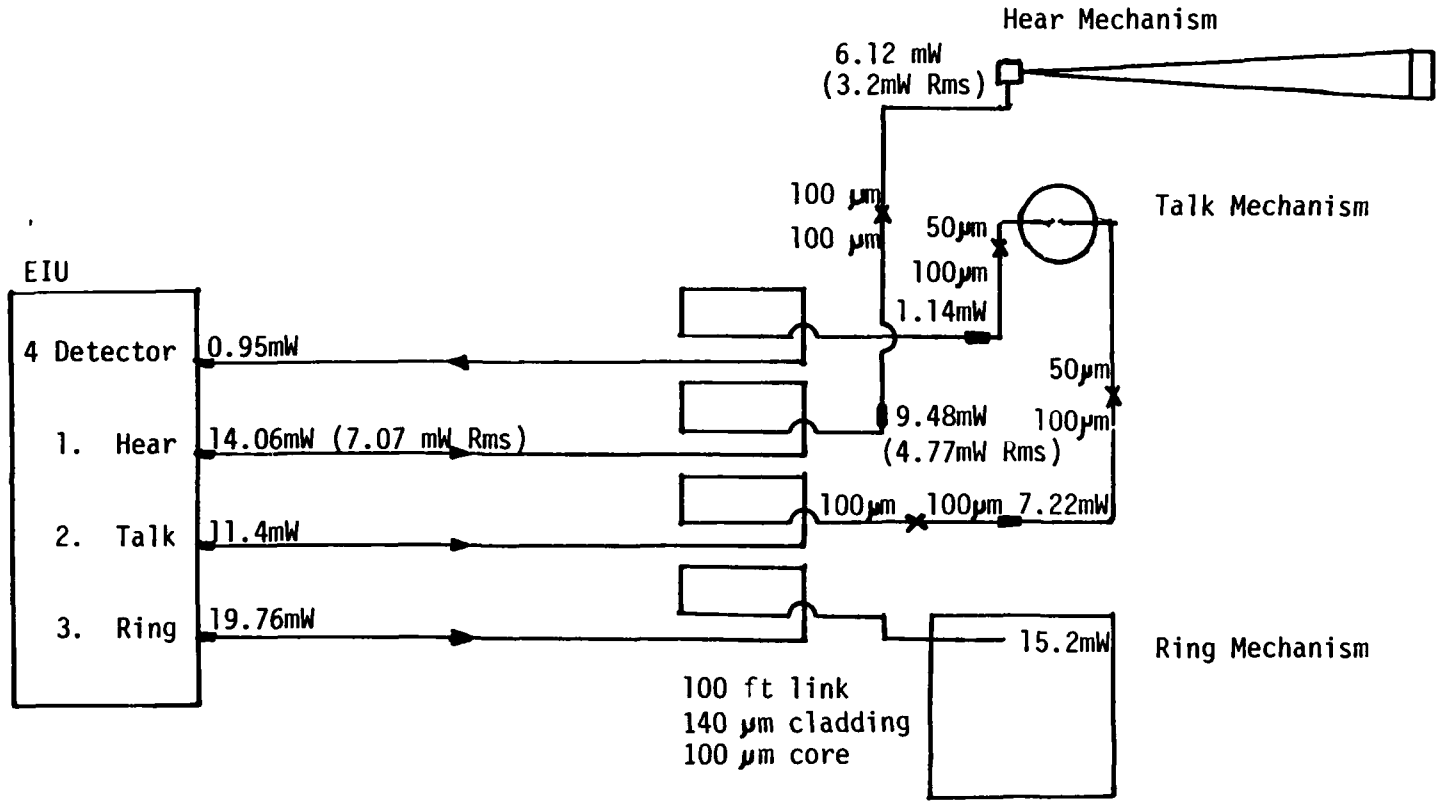

Figure 3.18 System layout with measured power budget.
X's mark location of low loss fusion splices
▬'s mark connectors

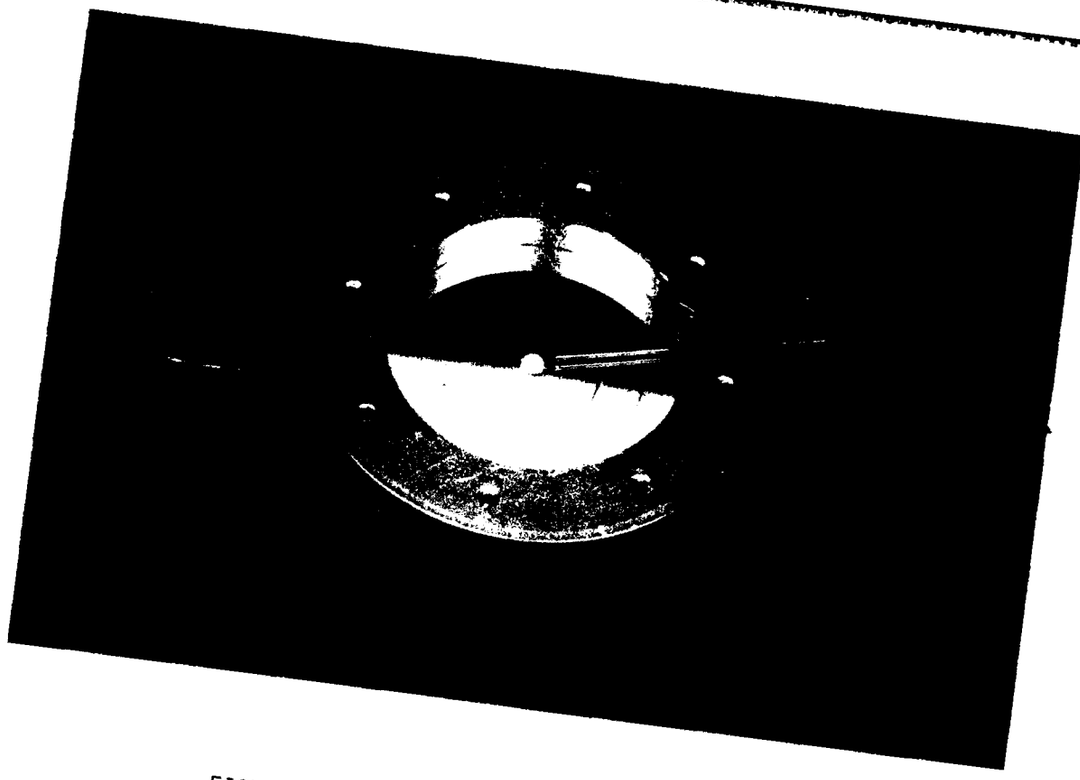

FIGURE 3.19 Photograph of Talk Mechanism

FIGURE 3.20 Photograph of Hear Mechanism

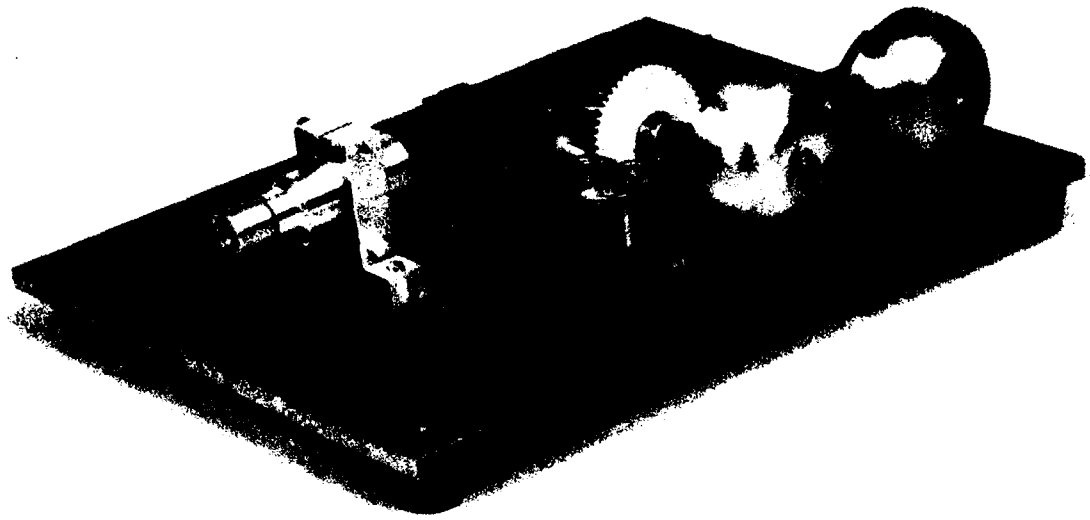

FIGURE 3.21 Photograph of Ring Mechanism

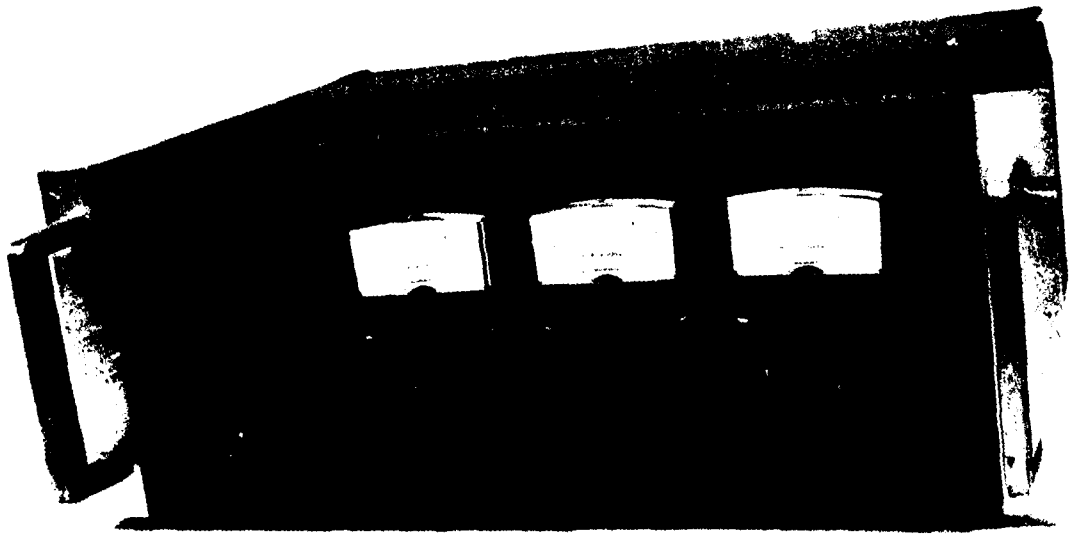

FIGURE 3.22 Photograph of Electronic Interface Unit

SECTION IV

SUMMARY, CONCLUSION AND RECOMMENDATIONS FOR FURTHER DEVELOPMENT

4.0 SUMMARY, CONCLUSIONS AND RECOMMENDATIONS FOR FUTURE DEVELOPMENT

The results of this study verify the technical feasibility of the opto-acoustic telephone concept. After an intensive literature survey of past research and brainstorming sessions for new ideas, those design and implementation techniques were selected, that provided the lowest risk for this program. Although system performance was slightly below the theoretically predicted level, significant improvement is possible in all three functions with some additional effort. The associated technology required for the desired capabilities and performance already exist, including low loss optical fibers and high power laser diodes.

Clearly, much work remains to be done in optimizing the performance parameters and manufacturability of the Talk, Hear, and Ring functions, and in implementing other functions such as hookswitch, optically generated sidetone at the receiver and dialing. Development and refinement for possible military applications is required in the areas of:

1) Device optimization
2) Link improvement
3) Switchboard functions and interfacing.

Device optimization - For device optimization, the individual opto-acoustic transducers should be optimized with increased emphasis on performance, manufacturability and low

cost. Other requirements, particularly for military applications, such as security, ruggedness and reliability must also be optimized. Improvements in the device operating features can be implemented such as:

A) Refine Hear and Talk transducers to increase their frequency response and output levels.

B) Improve Ring transducers by the implementation of the Harris Ring Horn design.

C) Reduce the physical volume of the optical telephone components and incorporate them within the size constraints of the standard telephone handset.

D) Implement dialing pulse generation by modulating light with a chopping wheel to send the required number of dial pulses or touch tone generation of the proper pairs of tones by vibrating reeds or grooves coupled by a suitable mechanical pickup.

E) Add passive side tone generation by using a low loss optical splitter directing light from Talk mechanism to the Hear mechanism.

Further improvements can reduce the number of link fibers required from 4 to 2. This can be accomplished using wavelength division multiplexing optical coupler technology developed by Harris on other fiber optic programs. Dual window fiber for 1.3 and 0.83 micrometer wavelengths and the corresponding high power laser diodes are commercially available. In this approach, one

wavelength could be used for the Talk and a different wavelength for the Hear. A dichroic splitter will direct the two wavelengths (traveling on a single fiber) to the Talk and Hear Functions when the hookswitch is raised and combine the two for increased power to the Ring mechanism when it is lowered. A Talk return fiber would be used to complete this 2 fiber link. An engineering conception drawing of a complete optical telephone is shown in Figure 4.1.

Switchboard functions and interfacing of the optical telephone is required for functional demonstration of the system. It should be possible to hook the interface to any node in the present military or Bell phone network. Some of the switchboard functions the interface unit should provide are off hook, on hook acknowledge, line busy monitoring, misdialing, receiver in permanent off hook position and touch tone or dial recognition. The wide bandwidth of the optical transmission line allows some of these supervisory signals, now operating in the voice band in some cases, to operate in the more desireable out of voice band frequencies. Implementation of the interfacing signal requirements will result in intelligent two way communication between the optical phone and existing telephone networks.

The optical telephone can form an integral part of a reliable communication system in a military environment. Although more work is required to fulfill the necessary performance requirements, Harris has demonstrated that the

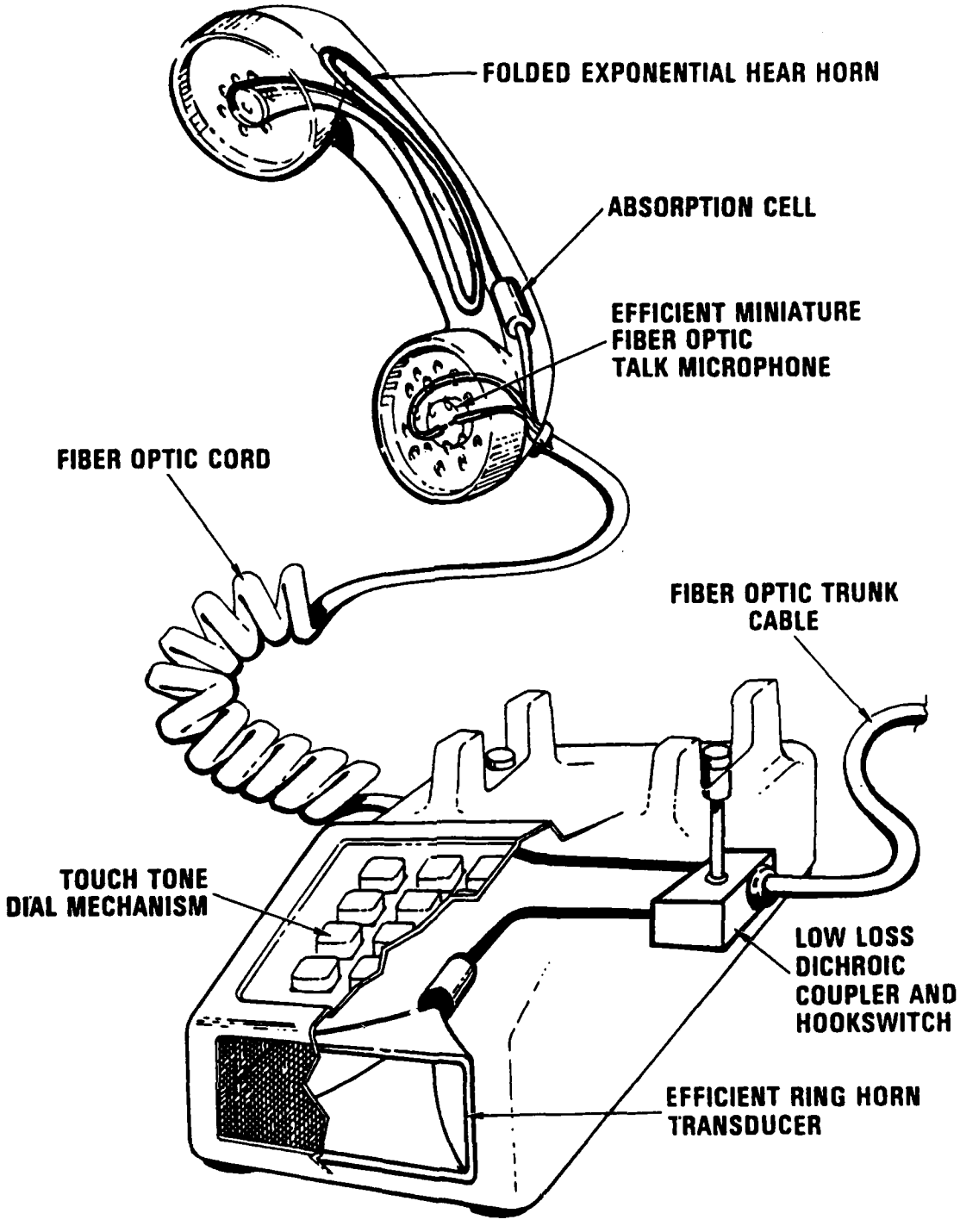

Figure 4.1 Engineering concept of the optical telephone of the future. Cutaway view shows all plastic-ceramic construction with no metal parts - feasible with present day technology.

concept is feasible and feels that the desired equipment is realizable.

References:

1. S. Edelman, U.S. Patent Pending

2. The Photophone - An Optical Telephone Receiver, D. Kleinman and D. Nelson, J. Acoust. Soc. Am., Vol. 59, No. 6, June 1976.

3. S. Edelman, Private Communications, Acoustic-optic Workshop, Ft. Monmouth, March 31, 1982.

4. Elements of Acoustical Engineering, H. F. Olson, D. Van Nostrand Co., NY, NY, 1940

5. Fundamentals of Acoustics, Kinsler and Frey., John Wiley and Sons, NY, NY, 1962

6. Nonlinear Analysis of a Photovoltaic Optical Telephone Receiver, D. Kleinman and D. Nelson, Bell System Technical Journal, Vol. 57, No. 5, May-June 1978

7. Photophone Performance, D. Nelson, K. Wecht, and D. Kleinman, J. Acoust. Soc. Am., Vol. 60, No. 1., July 1976

8. The Dynamical Theory of Sound, Horace Lamb, Dover Publication, NY, NY, 1960

9. Acoustic Measurements, L. L. Beranek, John Wiley and Sons, NY, NY., 1949

10. All Optical Telephone Development, B.G. Grossman, S.R. Adhav, L. M. Ralston R. K. Morse and N. Feldman, Fiber Optics and Communication Exposition, Sept. 1982

11. An All Optical Telephone set, N. Feldman, ICC-81, Denver, CO, June 1981.

AD-A164 919 OPTO-ACOUSTIC TELEPHONE STUDY(U) HARRIS CORP MELBOURNE FL GOVERNMENT COMMUNICATION SYSTEMS DIV S R ADHAV ET AL. 01 JAN 83 JA-1023 DAAB77-82-C-J011 2/2

UNCLASSIFIED F/G 20/6 NL

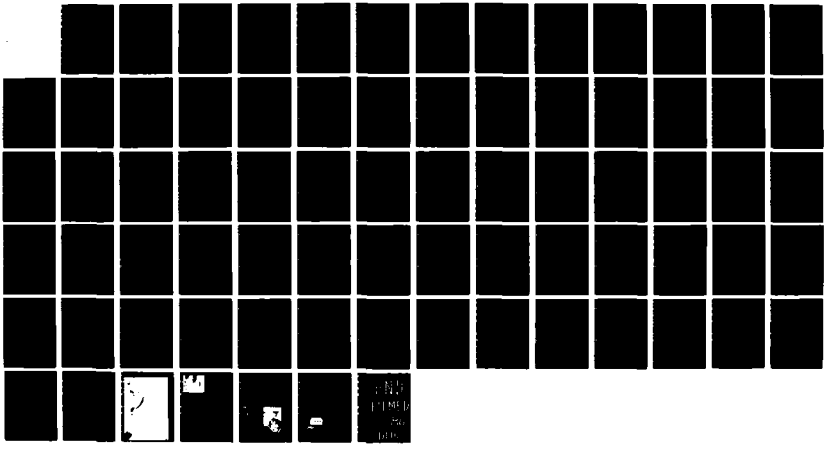

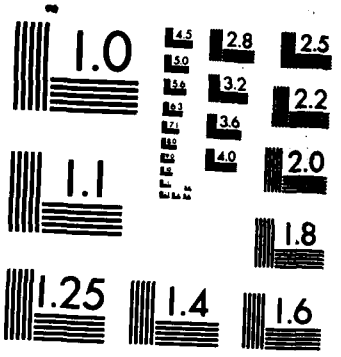

APPENDIX A

LITERATURE SURVEY

LITERATURE SURVEY

1. Nathan W. Feldman, "An All Optical Telephone Set," ICC-81, Denver, CO, June 1981.

2. D. A. Kleinman and D. F. Nelson, "The Photophone - An Optical Telephone Receiver", J. Acoust. Soc. Am., Vol. 59, No. 6, June 1976.

3. D. A. Kleinman and D. F. Nelson, "The Photophone - Physical Design", J. Acoust. Soc. Am., Vol. 59, No. 6, June 1976.

4. D. F. Nelson, K. W. Wecht, and D. A. Kleinman, "Photophone Performance", J. Acoust. Soc. Am., Vol. 60, No. 1, July 1976.

5. D. A. Kleinman and D. F. Nelson, "Nonlinear Analysis of a Photovoltaic Optical Telephone Receiver", Bell System Technology Journal, Vol. 57, No. 5, May-June 1978.

6. Dan Botez and G. J. Herskowitz, "Components for Optical Communications Systems: A Review", Proc IEEE Vol. 68, No. 6, June 1980.

7. J. C. Baker and D. N. Payne, "Expanded-beam Connector Design Study", App. Opt., Vol. 20, No. 16, August 15, 1981.

8. "Electro Acoustics", Reference Data for Radio Engineers, Chapter 35, Howard H. Sams and Co., Inc., 5th Ed., 1968.

9. G. T. Sincerbox and J. G. Gordon II, "Modulating Light by Attenuated Total Reflection", Laser Focus, November 1981.

10. D. H. McMahon, A. R. Nelson and W. B. Spillman, Jr., "Fiber-Optic Transducers", IEEE Spectrum, December 1981.

11. J. Free, "Piezoelectric Plastic - Changes Electricity into Motion", Popular Science, August 1981.

12. "Bell Labs Develops Telephone Powered by Lightwaves Alone", Electronics Magazine, November 23, 1978.

Appendix A continued,

13. M. R. Layton and J. A. Bucaro, "Optical Fiber Acoustic Sensor Utilizing Mode-Mode Interference,", App. Opt., Vol. 18, No. 5, March 1, 1979.

14. J. A. Bucaro and E. F. Carome, "Single Fiber Interferometric Acoustic Sensor", App. Opt., Vol. 17, No. 3, February 1, 1978.

15. J. A. Bucaro and H. D. Dardy and E. F. Carome, "Optical Fiber Acoustic Sensor", App. Opt., Vol. 16, No. 7, July 1977.

16. N. S. Nogar, M. Fisher, and W. Jalenak, "Photoacoustic Detection," Laser Focus, February 1979.

17. K. Wilner and N. P. Murarka, "Design Considerations and Test Results of an Evanescent Switch-Attenuator", App. Opt., Vol. 20, No. 20, October 15, 1981.

18. J. R. Hull, "Proposed Frustrated-Total-Reflection Acoustic Sensing Method," App. Opt., Vol. 20, No. 20, October 15, 1981.

19. J. A. Bucaro, A. D. Dardy and E. F. Carome, "Fiber-Optic Hydrophone", J. Acoust. Soc. AM, Vol. 72, No. 5, November 1977.

20. R. Santos and L. C. M. Miranda, "Photoacoustic Effect in Solids: Influence of Heat Loss", App. Opt., Vol. 70, No. 5, May 1980.

21. G. C. Wetsel Jr., "Photoacoustic Effect in Piezoelectric Ceramics", J. Opt. Soc. Amer., Vol. 70, No. 5, May 1980.

22. M. K. Barnoski and S. M. Jensen, "Fiber Waveguides - A Novel Technique for Investigating Attenuation Characteristics," App. Opt., Vol. 15, No. 9, September 1976.

23. F. T. Andrews and R. W. Hatch, "National Telephone Network Planning in the American Telephone and Telegraph Company", IEEE Trans. Commun. Tech., LDM-19, 302-314, 1971.

24. L. B. Kreuzer, "Ultralow Gas Concentration Infrared Absorption Spectroscopy", J. Appl. Phys., 42, 2934-2943, 1971.

Appendix A continued,

25. E. E. Mott and R. C. Miner, "The Ring Armature Telephone Receiver," Bell System Technology Journal, 30, HO-140, 1951.

26. H. Frederick and H. Dodge, "The Stethophone, an Electrical Stethoscope", Bell Sys. Tech. J., 3, 531-549, 1924.

27. W. P. Mason, "Wave Propagation in Fluids and Normal Solids", Physical Acoustics, Vol. 1, Part A, Academic, New York, 1964, P. 46., Eq. 201.

28. S. E. Miller, E. A. J. Marcatilli, and T. Li, "Research Toward Optical Fiber Transmission Systems", Proc. IEEE 61, 1703-1751, 1973.

29. A. H. Benade, "On the Propagation of Sound Waves in a Cylindrical Conduit", J. Acoust. Soc. Am. 44, 616-623, 1968.

30. W. C. Jones, "Instruments for the New Telephone Set", Bell Sys. Tech. J. 17, 338-357, 1938, See Figure 8, p. 352 for early type receiver.

31. G. M. Sessler and J. E. West, "Foil-Electric Microphones", J. Acoust. Soc. Am. 40, 1433-1440, 1966.

32. E. C. Wente, "The Thermophone," Phys. Rev. 17, 333-345, 1922.

33. A. Rosencwaig, "Photoacoustic Spectroscopy of Biological Materials", Science 181, 657-658, 1973.

34. M. E. Delany, "The Optic-Acoustic Effect in Gases," Sci. Prog. 47, 459-467, 1959.

35. "Bell's 1880 Photophone Invention Commemorated", Bell Laboratories Rec. 58: 132 Ap. 1980.

36. J. Gosch, "Light-Powered Phone Operates Without an Internal Light Source", Electronics, May 10, 1979, 39-40.

Appendix A continued.

37. H. J. Hindin, "Pieces of Plastic Filter Phone Voice", Electronics 52:46, July 5, 1979.

38. B. C. DeLoach, Jr., R. C. Miller, and S. Kaufman, "Sound Alerter Powered Over an Optical Fiber", Bell Sys. Tech. J. 57:3309-16, November 1978.

39. R. C. Miller and R. B. Lowry, "Optically Powered Speech Communication Over a Fiber Lightguide", Bell Sys. Tech. J. 58, 1735-41, September 1979.

40. Lord Rayleigh, "The Photophone", Nature XXIII, pp. 274-275, 1881

41. H. D. Arnold and I. B. Crandall, "The Thermophone as a Precision Source of Sound", Phys. Rev. 10, 22-38, 1917.

42. R. S. Quimby and W. M. Yen, "Photoacoustic Theory Including Energy Migration", J. Appl. Phys. 51 (9), September 1980.

43. W. R. Harshbarger and M. B. Robin, "The Quenching of Excited Iodine Atoms by Oxygen Molecules as Studied by Opto-Acoustic Spectroscopy", Chem. Phys. letters, 21, 462-465, 1973.

44. A. Rosencwaig, "Photoacoustic Spectroscopy of Solids", Commun. 7, 305-308, 1973.

45. W. R. Harshbarger and M. B. Robin, "The Opto-Acoustic Effect: Revival of an Old Technique for Molecular Spectroscopy", Acc. Chem. Res. 6, 329-334, 1973.

46. D. H. Leslie et al, "Fiber-Optic Spectrophone", Electronics Letters, 581-582, August 20, 1981.

47. G. T. Sincerbox and J. C. Gordon II, "Small Fast Large Aperature Light Modulator Using Attenuated Total Reflection", App. Optics 20-8.

APPENDIX B

ELECTRONIC INTERFACE UNIT SCHEMATIC

AND PARTS LIST

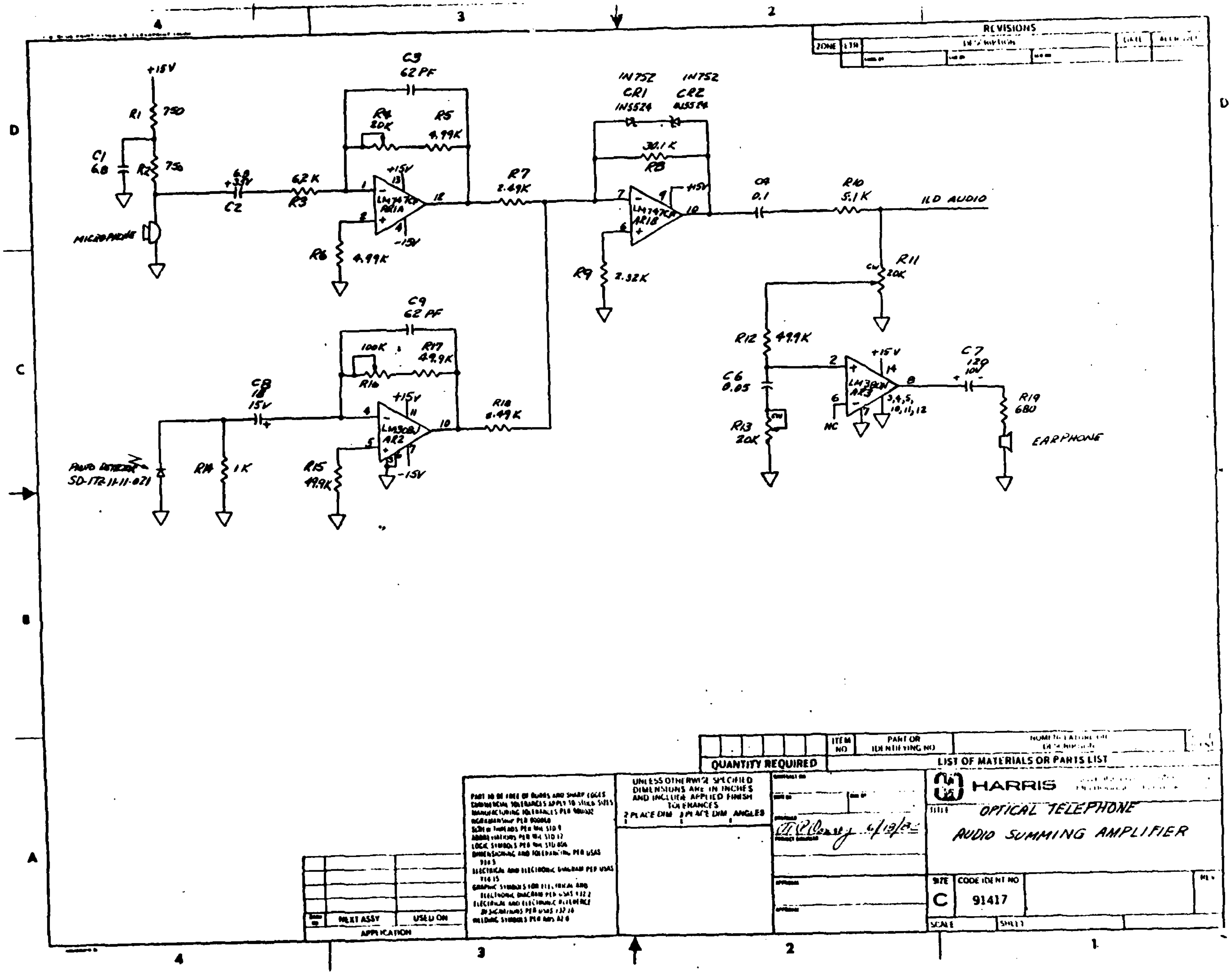

REVISIONS
+15V
R1 750
R2 750
C1 6.8
MICROPHONE
C2
R3 62K
C3 62 PF
R4 20K
R5 4.99K
R6 4.99K
LM747CP AR1A
-15V
R7 2.49K
IN752 CR1 IN5524
IN752 CR2 IN5524
30.1K R8
LM747CP AR1B
R9 2.32K
C4 0.1
R10 5.1K
ILD AUDIO
R11 20K
R12 49.9K
C6 0.05
R13 20K
LM380N AR3
NC
C7
R19 680
EARPHONE
C9 62 PF
100K
R16
R17 49.9K
C8 15V
LM308J AR2
R18 2.49K
R14 1K
R15 49.9K
PHOTO DETECTOR SD-172-11-11-021
QUANTITY REQUIRED
ITEM NO
PART OR IDENTIFYING NO
LIST OF MATERIALS OR PARTS LIST
UNLESS OTHERWISE SPECIFIED DIMENSIONS ARE IN INCHES AND INCLUDE APPLIED FINISH TOLERANCES
2 PLACE DIM 3 PLACE DIM ANGLES
NEXT ASSY
USED ON
APPLICATION
HARRIS
OPTICAL TELEPHONE
AUDIO SUMMING AMPLIFIER
SIZE C
CODE IDENT NO 91417
SCALE
SHEET

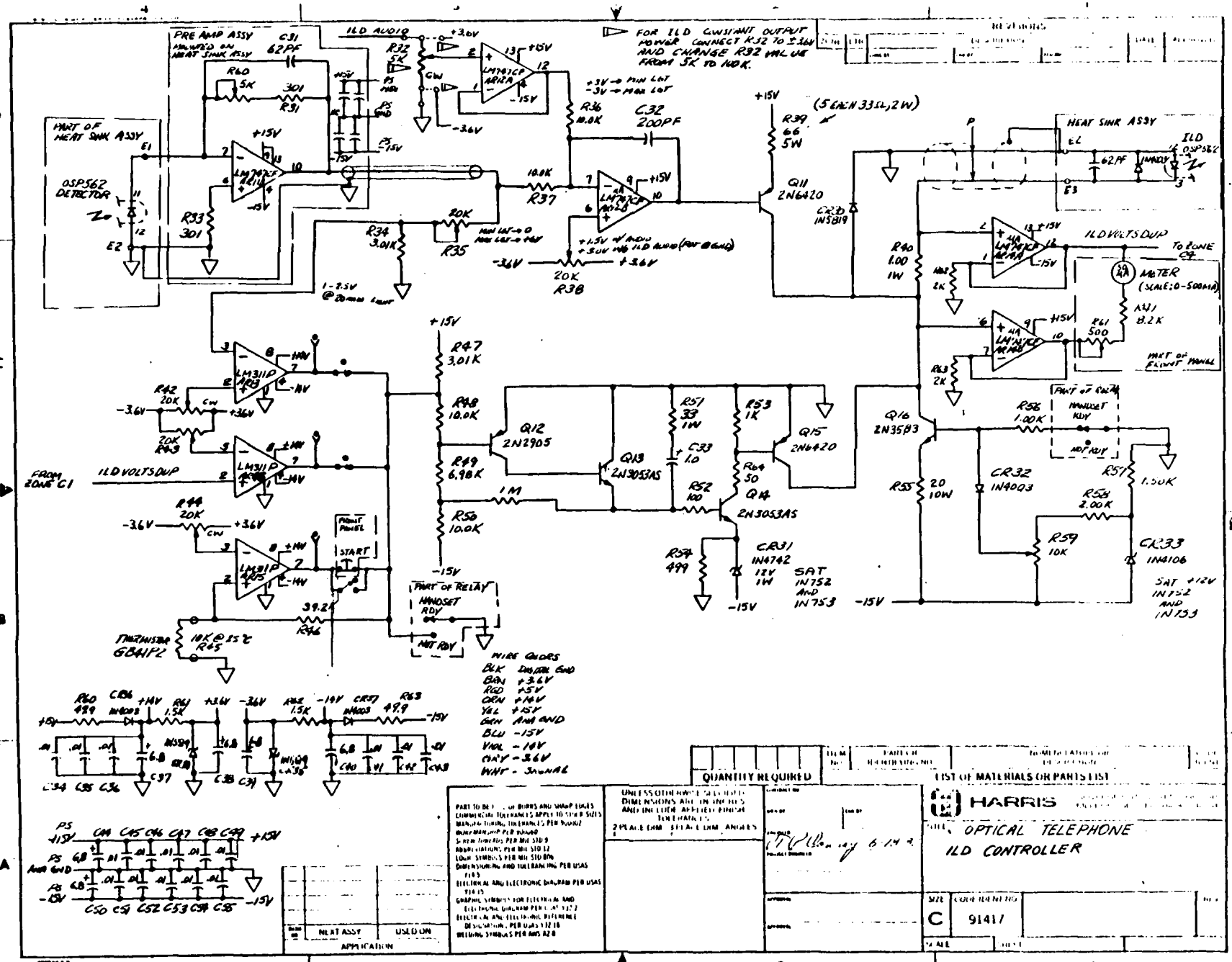
PRE AMP ASSY
MOUNTED ON HEAT SINK ASSY
PART OF HEAT SINK ASSY
OSP562 DETECTOR
ILD AUDIO
FOR ILD CONSTANT OUTPUT POWER CONNECT R32 TO ±3.6V AND CHANGE R32 VALUE FROM 5K TO 10K.
+3V → MIN LOT
-3V → MAX LOT
(5 EACH 33Ω, 2W)
HEAT SINK ASSY
ILD OSP562
ILD VOLTS DUP
TO ZONE CIR
METER (SCALE: 0-500mA)
PART OF FRONT PANEL
FROM ZONE C1
ILD VOLTS DUP
PART OF RELAY
HANDSET RDY
NOT RDY
START
PART OF CKT A
HANDSET RDY
NOT RDY
THERMISTOR 6BA1P2
10K @ 25°C R45
WIRE COLORS
BLK DIGITAL GND
BRN +3.6V
RED +5V
ORN +14V
YEL +15V
GRN ANA GND
BLU -15V
VIOL -18V
GRY -36V
WHT - SIGNAL
SAT +12V IN752 AND IN753
SAT IN752 AND IN753
PS +15V
PS ANA GND
PS -15V
QUANTITY REQUIRED
LIST OF MATERIALS OR PARTS LIST
HARRIS
OPTICAL TELEPHONE
ILD CONTROLLER
SIZE C
CODE IDENT NO 91417
HEAT ASSY
USED ON
APPLICATION
4
3
2
1
A
B
C
D

B-2

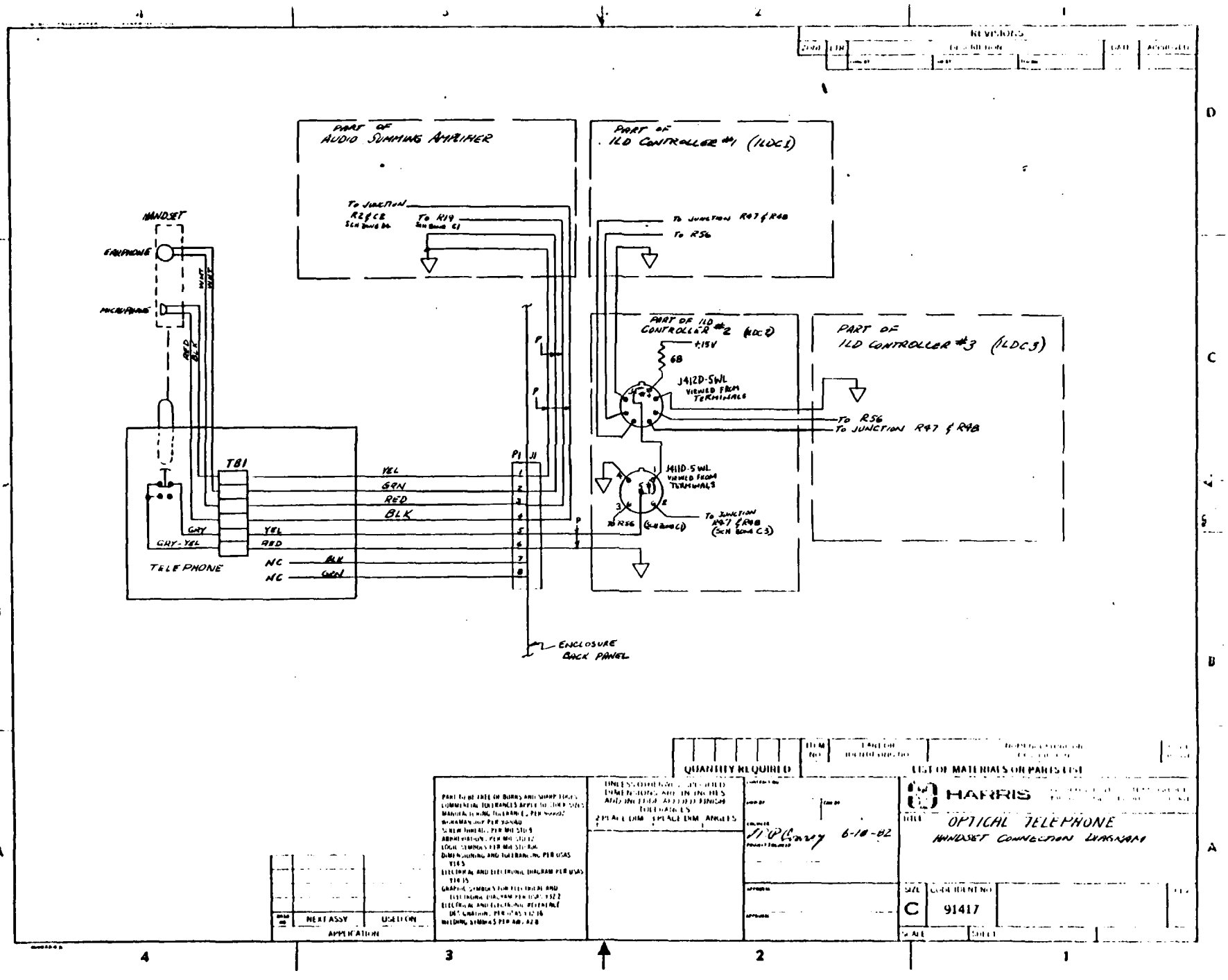

B-3

QUANTITY REQUIRED

LIST OF MATERIALS OR PARTS LIST

HARRIS

TITLE: OPTICAL TELEPHONE
HANDSET CONNECTION DIAGRAM

SIZE: C
CAGE IDENT NO: 91417

NEXT ASSY | USED ON
APPLICATION

6-10-82

APPENDIX B

ELECTRONIC INTERFACE UNIT PARTS LIST

All capacitors are in μf unless otherwise noted.

All resistors are in K ohm 1/4 watt unless otherwise noted.

Component No		Value		Quantity (each)
R1, R2		750 ohm		1
R3		620 ohm		1
R4, R11, R13	Pot	20		1
R5, R6		4.99		1
R7, R18		2.49		1
R8		30.1		1
R9		2.32		1
R10		15.0		1
R12, R15, R17		49.9		1
R14		11		1
R19		680 ohm		1
R33, R31		301 ohm		3
R32, R60	Pot	5		3
R36, R37, R48, R50		10		3
R34, R47		3.01		3
R42, R43, R44, R35, R38,	Pot	20		3
R39		100 ohm, 5 W		3
R49		6.98		3
R51		33 ohm, 1 W		3
R40		1 ohm, 1 W		3
R41		8.2		3
R66	Pot	500 ohm		3
R64, R65, R58		2		3
R52		100 ohm		3
R53, R56		1		3
R54		499		3
R55		30, 10 W		3
R59		10		3
R57		1.5		3
R60, R63		49.9		3
R62, R61		1.5		3
R70		1 M ohm		3
R71		68 ohm	Handset Con. Diag.	1
R64		50 ohm		3
C1, C2		6.8		1
C3, C9		62 pf		1
C4		.1		1
C5		.01		1
C6		.05		1
C7		120, 30 V		1
C8		18, 30 V		1

Component No.	Value	Quantity (each)
C31, C56	62 pf	3
C32	200 pf	3
C33	1	3
C34, C35, C36, C41, C42, C43, C45-C49, C51-C55	0.01	3
C37, C38, C39, C40, C44, C50	6.8, 30 V	3

SEMICONDUCTORS AND HARDWARE

Component No.	Part No.	Quantity
AR 1	LM 747	1
AR 2	LM 308	1
AR 3	LM 380	1
ITT Microphone		1
ITT Earphone		1
Photodetector	SD-172-11-11-021	1
CR 1, CR 2	1N5524	1
AR 11, AR 12, AR 15	747 CF	3
AR 13, AR 16, AR 15	LM 311 P	3
CR 38, CR 36, CR 37	1N4003	3
CR 34, CR 35	1N5519, 3.6 V	3
Q11, Q 15	2N6420	3
Q12	2N2905	3
Q13, Q14	2N3053	3
CR 31	1N4742, 12 V	3
Q16	2N3585	3
Meter	0-500 MA	3
ILD	OSP 562	3
SWI (Switch)		3
Relay		3
PIP-SW		3
CR 33	1N4106, 12 V	3
Power Supply	15 V, 1 A	3

APPENDIX C

TALK FUNCTION COMPUTER PROGRAM

AND VARIABLES SET

```
10 REM .....OPTICAL TELEPHONE.....
20 REM.....MEMBRANE VIBRATION.....
30 DIM Y[200],F[200]
35 PRINT
36 PRINT
40 D1=4
50 PRINT "40 DIAMETER OF CELL (CM)",D1
60 D2=0.036
70 PRINT "60 MEMBRANE DENSITY (G/CC)",D2
80 T1=0.5
100 PRINT "80 MEMBRANE THICKNESS (MIL)",T1
110 T2=12*1E+04
120 PRINT "110 MEMBRANE TENSION",T2
130 P=1
140 PRINT "130 DRIVE PRESSURE",P
150 N=0
160 R=0
170 PRINT "160 RADIUS POSITION (CM)",R
180 N1=200
190 PRINT "180 NUMBER OF STEPS",N1
191 PRINT
192 PRINT
200 F1=300
205 L1=LGT(F1)
210 F2=3300
215 L2=LGT(F2)
300 S=D2*T1
310 C=SQR(T2/S)
330 I=1
332 PRINT "   I","KA","FREQ(HZ)","   Y(I)"
333 PRINT
340 F3=(F2-F1)/N1
345 L3=(L2-L1)/N1
350 FOR L=L1 TO L2 STEP L3
352 F[I]=10↑L
355 W=2*PI*F[I]
356 K=W/C
360 X5=K*D1/2
370 X6=K*R
380 Z=X5
390 J1=FND(Z)
400 Z=X6
410 J2=FND(Z)
420 Y[I]=(P/(K*K*T2))*((J2/J1)-1)
422 Y[I]=ABS(Y[I])*(10↑4)
425 PRINT I,X5,F[I],Y[I]
430 I=I+1
440 NEXT L
445 PRINT
450 Y6=Y[1]
460 Y7=Y[1]
470 FOR I=2 TO N1
480 IF Y[I]<Y6 THEN 510
490 IF Y[I]>Y7 THEN 530
500 GOTO 540
510 Y6=Y[I]
```

Appendix C continued,

BESSEL ROUTINE

```
10 DEF FND(X)
20 Q2=X/2
30 Q1=0
40 Q3=Q4=1
50 FOR Q5=2 TO ABSN
60 Q3=Q3*Q5
70 NEXT Q5
80 Q0=Q3=1/Q3
90 Q3=-Q3*Q2/Q4*Q2/(N+Q4)
100 IF ABSQ3/Q0<1E-10 THEN 150
110 Q0=Q0+Q3*(Q3>0)
120 Q1=Q1+Q3*(Q3<0)
130 Q4=Q4+1
140 GOTO 90
150 E=10+LGTABS(1+Q1/Q0)
160 RETURN (Q0+Q1)*(Q2+(Q2=0)*(N=0))↑N
```

EXAMPLE OF PRINTED OUTPUT

```
40 DIAMETER OF CELL (CM)          4
60 MEMBRANE DENSITY (G/CC)        0.036
80 MEMBRANE THICKNESS (MIL)       0.5
110 MEMBRANE TENSION              120000
130 DRIVE PRESSURE                1
160 RADIUS POSITION (CM)          0
180 NUMBER OF STEPS               200

   I            KA              FREQ(HZ)          Y(I)

 1              1.460080323     300.0000000     0.136457302
 2              1.477691284     303.6184915     0.13853863
```

Appendix C continued,

```
515 F6=F[I]
520 GOTO 540
530 Y7=Y[I]
535 F7=F[I]
540 NEXT I
550 PRINT "Y MIN    ";F6;Y6
560 PRINT "Y MAX    ";F7;Y7
570 PRINT
580 PRINT
590 PRINT
600 END
```

PLOTTING ROUTINE

```
10 X1=2.4
20 X2=3.6
30 X3=(X2-X1)/8.5
40 X4=X1-1.5*X3
50 X5=X2+1*X3
60 F3=(F2-F1)/N1
70 Y1=0
80 Y2=1.1
90 Y3=(Y2-Y1)/6
100 Y4=Y1-1.5*Y3
110 Y5=Y2+1*Y3
150 SCALE X4,X5,Y4,Y5
160 XAXIS Y1,0.1,X1,X2
170 YAXIS X2,0.1,Y1,Y2
180 YAXIS X1,0.1,Y1,Y2
190 XAXIS Y2,0.1,X1,X2
200 L=L1
210 FOR I=1 TO N1
220 F9=LGT(F[I])
225 Y[I]=Y[I]/Y7
230 PLOT F9,Y[I]
250 NEXT I
260 END
```

APPENDIX C

TALK FUNCTION COMPUTER PROGRAM VARIABLES SET

In order of Appearance:

D1	-	cell membrane diameter (cm)
D2	-	membrane density (gm/cc)
T1	-	membrane thickness (mil)
T2	-	membrane tension (dynes/cm^2)
P	-	drive pressure (dynes/cm^2)
N	-	Bessel function order
R	-	radius of membrane amplitude position (cm)
N1	-	step counter
F1	-	minimum frequency (hz)
L1	-	log F1
F2	-	maximum frequency (hz)
L2	-	log F2
S	-	area density (gm/cm^2)
C	-	acoustic velocity (cm/sec)
I	-	counter
F3	-	linear frequency step
L3	-	log frequency step
Y(200)	-	amplitude array
F(200)	-	frequency array
L	-	counter
W	-	angular frequency (rad/sec)
K	-	propagation constant
X5	-	Ka
X6	-	Kr
Z	-	arguement for Bessel function program
J1	-	J_o (Ka)
J2	-	J_o (Kr)
F6	-	frequency at minimum amplitude
Y6	-	minimum amplitude
F7	-	frequency at maximum amplitude
Y7	-	maximum amplitude
X1	-	min X axis
X2	-	max X axis
X3	-	X axis scale factor
X4	-	min X scale
X5	-	max X scale
Y1	-	min Y axis
Y2	-	max Y axis
Y3	-	Y axis scale factor
Y4	-	min Y scale
Y5	-	max Y scale
F9	-	plotting frequency
I	-	counter

FND(X) Bessel approximation routine

APPENDIX D

HEAR AND RING COMPUTER PROGRAM

AND VARIABLES SET

```
10 DIM A$[50]
20 PRINT "SELECT GAS:A 1-RING 2-HEAR 3-KN AIR 4-KN XENON"
30 PRINT
40 DIM C[10]
50 Z3=0
60 INPUT K5
65 PRINT K5
70 IF K5=1 THEN 110
80 IF K5=2 THEN 130
90 IF K5=3 THEN 150
100 IF K5=4 THEN 170
110 RESTORE 3070
120 GOTO 180
130 RESTORE 3100
140 GOTO 180
150 RESTORE 3130
160 GOTO 180
170 RESTORE 3160
180 DIM Z[10],X[161],R[161]
190 READ A$
200 READ R1,R2,L,V2,V1,F1,F2,L4,R4,I7,P5
210 READ R0,C1,C2,M,H,N1,M2,M3,K1
220 PRINT "IMP EAR VOL 0 FREE SPACE 1 "
230 PRINT "   "
240 DISP "IMP EAR VOL 0 FREE SPACE 1";
250 INPUT K3
255 PRINT K3
260 IF K3=0 THEN 390
270 RESTORE 2910
280 FOR I=1 TO 45
290 READ X
300 K9=10*X+1
310 READ X[K9]
320 NEXT I
330 FOR I=1 TO 45
340 READ X
350 K9=10*X+1
360 READ R[K9]
370 NEXT I
380 N3=1
390 L1=(R0*L4/(PI*R4↑2)+2*R0/(4*R4))
400 A5=(LOG(R2/R1))/L
410 0=(M2↑0.5)/(2*H)
420 G1=FNG0
430 DEF FNG(Z3)
440 REM PLOTTING AND LABELING ROUTINE
450 P1=LGT(F1)
460 P2=LGT(F2)
470 X1=P1
480 X2=P2
490 X3=(X2-X1)/10
500 PRINT "PLOT 1/0,PRINT 1/0,AVG1/0"
510 PRINT
520 DISP "PLOT 1/0,PRINT 1/0,AVG 1/0";
530 INPUT Z0,Z1,Z5
535 PRINT Z0,Z1,Z5
540 PRINT "PARAMETERS FOR ";A$
```

```
550 PRINT "HORN INPUT RADIUS IS";R1;"CM"
560 PRINT "HORN OUTPUT RADIUS IS";R2;"CM"
570 PRINT "HORN LENGTH IS";L;"CM"
580 PRINT "CELL VOLUME IS";V1;"CUBIC CM"
600 PRINT "EAR VOLUME IS";V2;"CUBIC CM"
604 IF K3=0 THEN 610
605 PRINT "DISTANCE FROM MOUTH OF HORN IS 1  METER"
610 PRINT "OPTICAL POWER INPUT IS";P5;"MILLIWATTS"
620 PRINT "EQUALIZER TUBE LENGTH IS";L4;"AND RADIUS IS";R4;"CM"
630 IF Z0=0 THEN 1240
640 PRINT "YMIN,YMAX,INCRM.='
650 PRINT
660 DISP "YMIN,YMAX,INCRM.";
670 INPUT Y1,Y2,Y3
680 PRINT Y1,Y2,Y3
690 PRINT "AXIS?...YES 1 NO 0"
700 PRINT
710 DISP "AXIS?...YES 1 NO 0";
720 INPUT Z2
730 I=(X2-X1)/27
740 J=(Y2-Y1)/17
750 Y5=Y1-2*J
760 Y6=Y2+J
770 SCALE X1-2*I,X2+I,Y5,Y6
780 IF Z2=0 THEN 1240
790 PLOT X2,Y1
800 PLOT X1,Y1
810 PLOT X1,Y2,-1
820 U=Y1
830 V=Y2
840 T=Y3
850 Z=FNL0
860 U=X1
870 V=X2
880 T=X3
890 Z=FNL1
900 X3=I
910 Y3=J
920 Z=FNK0
930 LABEL (*,3,1,0,2/3)
940 GOTO 1240
950 FORMAT 2F7.1
960 RETURN 0
970 DEF FNL(Z)
980 X=ABSU
990 Y=ABSV
1000 P=INTLGT(X+(Y-X)*(Y>X))
1010 P0=(P<-1 OR P>2)
1020 LABEL (*,1.5,2,Z*ATN1E+99,2/3)
1030 IF Z=1 THEN 1100
1040 FOR K=U TO V STEP T
1050 PLOT X1* NOT Z+K*Z,K* NOT Z+Y1*Z,1
1060 CPLOT -7.3,-0.3
1070 LABEL (950)K/( NOT P0+P0*10↑P)"-";
1080 NEXT K
1090 GOTO 1180
1100 FOR K=U TO V STEP T
```

Appendix D continued,

```
1110 PLOT X1+ NOT Z+K*Z,K+ NOT Z+Y1+Z,1
1120 CPLOT -7.3,-0.3
1130 K5=K
1140 K=10↑K
1150 LABEL (950)K ; NOT P0+P0=(0↑P)"-";
1160 K=K5
1170 NEXT K
1180 IF P0=0 THEN 1200
1190 LABEL (*)" X10↑"P;
1200 RETURN 0
1210 DEF FNK(Z)
1220 PLOT X2+X3,Y2+Y3,1
1230 RETURN 0
1240 REM PHOTOPHONE CALCULATION: BIG LOOP
1250 P0=1.013E+06
1260 IF Z5=0 THEN 1290
1270 D4=50
1280 GOTO 1300
1290 D4=150
1300 FOR F5=P1 TO P2 STEP (P2-P1)/D4
1310 F3=10↑F5
1320 W=2*PI*F3
1330 K=W/C1
1340 IF (K↑2-A5↑2)<0 THEN 2470
1350 N=SQR(K↑2-A5↑2)
1360 R6=0
1370 I6=-W*L1
1380 R7=0
1390 I7=I7
1400 R8=0
1410 I8=M*P0/(W*V1)
1420 IF K3=1 THEN 1460
1430 R9=0
1440 I9=M*P0/(W*V2)
1450 GOTO 1510
1460 X4=2*K*R2
1470 X1=INT(X4*10)/10
1480 G1=FNR0
1490 R9=R0*C1/(PI*R2↑2)*R[K9]
1500 I9=-R0*C1/(2*PI*R2↑2)*X[K9]
1510 E1=SQR(2*A5/K)*(2*N*K↑2-A5*K↑2-2*0*A5*(A5*N-A5↑2-2*N↑2))/(A5*(K
1520 R5=2*H*(A5*C1)↑(-0.5)
1530 D9=R5/R1*(8*N↑2/A5/K)↑0.5*(K↑2-A5↑2*0)/(K↑2+3*N↑2)
1540 A=0
1550 B=W*R0/(PI*R1↑2)
1560 C=-A5
1570 D=N
1580 G1=FND0
1590 A=D5
1600 B=D6
1610 C=R8
1620 D=I8
1630 G1=FND0
1640 C[5]=D5
1650 C[6]=D6
1660 A=R6
1670 B=I6
1680 C=R8
1690 D=I8
```

Appendix D continued,

```
1700 G1=FND0
1710 C[1]=1+D5+C[5]
1720 C[2]=D6+C[6]
1730 A=0
1740 B=W*R0/(PI*R2↑2)
1750 C=-A5
1760 D=-N
1770 G1=FND0
1780 A=D5
1790 B=D6
1800 C=R9
1810 D=I9
1820 G1=FND0
1830 C[7]=D5
1840 C[8]=D6
1850 A=R7
1860 B=I7
1870 C=R9
1880 D=I9
1890 G1=FND0
1900 C[3]=C[7]-D5-1
1910 C[4]=C[8]-D6
1920 A=C[1]
1930 B=C[2]
1940 C=C[3]
1950 D=C[4]
1960 G1=FNM0
1970 REM"CALC MAGNITUDE AND PHASE OF G(K)"
1980 M7=(M5↑2+M6↑2)↑0.5
1990 A=M5
2000 B=M6
2010 G1=FNP0
2020 R3=(3*V1/4/PI)↑(1/3)
2030 T1=M*R3↑2/15/N1
2040 E=(15*W*T1/2)↑0.5
2050 F=-E
2060 A=EXP(2*E)*COS(2*F)+1
2070 B=EXP(2*E)*SIN(2*F)
2080 C=EXP(2*E)*COS(2*F)-1
2090 D=EXP(2*E)*SIN(2*F)
2100 G1=FND0
2110 A=D5
2120 B=D6
2130 C=E
2140 D=F
2150 G1=FNM0
2160 A=M5-1
2170 B=M6
2180 C=E
2190 D=F
2200 G1=FND0
2210 A=D5
2220 B=D6
2230 C=E
2240 D=F
2250 G1=FND0
2260 N5=((1-3*D5)↑2+(-3*D6)↑2)↑0.5
2270 N7=N5↑2
2280 A9=1-2*EXP(-D9)*COS(2*N*L+D9-2*P7)+EXP(-2*D9)
```

Appendix D continued.

```
2290 H5=K1*M3*(9.1E-04/R1↑2/R2↑2)*(N/K)↑2*(EXP(-(R5/R1)*E1)*N7/(M7↑2*A9))
2300 H6=H5*A9/(1-EXP(-2*D9))
2310 I5=10*LGT((680↑2*(M-1)↑2+(2*(M*P0)↑2)*(P5*10↑4)↑2)/(2E-04)↑2)
2320 IF Z5=0 THEN 2350
2330 S1=10*LGT(H6)+I5
2340 GOTO 2360
2350 S1=10*LGT(H5)+I5
2360 IF K3=0 THEN 2430
2370 P9=0.0002*10↑(S1/20)
2380 IF R9=0 AND I9=0 THEN 2410
2390 U0=P9/(R0*C1*PI*R2↑2)
2400 GOTO 2420
2410 U0=0
2420 Z4=100
2430 P6=K*P9*R2↑2/(2*2↑0.5*Z4)
2440 IF P6=0 THEN 2470
2450 S1=10*LGT((P6↑2/(0.0002)↑2))
2460 GOTO 2480
2470 S1=-1E+95
2480 IF Z1=0 THEN 2500
2490 PRINT F3,S1
2500 IF Z0=0 THEN 2520
2510 PLOT F5,S1,-2
2520 NEXT F5
2530 PEN
2540 END
2550 DEF FNM(Z3)
2560 REM COMPLEX MULT (A+JB)*(C+JD)=M5+JM6
2570 M5=A*C-B*D
2580 M6=B*C+A*D
2590 RETURN 0
2600 DEF FNP(Z3)
2610 REM PHASE OF A+JB
2620 IF A >= 0 THEN 2650
2630 P7=ATN(B/A)+PI
2640 RETURN 0
2650 P7=ATN(B/A)
2660 RETURN 0
2670 DEF FND(Z3)
2680 REM COMPLEX DIV (A+JB)/(C+JB)=D5+JD6
2690 IF C=0 AND D=0 THEN 2730
2700 D5=(A*C+B*D)/(C↑2+D↑2)
2710 D6=(B*C-A*D)/(C↑2+D↑2)
2720 GOTO 2740
2730 D5=D6=0
2740 RETURN 0
2910 DATA 0,0,0.2,0.0847,0.4,0.168,0.6,0.2486,0.8,0.3253,1,0.3969,1.2,0.4624
2920 DATA 1.4,0.5207,1.6,0.5713,1.8,0.6134,2,0.6468,2.2,0.6711,2.4,0.6862
2930 DATA 2.6,0.6925,2.8,0.6903,3,0.68,3.2,0.6623,3.4,0.6381,3.6,0.6081
2940 DATA 3.8,0.5733,4,0.5349,4.5,0.4293,5,0.3232,5.5,0.2299,6,0.1594
2950 DATA 6.5,0.1159,7,0.0989,7.5,0.1036,8,0.1219,8.5,0.1457,9,0.1663
2960 DATA 9.5,0.1782,10,0.1784,10.5,0.1668,11,0.1464,11.5,0.1216,12,0.0973
2970 DATA 12.5,0.0779,13,0.0662,13.5,0.0631,14,0.0676,14.5,0.077,15,0.88
2980 DATA 15.5,0.0973,16,0.1021
2990 DATA 0,0,0.2,0.005,0.4,0.0198,0.6,0.0443,0.8,0.0779,1,0.1199,1.2,0.1695
3000 DATA 1.4,0.2257,1.6,0.2876,1.8,0.3539,2,0.4233,2.2,0.4946,2.4,0.5665
3010 DATA 2.6,0.6378,2.8,0.7073,3,0.774,3.2,0.8367,3.4,0.8946,3.6,0.947
3020 DATA 3.8,0.9932,4,1.033,4.5,1.1027,5,1.131,5.5,1.1242,6,1.0922
3030 DATA 6.5,1.0473,7,1.0013,7.5,0.9639,8,0.9413,8.5,0.9357,9,0.9455
3040 DATA 9.5,0.9661,10,0.9913,10.5,1.015,11,1.0321,11.5,1.0397,12,1.0372
```

Appendix D continued,

```
3050 DATA 12.5,1.0265,13,1.0103,13.5,0.9944,14,0.9809,14.5,0.9733
3060 DATA 15,0.9727,15.5,0.9794,16,0.9887
3070 DATA "AIR HORN HARRIS RING"
3080 DATA 0.05,4,15,6,5E-04,1000,3000,20,0.02,0,18
3090 DATA 1.225E-03,3.403E+04,1.006E+07,1.403,0.565,0.2884,0.1461,1,1
3100 DATA "AIR HORN HARRIS HEAR"
3110 DATA 0.032,0.77,70,6,2.5E-03,250,4000,1.3,0.02,0,2.8
3120 DATA 1.225E-03,3.403E+04,1.006E+07,1.403,0.565,0.2884,0.1461,1,1
3130 DATA "AIR DATA K-N"
3140 DATA 0.036,0.85,85,6,2.5E-03,250,4000,1.8,0.02,0,2.8
3150 DATA 1.225E-03,3.403E+04,1.006E+07,1.403,0.565,0.2884,0.1461,1,1
3160 DATA "ZENON DATA K-N"
3170 DATA 0.024,1.27,56,6,6E-04,250,4000,2.1,0.02,0,2.8
3180 DATA 5.397E-03,1.769E+04,1.582E+06,1.667,0.375,0.1098,4.162E-02,2,5.245
3190 DEF FNR(Z3)
3200 X=X1
3210 T=INT(100*X)/100-INTX
3220 IF X >= 4 THEN 3400
3230 IF T >= 0 AND T<0.1 THEN 3300
3240 IF T >= 0.1 AND T<0.3 THEN 3320
3250 IF T >= 0.3 AND T<0.5 THEN 3340
3260 IF T >= 0.5 AND T<0.7 THEN 3360
3270 IF T >= 0.7 AND T<0.9 THEN 3380
3280 X=INTX+1
3290 GOTO 3440
3300 X=INTX
3310 GOTO 3440
3320 X=INTX+0.2
3330 GOTO 3440
3340 X=INTX+0.4
3350 GOTO 3440
3360 X=INTX+0.6
3370 GOTO 3440
3380 X=INTX+0.8
3390 GOTO 3440
3400 IF T >= 0 AND T<0.25 THEN 3300
3410 IF T >= 0.25 AND T<0.75 THEN 3430
3420 GOTO 3280
3430 X=INTX+0.5
3440 K9=10*INT(10*X)/10+1
3450 IF K9>161 THEN 3470
3460 GOTO 3480
3470 PRINT "2KA IS GREATER THAN 16!"
3480 RETURN 0
```

EXAMPLE OF PRINTED OUTPUT

```
SELECT DATA 1-RING 2-HEAR 3-KN AIR 4-KN XENON

 2
IMP EAR VOL 0 FREE SPACE 1

 0
PLOT 1/0,PRINT 1/0,AVG1/0

 0                0                1
PARAMETERS FOR AIR HORN HARRIS HEAR
HORN INPUT RADIUS IS 0.032    CM
HORN OUTPUT RADIUS IS 0.77     CM
HORN LENGTH IS 70    CM
CELL VOLUME IS 2.50000E-03    CUBIC CM
EAR VOLUME IS 6     CUBIC CM
OPTICAL POWER INPUT IS 2.8  MILLIWATTS
EQUALIZER TUBE LENGTH IS 1.8  AND RADIUS IS 0.02     CM
```

APPENDIX D

HEAR AND RING HORN COMPUTER PROGRAM VARIABLES SET

In order of Appearance:

A$(50)	-	Dimension of alphanumeric in DATA statements
C(10)	-	Dimension of scratph pad variables
Z3	-	Plotting Routine Variable
K5	-	User Input for DATA selection
X(161)	-	Dimension of complex impedance of circular piston DATA
R(161)	-	Dimension of real impedance of circular piston DATA
R1	-	horn input radius, R_1 (cm)
R2	-	horn output radius, R_2 (cm)
L	-	horn length, L (cm)
V2	-	ear volume, V_E (cc)
V1	-	cell volume, V_C (cc)
F1	-	plotting f min (Hz)
F2	-	plotting f max (Hz)
L4	-	length of input equalizer tube, (cm)
R4	-	radius of input equalizer tube (cm)
I7	-	complex part ouput equlization ($gm/sec\text{-}cm^4$)
P5	-	optical power input (ergs/sec)
K9	-	READ variable (2KR) for X(161) + R (161)
L1	-	inertance of input equalizer
A5	-	flare constant
Q	-	q, a gas constant
G1(Z3)	-	Define function calling variable
FNG	-	plotting routine
Po	-	Atmosphere pressure ($dyne/cm^2$)
Z5	-	Average or peak plotting variable
D4	-	plotting step variable
P1, 2	-	log F1,F2
F5	-	log frequency variable
F_3	-	linear frequency variable (Hz)
W	-	linear angular frequency, (rad/sec)
K	-	acoustic wave propagation constant, (rad/m)
N	-	complex part of lossless propogation solution, n
$R_{6,7,8,9}$ $I_{6,7,8,9}$	-	Real + Imaginary part of impedance for input equalizer, output equalizer, cell volume, output load (ear volume or free space)
X1	-	Operating argument for piston reactance function data
FNRØ	-	Piston reactance data handling subroutine
E1	-	ξ
R5	-	radius of boundary layer approximation, r_o
D9	-	Δ
AtjB	-	complex number (dividend) routine.
CtjD	-	complex number (divisor) for dividing & multiplying routine.
FNDØ	-	complex number dividing subroutine
FNMØ	-	complex number multiplying subroutine
D5 + jD6	-	returned complex number from complex dividing subroutine
M5 + jM6	-	returned complex number from complex multiplying subroutine
M7	-	$\|g(k)\|^2$
FNPØ	-	phase of g(k) computation subroutine
P7	-	Phase of g(k)
R3	-	radius of sphere volume, V_E
T1	-	Thermal relaxation time constant for volume V_E
E + jF	-	Ψ
N5	-	G_w

N7 - G_W^2
A9 - $1-2e^{-\Delta} \cdot \cos \Phi + e^{-2\Delta}$
H5 - H_W
H6 - $\langle H_W \rangle$
I5 - Intensity, I
S1 - SPL (dB)
P9 - pressure at output of horn (dynes/cm^2), P_E
UØ - volume flow of piston output - Uo
Z4 - measurement distance from months of horn (metres)
P6 - pressure P (100), pressure at 1 meter normal to source

APPENDIX E

PAPERS RELEVANT TO HARRIS DESIGN CONCEPTS

The photophone—an optical telephone receiver

D. A. Kleinman and D. F. Nelson

Bell Laboratories, Murray Hill, New Jersey 07974
(Received 15 December 1975, revised 28 February 1976)

A theoretical discussion is given of optical telephone receivers employing the optoacoustic effect, which are here called photophones, for use in an optical-fiber telephone subscriber loop. The basic receiver consists of an absorption cell, a response-equalizing device such as a gas column or diaphragm, a tapered acoustic tube acting as a transformer, and an earpiece similar to a conventional telephone earpiece including a response-equalizing device. These photophones are designed to give a flat (3-dB) response to intensity modulated light over the telephone voice band 300–3300 Hz. The optoacoustic effect is treated on the basis of a pseudo-gas model for solid absorbers in the form of a fine mesh disbusrsed in a gas. We find that the sensitivity (the optical power modulation required to produce a sound pressure level SPL = 81 dB in a closed volume of 6 cm³, representing the earpiece pressed against the ear) is 2.8 and 0.9 mW for the air-filled and xenon-filled photophones, respectively.

Subject Classification: [43]85.76,[43]85.40,[43]85.60,[43]35.65.

LIST OF SYMBOLS

a	radius (cell, gas column, tubes, diaphragm)
A	area
b	length (gas column, tubes); radius of load ring
c	sound speed
C	as subscript denotes cell
C_p, C_v	specific heats at constant pressure, constant volume
$C_{11}, \ldots, C_{22}$	matrix $[C]$, see Eq. (3)
d	see Eq. (38)
E	as subscript denotes earpiece
$f, \bar{f}$	frequency (Hz); resonant frequency
$g(k)$	see Eq. (19)
G_A, G_M, G_ω	see Eqs. (38), (55), (54)
$h(k)$	see Eq. (19)
H_ω	response function, see Eq. (8)
$\langle H_\omega \rangle$	smoothed response function, see Eq. (31)
I	sound intensity, see Eq. (5)
k	$= \omega/c$
l	length (acoustic tube, port)
L	inertance (g cm^{-4}), see Appendix A
m, n	see Eqs. (B19)
p	pressure (dyn cm^{-2})
p_0	$= 1.013 \times 10^6$ (dyn cm^{-2}) atm pressure
P, P_ω, P_0	optical power (erg sec^{-1}), see Eq. (1)
q	$= \mu^{1/2}/2\gamma'$
r_0	see Eq. (B18)
$r(x), r_1, r_2$	see Eq. (B16)
R	resistance (g sec^{-1} cm^{-4})
s	flow (cm^3 sec^{-1})
s_L	sound flow source, see Eq. (37)
S	entropy
t	time, thickness
T	absolute temperature (K), transformer
$T_{11}, \ldots, T_{22}$	transformer matrix, see Eq. (B9)
u, v	see Eqs. (B7)
V	volume (cm^3)
w	as subscript denotes cell wall
w	wall reflectivity
x	distance along tube
X	reactance (g sec^{-1} cm^{-4})
$\bar{y}$	see Eq. (50)
$Y(x)$	distributed admittance (cm^3 sec g^{-1})
z	$= p/s$ impedance (g sec^{-1} cm^{-4})
z_0	characteristic impedance of tube, see Eq. (B10)
z_1, z_2	characteristic impedances, see Eq. (20)
$Z(x)$	distributed impedance (g sec^{-1} cm^{-5})
Z	impedance
α	exponential taper, see Eq. (B16)
β	optical absorption coefficient; acoustic propagation constant
γ	$= C_p/C_v$ (γ_0 refers to air)
γ'	Kirchhoff's constant Eq. (B15)
Δ	see Eq. (B22)
η	viscosity coefficient (dyn sec cm^{-2})
κ	thermal conductivity (erg sec^{-1} cm^{-1} K^{-1})
μ	$= \eta/\rho$ (cm^2 sec^{-1})
ν	$= \gamma\kappa/\rho C_p$ (cm^2 sec^{-1})
ξ	see Eq. (B21)
ρ	density (g cm^{-3})
τ	relaxation time (sec)
φ	$= f/\bar{f}$
Φ	see Eq. (28)
χ	see Eq. (44)
ψ	see Eq. (28)
ω	$= 2\pi f$ angular frequency (rad sec^{-1})

INTRODUCTION

An optical telephone capable of performing the normal functions of transmitting, receiving, dialing, and ringing, using only power supplied through optical fibers from the central office, would be useful in order to reduce the use of copper wires in the telephone subscriber loop. This paper is concerned with only one of these functions, receiving, and with only one type of optical receiver which we call the *photophone*, a name originally coined by Alexander Graham Bell[1] in 1881. Although old in concept, the photophone has never been developed for communication purposes, and therefore the performance and design theory of this "new art"

had to be worked out from basic principles, and are presented here for the first time. The photophone can be equalized to give a flat (within 3-dB) frequency response to power-modulated light over the telephone band 300–3300 Hz. It can provide the average sound pressure level at the ear of 81 dB above the threshold of hearing with very small input optical powers of a few milliwatts or less. Recent telephone network surveys[2] have shown that the sound pressure level at the ear has a normal distribution with an average of 81 dB and a standard deviation of 7.8 dB.

The photophone has its origins in experiments of Alexander Graham Bell[1] in collaboration with Sumner Tainter on the production of sound when interrupted beams of sun light fall upon matter. Bell concluded that "sonorousness" under such circumstances is a general property of all matter whatever its physical state: solid, liquid, or gas. He also succeeded in demonstrating the "articulating photophone" which could audibly reproduce words and sentences spoken into his light modulating "photophonic transmitter." The greatest sonorousness was found to be produced by dark-colored solids in a loose, porous, spongy condition, in particular lampblack. Originally the term "photophone" meant Bell's whole system of optical telephony, but here we shall apply it just to receivers employing the "sonorousness" effect directly to produce sound (i.e., without intermediate electrical means). Bell also demonstrated an instrument for spectrum analysis in which the lampblack photophone was substituted for the eyepiece of a prism spectroscope. This device, which he said was particularly suited for infrared analysis, he called the "spectrophone."

Today the "sonorousness" of matter in a modulated beam of light is called the *optoacoustic* (or photoacoustic) *effect* and is widely used in the spectral analysis of gases, vapors, and solids. The modern spectrophone[3] differs from Bell's in that the gas or solid to be analyzed is the working substance of the photophone whereas Bell employed lampblack in his photophone and placed the gas sample in a separate absorption cell. Also, the sound produced in the photophone is detected by a microphone and electronically amplified. Recently Kreuzer[4] has estimated that fractional concentrations as low as 10^{-13} may be measurable with the optoacoustic effect when higher-power tunable infrared sources become available. Harshbarger and Robin[5] have applied the spectrophone to the study of several photochemical processes, and Rosencwaig[6] has reported spectrophone studies of various inorganic and organic solids including biological materials.

All of the relaxation mechanisms which transfer energy from the excited electronic and vibrational states of molecules to the translational motion are fast compared with audio frequencies. Therefore at audio frequencies a modulated light beam is equivalent to a modulated source of heat, a fact fully appreciated by Bell at the time of his early experiments. Obviously a modulated heat source can be obtained by means other than the absorption of light, and we mention one such device here. Arnold and Crandall[7] have discussed a device called the "thermophone" in which sound is produced when a modulated electric current is passed through a thin conducting foil or wire. They proposed that the acoustic output of the thermophone can be calculated from first principles to high accuracy and therefore it could be used as a precision absolute sound source. Wente[8] has performed careful measurements on the thermophone and obtained close agreement with theory.

In the case of absorption of light in a gas the mechanism of sound production is clear and can be accurately calculated from first principles just as in the thermophone. In the case of a solid absorber, however, more complicated mechanisms could be involved including, as suggested by Bell, adsorption and desorption of gas in the solid. Rosencwaig[6] has recently concluded from his experiments that the adsorbed gas plays no major role. Fortunately our discussion does not require detailed knowledge of the mechanisms involved, and we believe it applies quite well to both gaseous absorbers and tenuous solid absorbers disbursed in a gas. In any case the acoustic principles presented here do not depend on the absolute strength of the optoacoustic effect.

The photophone is presented descriptively in Sec. I, which explains the nature and function of all of the essential parts and outlines the analytical theory on the basis of a general equivalent circuit, leading to the definition of a response function. The presentation becomes analytical in Sec. II where the simplest equivalent circuit, necessarily somewhat hypothetical, is solved and optimized, leading to calculations of the response as a function of frequency. The presentation will become technical in a second paper[9] where the hypothetical aspects of the equivalent circuit are removed in favor of the actual properties of real materials and devices, leading to realistic calculations of the response and specific physical designs. The optoacoustic effect is treated in Sec. III. The main text is supported by four appendixes containing resource material essential to this work. A summary of results is presented in Sec. IV.

Our purpose in this discussion and that of the second paper[9] will not be to advocate the photophone, but only to give a sound technical appraisal of its capabilities.

I. GENERAL DESCRIPTION OF THE PHOTOPHONE

The basic parts of the photophone receiver are shown in Fig. 1. The input signal is an intensity modulated light beam conducted by an optical fiber into the absorption cell. For simplicity the fiber is shown as simply terminating inside the cell. This will result is significant reflection back down the fiber, so it would be advantageous to provide an optical termination for the fiber (not shown) to reduce this reflection to a minimum. The light is absorbed in the cell either by a special gaseous absorber or by a special solid absorber in thermal contact with an immersing gas; the absorber in either case must be strongly absorbing at the wavelength of light being used. Sound is produced in the cell by the optoacoustic effect and passes out of the cell into the small end of a tapered acoustic tube. The cell has a very small volume V_c of the order 10^{-3} cm^3 and there-

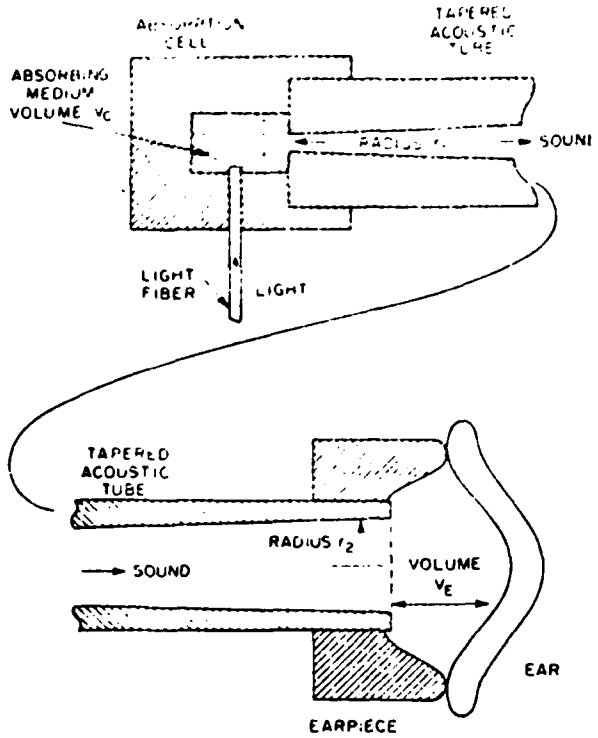

FIG. 1. The transformer-coupled photophone consisting of the absorption cell, tapered acoustic tube, and earpiece. Not shown are the equalizers at the input and output of the tube.

fore a very high acoustic impedance. Between the cell and the tube there must be some device (not shown) providing acoustic inertance for the purpose of equalizing the response across the desired band 300–3300 Hz. As sound is transmitted from the small end to the large end of the tapered acoustic tube it undergoes an impedance transformation from high (i.e., high pressure, low flow) to low impedance (i.e., low pressure, high flow). Thus the tube acts as a transformer. Typical values for its small radius, large radius, and length are 0.04, 0.9, and 85 cm, respectively. The tube could be coiled or folded so as to fit inside the handset. The sound is delivered to the earpiece at an impedance close to that of the volume V_E formed when the earpiece is pressed against the ear. The earpiece is very similar in shape and size to a conventional telephone receiver.[10] Since it is customary to test telephone receivers[11] with a closed volume of 6 cm^3, we adopt the value $V_E = 6$ cm^3 throughout the present work. The earpiece may include a device (not shown) to provide acoustic inertance to aid in frequency-response equalization. The nature of these equalizers will be thoroughly discussed in a succeeding paper.[9] The cell with equalizer, tapered acoustic tube, and earpiece with equalizer are the basic parts of the photophone. This design can be optimized to provide the desired sound level in the earpiece equalized across the band with the minimum optical power input to the cell. At the cost of considerably increased optical power the cell and earpiece can be directly coupled instead of coupled through a transformer; we shall refer to this case as the direct-coupled (DC) photophone and the case shown in Fig. 1 as the transformer-coupled (TC) photophone. The DC photophone will be discussed in the succeeding paper.[9] It allows a useful comparison with the TC photophone.

The equivalent circuit of the TC photophone is shown in Fig. 2. The optoacoustic effect is equivalent to a current generator s_L in parallel with the acoustic impedance z_C of the cell. Acoustic impedances needed in this paper are summarized in Appendix A. The quantities p and s in Fig. 2 are complex amplitudes for signals of pressure and flow having the time dependence $e^{-i\omega t}$. The instantaneous optical power delivered to the cell is

$$P(t) = P_0 + \mathrm{Re}(P_\omega e^{-i\omega t}) , \tag{1}$$

where P_0 is the average power and P_ω is the complex amplitude at angular frequency $\omega = 2\pi f$. We call $|P_\omega|$ the power modulation. Equation (1) is the model for the definition of all signal quantities in this paper. The sound source s_L is proportional to P_ω according to Eq. (37). The tapered acoustic tube is shown as a step-down transformer, but it is not an ideal transformer. In particular it is lossy due to thermoviscous damping (TVD) in the small end of the tube. Acoustic transformers are summarized in Appendix B. At this point we treat it as an unspecified two-port network represented by a matrix $[T]$ in the equations

$$\begin{aligned} p_1 &= T_{11} p_2 + T_{12} s_2 , \\ s_1 &= T_{21} p_2 + T_{22} s_2 . \end{aligned} \tag{2}$$

Similarly the equalizers are represented by matrices [EQ1] and [EQ2]. The overall coupling matrix is the matrix product

$$[C] = [\mathrm{EQ1}] \cdot [T] \cdot [\mathrm{EQ2}] , \tag{3}$$

and the solution of the circuit is

$$\frac{s_L}{p_E} = C_{21} + \frac{C_{11}}{z_C} + \frac{C_{22}}{z_E} + \frac{C_{12}}{z_C z_E} . \tag{4}$$

We regard the sound intensity in the earpiece

$$I = \langle p(t)_E^2 \rangle_{\mathrm{time}} = \tfrac{1}{2} |p_E|^2 \tag{5}$$

as the output of the photophone. It is customary and convenient to express this in sound-pressure-level decibels[11] SPL(dB)

$$\mathrm{SPL(dB)} = 10 \log_{10}[I/(2 \times 10^{-4} \text{ dyn cm}^{-2})^2] , \tag{6}$$

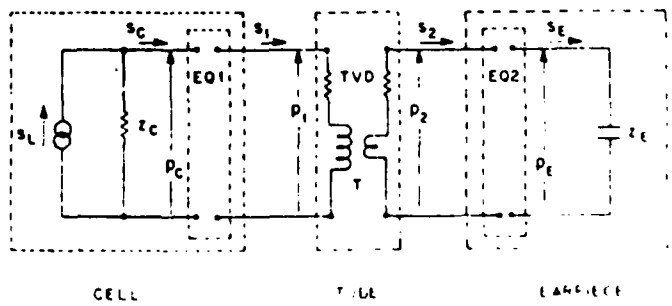

FIG. 2. Equivalent circuit for the transformer-coupled photophone. The unspecified 2-port networks EQ1, EQ2 are equalizers needed to obtain a flat frequency response.

where 2×10^{-4} dyn/cm^2 is the nominal rms pressure at the threshold of hearing. The present average level in the telephone network[2] is SPL = 81 dB, which we will use in this study to make numerical comparisons. Another requirement, called equalization, is that I should be flat (in a smoothed sense to be defined later) within 3 dB over the desired band 300–3300 Hz. It follows from Eq. (37) that I has the general form

$$I = [R_0^2 G_A^2 (\gamma_0 - 1)^2 / 2(\gamma_0 p_0)^2] \, |P_\omega|^2 H_\omega \,, \tag{7}$$

where the *response function* H_ω

$$H_\omega = |(p_E/s_L)|^2 (G_M^2/R_0^2) |G_\omega|^2 \tag{8}$$

contains all dependence on frequency, the properties of the coupling matrix $[C]$, the acoustic properties of the absorbing medium, and the cell volume V_C. The constant R_0 having the dimensions of an acoustic impedance is included to make H_ω dimensionless. The value adopted here, to normalize H_ω to a convenient magnitude, is

$$R_0 = 880 \text{ g/sec cm}^4 \,. \tag{9}$$

The quantity

$$(\gamma_0 - 1)^2 / 2(\gamma_0 p_0)^2 = 4.04 \times 10^{-14} \text{ (cm}^2\text{/dyn)}^2 \tag{10}$$

is a constant (approximately) of the atmosphere. Important acoustic properties of air and xenon are listed in Table I. The *utilization factor* for light absorption G_A is given by Eq. (38); it represents the fraction of light incident in the fiber which is actually absorbed in the interior of the cell. In a properly designed cell it should be very close to unity. The *figure of merit* for the absorbing medium is G_M defined by Eq. (55); it is a thermodynamic property of the absorbing medium which reduces to unity for a medium equivalent to air. The *dispersion function* G_ω defined by Eq. (54) and given for a spherical cell by Eq. (A15), contains the frequency dependence due to thermal conduction in the cell. For $V_C > 1 \times 10^{-3}$ cm^3, $|G_\omega|^2$ lies in the range 0.5–1.0 and increases monotonically with frequency.

TABLE I. Acoustic properties of air and xenon at 1 atm pressure $p_0 = 1.013 \times 10^6$ dyn/cm^2.

Property	Unit	Air[a] (288.16 °K, 1 atm)	Xenon (298 °K, 1 atm)
molecular weight		28.966	131.30[b]
density ρ	g/cm^3	1.225×10^{-3}	5.397×10^{-3}[b]
sound speed c	cm/sec	3.403×10^4	1.769×10^4
specific heat C_p	erg/g K	1.006×10^7	1.582×10^6[b]
specific heat ratio γ		1.403	1.667[b]
viscosity η	dyn sec/cm^2	1.789×10^{-4}	2.246×10^{-4}[c]
thermal conductivity κ	erg sec cm K	2.533×10^3	5.62×10^2[c]
Kirchhoff constant γ'	cm/sec$^{1/2}$	0.565	0.375
$\nu = \kappa/\rho C_p$	cm^2/sec	0.2884	0.1098
$\mu = \eta/\rho$	cm^2/sec	0.1461	4.162×10^{-4}

[a] Data for air refer to the standard atmosphere at sea level from L. Beranek, "Acoustic Properties of Gases," in *American Institute of Physics Handbook*, 2nd ed. (McGraw-Hill, New York, 1963), Chap. 3, pp. 3-59 to 3-70.

[b] Y. S. Touloukian and T. Makito, *Thermophysical Properties of Matter, Vol. 6* (Plenum, New York, 1970), Numerical Data 25a.

[c] *Handbook of Chemistry and Physics* (CRC Press, Cleveland, 1974), 55th ed., edited by R. C. Weast, p. F-59.

[d] Reference c, p. E-16.

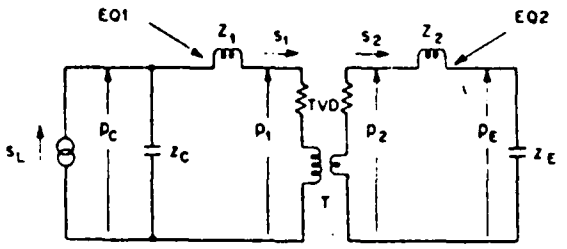

FIG. 3. Equivalent circuit analyzed in Sec. II having hypothetical pure-inertance equalizers.

Equations (7) and (8) reduce to

$$I = 3.13 \times 10^{-6} G_A^2 |P_\omega|^2 H_\omega \,, \tag{11}$$

$$H_\omega = 1.29 \times 10^{-6} G_M^2 \, |G_\omega|^2 \, |(p_E/s_L)|^2 \,, \tag{12}$$

when use is made of Eqs. (9) and (10) and cgs units are used throughout. For the presentation of our results we find it convenient to define a standard optical-signal power input to the absorbing medium

$$\text{standard } G_A |P_\omega| = 2.8 \text{ mW} = 2.8 \times 10^4 \text{ erg/sec} \,. \tag{13}$$

Referred to the standard input, H_ω can be expressed in SPL(dB)

$$\text{SPL(dB)} = 10 \log_{10} H_\omega + 87.9 \,. \tag{14}$$

Our discussion will now proceed in two phases: (a) in the first phase (contained in this paper and which we call analysis) we determine the simplest analytical models for the equalizers EQ1, EQ2 which can provide equalization, (b) in the second phase (contained in the succeeding paper[9] and which we call realization) we determine the specifications for actual physical devices of simple structure which approximate the analytical models determined in (a). In this paper it is established what the optimum level of response is after equalization. In the succeeding paper[9] the important result is established that simple devices, such as a column of air or a diaphragm of plastic, are capable of providing both equalization and optimum level of response.

II. ANALYSIS OF THE PHOTOPHONE

We consider the circuit of Fig. 3 in which EQ1 and EQ2 are series impedances. The equalizer matrices have the general form

$$[\text{EQ}] = \begin{bmatrix} 1 & Z \\ 0 & 1 \end{bmatrix} . \tag{15}$$

The solution of the circuit Eq. (4) reduces to

$$\frac{s_L}{p_E} = \frac{T_{11}}{z_C}\left(1 + \frac{Z_2}{z_E}\right) + \frac{T_{12}}{z_E z_C} + T_{21}\left(1 + \frac{Z_1}{z_C}\right)\left(1 + \frac{Z_2}{z_b}\right) + \frac{T_{22}}{z_E}\left(1 + \frac{Z_1}{z_C}\right) . \tag{16}$$

The transformer coefficients T_{mn} are given in general by Eqs. (B9). We specialize to an exponentially-tapered tube described by Eqs. (B16) and (B19) and cut-off frequency

$$f_0 = \alpha c/2\pi = 200 \text{ Hz} . \tag{17}$$

This value was chosen to be well below the lower limit 300 Hz of our desired passband. We next introduce two approximations which are reasonably well justified: (a) the boundary layer approximation Eq. (B17) for the sound propagation, and (b) the neglect of TVD except in exponents.

With these assumptions Eq. (16) gives

$$\left|\frac{p_E}{s_L}\right|^2 = \left(\frac{2}{\pi}\frac{\rho c n}{r_1 r_2 k}\right)^2 \frac{\exp[-(r_0/r_1)\xi(k)]}{|g(k)+h(k)\exp(2inl+i\Delta-\Delta)|^2} , \tag{18}$$

with

$$g(k) = \left(1+\frac{Z_1}{z_C}+\frac{z_1}{z_C}\right)\left(\frac{z_2}{z_E}\frac{m_+}{m_-}-\frac{Z_2}{z_E}-1\right) ,$$
$$h(k) = \left(1+\frac{Z_1}{z_C}+\frac{z_1}{z_C}\frac{m_+}{m_-}\right)\left(1+\frac{Z_2}{z_E}-\frac{z_2}{z_E}\right) . \tag{19}$$

Here n and $m_\pm$ given by Eqs. (B19) describe propagation in the lossless exponential tube, and the characteristic impedances z_1, z_2 are just those of a lossless tube

$$z_j = (i/m_+)(\omega\rho/\pi r_j^2) , \quad j = 1, 2 . \tag{20}$$

TVD is represented in Eq. (18) by r_0, $\xi(k)$, and $\Delta(k)$ given by Eqs. (B18), (B21), and (B22), respectively. The constants ρ, c, and r_0 refer to the gas in the tube which could be air, but it will be shown later than xenon gives considerably higher response. The most important effect of TVD is the attenuation factor in the numerator of Eq. (18). The squared magnitude in the denominator of Eq. (18) represents the interference of waves traveling in opposite directions in the tube. This interference sets up standing waves in the tube and causes oscillations in the response as a function of frequency. The peak-to-valley ratio of these oscillations depends on the round-trip attenuation $e^{-\Delta}$ due to TVD; if $e^{-\Delta} \ll 1$, the oscillations are damped out. The oscillations also depend on the round-trip reflection coefficient (one reflection off each end) $h(k)/g(k)$. Equations (12) and (18) now give

$$H_\omega = G_M^2\left(\frac{\rho c}{\rho_0 c_0}\right)^2\left(\frac{9.1\times10^{-4}\text{ cm}^4}{r_1^2 r_2^2}\right)\left(\frac{n}{k}\right)^2$$
$$\times\frac{\exp[-(r_0/r_1)\xi(k)]|G_\omega|^2}{|g(k)+h(k)\exp(2inl+i\Delta-\Delta)|^2} . \tag{21}$$

No assumption has yet been made as to the form of z_C, Z_1, z_E, or Z_2.

We base our analysis on the model in which z_C, z_E, Z_1, and Z_2 are all pure imaginary

$$z_C = i\gamma p_0/\omega V_C' , \quad z_E = i\gamma p_0/\omega V_E'$$
$$Z_1 = -i\omega L_1 , \quad Z_2 = -i\omega L_2 , \tag{22}$$

where V_C', V_E' are effective volumes defined by

$$V_C' = (\gamma/\gamma_C)(\partial\ln\rho/\partial\ln p)_T V_C ,$$
$$V_E' = (\gamma/\gamma_0)V_E , \tag{23}$$

and γ_C, γ, and γ_0 refer to the gases (possibly different) in the cell, tube, and earpiece (air) respectively. For generality we include in V_C' a thermodynamic factor from Eq. (56) to take account of possible nonideal behavior of the cell gas; otherwise z_C, z_E are just the ordinary approximation, Eq. (A10), for the adiabatic impedance of a closed volume. The important effects of thermal conduction are contained in the factor $|G_\omega|^2$ in Eq. (21). It now follows from Eqs. (19) that

$$h(k) = -g(k)^*$$
$$|g(k)|^2 = \left[\left(1+\frac{Z_1}{z_C}\right)^2+\left(\frac{kV_C'}{\pi r_1^2}\right)^2-\left(\frac{2\alpha V_C'}{\pi r_1^2}\right)\left(1+\frac{Z_1}{z_C}\right)\right]$$
$$\times\left[\left(1+\frac{Z_2}{z_E}\right)^2+\left(\frac{kV_E'}{\pi r_2^2}\right)^2+\left(\frac{2\alpha V_E'}{\pi r_2^2}\right)\left(1+\frac{Z_2}{z_E}\right)\right] . \tag{24}$$

This can be further simplified in appearance by defining resonant frequencies

$$\bar\omega_1 = (\gamma p_0/V_C' L_1)^{1/2}, \quad \bar\omega_2 = (\gamma p_0/V_E' L_2)^{1/2} , \tag{25}$$

so that

$$1+Z_1/z_C = 1-(\omega/\bar\omega_1)^2$$
$$1+Z_2/z_E = 1-(\omega/\bar\omega_2)^2 . \tag{26}$$

The only dissipation in this model is TVD in the transformer. *It follows that the reflection coefficient* $h(k)/g(k)$ has magnitude unity and the oscillations in response must have the maximum possible peak-to-valley ratio. The oscillations in H_ω in Eq. (21) are described by the function

$$|1+(h/g)\exp(2inl+i\Delta-\Delta)|^{-2} = (1-2e^{-\Delta}\cos\Phi+e^{-2\Delta})^{-1} , \tag{27}$$

where

$$g(k) = |g|e^{i\psi}$$
$$\Phi = 2nl+\Delta-2\psi . \tag{28}$$

Peaks correspond to $\cos\Phi = 1$, valleys to $\cos\Phi = -1$; the spacing of peaks is mainly determined by the rapidly varying function of frequency $2nl$. The average value of Eq. (27) over one cycle of Φ, treating Δ as constant, is

$$(2\pi)^{-1}\int_0^{2\pi} d\Phi(1-2e^{-\Delta}\cos\Phi+e^{-2\Delta})^{-1} = (1-e^{-2\Delta})^{-1} . \tag{29}$$

We can now write the response H_ω and the smoothed response $\langle H_\omega\rangle$ in the forms used for computation:

$$H_\omega = G_M^2\left(\frac{\rho c}{\rho_0 c_0}\right)^2\left(\frac{9.1\times10^{-4}\text{ cm}^4}{r_1^2 r_2^2}\right)\left(\frac{n}{k}\right)^2\frac{\exp[-(r_0/r_1)\xi(k)]|G_\omega|^2}{|g(k)|^2(1-2e^{-\Delta}\cos\Phi+e^{-2\Delta})} \tag{30}$$

$$\langle H_\omega\rangle = G_M^2\left(\frac{\rho c}{\rho_0 c_0}\right)^2\left(\frac{9.1\times10^{-4}}{r_1^2 r_2^2}\right)\left(\frac{n}{k}\right)^2\frac{\exp[-r_0/r_1)\xi(k)]}{|g(k)|^2(1-e^{-2\Delta})}|G_\omega|^2 . \tag{31}$$

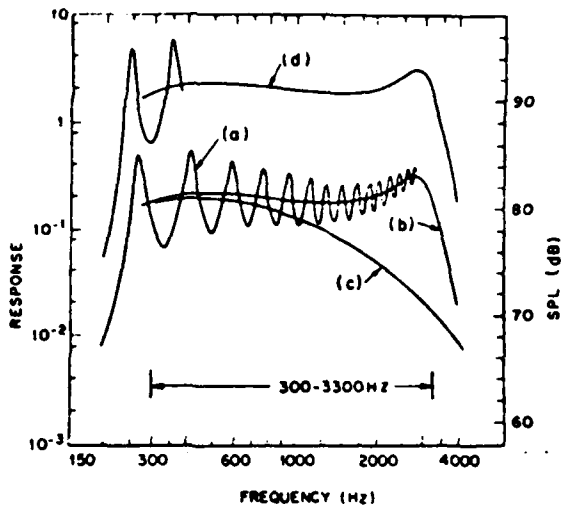

FIG. 4. Response versus frequency for optimized equalized photophone having pure-inertance equalizers. Curve (a) gives H_ω (scale on left) Eq. (30); (b) gives smoothed response Eq. (31); (c) gives smoothed response for no equalization, assuming parameters of Eq. (32); curve (d) gives response for same input power of xenon photophone with parameters Eq. (33). SPL scale refers to an input optical power modulation 2.8 mW.

Figure 4 curve (a) shows H_ω calculated for an optimized, equalized air photophone (cell, tube, and earpiece gases all air or equivalent to air) with the following specifications:

$$\begin{aligned} &G_M^2 = 1, && |G_\omega|^2 \text{ for air in sphere,} \\ &f_0 = 200, && \bar{f}_1 = \bar{f}_2 = 3100 \text{ Hz,} \\ &V_E = 6, && V_C = 2.5\times10^{-3} \text{ cm}^3, \\ &r_1 = 0.036, && r_2 = 0.85, \quad l = 85 \text{ cm.} \end{aligned} \tag{32}$$

We do not know *a priori* how close $G_M^2 = 1$ can be achieved for an absorbing gas or a solid suspended in air (see Sec. III). The oscillations in H_ω are seen to be very similar to those of a stethoscope.[12] The smoothed response $\langle H_\omega \rangle$ is shown in curve (b). Our *criterion of equalization* is that $\langle H_\omega \rangle$ should be flat within 3 dB over the band 300–3300 Hz; this requirement is satisfied as shown by curve (b). We do not know if the oscillations in H_ω would give the TC photophone an objectionable tone quality. The peak-to-valley ratio of these oscillations can be reduced by making r_1 smaller, which would increase Δ; we have not studied how far this can be carried before it becomes impossible to equalize the high-frequency end of the band in the present model. In this paper we assume it is sufficient just to equalize $\langle H_\omega \rangle$. With no equalization the smoothed response $\langle H_\omega \rangle_{NEQ}$ is shown in curve (c) of Fig. 4; this case corresponds to $f_1, f_2 \to \infty$ in Eqs. (32). Much use will be made of $\langle H_\omega \rangle_{NEQ}$ in the realization of equalizer devices using the method of equalization factors described in the succeeding paper.[9] The need for equalization is very apparent from curve (c) since $\langle H_\omega \rangle_{NEQ}$ is down at 3300 Hz by nearly 11 dB. The SPL(dB) scale in Fig. 4 is based on the standard input Eq. (13) and the relation Eq. (14). We see that curve (b) gives 81 dB at 1000 Hz, the required output, which is the reason for our choosing Eq. (13) as the standard input. Note that equalization brings up the high-frequency response without sacrificing low-frequency response.

Figure 4 curve (d) shows H_ω and $\langle H_\omega \rangle$ calculated for an optimized, equalized xenon photophone (xenon in cell and tube, air in earpiece) with specifications:

$$\begin{aligned} &G_M^2 = 2, && |G_\omega|^2 \text{ for xenon in sphere,} \\ &f_0 = 200, && \bar{f}_1 = \bar{f}_2 = 3100 \text{ Hz,} \\ &V_E = 6, && V_C = 6.0\times10^{-4} \text{ cm}^3, \\ &r_1 = 0.024, && r_2 = 1.27, \quad l = 56 \text{ cm.} \end{aligned} \tag{33}$$

We do not know how close $G_M^2 = 2$ can be achieved in practice. The improvement over the air photophone is 10 dB across the band; reduced TVD and increased impedance ρc both contribute to this improvement, as well as an increased material figure of merit G_M resulting from the largest specific-heat ratio γ possible. The xenon in the tube and cell could be retained by a thin plastic diaphragm at the junction of the tube and earpiece at the location shown by the dashed line in Fig. 1. It will be shown in the succeeding paper[9] that this diaphragm could also serve as the earpiece equalizer EQ2. For the xenon photophone an 81-dB-SPL output at 1000 Hz could be achieved with an optical input

$$G_A|P_\omega| = 0.89 \text{ mW (xenon)}. \tag{34}$$

This is the sensitivity of the xenon photophone; the air photophone has the sensitivity Eq. (13).

In arriving at the specifications Eqs. (32) and (33) we regarded $V_E = 6$ cm^3 and $f_0 = 200$ Hz as initially prescribed. Then r_1, r_2 were determined so as to maximize $\langle H_\omega \rangle_{NEQ}$ at a specific frequency $f_m = 2000$ Hz. Finally V_C and $\bar{f}_1, \bar{f}_2$ were determined to achieve equalization in $\langle H_\omega \rangle$ within 3 dB over the band. We believe the resulting design is very nearly optimum with regard to response level for equalized responses. However, a somewhat higher value of f_0, which would reduce TVD, would appear to be possible without giving up adequate response down to 300 Hz, and a somewhat lower choice of optimization frequency f_m might give a little higher level while still permitting equalization in the present model. In optimizing r_1, r_2 we ignore the factor $(1 - e^{-2\Delta})^{-1}$ in Eq. (31) which arises from the oscillations. If this factor were included in the optimization procedure, a larger value of r_1 would result. This would enhance the oscillations. Since we do not want to "encourage" these oscillations, which we regard as undesirable, by giving them weight in determining r_1, r_2, we omit the factor. It then follows from Eq. (31) that r_2 is determined by minimizing the quantity $r_2^2|g(k)|^2$; from Eq. (24) we obtain, with $Z_2 = 0$,

$$r_2 = (k_m V_E'/\pi)^{1/2} = (2f_m V_E'/c)^{1/2}. \tag{35}$$

Similarly r_1 is obtained by maximizing $r_1^{-2}|g(k)|^{-2} \times \exp[-(r_0/r_1)\xi_m]$; in practice this is almost independent of V_C so r_1 is actually determined by TVD

$$r_1 = \tfrac{1}{2} r_0 \xi_m \approx (\gamma'/2f_0)(f_m/\pi)^{1/2}. \tag{36}$$

Finally V_C and $\bar{f}_1 = \bar{f}_2 = \bar{f}$ were determined by trial using the complete expression Eq. (31) until curve (b) of Fig.

4 was obtained and the procedure terminated. The same procedure was followed for the xenon case, curve (d).

Because of the way of choosing r_2, earpiece equalization was not as important as cell equalization; in fact, equalization can be achieved with Z_1 alone, setting $Z_2 = 0$ in Fig. 3. Thus EQ2 is optional in the model being analyzed, but this is not necessarily true when realistic physical models of EQ1 are considered.

III. PRODUCTION OF SOUND

In this section it will be shown that the sound source s_L in Fig. 2 has the general form

$$s_L(\omega) = [(\gamma_0 - 1)/\gamma_0 p_0]\, G_A G_M G_\omega P_\omega \,, \tag{37}$$

where G_A is a utilization factor for the input light, G_M is a material figure of merit depending on the thermodynamic properties of the absorbing medium, and G_ω is a dispersion function depending on the dissipation in the cell.

To estimate G_A assume that all the light incident in the fiber is coupled out of the fiber into the interior of the cell by means of a suitable optical termination (not shown in Fig. 1); then the useful fraction of this light for the production of sound is

$$G_A = (e^{\beta d} - 1)(e^{\beta d} - w)^{-1} \,, \tag{38}$$

where β is the absorption coefficient of the absorbing medium, w is the wall reflectivity, and d is the mean distance between reflections off the wall. For practical purposes we take $d = (6V_C/\pi)^{1/3}$, the diameter of a sphere of volume V_C. If $\beta d \gg 1$, we have $G_A - 1$ but the thermal relaxation time becomes very short, as will be shown later, which causes G_ω to be small at low frequencies. Therefore $\beta d \gg 1$ is an undesirable condition. If $\beta d \ll 1$, it is essential at the same time to have high reflectivity $1 - w \ll 1$; then Eq. (38) reduces to

$$G_A \approx \{1 + [(1 - w)/\beta d]\}^{-1} \,. \tag{39}$$

By proper design it should be possible to achieve $G_A \approx 1$. From Eq. (39), which should hold in any practical case, we obtain a lower limit on β

$$\beta > (1 - w)/d \tag{40}$$

by requiring $G_A > 0.5$. The restriction, Eq. (40), is difficult to satisfy with gaseous absorbers in the visible region of the spectrum, but presents no problem for a solid absorber suspended in air. When $\beta d \ll 1$, the spatial distribution of the heat source in the cell is approximately uniform.

We proceed with a general analysis of the optoacoustic process in the absorption cell on the basis of a simplified model and obtain expressions for the sound source s_L and acoustic impedance z_C of the cell. In this model the absorbing medium is assumed to be a gas obeying some general equation of state

$$\rho = \rho(p, T) \,. \tag{41}$$

For generality we do not assume here that Eq. (41) is the ideal gas law, although for simplicity all of the numerical calculations presented in this paper are based on that assumption. The walls of the cell are a heat sink which is maintained at the constant temperature T_w. Within the cell $T(\vec{r}, t)$ varies with position $\vec{r}$ and time t, but the pressure $p(t)$ is spatially constant because the cell is much smaller than the wavelength of sound over the frequency range of interest. Imagine a massless piston at the opening of the cell into the tube which defines a time-dependent cell volume $V(t)$. The conservation of matter in $V(t)$ gives the relation

$$\frac{\partial}{\partial t} \int_{V(t)} \rho(\vec{r}, t)\, d\vec{r} = 0 \,. \tag{42}$$

The equation for thermal diffusion[13] with a uniform heat source is

$$-\kappa \nabla^2 T + \rho C_p \dot{T} = (G_A/V_C) P(t) + \chi \dot{p} \qquad (T = T_w = \text{constant on wall}) \,, \tag{43}$$

where

$$\chi = -(\partial \ln \rho / \partial \ln T)_p \tag{44}$$

has the value $\chi = 1$ for an ideal gas. Equation (43) is discussed and justified in Appendix C.

We believe the model is realistic for the case of a gaseous absorber in which the absorption does not involve dissociation or other type of chemical reaction. In this case Eq. (41) would be the ideal gas law. However, we believe the model may also apply to a wider range of situations to which the ideal gas law would not apply including gaseous absorbers that involve chemical reactions and tenuous solid absorbers disbursed in a gas. For example, when a fine mesh of cotton fibers is carbonized and used as the absorber, the combination of cottom charcoal and the air in which it is immersed may be regarded as a pseudo-gas. It is clear that an equilibrium equation of state like Eq. (41) exists for this pseudo-gas. It is also reasonable that this pseudo-gas has an effective thermal conductivity κ in the presence of a small temperature gradient. In applying the pseudo-gas model to a solid, three essential physical assumptions are involved: (a) under illumination by light (at levels of a few milliwatts) there is a sufficiently small difference between the average temperature of the gas and the temperature of the solid that the departure from local equilibrium is negligible, (b) all important gas adsorption–desorption processes are rapid compared to the highest frequency of interest, and (c) the solid and gas move together at the frequencies of interest. These assumptions represent an ideal which should be closely realizable in practice through the process of optimizing the absorbing medium. The breakdown of any of these assumptions will lead to a reduction of sound production. The fine-mesh solid we are considering here is similar to wool-like acoustic insulating materials that have been extensively studied theoretically and experimentally.[14,15] Our model corresponds to the low-frequency domain in which the solid is strongly coupled to the gas. As the decoupling frequency is approached from below there will be additional dissipation due to viscosity which is not in the model. However, we believe there should be no problem in getting the decoupling frequency well above 3300 Hz.[16] The assumption of a uniform heat source is not a serious limitation because it will be shown that at fre-

quencies high compared to the thermal relaxation rate (the frequency range of interest), the details of the heat-source distribution as well as the geometry of the cell become unimportant.

Write $V(t)$ in the form of Eq. (1):

$$V(t) = V_C + \mathrm{Re}(V_\omega e^{-i\omega t}) ,$$
$$V_\omega = i s_C/\omega , \tag{45}$$

where s_C is the flow out of the cell as shown in the circuit in Fig. 2. From Eqs. (42) and (43) we can compute s_C with and without $P(t)$; the general solution can be written in the form:

$$s_C = s_L - p_C/z_C , \tag{46}$$

where s_L is proportional to P_ω, which defines both s_L and z_C. Because the variation of $V(t)$ takes place at the wall where $\rho(\vec{r}, t) = \rho_w$, it follows from Eq. (42) to first order in sound amplitudes that

$$s_C = i\omega\rho_w^{-1} \int_C \rho_\omega(\vec{r})\, d\vec{r}$$
$$= i\omega\rho_w^{-1} \int_C \left\{\left(\frac{\partial\rho}{\partial p}\right)_T p_C + \left(\frac{\partial\rho}{\partial T}\right)_p T_\omega\right\} d\vec{r} , \tag{47}$$

where the integral is over the cell volume V_C. We neglect the spatial variation of the partial derivatives in Eq. (47) to obtain

$$s_C = \left(\frac{i\omega V_C p_C}{p_0}\right)\left(\frac{\partial \ln\rho}{\partial \ln p}\right)_T - \frac{i\omega\chi}{T_w} \int_C T_\omega(\vec{r})\, d\vec{r} , \tag{48}$$

where the partial derivatives are taken at p_0, T_w. This approximation is valid if the fractional rise in absolute temperature from the wall to the hottest spot in the interior is small compared with unity

$$|T(\vec{r}, t) - T_w| \ll T_w . \tag{49}$$

Let us write

$$\vec{r} = (-i\omega\rho C_p/\kappa)^{-1/2}\vec{y} , \tag{50}$$

$$T_\omega(r) = [i(G_A P_\omega/\omega\rho C_p V_C) + (\chi p_C/\rho C_p)]\, G(\vec{y}) . \tag{51}$$

The thermal diffusion equation, Eq. (43), then becomes simply

$$-\nabla_y^2 G + G = 1, \quad G = 0 \text{ on walls} . \tag{52}$$

It now follows from Eqs. (46), (48), and (51) that the sound source is

$$s_L = (\chi/\rho C_p T_w)\, G_A G_\omega P_\omega , \tag{53}$$

where the dispersion function

$$G_\omega = V_C^{-1} \int_C G(\vec{y})\, d\vec{r} \tag{54}$$

gives the frequency dependence due to thermal conduction. From the thermodynamic relation, Eq. (C5), the source can be written in the alternative form Eq. (37) with

$$G_M = \left(\frac{1-\gamma^{-1}}{1-\gamma_0^{-1}}\right)\left(\frac{\partial \ln T}{\partial \ln\rho}\right)_s , \tag{55}$$

the material figure of merit. For an ideal gas the partial derivative in Eq. (55) is unity. For air $G_M = 1$. Setting $P_\omega = 0$ in Eqs. (46), (48), and (51) gives the impedance

$$z_C = \left(\frac{i\gamma p_0}{\omega V_C}\right)[\gamma - (\gamma-1)G_\omega]^{-1}\left(\frac{\partial \ln\rho}{\partial \ln\rho}\right)_T . \tag{56}$$

The partial derivative is unity for an ideal gas; in this case Eq. (56) agrees with Eq. (A12). No assumption has been made about the shape of the wall, but it has been assumed that the heat source is spatially uniform. With this assumption the same function G_ω appears in s_L and z_C. For further discussion of G_ω, see Appendix A. In general G_ω depends on the wall shape and cell volume but always has the high- and low-frequency limits given by Eqs. (A13) and (A14), respectively. The function of interest here is $|G_\omega|^2$ which is shown in Fig. 5 for a sphere as a function of $\omega\tau$, where τ is the relaxation time in Eq. (A16). For an air-filled sphere, $|G_\omega|^2 > 0.5$ at all frequencies $f \geq 300$ Hz for a volume $V_C \geq 1.1\times10^{-3}$ cm^3.

We consider qualitatively the case in which the heat-source distribution is highly nonuniform due to large optical absorption $\beta d \gg 1$. We have already noted that this is an undesirable situation because it causes G_ω to be small at low frequencies. Physically this is due to the rapid escape of the optically generated heat to the wall. The thermal relaxation time τ for this case can be estimated from that for a sphere of radius a, Eq. (A18), by replacing $2a - \beta^{-1}$ to obtain

$$\tau \sim \rho C_p/60\,\kappa\beta^2 \quad (\beta d \gg 1) . \tag{57}$$

If we require $\omega\tau > 2$ for the lowest frequency of interest (300 Hz), we obtain an upper limit for β; combining this with Eq. (40) gives the range

$$(1-w)/d < \beta < (5\pi)^{1/2}(\rho C_p/\kappa)^{1/2} . \tag{58}$$

For air the value of the right side is 8.7 cm^{-1}; for $w = 0.98$, $V_C = 2.5\times10^{-3}$ cm^3 the left side is 0.12 cm^{-1}.

For a sphere of radius a the static temperature $T_0(r)$

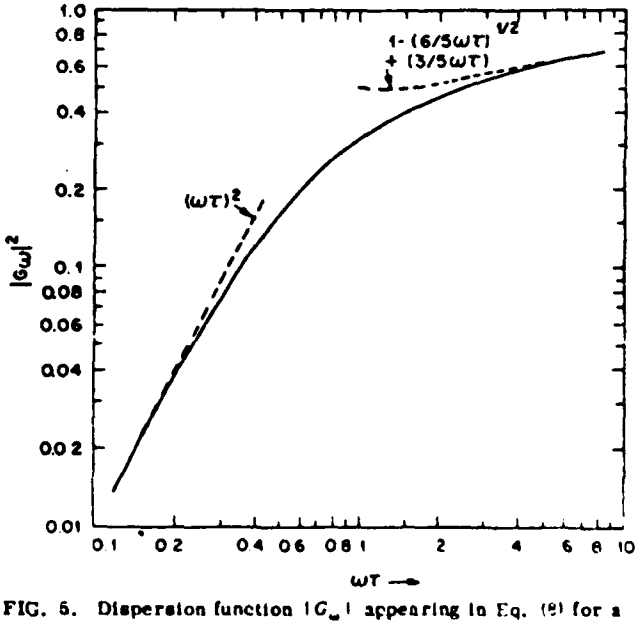

FIG. 5. Dispersion function $|G_\omega|$ appearing in Eq. (9) for a sphere according to Eq. (A15).

determined by Eq. (43) is

$$T_0(r) = T_\infty + (G_A P_0 a^2/6\kappa V_C)[1-(r/a)^2]\,. \tag{59}$$

It follows that the temperature rise ΔT is

$$\Delta T \leq 0.064\, G_A P_0/\kappa V_C^{1/3}\,, \tag{60}$$

with equality holding for a sphere. For $V_C = 2.5\times10^{-3}$ cm^3, Eq. (60) gives a rise of 1.9°K/mW, which completely justifies the assumption Eq. (49).

The absorption cell must contain some material which will absorb the incident light energy, transform the energy to heat, and transfer the heat to an immersing gas. The absorbing material can be the immersing gas itself, or a solid substance suspended in the gas volume, or a solid substance on the cell walls. In this section we have given a general theory for the optoacoustic effect on the assumption that the absorbing medium is a gas, or may be thought of as a gas, which is specified by its local pressure and temperature throughout the cell and has certain constant thermal properties. For example, a fine mesh of carbonized cotton immersed in air may be regarded as a pseudo-gas whose equation of state includes gas adsorption–desorption processes. When the amount of solid is very small, its only function is to provide optical absorption and the pseudo-gas is then acoustically very similar to the pure immersing gas. This justifies assuming $G_M = 1$ in Eq. (32) (air) and $G_M^2 = 2$ in Eq. (33) (xenon). The pseudo-gas concept enables us to treat formally one type of solid absorber without detailed knowledge of the physical mechanisms involved. Several observers[1,6] agree that the solids producing the largest optoacoustic signals are carbonaceous materials (lampblack, soot, charcoal) in a loose, porous, spongy condition. An important advantage of these materials is their broadband absorption with consequent usefulness for a large number of laser wavelengths.

We do not know whether the best gaseous abosrber is better or worse than the best carbonaceous absorber. If we assume that in either case β can be made to satisfy Eq. (58), the comparison comes down to the figure of merit G_M defined in Eq. (55). Taking $(\partial \ln T/\partial \ln p)_\gamma \approx 1$ we obtain the following illustrative values for several gases:

$$\begin{aligned} G_M^2 &\approx 1.0, && \text{air},\\ &\approx 2.0, && \text{Xe, Ar, etc.},\\ &\approx 0.67, && CO_2,\\ &\approx 0.12, && CClF_3. \end{aligned} \tag{61}$$

It is clear that gases having complex molecules (many atoms) tend to have small G_M because $\gamma - 1$ as the molecular size increases. Therefore it seems probable that a small amount of carbonaceous matter suspended in air, or preferably a monatomic gas, is a better absorbing medium than any gaseous absorber as complicated as $CClF_3$. This is only a tentative conclusion because we do not know how closely the pseudo-gas approaches the immersing gas in its acoustic properties or even how well the pseudo-gas model applies. Despite the above considerations it is of interest to learn whether suitable gaseous abosrbers exist for use with visible light. A brief discussion of this is given in Appendix D.

IV. SUMMARY

We have described the functional parts and basic principles of operation of optical telephone receivers employing the optoacoustic effect. The general theory of sound production by this effect has been presented on the basis of a model in which a dispersed solid absorber is treated as a pseudo-gas. This model avoids the need for detailed knowledge of the optoacoustic process in solid absorbers.

There are five functional parts of the transformer-coupled (TC) photophone, three of which are shown in Fig. 1: an absorption cell where sound is produced at high impedance by the absorption of intensity-modulated light, a tapered acoustic tube which transforms the sound to the impedance of the earpiece volume, and an earpiece which when pressed against the ear encloses a volume 6 cm^3. The parts not shown are devices, called equalizers, at the input and output of the tube to equalize the frequency response across the telephone band 300–3300 Hz. An important result of the analysis to be presented in a second paper[9] is that equalization can be achieved by simple means. Figure 4(a) shows the response for optimized cell, tube, and purely inertial equalizers; the SPL scale refers to an optical modulation of $|P_\omega| = 2.8$ mW. Figure 4(d) shows the improved response for a xenon-filled cell and tube.

A convenient measure of sensitivity for equalized optical receivers is the optical power modulation required to produce SPL = 81 dB in the earpiece volume of 6 cm^3. (When this quantity is small, the receiver is very sensitive.) We find the sensitivities 2.8 and 0.89 mW for the air and xenon photophones, respectively. These are independent of the average optical power. At present laser diodes[17] can emit as much as 25 mW of continuous optical power into an optical fiber and so qualify as sources of the optical carrier wave if a reasonable percentage modulation can be achieved. The tapered acoustic tube performs an essential function in bringing the photophone sensitivity within the capability of diode lasers.

We believe the xenon photophone represents the best receiver that can be achieved using the optoacoustic effect. Its use will require gas-tight construction including a diaphragm equalizer in the earpiece which will thus serve a dual function. When bought in quantities the xenon required for one photophone (whose gas volume is 32 cm^3) presently costs about $0.25. Thus, the higher performance of the xenon photophone may be obtained at only a modest increase in cost.

ACKNOWLEDGMENTS

We wish to thank J. K. Galt for stimulating our consideration of this problem. For helpful conversations we also acknowledge with thanks A. Rosencwaig, M. B. Robin, J. L. Peterson, C. D. Thurmond, R. L. Wallace, G. M. Sessler, and J. E. West.

APPENDIX A: ACOUSTIC IMPEDANCES

It is convenient to employ the analogy[A1] in which acoustic volume flow (s, $cm^3\,sec^{-1}$) is analogous to electric current, acoustic pressure (p, dyn cm^{-2}) is analogous to electric potential, and acoustic impedance ($z = p/s$, g sec^{-1} cm^{-4}) is analogous to electrical impedance. In this Appendix we present a concise resumé of the impedance formulas required in this work. Throughout we assume the time dependence $e^{-i\omega t}$ for all signals so that impedances have the general form $Z = R + (i/\omega C) - i\omega L$ for lumped resistance R, capacitance C, and inertance L.

A circular tube (duct, conduit) of radius a at low frequency $ka \ll 1$ is a transmission line with series distributed impedance $Z(x)$ and shunt distributed admittance $Y(x)$, where[A2]

$$Z = \left(\frac{-i\omega\rho}{\pi a^2}\right)\left[1 + \left(\frac{2}{r_v}\right)\frac{J_1(r_v e^{i\pi/4})}{J_0(r_v e^{i\pi/4})}\, e^{i(3\pi/4)}\right]^{-1}, \tag{A1}$$

$$Y = \left(\frac{-i\omega\pi a^2}{\rho c^2}\right)\left[1 - \left(\frac{2(\gamma-1)}{r_t}\right)\frac{J_1(r_t e^{i\pi/4})}{J_0(r_t e^{i\pi/4})}\, e^{i(3\pi/4)}\right], \tag{A2}$$

with

$$r_v = (\omega/\mu)^{1/2}a, \quad r_t = (\gamma\omega/\nu)^{1/2}a. \tag{A3}$$

The Bessel functions arise from the viscous and thermal boundary layers at the duct wall. In the boundary layer approximation, $r_v, r_t \gg 1$

$$Z \sim \left(\frac{-i\omega\rho}{\pi a^2}\right)\left[1 - \frac{2}{r_v}\, e^{i\pi/4} + \cdots\right]^{-1}, \tag{A4}$$

$$Y \sim \left(\frac{-i\omega\pi a^2}{\rho c^2}\right)\left[1 + \frac{2(\gamma-1)}{r_t}\, e^{i\pi/4} + \cdots\right]. \tag{A5}$$

In Eqs. (A5) and (A6) we may replace

$$a \to 2(\text{area})/(\text{perimeter}) \tag{A6}$$

for tubes of noncircular cross section. For a finite tube there is a contribution to the inertance L from the spreading of the flow at each end; for a tube of length l and area A with wide flanges (flow spreads into 2π solid angle to infinite)[A3]

$$L = (\rho l/A) + 2(\rho/4a), \tag{A7}$$

where the second term is for 2 flanges. In the narrow tube limit, $r_v, r_t \ll 1$

$$Z \sim (\omega\rho/\pi a^2)[(8/r_v^2) - (4i/3) + \cdots] \tag{A8}$$

$$Y \sim (\omega\pi a^2/\rho c^2)\{-i\gamma + [(\gamma-1)r_t^2/8] + \cdots\} \tag{A9}$$

valid only for circular tubes.

For a large enclosed volume V the impedance is approximately

$$z \approx i\gamma p_0/\omega V, \tag{A10}$$

corresponding to the adiabatic compression of the gas. In the limit $\omega \to 0$ Eq. (A10) breaks down and

$$z \xrightarrow[\omega\to 0]{} ip_0/\omega V \tag{A11}$$

corresponding to isothermal compression. In general z for a volume V filled with ideal gas is[A4]

$$z = (i\gamma p_0/\omega V)[\gamma - (\gamma-1)G_\omega]^{-1}, \tag{A12}$$

where G_ω depends on the size and shape of V. The effect of a nonideal gas is shown in Eq. (56). It is shown in Appendix C that

$$G_\omega \xrightarrow[\omega\to\infty]{} 1 \tag{A13}$$

in agreement with Eq. (A10). The low-frequency response can be used to define the thermal relaxation time τ

$$G_\omega \xrightarrow[\omega\to 0]{} -i\omega\tau. \tag{A14}$$

For a sphere of radius a

$$G_\omega = 1 - 3[(\varphi\coth\varphi - 1)/\varphi^2], \quad \varphi = (1-i)(15\omega\tau/2)^{1/2} \tag{A15}$$

with

$$\tau = \rho C_p a^2/15\kappa = \gamma a^2/15\nu. \tag{A16}$$

The limiting forms of Eq. (A15) are

$$G_\omega \xrightarrow[|\varphi|\gg 1]{} 1 - (3/\varphi) + (3/\varphi^2) + \cdots \tag{A17}$$

$$G_\omega \xrightarrow[|\varphi|\ll 1]{} (\varphi^2/15) - (2\varphi^4/315) + \cdots \tag{A18}$$

$$|G_\omega|^2 \xrightarrow[\omega\tau\gg 1]{} 1 - (6/5\omega\tau)^{1/2} + (3/5\omega\tau) + \cdots \tag{A19}$$

When the first two terms of Eq. (A17) give an adequate approximation, it is valid to write τ for any shape in the form

$$\tau \approx (9/15)(\gamma/\nu)(\text{volume/area})^2. \tag{A20}$$

The three-term approximation Eq. (A19) is shown in Fig. 5 along with the exact $|G_\omega|^2$ for a sphere. The impedance Eq. (A12) in the high-frequency limit reduces to

$$z \xrightarrow[\omega\tau\gg 1]{} (i\gamma p_0/\omega V)(1 - i\delta), \quad \delta = 3(\gamma-1)(30\omega\tau)^{-1/2}. \tag{A21}$$

APPENDIX B: ACOUSTIC TRANSFORMERS

An acoustic transformer is a duct whose cross sectional area A varies with distance x along the duct (tapered tube, horn). Such a tube can be treated as a transmission line with variable impedance $Z(x)$ and admittance $Y(x)$ per unit length

$$p' \equiv dp/dx = -Zs, \quad s' \equiv ds/dx = -Yp. \tag{B1}$$

Thermoviscous damping (TVD) is included in Z and Y. Eliminating s or p gives the horn equation

$$p'' - (\ln Z)'p' - ZYp = 0, \tag{B2}$$

$$s'' - (\ln Y)'s' - ZYs = 0. \tag{B3}$$

We shall assume that Eqs. (A1) and (A2) remain valid for a varying radius $a = a(x)$. This is confirmed by recent theoretical investigations of thermoviscous damping in tapered tubes.[B1] The lossless case (thermoviscous effects neglected) corresponds to the first terms of Eqs. (A4) and (A5), which give the usual form of the horn equation[B2]

$$p'' + (\ln A)'p' + k^2 p = 0, \tag{B4}$$

where $k = \omega/c$.

In general a transformer may be specified by a 2×2 matrix $[T]$ in the equation

$$\begin{bmatrix} p_1 \\ s_1 \end{bmatrix} = \begin{bmatrix} T_{11} & T_{12} \\ T_{21} & T_{22} \end{bmatrix} \begin{bmatrix} p_2 \\ s_2 \end{bmatrix} \tag{B5}$$

with sign conventions shown in Fig. 2. It can be shown[B1] from Eq. (B1) that $[T]$ satisfies the reciprocity relation

$$\det[T] = T_{11}T_{22} - T_{12}T_{21} = 1 , \tag{B6}$$

for arbitrary $Z(x)$, $Y(x)$. Let us take $x = 0$ at the input (p_1, s_1), $x = l$ at the output (p_2, s_2); let $p(x)_\pm$ denote a linearly independent pair of solutions of Eq. (B2); define

$$u = (\ln p_+)', \quad v = (\ln p_-)' \tag{B7}$$

and define the characteristic impedance

$$z(x) = -Z(x)/u(x) . \tag{B8}$$

Then T_{ij} can be expressed as follows[B1]:

$$\left.\begin{aligned} T_{11} &= M \\ T_{12} &= (1-M)z_2 \\ T_{21} &= N/z_1 \\ T_{22} &= (1-N)(z_2/z_1) \end{aligned}\right\} \times \exp\left(-\int_0^l u(x)\,dx\right)$$

$$M = \left[u_2 \exp\left(\int_0^l (u-v)\,dx\right) - v_2\right](u_2 - v_2)^{-1} , \tag{B9}$$

$$N = \left[u_2(v_1/u_1)\exp\left(\int_0^l (u-v)\,dx\right) - v_2\right](u_2 - v_2)^{-1} .$$

We assume $p(x)_+$ has been so chosen that $\mathrm{Re}[z(x)] > 0$; then if an impedance z_2 is put across the output, the input impedance will be $p_1/s_1 = z_1$.

For the uniform tube of constant radius a Eqs. (B7) and (B8) reduce to

$$\begin{aligned} &u = i\beta, \quad v = -i\beta , \\ &\beta = (-ZY)^{1/2}, \quad z(x) = z_0 = (Z/Y)^{1/2} . \end{aligned} \tag{B10}$$

For the lossless case this further reduces to

$$\beta = k, \quad z_0 = \rho c/\pi a^2 . \tag{B11}$$

In general β and z_0 are complex; for the case of air the real and imaginary parts can be read from the graphs given by Benade.[B3] If the tube has length b, Eqs. (B9) reduce to

$$[T] = \begin{bmatrix} \cos\beta b & -iz_0 \sin\beta b \\ (-i/z_0)\sin\beta b & \cos\beta b \end{bmatrix} \times e^{-i\beta b} . \tag{B12}$$

This is equivalent to the pi circuit (series impedance Z shunted fore and aft by impedance X) with[B4]

$$Z = -iz_0 \sin\beta b, \quad X = iz_0 \cot\tfrac{1}{2}\beta b . \tag{B13}$$

In the boundary layer (or "wide tube") approximation $(r_0, r_1 \gg 1)$ Eqs. (A4) and (A5) give the asymptotic expansion

$$\beta = k\left[1 + (\gamma'/a\omega^{1/2})\, e^{i\pi/4} + \cdots\right] , \tag{B14}$$

where

$$\gamma' = \mu^{1/2} + (\gamma - 1)(\nu/\gamma)^{1/2} \tag{B15}$$

is called Kirchhoff's constant. Recent calculations[B5] have shown that the fractional error in the γ' correction term in Eq. (B14) is about equal to the magnitude of the correction term. Although Eq. (B14) was long considered in substantial disagreement with experiment, recent experiments[B5–B7] have adequately confirmed it. Weston[B8] has carried the asymptotic expansion of β up to order $(a\sqrt{\omega})^{-3}$ and verified it experimentally[B7] for tubes as small as $a = 0.0127$ cm.

For the exponentially tapered tube

$$r(x) = r_1 e^{\alpha x}, \quad r_2 = r_1 e^{\alpha l} , \tag{B16}$$

a solution of Eq. (B2) is available[B1] only in the boundary layer approximation [order $(r\sqrt{\omega})^{-1}$]; for this solution Eqs. (B7) become

$$\left.\begin{matrix} u(x) \\ v(x) \end{matrix}\right\} = m_+ + \left(\frac{r_0}{r_1}\right)\left(\frac{\alpha}{k}\right)^{1/2} \frac{(k^2 + 2\alpha q m_+)}{\alpha \mp 2in}\, e^{-\alpha x} e^{i\pi/4} + \cdots , \tag{B17}$$

where

$$r_0 = 2\gamma'(\alpha c)^{-1/2} \tag{B18}$$

characterizes the boundary layer, m_+ characterize the lossless solutions[B9]

$$m_+ = -\alpha \pm in, \quad n = (k^2 - \alpha^2)^{1/2} , \tag{B19}$$

and $q = \mu^{1/2}/2\gamma'$. For the case of interest here $k \geq \alpha$, $r_0 \gg r_1$ we can write

$$\begin{aligned} &2\,\mathrm{Re}\left(\int_0^l u(x)\,dx\right) \approx -2\alpha l - (r_0/r_1)\,\xi(k) \\ &\int_0^l (u-v)\,dx \approx i\Delta - \Delta , \end{aligned} \tag{B20}$$

where

$$\xi(k) = \left(\frac{2\alpha}{k}\right)^{1/2}\left[\frac{2nk^2 - \alpha k^2 - 2q\alpha(\alpha n - \alpha^2 - 2n^2)}{\alpha(k^2 + 3n^2)}\right] , \tag{B21}$$

$$\Delta(k) = \left(\frac{r_0}{r_1}\right)\left(\frac{8n^2}{\alpha k}\right)^{1/2}\left[\frac{k^2 - \alpha^2 q}{k^2 + 3n^2}\right] . \tag{B22}$$

A discussion of the exponentially tapered electric line has been given by Burrows.[B10]

APPENDIX C: THERMODYNAMICS OF THE OPTOACOUSTIC EFFECT

We give here a thermodynamic discussion which confirms the correctness of Eqs. (43) and (55). A detailed derivation of Eq. (43) is given in Ref. 13. We offer the following simpler derivation based on three simple special cases: (a) For a reversible adiabatic compression, Eq. (43) reduces to

$$\begin{aligned} &\rho C_p (\partial T/\partial p)_s = \chi , \\ &(\nabla^2 T = 0, \quad P(t) = 0) , \end{aligned} \tag{C1}$$

which may be regarded as the definition of χ; (b) for a reversible constant-pressure heating Eq. (43) reduces to

$$\begin{aligned} &\rho C_p = \dot{V}_C^{-1}(\delta Q/\delta T)_p , \\ &(\nabla^2 T = 0, \quad \dot{p} = 0, \quad G_A P(t) = dQ/dt) \end{aligned} \tag{C2}$$

which is the definition of C_p; (c) for constant pressure Eq. (43) reduces to the standard equation for thermal diffusion.[C1] From the formulas[C2]

$$(\partial T/\partial p)_S = (\partial V/\partial S)_p$$
$$\rho C_p = (T/V)(\partial S/\partial T)_p \tag{C3}$$

it follows that χ can be written

$$\chi = \rho C_p (\partial V/\partial S)_p = -(T/\rho)(\partial \rho/\partial T)_p . \tag{C4}$$

These arguments confirm Eqs. (43) and (44). Other useful formulas involving χ are

$$\rho(C_p - C_v) = \chi(\partial p/\partial T)_V \tag{C5}$$

$$(\partial \rho/\partial p)_T = \chi^2/[T(C_p - C_v)] , \tag{C6}$$

which follow from Eq. (C4) and the formulas[C3]

$$\rho(C_p - C_v) = (T/V)(\partial V/\partial T)_p(\partial p/\partial T)_V$$
$$(\partial T/\partial P)_V(\partial V/\partial T)_p + (\partial V/\partial p)_T = 0 . \tag{C7}$$

If thermal transport can be neglected, the sound source and cell impedance can be calculated thermodynamically. The quantity $s_L/G_A P_\omega$ in Eq. (37) corresponds to $(\delta V/\delta Q)_p$. From Eqs. (C3), (C4), and (C5) we have

$$(\delta V/\delta Q)_p = (V\rho C_p)^{-1}(\partial V/\partial T)_p = (\rho C_p)^{-1}(\chi/T)$$
$$= p_0^{-1}(1-\gamma^{-1})(\partial \ln T/\partial \ln p)_V , \tag{C8}$$

which agrees with Eqs. (37) and (55) in the limit $G_\omega = 1$. The quantity $(i\omega z_C)^{-1}$ corresponds to $(\partial V/\partial p)_S$ which can be transformed as follows

$$(\partial V/\partial p)_S = -(\partial S/\partial p)_V(\partial V/\partial S)_p$$
$$= -(C_v/C_p)(\partial T/\partial p)_V(\partial V/\partial T)_p$$
$$= -(V/\gamma p)(\partial \ln \rho/\partial \ln p)_T . \tag{C9}$$

This agrees with Eq. (56) in the limit $G_\omega = 1$, which confirms the high-frequency limit Eq. (A14).

APPENDIX D: GASEOUS ABSORBERS

A gaseous absorber must have an optical absorption coefficient β in the range given by Eq. (58); for concreteness we write this in the approximate form

$$0.12\ \text{cm}^{-1} < \beta < 8.7\ \text{cm}^{-1} \tag{D1}$$

obtained by assuming $w = 0.98$, $V_C = 2.5\times10^{-3}$ cm^3, and $\rho C_p/\kappa$ for air from Table I. Practical considerations also require the gas to be chemically stable, noncorrosive, and nonpoisonous. Any temperature dependence of the absorption strength must be mild enough to leave β in the range Eq. (D1) from −30 °C to +40 °C, the range encountered by telephone sets. This will usually, but not always, rule out vapors in equilibrium with a condensed phase and gases whose boiling points fall within the above range. Thus the boiling point should preferably be below −30 °C (−22 °F). In a general way this requires low-molecular-weight compounds. The range Eq. (D1) lies rather high for gases at standard temperature and pressure and for absorption in the visible or near infrared. The reason for this is that the strong oscillator strength electronic absorption bands fall typically below 3000 Å wavelength while the strong oscillator strength vibrational–rotational transitions fall typically above 20 000 Å wavelength. Resonant absorptions between these limits are not common in gases and those occurring usually have low oscillator strengths.

Although we have not been able, as yet, to find a gas satisfying all the requirements, one gas which comes close is trifluoronitrosomethane (CF_3NO), a blue gas with a boiling point of −31 °C. This gas has a broad, fairly strong absorption band extending from 5000 Å to 7600 Å with a peak absorption near 6900 Å. The molar absorptivity ϵ is 15.9, 17.4, and 22.4 l mol^{-1} cm^{-1} at the wavelengths 6328 Å (HeNe laser line), 6471 Å (Kr laser line), and 6764 Å (Kr laser line).[D1] These values correspond to absorption coefficients $\beta \equiv \ln(I_0/I)/l$ of 1.4, 1.5, and 1.9 cm^{-1}, respectively, for atmospheric pressure and 300 K, values that fall within Eq. (D1). A problem with CF_3NO is its tendency by an excited-molecule mechanism, following light absorption in the band mentioned, to deposit on the walls of the vessel a decomposition product. Since the energy absorbed in this band is insufficient to cause dissociation of the molecule,[D1] it seems possible that a second gas could be found to use in a mixture with CF_3NO that would quench the excitation at a rate fast compared to the excited-molecule reaction rate. The quenching would, of course, convert the excitation energy to heat as desired. The related perfluoroalkanes have similar properties to CF_3NO.

A second gas worth consideration is nitrogen dioxide (NO_2) which has strong absorption[D2] from ~3200 to ~5000 Å giving it a red-brown color. However, it forms an equilibrium concentration of N_2O_4 whose absorption exists at wavelengths shorter than ~3700 Å. Further, NO_2 has its boiling point at 21 °C and its melting point at −9 °C. In spite of these disadvantages the absorption of the saturated NO_2 vapor comes close to remaining in the range Eq. (D1) throughout the temperature range of −30° to +40 °C. For the wavelength 4580 Å (cw Ar ion laser line) $\beta = 9.9$ cm^{-1} for $T = 40$ °C and $\beta = 0.090$ for $T = -30$ °C; for the wavelength 4880 Å (cw Ar ion laser line) $\beta = 5.3$ cm^{-1} at $T = 40$ °C and $\beta = 0.048$ cm^{-1} at $T = -30$ °C. The absorption measurements[D2] that these strengths are based on were made with a resolution of about 4 Å. Spectral measurements at high resolution[D3] (reciprocal dispersion of 0.1 Å/mm) show the absorption throughout the "band" discussed above is actually a dense forest of very sharp lines. Thus the absorption on some of these lines must be several times the values given above while at other wavelengths the absorption will vanish. Thus it is necessary to establish that the laser line chosen for use coincides with an absorption line. Other cw laser line wavelengths in this region which may fall in coincidence with an absorption line of NO_2 are 4545 Å, 4658 Å, 4727 Å, 4765 Å, 4965 Å, 5017 Å (all in Ar ion lasers), 4762 Å, 4825 Å (both in Kr ion lasers), and 4416 Å (in the HeCd laser).

Since at present only lasers whose emission can be transmitted at ultralow loss in glass-fiber waveguides would seem to be of interest, we will not give detailed

consideration to infrared lasers such as the CO and CO_2 lasers. However, it should be remarked that in the 5- and 10-μm wavelength regions characteristic of these lasers there are many gases with strong vibrational–rotational absorption bands. We have been unable as yet to find a gaseous absorber suitable for use with the Ga–Al–As heterostructure injection laser (~8800–9000 Å).

[1]A. G. Bell, "Upon the Production of Sound by Radiant Energy, Philos. Mag. 11, 510–528 (1881). See also U. S. Patent 241,909.

[4]F. T. Andrews and R. W. Hatch, "National Telephone Network Transmission Planning in the American Telephone and Telegraph Company," IEEE Trans. Commun. Tech., COM-19, 302–314 (1971).

[3]M. E. Delaney, "The Optic–Acoustic Effect in Gases," Sci. Prog. 47, 459–467 (1959).

[4]L. B. Kreuzer, "Ultralow Gas Concentration Infrared Absorption Spectroscopy," J. Appl. Phys. 42, 2934–2943 (1971).

[5]W. R. Harshbarger and M. B. Robin, Acc. Chem. Res. 6, 329–334 (1973); Chem. Phys. Lett. 21, 462–465 (1973).

[6]A. Rosencwaig, Opt. Commun. 7, 305–308 (1973); Science 181, 657–658 (1973).

[7]H. D. Arnold and I. B. Crandall, "The Thermophone as a Precision Source of Sound," Phys. Rev. 10, 22–38 (1917).

[8]E. C. Wente, Phys. Rev. 17, 333–345 (1922).

[9]D. A. Kleinman and D. F. Nelwon, "Physical Design of the Photophone," to appear in J. Acoust. Soc. Am. 59 (1976).

[10]E. E. Mott and R. C. Miner, "The Ring Armature Telephone Receiver," Bell Sys. Tech. J. 30, 110–140 (1951).

[11]USA Standards, "The Coupler Calibration of Earphones," USAS Z24.9-1949 (R1971).

[12]H. Frederick and H. Dodge, Bell Sys. Tech. J. 3, 531–549 (1924).

[13]R. N. Thurston, "Wave Propagation in Fluids and Normal Solids," in *Physical Acoustics, Vol. 1, Part A*, edited by W. P. Mason (Academic, New York, 1964), p. 47, Eq. (201).

[14]C. Zwikker and C. W. Kosten, *Sound Absorbing Materials* (Elsevier, New York, 1949), pp. 52–75.

[15]L. Beranek and S. Labate, "Properties of Porous Acoustic Materials," in *Noise Reduction*, edited by L. Beranek (McGraw-Hill, New York, 1960).

[16]Reference 14, p. 63.

[17]S. E. Miller, E. A. J. Marcatili, and T. Li, "Research Toward Optical Fiber Transmission Systems," Proc. IEEE 61, 1703–1751 (1973), Table V, p. 66.

[A1]H. F. Olson, *Acoustical Engineering* (Van Nostrand, New York, 1957), 3rd ed. Chap. 4, pp. 71–87.

[A2]A. H. Benade, "On the propagation of Sound Waves in a Cylindrical Conduit," J. Acoust. Soc. Am. 44, 616–623 (1968).

[A3]P. M. Morse and K. U. Ingard, *Theoretical Acoustics* (McGraw-Hill, New York, 1968), pp. 480–483.

[A4]F. B. Daniels, "Acoustical Impedance of Enclosures," J. Acoust. Soc. Am. 19, 569–571 (1947).

[B1]D. A. Kleinman, "Thermoviscous Damping of Sound in Tapered Tubes" (unpublished).

[B2]See Ref. A1, p. 101.

[B3]See Ref. 12, Figs. 6–9.

[B4]See Ref. 13, p. 62.

[B5]F. D. Shields, K. P. Lee, and W. J. Wiley, "Numerical Solution for Sound Velocity and Absorption in Cylindrical Tubes," J. Acoust. Soc. Am. 37, 724–729 (1965).

[B6]F. Shields and R. Lageman, "Tube Corrections in the Study of Sound Absorption," J. Acoust. Soc. Am. 29, 470–475 (1957).

[B7]D. E. Weston and J. D. Campbell, "Experiments on the Propagation of Plane Sound Waves in Tubes," Proc. Phys. Soc. 66, 769–774 (1953).

[B8]D. E. Weston, "The Theory of Propagation of Plane Sound Waves in Tubes," Proc. Phys. Soc. B66, 695–709 (1953).

[B9]J. B. Crandall, *Theory of Vibrating Systems and Sound*, (Van Nostrand, New York, 1927), 2nd ed., p. 158.

[B10]C. H. Burrows, "The Exponential Transmission Line," Bell Sys. Tech. J. 17, 555–573 (1938).

[C1]H. Carslaw and J. Jaeger, *Conduction of Heat in Solids* (Oxford, London, 1959), p. 10.

[C2]See Ref. 15, p. 35.

[C3]See Ref. 15, p. 45, Eq. 186.

[D1]J. Mason, J. Chem. Soc. 3904–3912 (1957).

[D2]T. Hall and F. Blacett, J. Chem. Phys. 20, 1745–1749 (1952).

[D3]A. Douglas and K. Huber, Can. J. Phys. 43, 74–81 (1965).

The photophone—physical design

D. A. Kleinman and D. F. Nelson

Bell Laboratories, Murray Hill, New Jersey 07974
(Received 15 September 1975; revised 28 February 1976)

The physical design of the response-equalizing components of the acoustic transformer-coupled photophone is presented. Two possible equalizers for the absorption cell—a gas column and a loaded diaphragm—are discussed; one equalizer for the earpiece, consisting of a diaphragm and screen, is also discussed. The optimization, equalization, and physical realization of a direct-coupled photophone (one not containing an exponentially tapered tube acting as an acoustic transformer) is also presented. It is found that its response is poorer than the transformer-coupled photophone by 25 dB.

Subject Classification: [43] 85.76, [43] 85.40, [43] 85.60.

LIST OF SYMBOLS

a	radius (cell, gas column, tubes, diaphragm)
A	area
b	length (gas column, tubes); radius of load ring
B	$=E_0/12(1-\sigma^2)$, E_0 = Young's modulus, σ = Poisson's ratio
c	sound speed
C	as subscript denotes cell
C_p, C_v	specific heats at constant pressure, constant volume
$C_{11}, \ldots, C_{22}$	matrix $[C]$, see Eq. (3), KN:I
d	see Eq. (38), KN:I
E	as subscript denotes earpiece
$f, \bar{f}$	frequency (Hz); resonant frequency
F	diaphragm reactance function, see Eq. (B6)
$g(k)$	see Eq. (19), KN:I
G_A, G_M, G_ω	see Eqs. (38), (55), (54), KN:I
$G_1(\omega), G_2(\omega)$	equalization factors, see Appendix A
h	porosity, see Eq. (44)
$h(k)$	see Eq. (19), KN:I
H_ω	response function, see Eq. (8), KN:I
$\langle H_\omega \rangle$	smoothed response function, see Eq. (31), KN:I
I	sound intensity, see Eq. (5), KN:I
J	diaphragm stress function, see Eq. (B12)
k	$=\omega/c$
l	length (acoustic tube, port)
L	inertance (g cm^{-4}), see Appendix A, KN:I
m	diaphragm loading mass
m_s, n	see Eqs. (B19), KN:I
n	number of tubes in porous leak
p	pressure (dyn cm^{-2})
p_0	$=1.013\times10^6$(dyn cm^{-2}) atmospheric pressure
P, P_ω, P_0	optical power (erg sec^{-1}), see Eq. (1), KN:I
q	$=\mu^{1/2}/2\gamma'$
Q	diaphragm loading parameter see Eq. (B8); heat in Appendix C, KN:I
r_0	see Eq. (B18), KN:I
$r(x), r_1, r_2$	see Eq. (B16), KN:I
R	resistance (g sec^{-1} cm^{-4})
s	flow (cm^3 sec^{-1})
s_L	sound flow source, see Eq. (37), KN:I
S	entropy
t	time, thickness
T	absolute temperature (K), transformer
$T_{11}, \ldots, T_{22}$	transformer matrix, see Eq. (B9), KN:I
u, v	see Eq. (B7), KN:I
V	volume (cm^3)
w	as subscript denotes cell wall
w	wall reflectivity
$w(r)$	diaphragm displacement
x	distance along tube
X	reactance (g sec^{-1} cm^{-4})
$X_d(\omega)$	diaphragm reactance
y	see Eq. (50), KN:I
$Y(x)$	distributed admittance (cm^3 sec g^{-1})
z	$=p/s$ impedance (g sec^{-1} cm^{-4})
z_0	characteristic impedance of tube, see Eq. (B10), KN:I
z_1, z_2	characteristic impedances, see Eq. (20), KN:I
$Z(x)$	distributed impedance (g sec^{-1} cm^{-6})
Z	impedance
α	exponential taper, see Eq. (B16), KN:I
β	optical absorption coefficient; acoustic propagation constant
γ	$=C_p/C_v$ (γ_0 refers to air)
γ'	Kirchhoff's constant Eq. (B15), KN:I
Δ	see Eq. (B22), KN:I
ϵ	see Eq. (45)
η	viscosity coefficient (dyn sec cm^{-2})
κ	thermal conductivity (erg sec^{-1} cm^{-1} K^{-1})
μ	$=\eta/\rho$ (cm^2 sec^{-1})
ν	$=\gamma\kappa/\rho C_p$(cm^2 sec^{-1})
ξ	see Eq. (B21), KN:I
ρ	density (g cm^{-3})
ρ_d	diaphragm density
σ	Poisson's ratio in Appendix B
τ	relaxation time (sec)
ψ	$=f/\bar{f}$
Φ	see Eq. (28), KN:I
χ	see Eq. (44), KN:I
ψ	see Eq. (28), KN:I
ω	$=2\pi f$ angular frequency (sec^{-1})
Ω	see Eq. (B7)

INTRODUCTION

In the preceding paper,[1] which will be referred to as KN:I, we presented the design principles of the photophone, a telephone receiver which produces voice-band sound in an earpiece directly from a power-modulated light wave from an optical fiber via the optoacoustic effect. The optimization of the response of the photophone for a given optical input was also presented. This led to the absorption cell, that produces the sound, being very small ($\sim 10^{-3}$ cm^3) and being coupled to the earpiece volume by an acoustic transformer in the form of an exponentially tapered tube. The resulting design is referred to as a transformer-coupled (TC) photophone. Consideration was also given to equalization of the response, that is, making it flat versus frequency to within 3 dB over the voice band 300–3300 Hz. This was accomplished by adding *equalizers* between the absorption cell and acoustic tube (EQ1) and between the acoustic tube and the earpiece volume (EQ2). The equalizers were represented in the analysis of KN:I by impedances of simple form—no specific physical realizations for equalizers were considered there. We assume the reader is acquainted with at least the Summary Section of KN:I.

In this paper we go on to consider two further aspects of the photophone. First, in Sec. II we present design criteria for specific physical equalizers that approximate the performance of the idealized equalizers assumed in the previous analysis. For EQ1 both a gas column and a loaded diaphragm will be considered; for EQ2 a combination of a diaphragm and a screen will be considered. Two Appendixes support the physical design discussion.

The second aspect to be considered is a comparison to a direct-coupled (DC) photophone, that is, a photophone without the tapered tube acoustic transformer. In Sec. III we present the optimization, the equalization, and the physical design of the DC photophone. This device, though simpler than the TC-photophone, has a poorer sensitivity than the latter by 25 dB. This demonstrates the importance of the tapered tube.

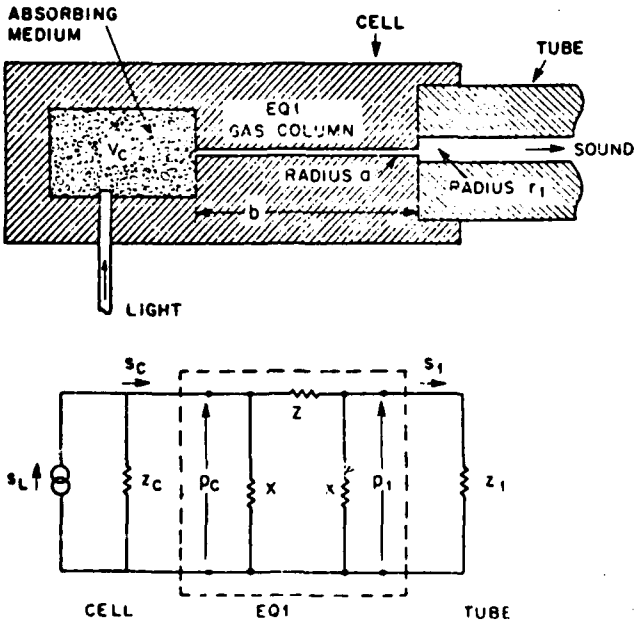

FIG. 1. The cell with gas-column equalizer and equivalent circuit.

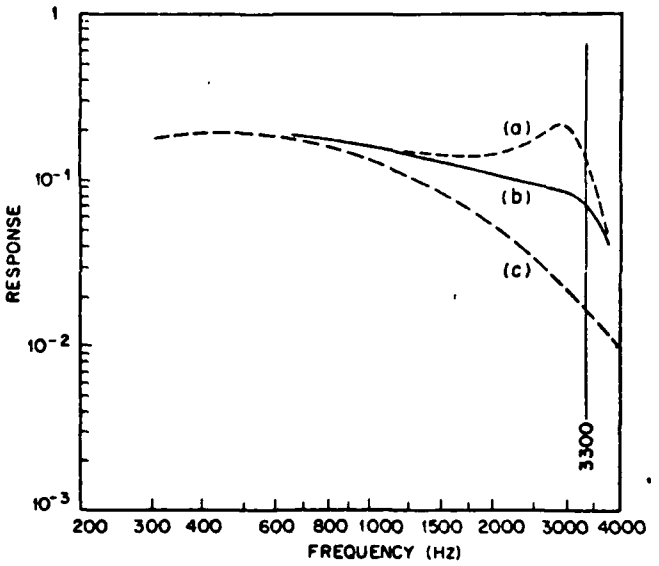

FIG. 2. Response of the air-column-equalized photophone with no earpiece equalization. Curve (a) gives response for a pure inertance equalizer, curve (b) gives Eq. (1) for the air column and cell Eq. (6), curve (c) gives the smoothed response for no equalization [see curve (c) of Fig. 4 of KN:I].

I. REALIZATION OF EQUALIZERS

The simplest physical model of an equalizer between the cell and the input to the tapered tube (EQ1) is a column of gas as shown in Fig. 1. The matrix for a gas column was developed in Eq. (E12) of KN:I. It is equivalent to that of the *pi*-circuit shown in Fig. 1 with X, Z given by Eq. (B13) of KN:I. The general equivalent circuit of the photophone is given in Fig. 2 of KN:I. We shall treat the effect of equalizers on the basis of a simplified circuit as shown in Fig. 1 in which the input to the tapered tube is regarded as the characteristic impedance z_1. We call this the *method of equalization factors*; a full discussion is given in Appendix A. The response of the photophone has been defined in Eqs. (7) and (8) of KN:I; the frequency response function H_ω contains structure due to standing wave resonances in the tube which is of no interest here, so we shall work with the smoothed response function $\langle H_\omega \rangle$ introduced in Eq. (31) of KN:I. According to our method the effect of EQ1 on the frequency response function $\langle H_\omega \rangle$ is given by

$$\langle H_\omega \rangle = \langle H_\omega \rangle_{NEQ}\, G_1(\omega)\,, \tag{1}$$

where $\langle H_\omega \rangle_{NEQ}$ is the response function with no equalization, curve (c) of Fig. 4 of KN:I, and

$$G_1(\omega) = |(s_1(EQ)/s_1(NEQ))|^2 \tag{2}$$

is the *equalization factor* calculated from the circuit of Fig. 1. In Eq. (2) the volume flow $s_1(EQ)$ is calculated for the circuit shown, $s_1(NEQ)$ is calculated for $Z = 0$,

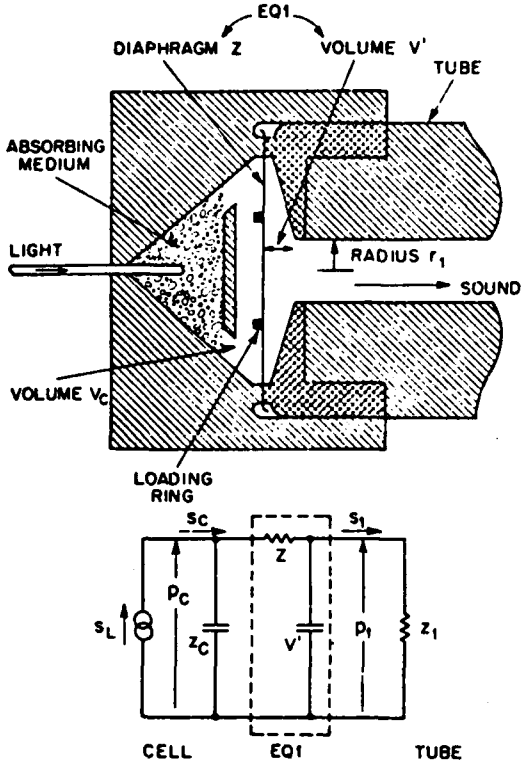

FIG. 3. The cell with loaded-diaphragm equalizer and equivalent circuit. Proportions agree with Eqs. (15) and (16).

$X = \infty$ and an air-filled cell of volume $V_C = 2.5\times10^{-3}$ cm^3 as called for in Eq. (32) of KN:I. Here we shall assume an air-filled cell of volume of the order 1×10^{-3} cm^3, the exact value to be determined so as to achieve equalization. The optoacoustic effect produces the volume flow source s_L in Fig. 1 given in general by Eq. (37) of KN:I. Although s_L depends on V_C through the dispersion function $|G_\omega|^2$ (which results from the finite thermal relaxation time of the absorption cell), the change in $|G_\omega|^2$ over the range of V_C we need to consider is unimportant and will be neglected. Then s_L is the same as that in $\langle H_\omega\rangle_{NEQ}$ and cancels out of $G_1(\omega)$. Thus the simple circuit is only used to compute ratios, the absolute response being determined by $\langle H_\omega\rangle_{NEQ}$. In practice we further simplify the circuit by replacing $z_1 \to |z_1|$, where from Eq. (20) of KN:I

$$z_1 \to |z_1| = c\rho/\pi r_1^2 = 1.02\times10^4 \text{ g/sec cm}^4. \qquad (3)$$

It is shown in Appendix A that the error in using Eq. (3) is unimportant.

The solution of the circuit of Fig. 1 is

$$\left(\frac{s_L}{s_1}\right)_{EQ} = \left(1+\frac{Z}{z_C}\right)+\frac{z_1}{z_C}+\frac{z_1}{X}\left(2+\frac{Z}{X}+\frac{Z}{z_C}\right)+\frac{Z}{X}$$

$$= \cos\beta b - \frac{iz_0}{z_C}\sin\beta b - i\frac{z_1}{z_0}\left(\sin\beta b + i\frac{z_0}{z_C}\cos\beta b\right), \qquad (4)$$

where β, z_0 are the propagation constant and characteristic impedance of the gas column given by Eqs. (B10) of KN:I. The real and imaginary parts of β and z_0 are given for air in Figs. 6–9 of Ref. 2. For z_C we have assumed the form Eq. (A22) of KN:I using τ calculated from Eq. (A17) of KN:I for a sphere of air of volume V_C. This includes dissipation in the cell and therefore is more general than Eq. (22) of KN:I used in the analytical model. However, it turned out that the effects of the dissipation to be expected from air are unimportant. The possibility exists that the presence of the solid absorber in the cell would significantly reduce the relaxation time τ and make the dissipation more important. Setting $Z = 0$, $X = \infty$, $V_C = 2.5\times10^{-3}$ cm^3 and using Eq. (3) we obtain from Eq. (4)

$$(s_L/s_1)_{NEQ} = 1 + 1.28\times10^{-6} f^2, \quad f \text{ in hertz.} \qquad (5)$$

We have computed $G_1(\omega)$ from Eqs. (2), (4), and (5) for an optimized air column. The best equalization we were able to obtain is shown in Fig. 2(b) corresponding to the following specifications:

$$a = 0.02, \quad b = 1.80 \text{ cm}, \quad V_C = 7.5\times10^{-4} \text{ cm}^3. \qquad (6)$$

Comparing curves (a) and (b) we see that the air column falls well short of the performance of an hypothetical pure inertance in providing equalization. Nevertheless, it does provide a worthwhile improvement in the high end of the band, and can provide equalization (flatness within 3 dB) with the aid of about 1.5 dB from the earpiece equalizer, an amount easily realized. Curve (c) of Fig. 2 is $\langle H_\omega\rangle_{NEQ}$, identical with curve (c) of Fig. 4 of KN:I. Comparing curves (b) and (c) shows that the air column gives 6-dB improvement at 3300 Hz.

A diaphragm can give a higher performance than an air column, and in addition can serve the second function of sealing the cell to keep out dirt and moisture or retain a special gas in the cell. Figure 3 shows a possible physical configuration for a cell with EQ1 provided by a diaphragm (clamped plate). The acoustic impedance $Z = iX_d(\omega)$ of a flat-loaded diaphragm is reviewed in Appendix B. The reactance $X_d(\omega)$ of a flat-loaded diaphragm is given by Eq. (B6). The structure of such a diaphragm and our notation is shown in Fig. 4. The dimensionless reactance function F appearing in Eq. (B6) is plotted in Fig. 5 for the case we have found to be optimum.

The solution of the circuit of Fig. 3 is

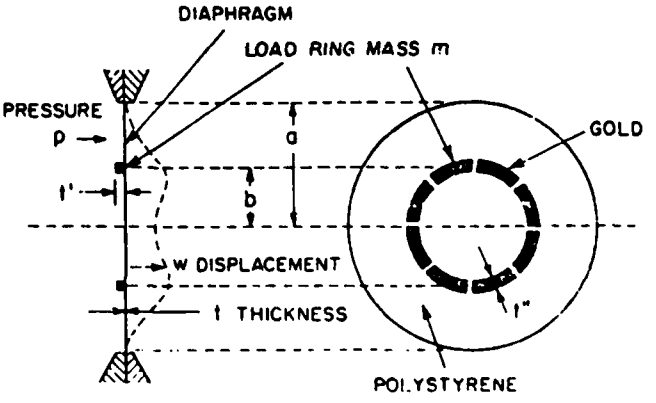

FIG. 4. Details of the ring-loaded diaphragm of Fig. 3. Also shown is the displacement for frequencies greater than 13000 Hz where the diaphragm reacts inertially.

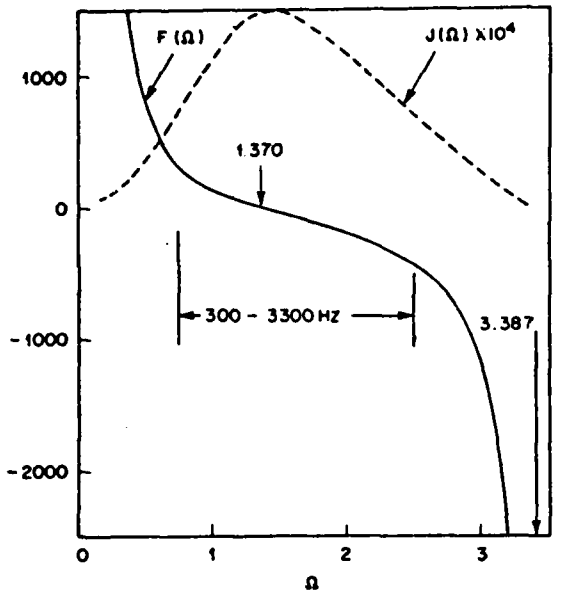

FIG. 5. Reactance function F defined in Eq. (B6) for loaded diaphragm with $Q = 35$, $b/a = 0.47$. Also shown (dashed) is $10^4 \times J(\Omega)$ where $J(\Omega)$ is the stress function appearing in Eq. (B12) and Eq. (17).

$$\left(\frac{s_L}{s_1}\right)_{EQ} = \left(1 + \frac{V_C \omega X_d(\omega)}{\gamma_0 p_0}\right) - i\left(\frac{kV_C}{\pi r_1^2}\right) , \tag{7}$$

where V' has been neglected, Eq. (A11) of KN: I and Eq. (3) have been used, and the cell has been assumed to be air filled. We define the resonant frequency $\bar{\omega}_1$ by the relation

$$1 + (V_C/\gamma_0 p_0)\,\bar{\omega}_1 X_d(\bar{\omega}_1) = 0 \ . \tag{8}$$

[In the design that we shall obtain Eq. (8) has only a single solution in the desired band.] It follows from Eqs. (8), (B6), and (B7) that

$$\frac{a^2}{t} = \frac{\bar{\Omega}^2 (B/\rho_d)^{1/2}}{\bar{\omega}_1} \tag{9}$$

and

TABLE I. Density ρ_d, flexural modulus $B = E_0/12(1-\sigma^2)$, and fatigue limit stress T_m for various materials. Here B has been calculated from Young's modulus E_0 using $\sigma = 0.33$. Values of T_m in parenthesis have been estimated by taking $\frac{1}{4}$ the rupture stress.

	ρ_d(g/cm³)	B(dyn/cm²)	T_m(dyn/cm²)	ϵ_c	ϵ_0
Teflon[a]	2.2	3.8×10^{5}	(2.8×10^{7})	1.4	6.0×10^{-4}
PMMA[b]	1.2	2.4×10^{5}	1.4×10^{8}	9.0	3.7×10^{-3}
Al 7075-T6	2.8[c]	6.7×10^{10}[d]	1.4×10^{9}[d]	14.0	5.9×10^{-3}
Stainless 446	7.8[e]	1.8×10^{11}[f]	3.2×10^{9}[f]	4.7	2.0×10^{-3}
Phos. bronze 8%[g]	8.8	9.2×10^{10}	1.9×10^{9}	2.8	1.2×10^{-3}
Polystyrene[h]	1.1	3.3×10^{5}	(1.5×10^{7})	12.0	5.0×10^{-3}

[a]D. F. Miner and J. B. Seastone, *Handbook of Engineering Materials*, 1st. ed. (Wiley, New York, 1955), p. 3-208.
[b]Ref. a, p. 3-198.
[c]Ref. a, p. 2-233.
[d]Ref. a, p. 2-237.
[e]Ref. a, p. 2-140.
[f]Ref. a, p. 2-132.
[g]Ref. a, p. 2-334.
[h]Ref. a, p. 3-215.

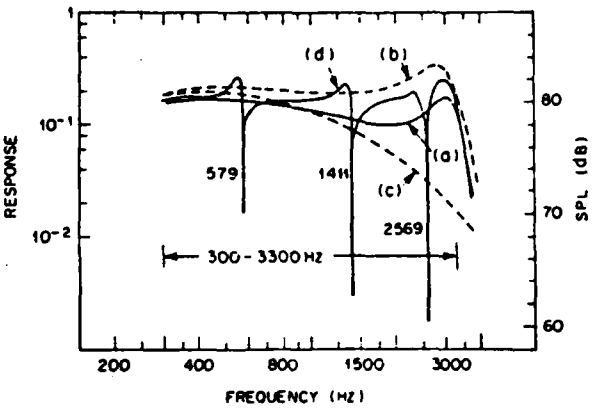

FIG. 6. Response of diaphragm-equalized photophone. Curve (a) gives Eq. (1) (left scale) for cell diaphragm Eq. (15) and no earpiece equalization. Curves (b), (c) are the same as curves (b) and (c) in Fig. 4 of KN: I. Curve (d) shows Eq. (23) for cell diaphragm and earpiece diaphragm specified by Eq. (37). SPL scale refers to 2.8-mW input.

$$-\frac{F}{\bar{\Omega}^4} = \epsilon_C \equiv \frac{\pi \gamma_0 p_0}{V_C \bar{\omega}_1^2}\left(\frac{B}{\rho_d}\right)^{1/2} , \tag{10}$$

where $\bar{F}$ and $\bar{\Omega}$ are evaluated at $\omega = \bar{\omega}_1$. From Eqs. (7) and (8)

$$\left|\frac{s_L}{s_1}\right|^2_{EQ} = \left[1 - \left(\frac{\Omega}{\bar{\Omega}}\right)^2 \frac{F}{\bar{F}}\right]^2 + \left(\frac{2\bar{f}_1 V_C}{c_0 r_1^2}\right)^2 \left(\frac{\Omega}{\bar{\Omega}}\right)^4 \tag{11}$$

$$\Omega/\bar{\Omega} = (\omega/\bar{\omega}_1)^{1/2} \ .$$

$G_1(\omega)$ can now be computed from Eqs. (2), (5), and (11) and a computer program which gives $F(\Omega, Q, b/a)$. The general nature of F is discussed in Appendix B. We regard $\bar{f}_1 = 3100$ Hz and $r_1 = 0.036$ cm as prescribed according to Eq. (32) of KN: I; still to be determined are V_C, $\bar{\Omega}$, Q, b/a, and the diaphragm material.

Table I lists selected values of ρ_d, B, and ϵ_C for various materials that might be considered for the diaphragm, assuming in ϵ_C the volume $V_C = 2.5\times10^{-3}$ cm³ as used in Eq. (32) of KN: I. The order of magnitude of ϵ_C immediately rules out the unloaded diaphragm, which, if made of any ordinary material, could not provide the required inertance without being too stuf. Doming the diaphragm would increase the stiffness. Thus the domed diaphragm used in telephone receivers for many years[3,4] to avoid the antiresonances ($Z \to \infty$) of the flat diaphragm is inappropriate here. Thus it is clear that heavy loading $Q \gg 1$ is required, which dictates choosing a light material for the diaphragm, polystyrene, and a heavy material for the loading ring, gold. For polystyrene Eqs. (9)–(11) become

$$a^2/t = 2.8\,\bar{\Omega}^2 , \tag{12}$$

$$-F/\bar{\Omega}^4 = 0.030 \text{ cm}^3/V_C , \tag{13}$$

$$\left|\frac{s_L}{s_1}\right|^2_{EQ} = \left[1 - \left(\frac{\Omega}{\bar{\Omega}}\right)^2 \frac{F}{\bar{F}}\right]^2 + 1.98\times10^{4} \text{ cm}^{-6}\, V_C^2 \left(\frac{\Omega}{\bar{\Omega}}\right)^4 \tag{14}$$

and Eq. (5) remains valid.

The best equalization we could achieve by trial calculations and adjustments of the parameters $\bar{\Omega}$, Q, b/a is shown in Fig. 6 curve (a), which corresponds to the

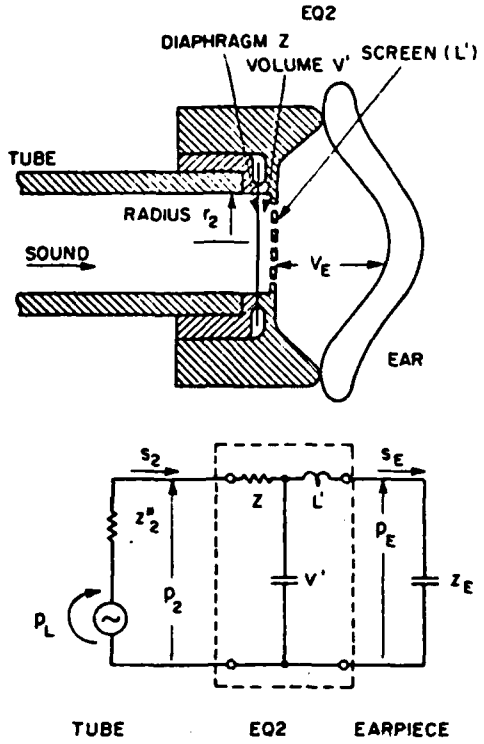

FIG. 7. Earpiece with diaphragm and screen, and equivalent circuit.

$F(\Omega)$ shown in Fig. 5, and the specifications

$$\bar{\Omega}=2.40,\quad Q=35,\quad b/a=0.47,$$
$$V_C=2.64\times10^{-3}\ \text{cm}^3, \tag{15}$$
$$a^2/t=16.1\ \text{cm}.$$

The frequency band 300–3300 Hz is indicated in Fig. 5; it will be seen that this band is approximately centered between $\Omega=0$ and $\Omega=3.387$ where $|F|\to\infty$. Curves (b) and (c) of Fig. 6 are taken from Fig. 4 of KN: I; they represent, respectively, the response with the optimum pure inertance equalization and with no equalization. Note that although equalization has been achieved in curves (a), the level lies below curve (c) at low frequencies less than 1000 Hz. This is because, as Fig. 5 shows, the diaphragm ceases to act like an inertance ($F<0$) for $f<1000$ Hz and becomes stiffness controlled like a capacitance.

A possible set of specifications for the loaded diaphragm is the following:

$$a=0.127,\quad t=1.00\times10^{-3}\ \text{cm}\ \text{(polystyrene)}$$
$$t'=t''=0.0109,\quad b=0.060\ \text{cm}\ \text{(gold)} \tag{16}$$
$$m=8.6\times10^{-6}\ \text{g}\ \text{(gold)}.$$

Figure 4 shows the structure approximately to proportion. Also shown is the displacement $w(r)$ for frequencies in the inertial range $1000<f<3300$ Hz. The ring is segmented to avoid stiffening the diaphragm. Figure 3 shows approximately to proportion this diaphragm installed at the base of a conical absorption cell of volume $V_C=2.6\times10^{-3}$ cm^3. The conical shape is dictated by the values of a and V_C. The volume V', neglected in Eq. (7), in the design shown is about 1×10^{-3} cm^3 corresponding to an impedance $z'\sim7\times10^4$ g/sec cm^4 about seven times greater than $|z_t|$ given by Eq. (3) at the highest frequency of interest 3300 Hz. This justifies neglecting V'.

We have considered the concentration of tensile stress in the diaphragm at the loading ring. The theory of this stress is given in Appendix B. The maximum permissible flow $s_m(\omega)$ is given by Eq. (B12) in terms of a computer calculated function J and the fatigue limit tensile stress T_m of the material. The function $10^4\times J$ for the diaphragm Eq. (15) is plotted in Fig. 5. Table I lists values of T_m, some of which are measured values from fatigue tests and others are estimated as one-quarter the rupture stress. The fatigue stress relevant here is that for completely reversed stress indefinitely cycled. We use Eq. (B12) to estimate the maximum optical power $G_A|P_\omega|$ which can safely be applied to the diaphragm. In making this estimate we take $s_C\sim s_L$ in Fig. 3, $G_M\sim1$, $|G_\omega|\sim1$ in Eq. (37) of KN: I, and obtain

$$G_A|P_\omega|<\frac{\pi\gamma_0p_0a^2T_m}{6(\gamma_0-1)(\rho_dB)^{1/2}}J(\Omega,Q,b/a)\ ,$$
$$=(7\times10^7\ \text{erg/sec})J\ . \tag{17}$$

We see from Fig. 5 that the smallest values of J occur at the low and high ends of the band where $J\sim0.07$; thus

$$G_A|P_\omega|<5\times10^5\ \text{erg/sec}=50\ \text{mW}. \tag{18}$$

Figure 7 shows the earpiece with both a diaphragm and screen (or grid). If a diaphragm is used either to seal the end of the tube or to act as EQ2, the screen would be needed to protect it from damage. If no diaphragm is used, the screen alone can act as EQ2. The small volume V' between diaphragm and screen can be neglected. Consider first the screen alone; the required value of L' is given by Eq. (25) of KN: I

$$L'=L_2=\gamma_0p_0/V_E\bar{\omega}_2^2=6.23\times10^{-4}\ \text{g cm}^{-4} \tag{19}$$

for a resonant frequency $\bar{f}_2=3100$ Hz. If the screen has radius r_2, thickness t, and porosity h (ratio of open to total area), the inertance according to Eq. (A8) of KN: I is approximately given by

$$L'\approx(\rho_0t/\pi r_2^2h)+(\rho_0/4r_2)\ , \tag{20}$$

where the first term is the inertance of the air in the pores of the screen and the second term corrects for the spreading of the flow into the volume V_E. One possible design satisfying Eqs. (19) and (20) is

$$h=0.21,\quad t=0.1\ \text{cm}. \tag{21}$$

The realization in this case is perfect, which is to say that it corresponds exactly to that assumed in the analytical model of Fig. 3 and Eq. (22) both in KN: I.

Now assume that EQ2 is to be realized by a diaphragm, the screen L' being negligible; this is easy to arrange, e.g., by taking $h=0.8$, $t=0.05$ cm. We take $V_E=6$ cm^3 and $r_2=0.85$ cm from Eq. (32) of KN: I. In the circuit of Fig. 7 the sound transmitted down the tube is replaced by an equivalent pressure source p_t in series with the impedance z_2''. This procedure is justified

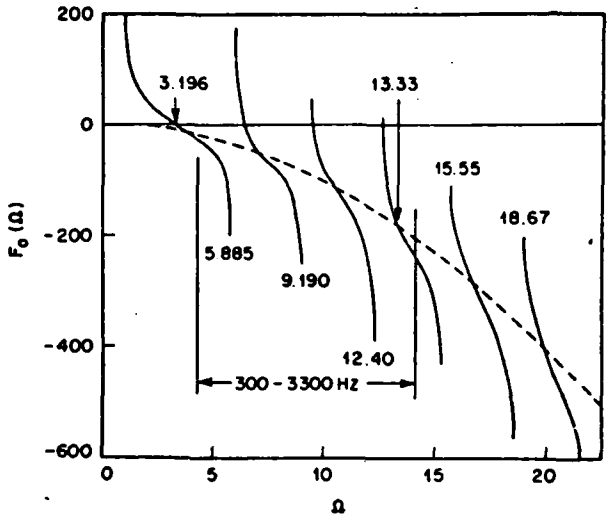

FIG. 8. Reactance function Eq. (B9) for unloaded diaphragm, and pure inertance function Eq. (B10).

in Appendix A. The equalization factor is defined by

$$G_2(\omega) = |p_E(\mathrm{EQ})/p_E(\mathrm{NEQ})|^2 \ , \tag{22}$$

and the overall smoothed response is given by

$$\langle H_\omega \rangle = \langle H_\omega \rangle_{\mathrm{NEQ}} G_1(\omega)\ G_2(\omega) \ , \tag{23}$$

where $\langle H_\omega \rangle_{\mathrm{NEQ}}$ is curve (c) of Fig. 6. We do not need the value of p_L to compute $G_2(\omega)$. As in Eq. (3) we shall replace

$$z_2^* \to |z_2| = c\rho/\pi r_2^2 = 18.4 \text{ g/sec cm}^4 \tag{24}$$

which is justified in Appendix A. Thus

$$\left(\frac{p_L}{p_E}\right)_{\mathrm{EQ}} = 1 + \frac{Z + |z_2|}{z_E} \ , \tag{25}$$

where z_E is given by Eq. (A11) of KN: I. For Z we write for generality

$$Z^{-1} = R^{-1} + (iX_d)^{-1} \ , \tag{26}$$

where R is the resistance of an optional small leak in the center of the diaphragm, and $Z = iX_d$ is the diaphragm impedance without a leak. We define the resonant frequency $\bar{\omega}_2$ just as in Eq. (8)

$$1 + (V_E/\gamma_0 p_0)\,\bar{\omega}_2 X_d(\bar{\omega}_2) = 0 \ ; \tag{27}$$

it follows that

$$\frac{a^2}{t} = \frac{\bar{\Omega}^2 (B/\rho_d)^{1/2}}{\bar{\omega}_2} \ , \tag{28}$$

$$\frac{-F}{\bar{\Omega}^4} = \epsilon_E \equiv \frac{\pi \gamma_0 p_0}{V_E \bar{\omega}_2^3}\left(\frac{B}{\rho_d^3}\right)^{1/2} \tag{29}$$

exactly as in Eqs. (9) and (10). The equation analogous to Eq. (11) can be written

$$\left|\frac{p_L}{p_E}\right|^2_{\mathrm{EQ}} = \left[1 - \frac{W}{1 + (W/\lambda\Gamma\varphi)^2}\right]^2 + \left[1 + \frac{\lambda}{1 + (\lambda\Gamma\varphi/W)^2}\right]^2 \Gamma^2\varphi^2 \ , \tag{30}$$

where

$$\varphi = \omega/\bar{\omega} = (\Omega/\bar{\Omega})^2 \ , \quad W(\varphi) = \varphi F/\bar{F} \ , \tag{31}$$

$$\lambda = R/|z_2| \ , \qquad \Gamma = 2\bar{f}_2 V_E/c_0 r_2^2 \ . \tag{32}$$

For no equalization $Z \to 0$,

$$\left|\frac{p_L}{p_E}\right|^2_{\mathrm{NEQ}} = 1 + \frac{2V_E f}{c_0 r_2^2} = 1 + (2.38\times 10^{-7}\ \mathrm{sec}^2) f^2 \ . \tag{33}$$

$G_2(\omega)$ can now be calculated from Eqs. (30) and (33) and computer evaluations of $F(\Omega, Q, b/a)$.

The values of ϵ_E for various materials are listed in Table I assuming $\bar{f}_2 = 3100$ Hz, $V_E = 6$ cm^3. The order of magnitude of ϵ_E is consistent with an unloaded diaphragm. The reactance function $F_0(\Omega)$ for the unloaded diaphragm is given by Eq. (B9) and plotted in Fig. 8. The dashed curve is $F_{00}(\Omega)$ given by Eq. (B10) representing a freely moving piston of the same area and mass (i.e., a pure inertance). We see that the diaphragm is similar to a piston only over certain narrow ranges of Ω near the intersections of $F_0(\Omega)$ and $F_{00}(\Omega)$. Therefore we choose one of these intersections to correspond to the desired resonant frequency $\bar{f}_2$ near 3100 Hz

$$\Omega = 13.33, \quad F_0 = -178, \quad \epsilon_E = 5.64\times 10^{-3} \ . \tag{34}$$

Again we choose polystyrene for the diaphragm; it follows from Eqs. (29) and (32) that

$$\bar{f}_2 = 2058 \text{ Hz}, \quad \Gamma = 1.44, \tag{35}$$

and Eq. (28) becomes

$$a^2/t = 519 \text{ cm}. \tag{36}$$

Since the diaphragm is mounted at the end of the tube,

$$a = r_2 = 0.85, \quad t = 1.39\times 10^{-3} \text{ cm (polystyrene)}. \tag{37}$$

Curve (d) of Fig. 6 shows the overall smoothed response Eq. (23) for the two diaphragms characterized by Eqs. (16) and (37). The three antiresonances in Fig. 8 lying below $\Omega = 13.33$ show up in $\langle H_\omega \rangle$ as very sharp holes in the response at frequencies 579, 1411, and 2569 Hz. These holes go to zero if there is no leak ($\lambda \to \infty$) in the diaphragm; the case plotted corresponds to $\lambda = 10$. Equalization is achieved apart from these holes, and the earpiece diaphragm significantly raises the level of response in the range $1000 > f < 3300$ Hz. We do not know if the holes would give the photophone an objectionable tone quality, but we note that the effect of such holes is probably inversely proportional to the number of holes, and for many years the standard telephone receiver[5] had a single antiresonance in the band.

II. DIRECT-COUPLED PHOTOPHONE

In order to determine the efficacy of the exponentially tapered tube in the optimized transformer-coupled (TC) photophone it is necessary to consider what is the best response from an equalized photophone that does not contain such a tube, which we call a direct-coupled (DC) photophone.[6] The optimized DC-photophone structure, which will now be discussed, is shown in Fig. 9 along with its equivalent circuit.

In our consideration of this circuit we will ignore l''' since this is not helpful for equalization. Since $V_L \gg V_E$, we also ignore V_C; thus $s_C = s_L$. The solution of the circuit is then

$$(p_L/s_L)_{\mathrm{EQ}} = (Z^{-1} + z_E^{-1})^{-1} \ , \tag{38}$$

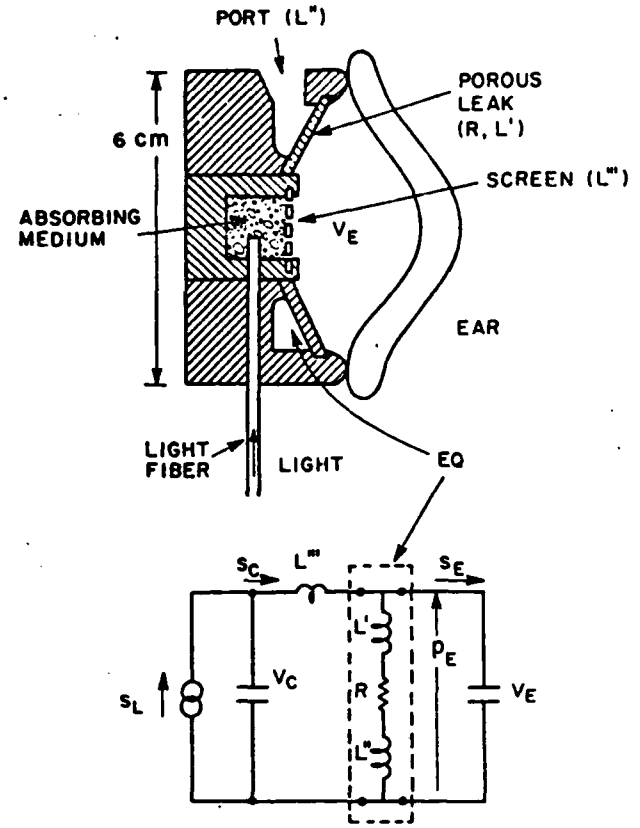

FIG. 9. The direct-coupled photophone including the equalizer EQ.

where z_E is given by Eq. (A11) of KN:I and

$$Z = R - i\omega L = R - i\omega(L' + L'') \tag{39}$$

is the impedance of the porous leak and port. We define the resonant frequency $\bar{\omega}$ and damping parameter δ by

$$\bar{\omega} = (\gamma_0 p_0 / L V_E)^{1/2} \ , \qquad \delta = R/\bar{\omega}L \ . \tag{40}$$

The response may be expressed in terms of H_ω according to Eq. (12) of KN:I with

$$\left|\frac{p_E}{s_L}\right|^2 = \left(\frac{\gamma_0 p_0}{\omega V_E}\right)^2 \left[\frac{\delta^2 + \varphi^2}{\varphi^2\delta^2 + (1-\varphi^2)^2}\right] \ , \qquad \varphi = \omega/\bar{\omega} \ . \tag{41}$$

The case of no equalization corresponds to $\delta \to \infty$. The cell is large so we can safely assume $|G_\omega|^2 \approx 1$; it is also reasonable as in Eq. (32) of KN:I to set $G_y^2 \approx 1$ for an air photophone. We have found the best equalized response for the case (using $V_E = 6$ cm^3)

$$\bar{f} = 3705 \text{ Hz}, \ \delta = 1.73 \ , \qquad R = 17.6 \text{ g/sec cm}^4, \ L = 4.36 \times 10^{-4} \text{ g cm}^{-4} \ . \tag{42}$$

The resulting H_ω is plotted as curve (a) of Fig. 10. The unequalized response is shown in curve (b), which varies like f^{-2}. We regard such an unequalized response curve as completely unsatisfactory for use. Comparing curves (a) and (c) shows that the equalized DC photophone is down from the equalized TC photophone by about 25 dB; this means that the sound level of 81 dB SPL [see defining Eq. (6) in KN:I] can be produced with the optical input (the sensitivity)

$$G_A |P_\omega| = 51 \text{ mW} \ . \tag{43}$$

It should be possible to achieve a utilization factor $G_A \approx 1$. This sensitivity of the DC photophone (51 mW) is to be compared to the 2.8-mW sensitivity of the TC photophone (filled with air). This comparison proves the importance of the acoustic tube transformer.

The question remains as to the actual physical nature of the porous leak, its dimensions, the dimensions of the port, and the feasibility of incorporationg these into a telephone receiver. Consider a bundle of n parallel tubes of length $b \ll k^{-1}$ and radius $a \ll b$; neglecting end effects we obtain for the impedance $R - i\omega L'$ of the bundle, according to Eq. (A9) of KN:I,

$$L' = (4/3n)(\rho/\pi a^2) b \ , \qquad R = (8/n)(\rho\mu/\pi a^4) b \ . \tag{44}$$

It follows that

$$a = (6\mu L/R)^{1/2} \epsilon^{1/2} \ , \qquad b = (9\pi/2)(L^2\mu/R\rho) n\epsilon^2 \ , \qquad \epsilon = L'/L \ . \tag{45}$$

The tubes are holes drilled in a plate of thickness b and area A; define the *porosity* (cavity factor)

$$h = n\pi a^2/A \ , \qquad 0 < h < \pi/2\sqrt{3} = 0.907 \ . \tag{46}$$

The upper limit $\pi/2\sqrt{3}$ corresponds to the close packing of circles. Now assume that the port has area A and length l; neglecting end effects we obtain from Eq. (A8)

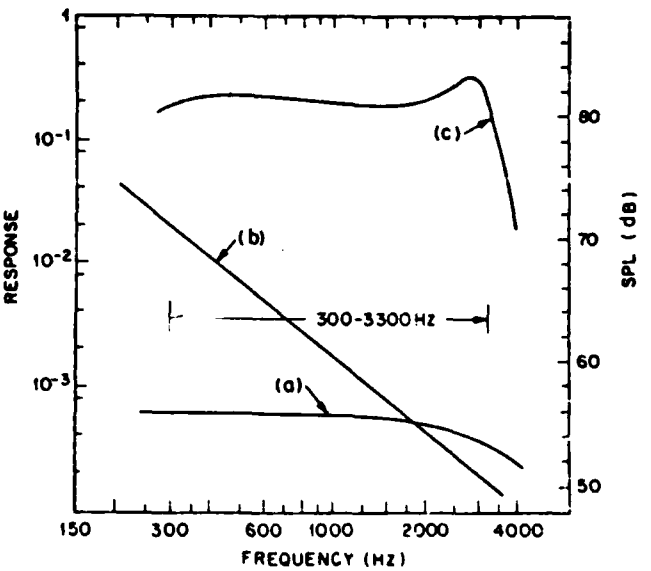

FIG. 10. Response of DC photophone. Curve (a) shows the equalized DC photophone specified by Eq. (42) and depicted in Fig. 9, curve (b) shows the unequalized response of the DC photophone, curve (c) shows the pure inertance equalized response of the TC photophone for comparison (same as curve (a), Fig. 2).

of KN: I

$$L'' = \rho l/A \ . \tag{47}$$

It follows that

$$l = (6\pi/h)(L^2\mu/R\rho)n\epsilon(1-\epsilon) \ . \tag{48}$$

We choose $\epsilon = 0.5$ to maximize l; we then have

$$\begin{aligned} &a = (3\mu L/R)^{1/2} = 3.30\times10^{-3} \text{ cm}, \\ &l = (3\pi/2h)(L^2\mu/R\rho)n = 6.07\times10^{-6}\,(n/h) \text{ cm}, \\ &b/l = 3h/4 \ , \\ &A/l = 2\rho/L = 5.62 \text{ cm}, \\ &A = 3.41\times10^{-5}(n/h) \text{ cm}^2. \end{aligned} \tag{49}$$

For practical reasons l must be in the range 2–2.5 cm and b should not be less than about 0.1 cm; therefore we choose the following specifications for illustrative purposes:

$$\begin{aligned} &l = 2.2 \text{ cm}, \quad b = 0.2 \text{ cm}, \\ &A = 12.4 \text{ cm}^2, \\ &h = 0.121, \quad n = 4.39\times10^4. \end{aligned} \tag{50}$$

The area A can be achieved if the port extends all around the circumference of the earpiece except for structural ribs. The perforated plate is the "porous leak" of Fig. 9.

This calculation establishes that the realization of EQ is physically possible using elements of the approximate size and proportion shown in Fig. 9. In practice it would probably not be economical to use a drilled plate because of the large value of n, but the desired acoustic properties could be obtained using one of the standard acoustic insulating materials[7,8] in the port. Alternatively the porous leak could be a rigid composite material that requires no drilling. An interesting example of this latter type is afforded by the close packing of fibers. Consider a plate of area A and thickness b formed by close packed circular fibers of radius a which adhere along their lines of contact. The tubes which conduct sound in this case are the interstices between the fibers. For this geometry Eq. (46) is replaced by

$$h = 0.0931, \quad hA/n = 0.1613\,a^2 \ , \tag{51}$$

where the number of fibers is $n/2$, the number of tubes is n. An exact solution is known for viscosity limited flow in triangular ducts[9]; in the approximation that the tubes are considered as having an equilateral triangular cross section we have

$$\begin{aligned} &L' = 1.43(\rho/hA)b \ , \\ &R = 34.6(\rho\mu/h^2A^2)bn \ , \end{aligned} \tag{52}$$

which replace Eq. (44). Corresponding to Eqs. (49) we now obtain

$$\begin{aligned} &a = 8.66(\mu L/R)^{1/2} = 0.0165 \text{ cm}, \\ &l = 65.0(L^2\mu/R\rho)n = 8.37\times10^{-5}n \text{ cm}, \\ &b/l = 0.70\,h = 0.0651, \\ &A/l = 2\rho/L = 5.62 \text{ cm}, \\ &A = 4.72\times10^{-4}n \text{ cm}^2 \ . \end{aligned} \tag{53}$$

Again choosing $l = 2.2$ cm as in Eq. (50) gives the specifications

$$\begin{aligned} &l = 2.2 \text{ cm}, \quad b = 0.143 \text{ cm}, \\ &A = 12.4 \text{ cm}^2, \quad n = 2.63\times10^4. \end{aligned} \tag{54}$$

In this analysis we have assumed that L''', the inertance of the screen protecting the absorbing medium, is negligible. Suppose this screen has radius a, thickness t, and porosity h; then from Eq. (A8) of KN: I we obtain

$$L''' \approx (\rho t/h\pi a^2) + (\rho/4a) \tag{55}$$

counting only one end effect instead of two. For illustrative purposes take

$$\begin{aligned} &a = 1.0 \text{ cm}, \quad t = 0.1 \text{ cm}, \quad h = 0.8, \\ &L''' \approx 3.5\times10^{-4} \text{ g cm}^{-4}, \\ &V_C = 1 \text{ cm}^3; \end{aligned} \tag{56}$$

then we have

$$|\omega L'''/z_C| = \omega^2 L''' V_C/\gamma p_0 = 0.1(f/3300)^2 \ , \tag{57}$$

with f in hertz. This justifies our assumption $s_C = s_L$ for the band of interest 300–3300 Hz.

III. SUMMARY

In the preceding paper[1] (KN: I) we presented the design principles and optimization of the equalized response of photophones containing either air or xenon. The equalizers considered in that paper were hypothetical ones represented only by impedances. One of the purposes of this paper is to show that the equalizer impedances found necessary in KN: I can be obtained from practical physical components. Since most of the equalization of the frequency response must be accomplished by an equalizer between the absorption cell and the tapered tube, most of the calculations have concerned it; the additional equalization needed from the equalizer between the tapered tube and the earpiece can be obtained from a simple tensionless plastic membrance in conjunction with a screen.

The simplest physical equalizer at the absorption cell is an air column shown in Fig. 1; when optimized this gives the response shown by curve (b) of Fig. 2. These calculations take into account thermoviscous damping in the tube and air column. We have also considered diaphragm equalizers and arrived at specific diaphragm designs. Figure 3 shows one possible design approximately to scale for a cell equipped with a polystyrene diaphragm loaded with a ring-shaped mass of heavy metal. The averaged response obtainable with this diaphragm is shown by curve (a) of Fig. 6. With the addition of an optimized unloaded diaphragm in the earpiece the overall response including equalizer resonances is that of curve (d) of Fig. 6.

We have also presented here an analysis of an equalized direct-coupled (DC) photophone in order to demonstrate the importance of the acoustic transformer in the form of an exponentially tapered tube present in the pre-

ferred design. The DC-photophone is shown in Fig. 9 and its equalized response is shown as curve (a) of Fig. 10. Its sensitivity of 51 mW compares unfavorably with the sensitivities of the xenon and air transformer-coupled (TC) photophones which are 0.89 and 2.8 mW, respectively.

If optical subscriber loops are ever installed in the telephone network, they will have to be compatible with the existing telephone plant. The question is then whether the present electrical signal power at the central office is sufficient to meet the sensitivity requirement of any of these three versions of the photophone. In a study to be published elsewhere[10] we consider design requirements of optical loops including their interfacing with the present telephone plant. We show in this study that the optical signal power available from an electrical–optical interface at a central office could be sufficient to meet the requirement of the xenon or air TC photophones but not that of the DC photophone. Losses in an optical fiber transmission medium will be significant, however, and will prevent the use of the TC photophone with fibers greater than a certain length.

ACKNOWLEDGMENTS

We wish to thank W. M. Hubbard and D. Gloge for helpful suggestions.

APPENDIX A: EQUALIZATION FACTORS

For the purpose of equalizer design we have used simplified circuits shown in Figs. 1, 3, and 7 to compute the smoothed response $\langle H_\omega \rangle$ in the form

$$\langle H_\omega \rangle = \langle H_\omega \rangle_{NEQ}\, G_1(\omega)\, G_2(\omega)\,, \tag{A1}$$

where $\langle H_\omega \rangle_{NEQ}$ is curve (b) of Fig. 10, and $G_1(\omega)$ and $G_2(\omega)$ are independent equalization factors depending only on the parameters of the simplified circuits. This approximation is only appropriate for the smoothed response, since the oscillations in H_ω depend on the coupling between the cell and earpiece circuits through reflected waves in the tube. For large TVD the round-trip amplitude attenuation factor is very small

$$e^{-2\Delta} \ll 1\,, \tag{A2}$$

where Δ is given in Eq. (B22) of KN: I; in this case Eq. (B9) of KN: I gives the relations

$$T_{11} = z_1\, T_{21}, \quad T_{12} = z_1\, T_{22}\,, \tag{A3}$$

and it follows from Eq. (B5) of KN: I that

$$\begin{aligned} p_1/s_1 &= z_1\,, \\ p_2 &= (p_1/T_{11}) - (z_1\, T_{22}/T_{11})\, s_2\,. \end{aligned} \tag{A4}$$

Our calculations only retain TVD in the exponential factors; in this approximation

$$\begin{aligned} z_1 &\approx (i/m_*)\,(\omega\rho/\pi r_1^2) \xrightarrow[(\omega>a)]{} \rho c/\pi r_1^2\,, \\ z_2 &\approx (i/m_*)\,(\omega\rho/\pi r_2^2) \longrightarrow \rho c/\pi r_2^2\,, \\ (z_1 T_{22}/T_{11}) &\approx z_c^* \longrightarrow \rho c/\pi r_2^2\,. \end{aligned} \tag{A5}$$

Thus in the large TVD limit the input to the tube has impedance z_1 and the output is equivalent to a pressure source (p_1/T_{11}) in series with an impedance z_c^*. This agrees with the circuits of Figs. 1, 3, and 7. Actually, the values of the sources s_L, $p_L = (p_1/T_{11})$ in these circuits are not relevant since the circuits are only used to compute ratios; they are never used to compute the absolute response which rests on curve (b) of Fig. 10. For this reason the further liberty was taken in the calculations of $G_1(\omega)$, $G_2(\omega)$ of replacing $z_1 \to |z_1|$, $z_2^* \to |z_2|$.

The presence of reflected waves in the tube does not invalidate the simple circuits as long as they are only used to compute $\langle H_\omega \rangle$, not H_ω. For the circuit of Fig. 3 of KN: I we have shown in Eqs. (24) of KN: I that $\langle H_\omega \rangle$ does factor into the form Eq. (A1). The effect of reflected waves on $\langle H_\omega \rangle$ is to increase it by a factor $(1 - e^{-2\Delta})^{-1}$ which does not depend on the terminations of the tube. This applies rigorously only to reactive (pure imaginary) terminations; if EQ1 or EQ2 are dissipative the effective values of Δ is increased by the end losses. From Eq. (24) of KN: I we see that $G_1(\omega)$ is

$$G_1(\omega) = \left[\left(1 + \frac{Z_1}{z_C}\right)^2 + \left(\frac{kV_C'}{\pi r_1^2}\right)^2 - \left(1 + \frac{Z_1}{z_C}\right)\left(\frac{2\alpha V_C'}{\pi r_1^2}\right)\right]^{-1} \times \left[1 + \left(\frac{kV_C''}{\pi r_1^2}\right)^2 - \left(\frac{2\alpha V_C''}{\pi r_1^2}\right)\right], \tag{A6}$$

where V_c'' is the volume assumed in curve (b) of Fig. 10, $V_C'' = 2.5 \times 10^{-3}$ cm^3. Essentially the same numerical results are obtained from the simpler form

$$G_1(\omega) = \left[\left(1 + \frac{Z_1}{z_C}\right)^2 + \left(\frac{kV_C'}{\pi r_1^2}\right)^2\right]^{-1} \times \left[1 + \left(\frac{kV_C''}{\pi r_1^2}\right)^2\right]. \tag{A7}$$

It is easy to show that Eq. (A6) agrees with the circuit of Fig. 3 (neglecting V') and the general definition

$$G_1(\omega) = |s_1(EQ)/s_1(NEQ)|^2\,, \tag{A8}$$

where $s_1(NEQ)$ is calculated for volume V_C'' and $Z = 0$. Replacing $z_1 \to |z_1|$ in the circuit gives Eq. (A7). Similarly, it follows from Eq. 24 of KN: I that $G_2(\omega)$ for the circuit of Fig. 3 of KN: I is

$$G_2(\omega) = \left[\left(1 + \frac{Z_2}{z_E}\right)^2 + \left(\frac{kV_E'}{\pi r_2^2}\right)^2 + \left(1 + \frac{Z_2}{Z_E}\right)\left(\frac{2\alpha V_E'}{\pi r_2^2}\right)\right]^{-1} \times \left[1 + \left(\frac{kV_E'}{\pi r_2^2}\right)^2 + \left(\frac{2\alpha V_E'}{\pi r_2^2}\right)\right], \tag{A9}$$

which agrees with the circuit of Fig. 7 (neglecting L' and V') and the general definition

$$G_2(\omega) = |p_E(EQ)/p_E(NEQ)|^2\,, \tag{A10}$$

where $p_E(NEQ)$ is calculated for $Z = 0$. Again it is valid to use the simpler form like Eq. (A7) of KN: I which corresponds to replacing $z_2^* \to |z_2|$.

We have given Eqs. (A6), ..., (A10) to establish the validity of the equalization factor method in a particular case, the circuit of Fig. 3 of KN: I. However, we believe the method applies equally well to more complicated equalizer networks EQ1, EQ2 in Fig. 2 of KN: I.

APPENDIX B: IMPEDANCE OF FLAT-LOADED DIAPHRAGMS

Here we summarize the theory of the acoustic impedance $iX(\omega)$ of a circular elastic plate (diaphragm) clamped without tension at a radius a and carrying a concentrated mass m in the form of a concentric ring of radius $b \leq a$. The case $m = o$ or $b = a$ correspond to the uniform diaphragm whose properties are well known.[B1] The displacement $w(r)$ satisfies the equation[B2]

$$t^3 B \nabla^4 w - t\rho_d \omega^2 w - p = 0 , \tag{B1}$$

where p is the pressure difference, ρ_d the plate density, t the thickness, and $B = E_0/12(1-\sigma^2)$ specifies the elastic constant of the plate for flexure. The normal shear force per unit length is[B3]

$$N = -t^3 B \nabla^2 (dw/dr) . \tag{B2}$$

At $r = 0$ $w(r)$ must be finite. At $r = b$ there is a discontinuity in N due to the acceleration of the load

$$\Delta N = -(m\omega^2/2\pi b)\, w(b) , \tag{B3}$$

and at $r = a$ the clamped edge satisfies

$$w(a) = (dw/dr)_a = 0 . \tag{B4}$$

There is no discontinuity at b in w, dw/dr, or $\nabla^2 w$. We are neglecting the rotation of the plate and of the loading mass and assuming that the loading ring does not stiffen the plate. Figure 4 shows how the loading ring can be broken up into segments to avoid any stiffening effect. The width t'' of the ring will be considered negligible. The reactance $X(\omega)$ is defined by

$$X(\omega) = \frac{p}{\omega}\left(\int_0^a 2\pi r w(r)\, dr\right)^{-1} . \tag{B5}$$

We have evaluated $X(\omega)$ using a computer program based on expressing $w(r)$ in terms of Bessel functions with six unknown coefficients which are determined from the six simultaneous linear equations representing the boundary condition at $r = a$ and $r = b$. The result can be written for the reactance

$$X_d(\omega) = (t^2/\pi a^4)(B\rho_d)^{1/2} F(\Omega, Q, b/a) , \tag{B6}$$

where

$$\Omega = (\rho_d a^4/t^2 B)^{1/4} \omega^{1/2} , \tag{B7}$$

$$Q = m/2\pi b^2 t \rho_d , \tag{B8}$$

and F is the computer calculated function. For the *uniform diaphragm*[B4] ($Q = 0$ or $b = a$)

$$F_0(\Omega) = \Omega^2\left[\frac{4}{\Omega}\left(\frac{J_0(\Omega)}{J_1(\Omega)} + \frac{I_0(\Omega)}{I_1(\Omega)}\right)^{-1}\right]^{-1} . \tag{B9}$$

If the uniform diaphragm is free at the edge and moves like a rigid piston (i.e., a pure inertance), the reactance $X = -(\omega\rho_d t/\pi a^2)$ is equivalent to

$$F_\infty(\Omega) = -\Omega^2 . \tag{B10}$$

The general nature of $F(\Omega)$ may be seen in Fig. 8. The modes of vibration of the uniform diaphragm correspond to the zeros of $F_0(\Omega)$, the lowest being at 3.196. Of greater importance are the singularities, or antiresonances, the first few being at 5.885, 9.190, 12.40, 15.55, 18.67, ... For $\Omega > 3.196$, $F_0(\Omega)$ is mostly inertial ($F(\Omega)$ and may be considered to oscillate about Eq. (B10) shown dashed. The smallest slope $|(dF/d\Omega)|$ occurs close to the intersections of Eqs. (B9) and (B10). The general nature of $F(\Omega, Q, b/a)$ is similar except the lowest resonance is depressed and the antiresonances are not uniformly spaced. Figure 5 shows $F(\Omega, 35, 0.47)$ which has its lowest resonance at 1.370 and first antiresonance at 3.387. It follows that this diaphragm has an inertial range ($F < 0$) over which ω varies by a factor $(3.387/1.370)^2 = 6.112$, which may be compared with the corresponding inertial range factor $(5.885/3.196)^2 = 3.391$ of the uniform diaphragm. This is one advantage of loading, a larger inertial range; the other is that large values of $-F/\Omega^4$ can be achieved in the slowly varying region of F, which is the useful region for equalization. The displacement $w(r)$ in the inertial range is sketched in Fig. 4.

The significance of choosing $b/a = 0.47$ lies in the fact that the displacement $w(r)$ of the uniform diaphragm at the first antiresonance (5.885) has a node at $r = 0.47$. Therefore, if $b/a = 0.47$ there is always an antiresonance at 5.885 for any value of Q. As Q is increased from zero the lowest resonance is depressed, the lowest antiresonance remains fixed, and the inertial-range-frequency-factor increases. However, there is a limit to this factor because at very high $Q \gg 1$ antiresonances appear below 5.885; these can be continuously traced as functions of Q back to higher antiresonances of the uniform plate. Nevertheless, $b/a = 0.47$ is the optimum choice for achieving the maximum inertial range factor.

It is clear that a loading as high as $Q = 35$ must cause a concentration of stress in the diaphragm at $r = b$. To estimate the maximum rating for the diaphragm expressed as the maximum permissible flow $s_m(\omega)$, we assume failure will occur at the loading ring due to excessive tensile stress in the diaphragm. The tensile stress varies linearly through the thickness of the diaphragm, being maximum in magnitude at the surfaces. The maximum tensile stress at any radius r is given by[B3]

$$T = 6tB\left|\nabla^2 w - (1-\sigma)(dw/r dr)\right| . \tag{B11}$$

For nearly all materials of interest it is permissible to take $\sigma = \frac{1}{3}$; then the maximum flow can be written

$$s_m(\omega) = (\pi a^2 T_m/6(\rho_d B)^{1/2}) J(\Omega, Q, b/a) , \tag{B12}$$

where J is a computer calculated function and T_m is the fatigue limit tensile stress of the diaphragm (completely reversed stress cycled indefinitely). Figure 5 shows $J(\Omega, 35, 0.47) \times 10^1$ plotted on the same scale as F. The smallest value of J in the frequency range 300–3300 Hz determines the rating of the diaphragm.

[1] D. A. Kleinman and D. F. Nelson, "The Photophone—An Optical Telephone Receiver," J. Acoust. Soc. Am. 59, 1492–1494 (1976).
[2] A. H. Benade, "On the Propagation of Sound Waves in a Cylindrical Conduit," J. Acoust. Soc. Am. 44, 616–623 (1968).
[3] E. E. Mott and R. C. Miner, "The King Armature Telephone Receiver," Bell Syst. Tech. J. 30, 110–140 (1951).
[4] W. P. Mason, *Electromechanical Transducers and Wave*

Filters (Van Nostrand, Princeton, NJ, 1948), 2nd ed., p. 173.

[5]W. C. Jones, "Instruments for the New Telephone Sets," Bell Sys. Tech. J. 17, 338–357 (1938). See Fig. 8, p. 352, for early type receiver.

[6]A. Rosencwaig has recently constructed and demonstrated a DC photophone (having no equalization) using a carbon black absorber and telephone earpiece. We wish to thank him for the opportunity to make measurements on his device.

[7]C. Zwikker and C. W. Kosten, *Sound Absorbing Materials* (Elsevier, New York, 1949), pp. 52–75.

[8]L. Beranek and S. Labate, "Properties of Porous Acoustic Materials," in *Noise Reduction*, edited by L. Beranek (McGraw–Hill, New York, 1960).

[9]R. Berker, "Integration des equations du movement d'un fluide visqueix incompressible," *Handbuch der Physik VIII/2*, edited by S. Flugge and C. Trusedell (Springer, Berlin, 1963), p. 71.

[10]D. A. Kleinman and D. F. Nelson, Bell Syst. Tech. J. (to be published).

[B1]Ref. 4, pp. 167–173.

[B2]Ref. 4, Eq. 5.34, p. 167.

[B3]A. E. H. Love, *A Treatise on the Mathematical Theory of Elasticity* (Dover, New York, 1944, originally Cambridge, 1927), 4th ed., pp. 488–489.

[B4]Ref. 4, Eq. 5.45, p. 170.

Photophone performance

D. F. Nelson, K. W. Wecht, and D. A. Kleinman

Bell Laboratories, Murray Hill, New Jersey 07974
(Received 15 September 1975; revised 28 February 1976)

A photophone consisting of a light guiding fiber, an absorption cell containing charred cotton suspended in air, an exponentially tapered tube, and a standard earpiece volume has been made and tested. The pressure in the earpiece versus the frequency in the 300–3300-Hz telephone band for a given optical power input agrees well with the theory of the preceding paper. We conclude that the charred cotton suspended in air can be treated simply as light-absorbing air. Measurements were also made on a photophone which included an air column equalizer to resonate with the absorption cell in order to flatten the frequency response. The high-frequency (1500–3300 Hz) response was enhanced as expected thought not quite as much as predicted.

Subject Classification: [43]85.76, [43]85.40, [43]85.60.

INTRODUCTION

With optical-fiber communication systems being extensively studied[1] it is worthwhile to consider the possibility of direct production of sound from light which is modulated at audio frequencies. By direct production we mean a conversion process which does not involve audio frequency electricity as an intermediary in the process. With this motivation we have been led to consider the generation of sound waves from the absorption of a modulated light beam in a gas or in a tenuous substance distributed in a gas. We have found that this is an old idea, first studied by A. G. Bell[2] in 1881. We follow his usage in calling it a photophone. Since his study was only of an empirical nature, we have carried out in the preceding papers[3] an extensive analytical study of the design principles and optimization of a photophone. That study led to a photophone structure differing markedly from the simple structure studied by Bell. The purpose of the work reported in this paper is to test experimentally the main predictions of that study.

I. STRUCTURE

The photophone structure developed in the preceding papers[3] consists of a glass fiber which guides intensity-modulated light into a small absorption cell, a volume representing the ear plus earpiece, and a tapered acoustic tube which acts as an acoustic transformer between the absorption cell and the ear volume. It may also contain acoustic elements for resonating the absorption cell and/or the ear volume so as to enhance the high-frequency response. This is done to make the response of the photophone as nearly flat as possible over the normal telephone frequency range of 300–3300 Hz. A schematic, cross-sectional drawing of the photophone is shown in Fig. 1.

The characteristics of the light-guiding fiber are not crucial to the photophone structure. The one used had a germania doped silica core of 0.004 cm diameter and a silica cladding with an outside diameter of 0.015 cm. It had a numerical aperture of 0.14 for coupling light into a flat end. A length of fiber of a few meters was used. The output end was glued into an entry hole to the absorption cell so as to avoid any air leaks.

The absorption cell has a volume of 4.5×10^{-3} cm^3 and contains charred cotton fibers suspended in air. The exact volume is not crucial when no attempt at resonating the cell volume is made. The volume is chosen within a range which is large enough to be in the thermal high-frequency or adiabatic limit[3] and small enough to have a large acoustic impedance. The acoustic impedance must be large compared to the tapered tube input impedance so that the former does not act as a short circuit across the sound source. A charge of approximately 15 μg of charred cotton fibers has been found empirically to be optimum for this cell volume. When distributed throughout the volume, this charge appears just barely opaque to the eye. Under this condition substantially all the light entering the cell is absorbed by the charred cotton. It is produced by heating at a temperature of about 500 °C for a minute or two in an atmosphere of flowing nitrogen. The absorption cell is contained in an aluminum block of centimeter-size dimensions. This size is believed adequate to carry heat away from the absorption cell so that a constant temperature cell wall, as assumed in the theory,[3] is maintained.

Joining the absorption cell in Fig. 1 with the standard[4] 6-cm^3 volume representing the ear plus earpiece is an air-filled exponentially tapered tube which acts as an acoustic transformer to convert the high pres-

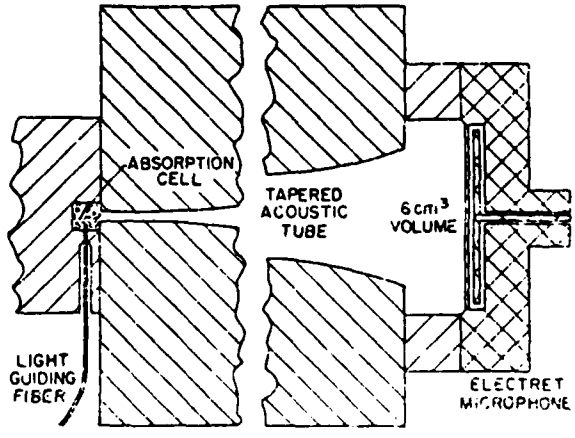

FIG. 1. Schematic cross-sectional view of the photophone with an electret microphone attached for measurement.

sure, low volume flow, acoustic source of the absorption cell to the maximum pressure attainable in the 6-cm³ volume. The optimization procedure[3] determines the cross-sectional area A of the exponentially tapered tube to be

$$A = A_1 e^{2\alpha x}, \quad 0 \leq x \leq l, \qquad (1)$$
$$A_1 = 4.07 \times 10^{-3} \text{ cm}^2, \quad \alpha = 0.037 \text{ cm}^{-1}, \quad l = 85 \text{ cm}.$$

A circular cross section for the tube is best since the perimeter to area ratio, which determines roughly the thermoviscous damping losses to useful acoustic transmission, is smallest. Ease of construction, however, dictated the use of a square cross section tapered tube. A numerically controlled milling machine produced two aluminum pieces having exponential surfaces which, when joined with two flat surface pieces, produced a tube satisfying Eq. (1). The sides of the square are 0.064 cm at the input end and 1.54 cm at the output end. Air leaks in the joints of the photophone assembly were prevented either with a viscous grease or with thin Teflon gaskets (7.6×10^{-3} cm thick).

The design studies[3] indicate that the simplest method of resonating the absorption cell volume is to couple it to the tapered tube via an air column. The inertial character of the latter can be made to compensate for the capacitive character of the cell volume at 3300 Hz and so produce an acoustic resonance at that frequency. The thermoviscous damping losses in the system make the resonance quite broad. When these losses were included in the calculation of the air column performance, it was found[3] that an air column 1.8 cm long and 0.02 cm in diameter in conjunction with an absorption cell volume of 7.5×10^{-4} cm³ would be expected to produce the best resonant enhancement in the high frequency range. A proportionately smaller amount of charred cotton is used in this cell in comparison with the amount used in the absorption cell of Fig. 1. A schematic diagram of the photophone with the air column equalizer is shown in Fig. 2.

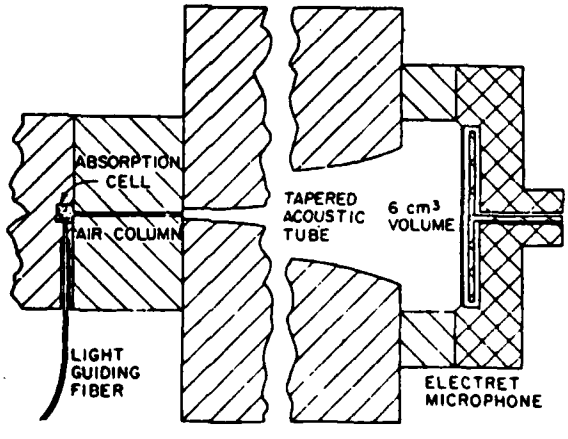

FIG. 2. Schematic cross-sectional view of the photophone with an electret microphone attached for measurement. This version of the photophone contains an air column coupler to resonate with the absorption cell so as to enhance the response of the high-frequency end of the normal telephone band (300–3300 Hz).

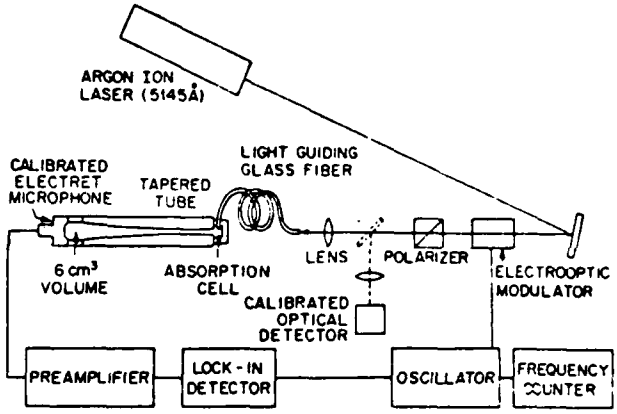

FIG. 3. Schematic arrangement of the optic, acoustic, and electric components used in measuring the photophone performance.

A third structure studied was similar to Fig. 1 except the tapered tube was a single piece plastic casting. It was made by using the four-piece aluminum tube as a mold in which to form a wax core. The core consisted of a mixture of 80% by volume of a microcrystalline wax[5] and 20% of polyisobutylene[6] having a molecular weight of 40 000. The core was molded around a 0.025-cm-diam reinforcing wire. A wax core of this type can be cast in a straight housing or after warming can be coiled inside the hand-held portion of a telephone set before casting. After the casting resin[7] has hardened, the entire casting is heated to about 80 °C to melt out the wax core.

II. TEST ARRANGEMENT

A schematic diagram of the arrangement used for testing the photophone is shown in Fig. 3. Because the absorber, charred cotton, is black, the laser wavelength used for testing is of little consequence. The 5145-Å line of an argon-ion laser was used because of the laser's availability. Its beam, adjusted to be in the lowest order transverse mode and in a state of complete linear polarization, was directed by a mirror through a modulator driven by an audio frequency oscillator whose frequency was determined by a frequency counter. The optical modulator was a commercial model[8] that uses an electrically biased quadratic electro-optic effect to obtain in conjunction with the polarizer a range of linear amplitude modulation. The intensity of the output beam, which is the square of its amplitude, can have a linear modulation range provided the biasing field on the modulating crystal is adjusted so that the two polarization components of the beam emerging from the modulator have a $\frac{1}{2}\pi$ phase difference in the absence of any modulation. Such an adjustment necessarily produces an unmodulated component to the output beam. This component, however, produces no significant effect on the measurements.

Following the polarizer a mirror can be inserted to direct the modulated beam into a calibrated photoelectric detector.[9] This allows a measurement of the power of the light which is modulated at the frequency of the

audio oscillator. With the insertable mirror removed, the modulated beam is focused onto a cleaved end of the light-guiding glass fiber by a 6.3× microscope objective lens.

The sound at the output of the photophone was measured with an electret microphone[10] which had a measured calibration of 1.1 dyn cm^{-2}/mV through the frequency range of interest. Its output was amplified 100 times by a low noise, junction field effect transistor input preamplifier before being measured with a lock-in detector.

Several tests were made on the system prior to measuring the photophone performance. One was the measurement of the transmission of the glass fiber including coupling losses at the ends. This was done prior to gluing the fiber into the absorption cell so that the output could be directed into the calibrated optical detector (Fig. 3) just as the input could be. With the modulator in place this transmission factor was found to be 0.5 while with the optical modulator removed it was 0.9 showing that distortion of the wave front by the electrooptic modulator lessened the coupling of the focused beam into the fiber.

Because the charred cotton is an incompletely understood component in the system, we have measured the sound pressure versus the input modulated laser power. To simplify this test the arrangement shown schematically in Fig. 4 was used. The absorption cell is connected directly to a 2-cm^3 volume in which the pressure variation is measured by the electret microphone. In order to reach higher laser power levels in the cell the electrooptic modulator was replaced by a chopping wheel which produced a 750-Hz square wave optical signal of up to 15 mW in the absorption cell. The pressure amplitude (one-half of the peak-to-peak signal) of the resulting triangular pressure wave is plotted in Fig. 5 versus the average laser power.

We also plot in Fig. 5 the predicted behavior of the pressure amplitude versus average power for a simple air-heating model. The linear relationship plotted is

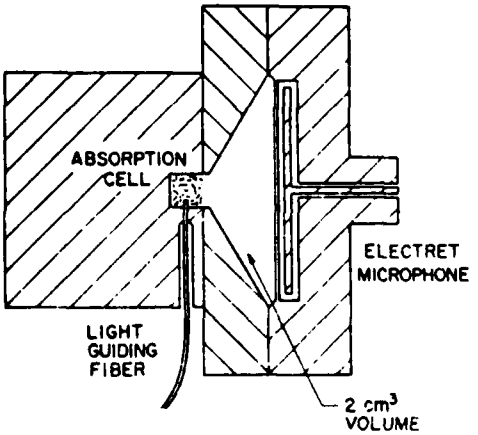

FIG. 4. Schematic cross-sectional view of the arrangement used to test the opto-acoustic performance of the charred-cotton-suspended-in-air absorption cell.

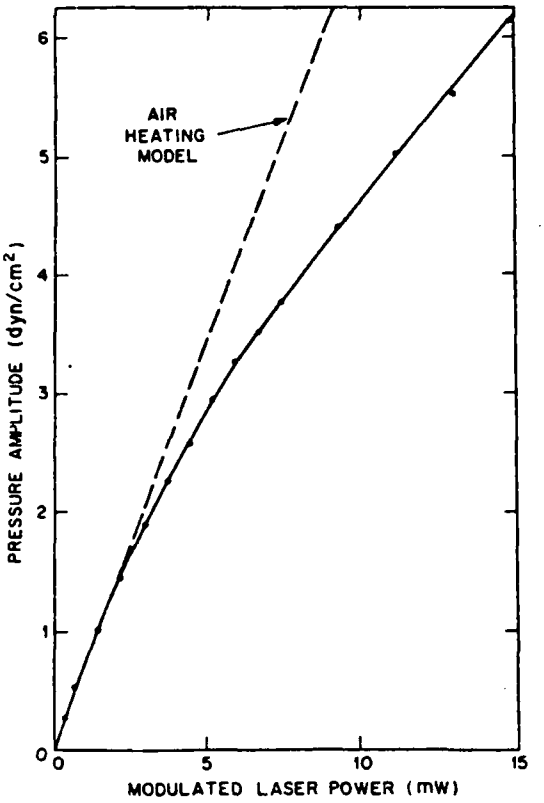

FIG. 5. Plot of the pressure amplitude (one half of the peak-to-peak signal) of a triangular wave versus the average optical power in a square wave that reaches the absorption ceil. The dashed curve is a plot of Eq. (5) which represents an air-heating model.

derived as follows. From Eq. (A11) of the first paper[3] we have that the pressure p [not specialized to a single-frequency component as in Eq. (A11)] is related to the volume flow s in a small volume V of gas by

$$dp/dt = \gamma p_0 s/V \,, \tag{2}$$

where γ is the specific heat ratio and p_0 is the static gas pressure. It was shown in the first paper[3] [Eq. (37)] that the volume flow s is related to the optical power P which is converted to heat in the cell by

$$s = (\gamma - 1)P/\gamma p_0 \tag{3}$$

in the high-frequency or adiabatic limit. Equations (2) and (3) combine to yield

$$dp/dt = (\gamma - 1)P/V \,. \tag{4}$$

If the power P is in the form of a square wave of period T with a peak-to-peak signal of $2P_A$, then the resultant triangular pressure wave p has a peak-to-peak signal of $2p_A$ where

$$p_A = (\gamma - 1)TP_A/4V \,. \tag{5}$$

The plot of this equation in Fig. 5 is in excellent agreement with the data for power levels below 2.5 mW despite the fact that the actual absorption cell contains not just air but charred cotton suspended throughout the air. This justifies treating the absorption cell as containing "light-absorbing air." We have not explored the origin

of the nonlinearity evident in the data of Fig. 5 at higher power levels.

III. PERFORMANCE

Because of the nonlinearity present in Fig. 5 the power absorbed in the cell was held to 1 mW for performance-versus-frequency tests on the photophone. The aluminum walled photophone of Fig. 1 was tested in the frequency range of 150 to 4000 Hz, a range somewhat in excess of the standard telephone range of 300–3300 Hz. In Fig. 6 the pressure amplitude of the sound wave as detected by the electret microphone is plotted versus the modulation frequency in curve A. Curve B represents the predicted performance[3] with the tube resonances averaged out. No adjustable parameters are used in this comparison which can be seen to be very good. The predicted performance including the tube resonances is shown displaced for clarity as curve D; curve C is a repetition of curve B. Though there is some shift of the tube resonances between the predicted and observed responses and a somewhat lower amplitude of the observed tube resonances, the overall agreement is felt to be very good. The triangular points in Fig. 6 represent the response of the same charge of cotton as used in obtaining curve A when the absorption cell is connected to the 2-cm³ test volume as shown in Fig. 4. Curve E is the predicted response for this

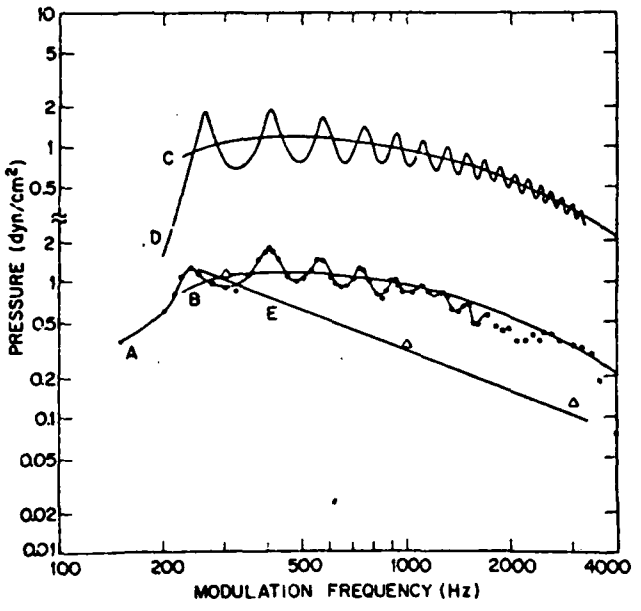

FIG. 6. Plot of pressure amplitude versus modulation frequency for the structure of Fig. 1 for 1 mW of modulated optical input to the absorption cell. Curve A: measurements; curve B and C: theory with tube resonances averaged out; curve D: theory with tube resonances shown; curve E: plot of magnitude of Eq. (7) for the air volume of Fig. 4; triangular points: measurements on the structure of Fig. 4 for the charred cotton charge used for curve A measurements. The pressure amplitude p in dyn/cm² may be converted to sound pressure level (SPL) measured in dB by SPL = $20\log(p/\sqrt{2}\times 2\times 10^{-4})$. Thus an SPL of 81 dB, the average level present at the ear in the telephone network,[11] corresponds to 3.17 dyn/cm².

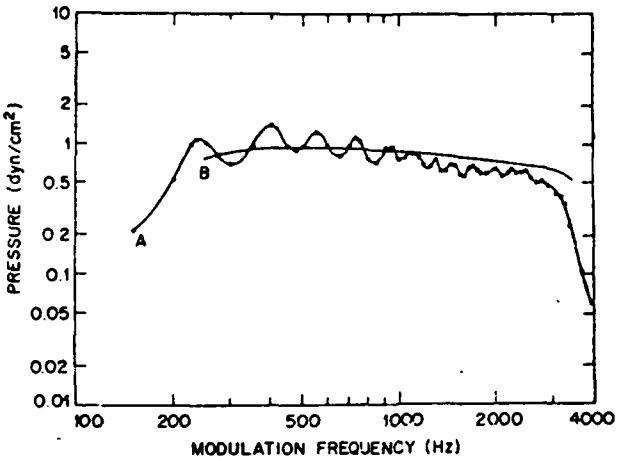

FIG. 7. Plot of pressure amplitude versus modulation frequency for the structure of Fig. 2 for 1 mW of modulated optical input to the absorption cell. Curve A: measurements; curve B: theory with tube resonances averaged out.

arrangement versus frequency. It is obtained by specializing the time dependence in Eq. (2) to a single angular frequency ω,

$$p = i\gamma p_0 s/\omega V\,, \tag{6}$$

combining this with Eq. (3) to obtain

$$p = i(\gamma - 1)P/\omega V\,, \tag{7}$$

and then plotting the magnitude of p versus the circular frequency $f \equiv \omega/2\pi$. Once again this demonstrates that the charred cotton suspended in air responds very closely to "light-absorbing air" in the absorption cell.

The photophone with the air column equalizer shown in Fig. 2 and described in Sec. II was tested next. Figure 7 shows a plot of the measured pressure versus the modulating frequency in curve A and the expected[3] response in curve B with the tube resonances averaged out. The experimental curve was measured for an absorption cell with a volume of 5×10^{-4} cm³ since this enhanced the output somewhat over the calculated 7.5×10^{-4} cm³ volume. From a comparison with Fig. 6 it can be seen that the resonance between the air column and absorption cell flattens the expected response curve by boosting the high-frequency response. A similar comparison of the measured response shows that it is larger at frequencies higher than about 1500 Hz though it does fall somewhat below the expected response curve. Though these data do not represent the ultimate for a resonant absorption cell photophone, they do confirm the usefulness of the concept for flattening the frequency response curve.

A performance test was made on a straight one-piece plastic tapered tube for comparison to the aluminum tapered tube. The configuration was the same as in Fig. 1. The experimental points are shown on curve A of Fig. 8. More measurements were made in the high-frequency region in the experiment in order to better resolve the tube resonances which can be seen clearly out to 3100 Hz. The fit of curve A to the predicted[3] response (with the tube resonances averaged out)

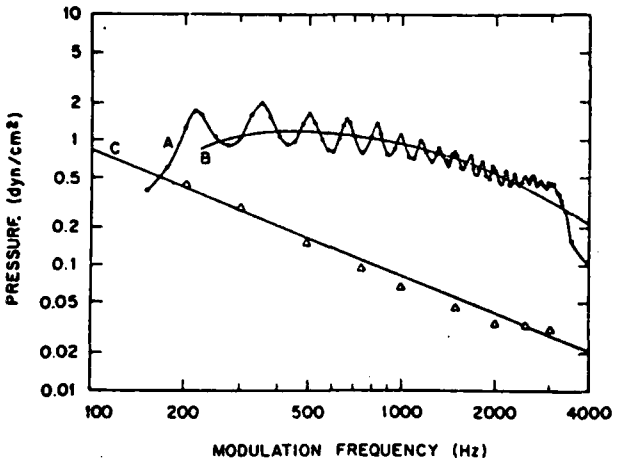

FIG. 8. Plot of pressure amplitude versus modulation frequency for the cast plastic tapered tube in the structure of Fig. 1 for 1 mW of modulated optical input to the absorption cell. Curve A: measurements; curve B: theory with the tube resonances averaged out; curve C: plot of Eq. (7) for the air volume of 7.7 cm^3; triangular points; measurements of curve C.

shown in curve B is very good. The experimental curve is also a bit higher in average response and in the amplitude of the tube resonances compared to the data of Fig. 6 for the aluminum tapered tube. The triangular data points are test measurements of the same charge of charred cotton as used for the measurements of curve A but are made in the configuration of Fig. 4 except an extra spacer made the test volume 7.7 cm^3. These measurements are in good agreement with curve C which represents Eq. (7) for this volume. Once again this shows that, for the amount of charred cotton used, the "light-absorbing air" model of the absorption cell employed in calculating curves B and C is valid. The results of Fig. 8 in comparison with Fig. 6 show that no substantial air leaks were present in the aluminum horn. Though the plastic horn tested here was straight, the wax core from which it is cast can be bent easily when warmed. This would allow it to be coiled within the hand-held portion of a telephone set before the casting is done. Thus the length of the tapered tube need not be an impediment to the use of the photophone described here.

Finally, we remark that a simple demonstration of voice reception by the photophone was made. For this demonstration the amplified output of a microphone was used to drive the electrooptic modulator. The photophone of Fig. 1 with the aluminum tapered tube was used. In this test the ear was pressed against a standard earpiece attached to the output end of the tapered tube.

ACKNOWLEDGMENTS

We wish to thank G. M. Sessler for the calibrated electret microphone, G. L. Miller for the design of the preamplifier, and J. R. Klauder for encouraging this work.

[1]S. E. Miller, E. A. J. Marcatili, and T. Li, "Research Toward Optical-Fiber Transmission Systems Part 1: The Transmission Medium," Proc. IEEE 61, 1703–1726 (1974); S. E. Miller, T. Li, and E. A. J. Marcatili, "Research Toward Optical Fiber Transmission Systems Part 2: Device and Systems Considerations," Proc. IEEE 61, 1726–1751 (1974).
[2]A. G. Bell, "Upon the Production of Sound by Radiant Energy," Philos. Mag. 11, 510–528 (1881).
[3]D. A. Kleinman and D. F. Nelson, "The Photophone-An Optical Telephone Receiver," J. Acoust. Soc. Am. 60, 1492–1494; "The Photophone—Physical Design," J. Acoust. Soc. Am. 60, 240–250 (1976).
[4]USA Standard, Z24.9-1949, "Method for the Coupler Calibration of Earphones."
[5]Sunproof Super Wax, Uniroyal Chemical, Naugatuck, CT.
[6]Vistanex, Exxon Chemical Co., Houston, TX.
[7]Bio-Plastic, Ward's Natural Science Establishment, Inc., Rochester, NY.
[8]Model BC4800, Laser Precision Corp., Yorkville, NY.
[9]Model 560B Lite-Mike, EG & G Inc., Salem, MA.
[10]G. M. Sessler and J. E. West, "Foil-Electret Microphones," J. Acoust. Soc. Am. 40, 1433–1440 (1966).
[11]F. T. Andrews and R. W. Hatch, National Telephone Network Transmission Planning in the American Telephone and Telegraph Company, IEEE Trans. Commun. Technol, COM-19, 302–314 (1971).

(No Model.) 2 Sheets—Sheet 1.

A. G. BELL & S. TAINTER.

Photophonic Receiver.

No. 241,909. Patented May 24, 1881.

Fig. 1.

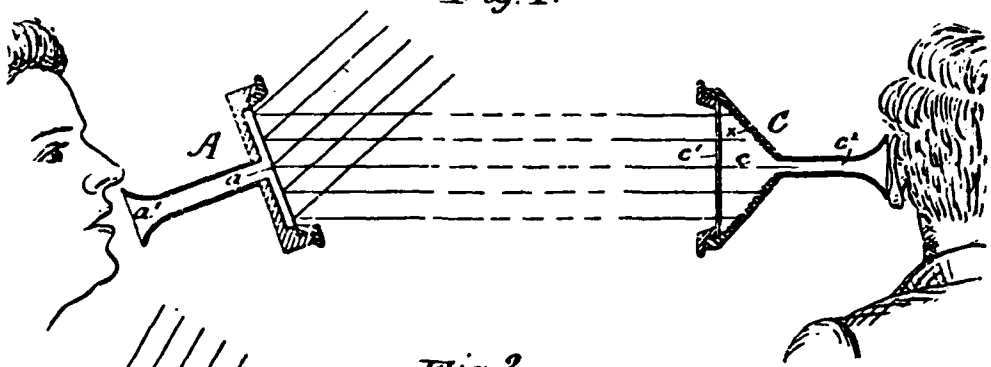

Fig. 2.

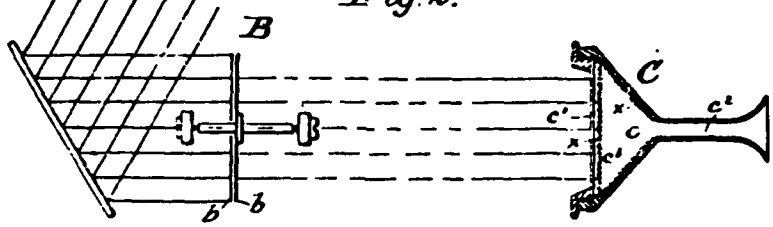

Fig. 2ª

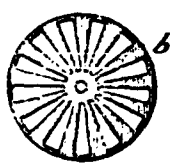

Fig. 2ᵇ

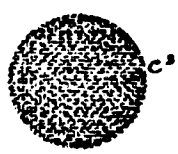

Fig. 3.

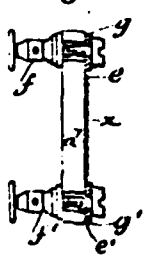

Fig. 4.

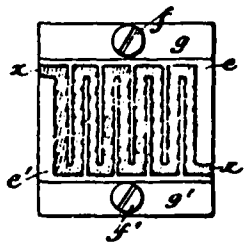

Witnesses:

E. E. Masson

Philip Abbey

Inventors.

Alexander Graham Bell

Sumner Tainter by

A. Pollok their attorney

(No Model.) 2 Sheets—Sheet 2.

A. G. BELL & S. TAINTER.

Photophonic Receiver.

No. 241,909. Patented May 24, 1881.

Fig. 5.

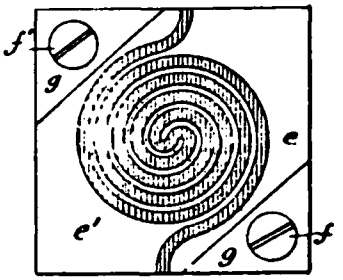

Fig. 6.

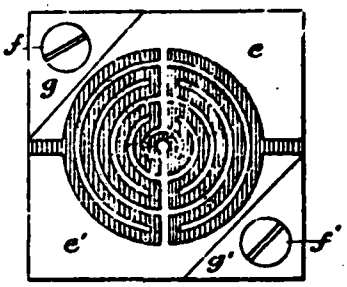

Fig. 7.

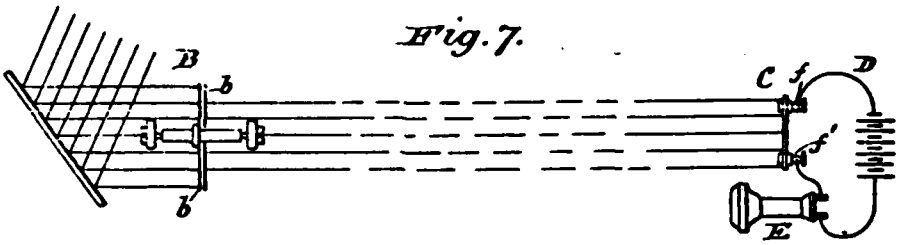

Fig. 8.

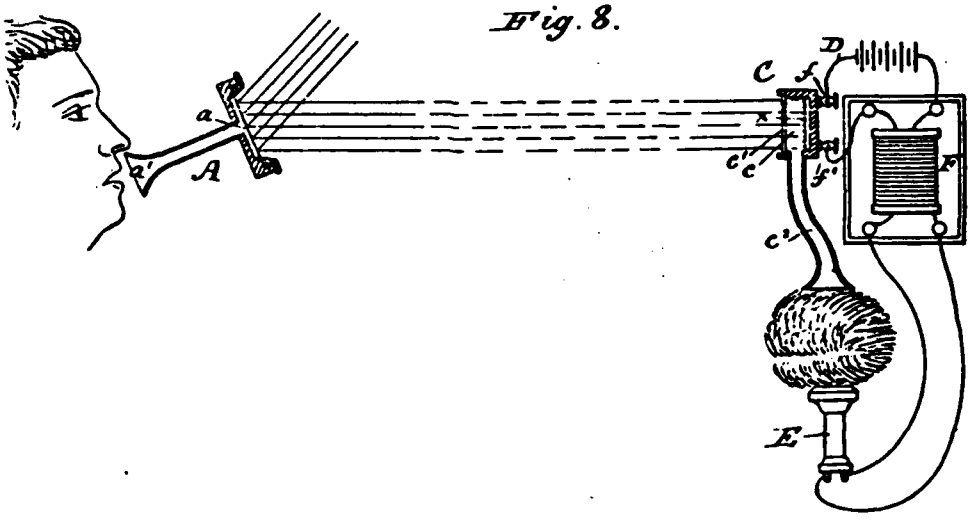

Witnesses.

E. E. Masson

Philip Lamb

Inventors:

Alexander Graham Bell &
Sumner Tainter by
F. Pollok their atty.

UNITED STATES PATENT OFFICE.

ALEXANDER G. BELL AND SUMNER TAINTER, OF WASHINGTON, D. C.

PHOTOPHONIC RECEIVER.

SPECIFICATION forming part of Letters Patent No. 241,909, dated May 24, 1881.

Application filed March 24, 1881. (No model.)

To all whom it may concern:

Be it known that we, ALEXANDER GRAHAM BELL and SUMNER TAINTER, both of Washington, in the District of Columbia, have invented a new and useful Improvement in Photophonic Receivers for the Production and Reproduction of Sound by the Action of Radiant Energy, which invention is fully set forth in the following specification.

The invention relates more particularly to the reproduction of articulate speech photophonically—that is, by the action of radiant energy from the sun or other suitable source—but is also applicable, in whole or in part, to the production or reproduction of other sounds, to the production of electrical and other effects, and to other purposes. It is intended as an improvement upon the photophone for which Letters Patent No. 235,199 were granted to Alexander Graham Bell, December 7, 1880.

The said photophone consists, generally, of a photophonic transmitter, by which a vibratory or undulatory beam or pencil of rays is produced, corresponding in its vibrations or undulations with the atmospheric vibrations that represent the sound to be produced or reproduced, and a photophonic receiver, by which the vibrations or undulations in the said beam or pencil of rays are converted into sound-waves, or into vibrations in an electric current that can be converted into sound-waves.

The present invention has reference to the photophonic receiver, and comprises means for converting the "radiant vibrations," as the vibrations or undulations of the beam of rays may be called, into sound-waves, and also into electric vibrations.

As described in the aforesaid patent, the radiant vibrations were converted into sound-waves by means of thin diaphragms of hard rubber, mica, and various other materials, upon which the radiant vibrations were allowed to fall. The sound was conveyed to the ear by a hearing-tube connected with a sound-chamber in the rear or unexposed side of the diaphragm, which itself formed one side of said chamber, or a part of one side. With this apparatus, although it is not very sensitive, musical notes were produced by rapidly interrupting a beam which was allowed to fall upon the diaphragm. The musical notes corresponded in pitch to the rate of interruption, and were loud enough to be easily heard.

We have discovered that the loudness of the sound is increased by having the illuminated or exposed side of the sensitive medium in contact with the air of the sound-chamber with which the ear-tube is connected, and by allowing the radiant beam to fall upon said medium through a plate of glass or similar material which is transparent to radiant energy, but opaque or less transparent to sound-waves. In this way the full effect of the radiant vibrations upon the sensitive medium is obtained, and the resulting sound-waves are shut in and conveyed to the ear with approximately their full force.

We have further discovered that a dark or black color in the sensitive medium is advantageous, and that with substances in an open, porous, or subdivided condition louder sounds are in general obtained than with diaphragms. The best effects are obtained with lamp-black deposited upon a surface of glass or other hard or rigid material. With a layer of this substance as the sensitive medium, articulate speech has been reproduced by the direct action of radiant energy upon said medium. In the experiments in which this result was obtained sunbeams were reflected from a mirror of thin glass silvered, (as described in Letters Patent No. 235,496, granted to us December 14, 1880,) and the mirror, being thrown into vibration by the voice, caused more or less of the sunbeams to fall upon the lamp-black. The latter was deposited upon the inner walls of a sound-chamber having one side formed of a glass plate to transmit the radiant beam, and having an ear-tube communicating with the interior, as explained above.

Articulate speech has also been reproduced with a receiver containing a mass of lamp-black in a loose pulverulent condition. A lump of lamp-black, when exposed in the sound-chamber to the action of an intermittent beam, gives a loud sound, but inferior to that given by the same substance in the form of loose powder or a deposited layer.

Instead of smoking the walls of the sound-chamber, a plate of glass, mica, or other material can be smoked and placed in said chamber so that the light falls upon the smoked surface.

The loudest sounds with the intermittent beam have been obtained by means of an open wire-gauze smoked or covered with a deposit of lamp-black. With a tubular resonator having the interior smoked a loud sound is produced when an intermittent beam having the proper rate of vibration is allowed to fall into it.

Numerous experiments have been made with various other substances. Black worsted may be mentioned as giving, with the intermittent beam, a good sound, although much inferior to lamp-black. Fibrous material coated with lamp-black has also been used.

Conducting-bodies generally, in a physical condition similar to lamp-black, especially if of dark or black color, yield good sound. Spongy platinum should be particularly mentioned. Other metals or metallic compounds—as silver, copper, black oxide of manganese, and the like—are also sensitive to radiant energy, and give out sound by the direct action of a vibratory beam. The production of sound in this way is conceived to be due to an absorption and expulsion of the air by the vibratory medium acting, as it were, like a sponge. Thus when the energy of the radiant beam increases the particles composing the vibratory medium expand and expel the air from between them, and when it decreases the reverse action takes place and the air is again absorbed. These repeated expulsions and absorptions are *proportionate to the rise and fall of radiant energy*, and produce corresponding condensations and rarefactions—or, in other words, sound-waves—in the surrounding atmosphere. Heat due to the absorption of the radiant energy seems therefore to be the principal agent in producing the sound-waves.

In the photophone as desbribed in Patent No. 235,199, above mentioned, the radiant vibrations were converted into electrical vibrations by a different material from any used for the direct production of sound-waves, the peculiar substance selenium being employed. The resistance which selenium, when properly prepared, offers to an electric current was known to vary under the influence of rays from the sun or other suitable source of radiant energy, and it was therefore employed as the medium for converting the radiant into electric vibrations. It was included in the circuit of a galvanic battery and placed in such position that the radiant beam fell upon it. The variations in the radiant energy due to the vibrations in the beam produced corresponding variations in the resistance of the selenium and in the galvanic circuit of which it formed a part, and consequently in the tension of the current on said circuit, or, in other words, they produced electrical vibrations in that circuit. By the aid of cells constructed to expose a large surface of the selenium, and the proper preparation of the latter, an apparatus was produced so sensitive to variations in radiant energy that, with a suitable photophonic transmitter and with an ordinary hand-telephone and galvanic circuit connected with the photophonic receiving apparatus, articulate speech was reproduced photophonically.

We have discovered that the same medium used to produce musical notes or to reproduce speech by the direct action of the radiant vibrations can be used to convert the latter into electric vibrations.

If a layer of lamp-black is included in an electric circuit and is exposed to the action of a vibratory beam of rays from the sun or other source, variations are produced in the electric resistance of the lamp-black, which variations correspond to those in the energy of the vibratory beam. If an intermittent beam is allowed to fall upon the lamp-black, electrical impulses are produced in the circuit in which the lamp-black is included corresponding to the radiant impulses of the beam, and if a telephonic receiver is also included in the circuit a musical note will be heard. If an undulatory or vibratory beam from the reflecting-transmitter before mentioned, or other speaking-transmitter which gives to the beam vibrations similar in rate, amplitude, and quality to the sound-waves of articulate speech, is allowed to fall upon the lamp-black, the electric undulations or vibrations in the galvanic circuit will represent the words and sentences which produced the vibratory beam, and if the apparatus is sufficiently sensitive these words and sentences can be reproduced by an ordinary telephonic receiver. The use of selenium, which is objectionable for reasons based upon the nature of the substance itself, as well as upon its high price and scarcity, can therefore be dispensed with. The same objections do not apply to lamp-black.

The action of radiant energy upon the vibratory medium to produce variations in the electrical resistance of the latter appears to be similar to that in producing sound by direct action—that is to say, the particles are brought together or moved apart according to the increase or decrease of the energy of the beam. They consequently furnish to the electric current a path of less or greater resistance.

All conductors in a physical condition similar to lamp-black have their electrical resistance affected by radiant energy. Spongy platinum is an example.

We have devised a form of cell whereby any desired extent of surface of the lamp-black can be exposed to the radiant energy without introducing undue resistance into the electric circuit.

Reference has hereinbefore been made to the cells used with selenium. These cells, the construction of which is fully described in Letters Patent Nos. 235,497 and 235,588, both dated December 14, 1880, consist, mainly, of two or more conducting strips, plates, or disks, placed side by side and separated by thin sheets of insulating material, which extend nearly to the edges of the plates, so as to leave a narrow

and shallow but long space to receive the selenium. The poles of the battery being connected with the plates which form the conductors of the cell, the current flows from one to the other through the selenium, meeting but small resistance on account of the thinness of the selenium layer. In some cases the selenium was cast around metallic pins embedded in insulating material connected with the poles of the battery.

In the present invention the conductors are formed of thin strips, plates, sheets, wires, or films fixed or mounted upon an insulating backing or support with their edges opposed and near together, so as to leave one or more narrow channels to receive the sensitive medium. Cells of this character are much simpler than those already patented, and they are, besides, better adapted to use in connection with lamp-black. The improved cells can be made with a curved or cylindrical surface, although a flat surface would generally be preferred, and the conductors can be made of various forms and metals.

Excellent results have been obtained with a cell having two conductors which resemble in appearance combs with wide-spaced teeth, and which are secured to the insulating-backing in such relative position that the teeth of one comb alternate or intermesh with the teeth of the other, but are not in contact with them. The sensitive medium fills the spaces between the teeth of the two conductors, and by increasing the number and length of the teeth the surface can be increased to any desired extent. The resistance to the electric current will, of course, depend upon the mass or area of sensitive medium, and upon the distance which separates the teeth of one comb from those of the other.

In order that the electric current may flow equally from the several teeth, or generally from one conductor to another, it is necessary that the spaces between their adjacent edges should be everywhere the same.

We have found that a film of silver deposited upon a glass plate by the methods ordinarily employed for silvering mirrors is possessed of great toughness, and can, with a suitable tool, be ruled or scraped off in stripes, so as to leave sharp edges which appear clean and well defined, even under a microscope. As the silvered film is not affected injuriously by lamp-black, it is, from its great conductivity and the accuracy with which it can be ruled, eminently adapted to use in this invention as the conductor of the photophonic receiver. The silvered film can be deposited upon a curved or flat surface, and can be scraped off in straight, zigzag, circular, spiral, or other suitable lines. The width of the stripe or stripes removed is regulated by the scraping-tool, and the position of the latter in operation is controlled and adjusted by mechanical means, so that the utmost exactness can be obtained.

In the cell before referred to as giving excellent results the intermeshing combs were formed by scraping a silvered film from a flat glass plate, as just described. This form of conductor is, however, obviously of general application, and can be employed with various metals. For example, the combs can be cut from tin-foil and pasted upon glass. The lamp-black is applied to these cells by smoking the proper surface over a flame from a coal-oil lamp or other suitable burner. The lamp-black will be deposited on the conductors as well as between them; but this does not interfere with the practical workings of the apparatus. The depth of the layer deposited may be just sufficient to render the surface sensibly opaque. The character of the result is affected by the depth and also by the extent of surface exposed to the radiant energy. Although no special extent is requisite, a very large surface is not desirable, and there is a certain limit at which the best results are obtained in any case; but this limit varies with the energy of the radiant beam, the strength of the battery, and other conditions, so that no simple rule can be given. By depositing upon the silvered glass, ruled or scraped as explained, a layer which is sensibly opaque and wiping it off gradually around the edges, a spot of suitable size and character can be readily obtained.

The cell is ordinarily secured in position in a sound-chamber having a glass plate for the entrance of the radiant beams, and it is so placed that said beams fall upon the lamp-black. If it is desired to receive a message or signal directly, as well as through the intermediary of the electric current, the sound-chamber is provided with one or more ear-tubes.

The lamp-black cell can be located in the main circuit in which the electrical or telephonic receiving apparatus is placed, or it can be connected with a receiving-circuit by means of an induction coil or coils, as telephonic transmitters using a battery have been connected.

Having explained the general principles of our invention, we will now proceed to describe apparatus constructed in accordance with the same, reference being had to the accompanying drawings, which form a part of this specification.

Figure 1 is a sectional view, illustrating apparatus for transmitting speech photophonically without the aid of an electric circuit; Fig. 2, a sectional view of a slightly altered form of a receiver, shown in connection with the apparatus for producing an intermittent beam; Fig. 2^a, a front view of one of the disks of the intermittent-beam apparatus; Fig. 2^b, a similar view of a wire-gauze disk used in the receiver; Figs. 3 and 4, views, in section and plan, of the lamp-black cell with intermeshing combs of silver film; Figs. 5 and 6, plan views of other forms of the cell; Fig. 7, a view showing the cell in circuit with galvanic battery and hand-telephone and the intermittent-beam apparatus as the photophonic transmitter; and Fig.

8, a view, partly in section, illustrating the apparatus for transmitting speech, and showing a photophonic receiver connected with a telephonic circuit, and also provided with means for collecting and conveying to the ear of the listener sound-waves directly produced.

The same letters of reference indicate like parts in the several figures in which they occur.

A is a reflecting photophonic transmitter; B, the intermittent-beam apparatus; C, the photophonic receiver; D, a galvanic circuit; E, an ordinary hand telephone; F, an induction coil.

The reflecting-transmitter A consists of a mirror of thin silvered glass, *a*, which is thrown into vibrations by the voice of a person speaking into the tube *a'*, and reflects more or less of the beam of sunlight or other radiant beam toward the receiver C.

The intermittent-beam apparatus B comprises two disk-wheels, *b*, with a series of radial openings in the path of the beam. One of these disk-wheels is stationary and the other revolves, or they both revolve in opposite directions, or in the same direction at unequal velocities. The beam, being consequently cut off by the blank spaces and allowed to pass through the openings when those in one disk register with those in the other, is intermittent in its action. A beam from the sun or from an artificial source can be employed with this apparatus. The beam can be concentrated before or after passing through the disk-wheels, and can be reflected by mirrors to the proper path, or allowed to fall directly upon the wheels.

These two forms of transmitting apparatus are shown as types. Any photophonic transmitter of ordinary or suitable construction can be used with the improved receiver.

In Fig. 1 the receiver C consists of a funnel-shaped sound-chamber, *c*, the interior flaring walls of which are smoked or covered with a deposit of lamp-black, *x*. The mouth is covered with a glass plate, *c'*, and a sound-conveying tube, *c²*, communicates with the contracted portion in the rear. Speech or other sound uttered into the tube *a'* of the transmitter A can be heard by listening at the tube *c'* of the receiver C. The distance over which speech can be transmitted in this way and the distinctness of the sounds reproduced depend upon the energy of the beam employed.

In Fig. 2 the receiver C contains a piece of wire gauze, *c³*, upon which the lamp-black *x* is deposited. The walls of the sound-chamber *c* can also be smoked, as shown, or not, as desired. The sound is received by the tube *c²*, as before.

In Figs. 3 and 4 the receiver is a lamp-black cell, and comprises the glass plate or insulating support *d*, the intermeshing combs or conductors *e e'*, of silver film, the binding-posts *f f'*, connected with the conductors *e e'*, respectively, by the metallic plates *g g'*, and the lamp-black *x*.

In forming the cell the silver is deposited in any ordinary or suitable way. The desired portions are removed or scraped off by means of a tool with a flat end. This tool can be made like a chisel, or a punch with conical point can be ground off or cut at right angles to the axis, so as to leave a flat end with a diameter equal to the desired width of the stripe to be removed. The mechanical ruling or scraping of the plate can be easily effected by means of an ordinary lathe provided with a slide rest. The tool is held in a frame supported between centers. The plate is clamped to a bed-plate beneath with the silvered side uppermost, in such position that when the tool is pressed down and penetrates the film its operating end rests flat upon the surface of the glass. The bed-plate carrying the silvered plate can be worked lengthwise of the lathe to rule or scrape off the lines in one direction, and then moved across at right angles to the length to bring the plate into position for scraping a new line.

It is not necessary to remove the tool from the plate. The lengthwise movement under the tool removes the film so as to form the spaces between the teeth of the combs, and the transverse movement connects these spaces with each other alternately at opposite ends.

The binding-posts are fastened to the glass plate in any ordinary or suitable way, and are in electrical connection with the two parts of the conducting-film. To apply the carbon the silvered side of the glass plate is smoked over a suitable burner.

In Fig. 5 the silver film is scraped off in the form of a double spiral, leaving the conductors *e e'*. In Fig. 6 the conductors *e e'* have curved intermeshing teeth. In these figures the lamp-black *x* is shown as confined to the spaces between the conductors in order to show the latter more clearly; but in practice the conductors would ordinarily be themselves coated.

In Fig. 7 the poles of the galvanic circuit D are connected with the binding-posts *f f'*. A musical note produced by the action of the intermittent beam can be heard by applying the telephone E to the ear.

In Fig. 8 the lamp-black cell is placed in a sound-chamber, *c*, and is connected with a battery in the primary circuit of the induction-coil F, the telephone E being connected in the secondary circuit of the coil. The chamber C has a glass plate, as in Fig. 1, through which the radiant energy is transmitted, and a hearing-tube, *c²*, for conveying the sound-waves produced in the receiver to the ear. Sounds uttered into the tube *a'* of the transmitter can be heard either by listening at the tube *c²* or by means of the telephone E.

It is obvious that various modifications may be made without departing from the spirit of the invention, and that parts of said invention could be used without the others. The forms of cells used for selenium can be used with lamp-black, and the improved cell can be em-

ployed with any suitable form of sensitive medium; but the metal composing the conductors should be such as not to be injuriously affected by the action of the sensitive medium.

The insulating-plate with the ruled or scraped silver film thereon can be employed to measure the electric conductivity of various substances, liquids, and gases by connecting the binding-posts with the poles of a galvanometer-circuit and immersing the plate with the substance to be tested, or covering the silvered side with the same. In some cases the silver film can be deposited on both sides of the plate and ruled as before described.

Telephonic transmitters and receivers can be formed by means of apparatus like the lamp-black cell; but these will form the subject of separate applications.

That part of the invention which relates to the conversion of the radiant vibrations into electrical vibrations is not limited to lamp-black, but includes other forms of carbon, and also other materials which operate in a substantially similar manner to lamp-black.

Having now fully described our said invention and the manner of carrying the same into effect, what we claim is—

1. In a photophonic receiver, the sound-chamber for containing the sensitive medium, having a wall transparent to light or radiant energy, but opaque or less transparent to sound, substantially as described.

2. *The combination of the sound-chamber*, having a wall transparent to radiant energy, but opaque or less transparent to sound, with the sensitive medium therein contained, and a sound conveyer or opening communicating with the interior of said chamber, substantially as described.

3. In a photophonic receiver, the sensitive medium, composed of vibratory material in an open, porous, or subdivided condition, substantially as described.

4. In a photophonic receiver, a sensitive medium of lamp-black or similar material, substantially as described.

5. A photophonic receiver having as the sensitive medium a deposit of vibratory material in a loose, porous, subdivided, flocculent, or spongy condition, substantially as described.

6. In a photophonic receiver, the combination of a sensitive medium conductive of electricity, in a loose, porous, or subdivided condition such as lamp-black, and conductors for including the same in an electric circuit, substantially as described, so that radiant vibrations can be thereby converted into electric vibrations, as set forth.

7. The combination of the lamp-black or other vibratory conducting material in loose particles, the rigid or substantially inextensible support of insulating material, and conductors by which the lamp-black can be included in an electric circuit, as set forth.

8. A cell comprising sheets, plates, or strips of conducting material, fixed or mounted upon a support of insulating material, with their edges opposite each other and separated by a suitable distance, and sensitive conducting material in the space or spaces between said edges, substantially as described.

9. A support of insulating material, having comb shaped conductors fixed or mounted on said support, as indicated, so that the teeth of the combs intermesh but are not in contact with each other, substantially as described.

10. A silvered plate having the silver film mechanically ruled or scraped, as described, so as to leave parallel lines or stripes of equal width, and with sharp, clean edges, substantially as set forth.

11. The insulating-plate having on one or both sides a silver film ruled or scraped, as described, so as to divide the silver film into two or more conductors, in combination with binding-posts connected with the parts of said film or films, substantially as set forth.

12. The combination of the insulating-plate and ruled silver film with the lamp-black or sensitive medium included in the ruled or scraped spaces in said film, substantially as set forth.

13. The combination, with a galvanic circuit, of a photophonic cell comprising a glass plate with ruled silver film thereon, lamp-black deposited in the ruled spaces in said film, and connections for completing the galvanic circuit through said cell, substantially as described.

14. The combination, with a photophonic cell, of an induction-coil, electric connections for including said cell in one circuit of said coil, and a telephone-circuit connected with the other circuit of said coil, substantially as described.

15. A photophonic receiver comprising a sound-chamber having a wall transparent to radiant energy, but opaque or less transparent to sound, a cell having a vibratory sensitive medium, such as lamp-black, electrical connections for connecting said cell in an electrical circuit, and a hearing-tube connected with the interior of said sound-chamber, substantially as described.

In testimony whereof we have signed this specification in the presence of two subscribing witnesses.

ALEXANDER GRAHAM BELL.
SUMNER TAINTER.

Witnesses:
PHILIP MAURO,
A. POLLOK.

ALL OPTICAL TELEPHONE DEVELOPMENT

by

B. G. Grossman, S. R. Adhav, L. M. Ralston, and R. K. Morse,
Harris Corporation, N. Feldman, CECOM

1. INTRODUCTION

The optical fiber, as a medium for communications, has been successfully replacing metallic cable trunks. It is presently serving the communication industry in both high capacity and low capacity links. Thus far, with few exceptions, the highest volume users of transmissions lines, subscribers, have been neglected.

When Mr. Feldman discussed his "All Optical Telephone" at ICC-81 in Denver, Colorado in June 1981, it was a step toward correcting this neglect. He described an instrument served by optical fibers, simple, and inexpensive, requiring no electrical power. His conceptual system contained six components, two of which, earphone and ringer, seemed to present some measure of barrier to successful implementation. A government contract was awarded to Harris Corporation, Melbourne, Florida, in November 1981, to demonstrate the feasibility of the concept. The barrier items would get special attention in the execution of this contract.

In this paper, we will describe the work pursued and accomplished by Harris. Three of the six components, hear (earphone), talk, and ring, will be addressed. The expended effort has consisted of a judicious mix of computer modeling, brainstorming, engineering, and model shop work. Our efforts will be described, our results documented, and our designs discussed.

It should be noted that one barrier component, the optical to sound converter, was addressed 100 years ago by Alexander Graham Bell. Though several experimenters have worked on it since, we believe that this is the first work directed at its use in a complete telephone instrument. What is reported here is a first cut effort to demonstrate feasibility. We realize these efforts are primitive, but, fully expect that the refinement process and optimization will follow rapidly.

Presented at the Sixth International Fiber-Optics and Communications Exposition.
September 15-17, 1982
Los Angeles

2. TALK FUNCTION

The function of the TALK mechanism is to convert spoken words into modulated light. This light is coupled by optical fiber to an electronic switchboard and then reconverted into sound at a HEAR mechanism. The frequency response of the TALK mechanism must be reasonably flat over the voice band, 300 to 3300 Hz, and typical voice levels must generate sufficient optical modulation to be detected and reconverted to sound with a sufficient signal to noise ratio, as in a conventional telephone set.

Two basic modulation methods, phase modulation and amplitude modulation, were considered for the talk mechanism. Phase modulation of light by pressure waves recently has been explored and optimized using optical fibers for underwater sensor applications. The major disadvantage of this method is that complicated interferometric techniques are usually required to demodulate the phase encoded information. It was decided, therefore, because of their easier implementation, to concentrate on amplitude modulation techniques. There are numerous passive amplitude modulation techniques, including sound dependent fiber misalignment, frustrated total internal reflection, microbending loss modulation, etc. The approach selected by Harris for the TALK function was the first represented as loss modulation by variable optical coupling between two end-to-end coaxially aligned fibers. In this technique, one of the fibers is fixed in position, while the other is attached to the center of a thin membrane diaphragm. Sound waves incident on the membrane cause it to vibrate resulting in changes in the coupling efficiency between the two fibers. The amount of coupling, and therefore the magnitude of the intensity variations, depends on the amplitude of the diaphragm vibrations.

The TALK mechanism model is a homogeneous circular membrane driven by a constant pressure across the surface with no damping forces. Solution of the wave equation of this system for the amplitude of the membrane displacement, y, results in:

$$y = \frac{P}{kT}\left(\frac{Jo(kr)}{Jo(ka)} - 1\right)$$

where:

Jo(kr), Bessel function of order zero.
P, drive pressure, dynes/cm^2.
T, membrane tension, dynes/cm^2
$k = \omega\sqrt{s/T}$, rad/cm.
s, area density, gm/cm^2.
a, cell radius, cm^2.
ω, frequency, rad/sec.
r, the radius at which the displacement is measured, cm

This equation was used to generate plots of membrane displacement at the center of the cell, where the fiber ends were placed, as a function of frequency. Since the fiber ends, one fixed and one moving with the membrane, are at the center, the plots represent instantaneous fiber coupling and thus, light amplitude. A typical plot is shown in Figure 2.1. As mentioned previously, in order to reproduce ideally the individual voice characteristics of the user, the response of the TALK mechanism should be flat across the voice band from 300 to 3300 Hz. One way to accomplish this is to set the membrane parameters such that the first resonance is above the band of interest. The other option is to generate resonances across the frequency band, especially at the high frequency end where overtones typically give voices their individuality.

The Harris design for the talk mechanism is shown in Figure 2.2. A disk of 12.7 micron thick mylar was stretched across a 4 cm ring and fixed at the edges. The input fiber was attached to the mounting ring and to the center of the membrane by a small drop of epoxy. The output fiber was mounted inside a hypodermic needle cut and polished flat at both ends. The 50μm core input and output fibers were aligned to maximize the coupling efficiency of the light in the static mode, and then the needle attached to the ring mount by epoxy to hold the fiber stationary.

3. HEAR FUNCTION

The passive HEAR mechanism must convert light into sound with a bandwidth of 300-3300 Hz and a sound pressure level at the ear of at least 81 dB. Two design approaches were considered. In the first, the Edelman[1] approach shown in Figure 3.1, the optical energy is absorbed as heat in optical fibers having a high Youngs modulus, low specific heat and a large coefficient of thermal expansion. The fibers expand and contract under tension as a function of the modulated optical input and drive a diaphragm element which is impedanced matched for the desired voice bandwidth. Input modulated light is thus converted into sound pressure waves by the moving diaphragm.

The second approach, the Kleinman-Nelson[2] approach shown in Figure 3.2, consists of a small photo-acoustic cell, which converts the light modulation into sound waves, and an acoustic impedance matching system. The last impedance matching element is an exponentially tapered horn which couples sound to the ear. The photo-acoustic interaction occurs between the light and a small quantity of suspended carbonized cotton. As the input light intensity varies with the HEAR signal, the cotton and surrounding gas heat and cool and thus expand and contract producing an acoustic pressure wave. The impedance matching system maximizes the acoustic energy transmitted to the ear. Calculations made of the expected performance of the Edelman[3] and the Kleinman-Nelson[4] approaches indicated that the latter approach had a 10 dB higher conversion efficiency. Because of this and the proven nature of the Kleinman-Nelson approach, it was decided to incorporate this technique in the Harris design.

The Harris HEAR mechanism design consists of an exponential horn similar to that of Kleinman-Nelson approach. The Harris design was computer optimized and resulted in a mechanism with 10% less overall length and an increase of approximately 3 dB in output over the desired bandwidth as compared to the Kleinman-Nelson approach. Air was chosen as the internal gaseous medium for ease of fabrication, although it has been shown[3] that other internal gases can increase sensitivity. However, this requires added complexity of a diaphragm for gas confinement.

It was decided to fabricate the horn by machining a two piece aluminum mandril on a lathe, electroplating copper on the outside of the mandril and, subsequently, etching the aluminum in a hot sulphuric acid bath. The resulting form is a rigid copper horn whose inside dimensions are the same as the outside dimensions of the aluminum mandril. Inertance tube equalizers, photo-acoustic cell and ear-piece coupler can then be attached.

Following the nomenclature of Kleinman-Nelson (K-N)[3], the equivalent circuit of the photophone is shown in Figure 3.3. The solution of the circuit shown reduces to:

$$\left|\frac{P_E}{S_L}\right|^2 = \left(\frac{2}{\pi}\frac{j\omega\rho}{r_1^2 r_2^2 k}\right)^2 \cdot \frac{\exp\{(-r_o/r_1)\xi\}}{|g(k) + h(k)\exp(2j\alpha l + j\Delta - \Delta)|^2}$$

where: $g(k) = -h(k)^* = (1 + \frac{Z_1}{Z_c} + \frac{Z_1}{Z_c}) \cdot (\frac{Z_2}{Z_e} - \frac{Z_2}{Z_e} - 1)$

$Z_{1,2} = \frac{j\omega\rho}{m \pm \pi r^2_{1,2}}$, characteristic impedance of a lossless tube.

$m \pm = \alpha \pm j\alpha$, lossless solutions.

$\alpha = (\ln(r_2/r_1))/l$, exponential taper constant.

l, length of horn, cm.

P_E, pressure at ear-piece coupler, dynes/cm^2.

Z_e, acoustic impedance of ear coupler, gm/sec cm^4.

Z_c, acoustic impedance of source volume, gm/sec cm^4.

S_L, velocity flow of photo-acoustic source, cc/sec.

$Z_{1,2}$, equalizer impedances, gm/sec cm^4.

TVD, thermoviscous damping, gm/sec cm^4.

ρ, density of medium, gm/cc.

c, velocity of sound, cm/sec.

$r_{1,2}$, input and output radii of the horn, cm.

r_o, boundary layer radius, cm.

α, complex term of propagation constant.

$k = \omega/c$, rad/cm.

ξ, Δ, frequency dependent functions for boundary layer approximation.

Further manipulation yields the transfer function, H_ω:

$$H_\omega = G_m^2 \left(\frac{9.1 \times 10^{-4}\ \text{cm}^4}{r_1^2 r_2^2}\right) \cdot \left(\frac{\alpha}{k}\right)^2 \frac{\exp\{(-r_o/r_1)\xi\}|G_\omega|^2}{|g(k)|^2(1 - 2e^{-\Delta}\cos\phi + e^{-2\Delta})} \quad (3)$$

where: G_m, figure of merit for the gas; air = 1.

G_ω, dispersion function for a sphere volume approximation of the cell.

$\phi = 2\alpha l + \Delta - 2\varphi$

$\varphi = g(k)$

Integration of $1 - 2e^{-\Delta}\cos\phi + e^{-2\Delta}$ over 2π in equation 3 (the term of which arises from oscillations due to resonances of travelling waves in the tube) results in an average or a smoothed response, $\langle H_\omega \rangle$:

$$\langle H_\omega \rangle = G_m^2 \left(\frac{9.1 \times 10^{-4}\ \text{cm}^4}{r_1^2 r_2^2}\right) \cdot \left(\frac{\alpha}{k}\right)^2 \frac{\exp\{(-r_o/r_1)\xi\}|G_\omega|^2}{|g(k)|^2\{1 - e^{-2\Delta}\}}$$

The output intensity is the product of H_ω with the following function, D_ω.

$$D_\omega = \frac{R_o^2(\gamma - 1)^2(P_{opt} \times 10^4)^2}{2(\gamma_o P_o I_o)^2}$$

where:

R_o, 880 gm/sec cm^4, a constant to normalize H_ω.

γ_o, specific heat ratio of gas.

P_{opt}, RMS optical power, mW.

P_o, atmospheric pressure, dynes/cm^2.

I_o, 2×10^{-4} dynes/cm^2.

A computer predicted plot of the Harris HEAR mechanism response compared to the K-N photophone appears in Figure 3.4.

4. RING FUNCTION

As in the case of the HEAR function, the technical challenge of the RING implementation lies in the need to obtain a noticeable acoustic output from the telephone set at a level of approximately 75 dB sound pressure level (SPL) at 1 meter with only an optical input from the fiber link. However, the RING function, unlike the HEAR, does not convey detailed communications, but serves only to alert the telephone user to an incoming call. There are two possible means for producing the required sound; direct conversion of the optical RING signal to acoustical energy as in the HEAR function and the use of the optical ring signal to trigger the release of stored mechanical energy into a predetermined acoustic signal, loud and noticeable enough to attract the attention of the telephone user. Both approaches were investigated.

The direct conversion of optical to acoustical energy can be obtained, as in the HEAR function, by the photo-acoustic effect. The problem is the same as that of the HEAR function, except for the value of the load impedence. The HEAR couples into a fixed volume load, whereas, to be useable in a manner comparable to existing systems, the RING must couple into free space. Using the HEAR computer programs, a design for a RING horn which optimized the sound output for a load impedance of a massless air piston was derived. In this case, bandwidth was not a major concern and was traded off for increased response over a narrow band. The RING horn is similar in design to the HEAR horn but the larger diameters are due to the different load impedance. The input radius is 0.05 cm and the output radius is 15.0 cm. The overall length is 17 cm. The cell volume is 5.0×10^{-4} cm^3 and the equalizer tube diameter and lengths are 0.02 cm and 20 cm respectively. The predicted acoustic output is shown in Figure 4.1. The predicted peak response 1 meter from the horn is 75 dB with 2.5 mW of light and increases to 92 dB with 18 mW of light.

The second approach investigated utilized the optical ring signal to trigger the release of mechanically stored energy which was then converted into acoustic energy to alert the user of an incoming call. The released mechanical energy is restored at the conclusion of the call through the action of the hook switch which, when depressed, can be used to compress a spring, twist a torsion bar, or displace a weight, etc. The actual production of sound can be accomplished with a bell type device, a bellows/vibrating reed, etc.

The initial investigation concentrated on the trigger mechanism. When irradiated, the trigger released a predetermined amount of mechanical energy into the sound producing device. The designed mechanism incorporated a bimetallic strip; when heated by optical energy, the strip bends from its normal position releasing the mechanical energy. After the light pulse ends, only a few seconds is required for the strip to cool to ambient and return to its initial latching position. Thus, each light pulse can trigger a ring cycle.

The Harris RING mechanism, incorporating the bimetallic trigger, is shown in Figure 4.2. Mechanical energy is stored by means of a spring geared to a low torque governor. The bimetallic trigger in its normal off position latches the governor. When a ring signal is sent, the light output from the fiber is focused by two lenses onto a blackened bimetal strip which deflects as it heats up, releasing the governor. The drum rotates, causing a set of bells to be struck, producing a sound much like that of a conventional phone. Although the feasibility design implemenatated was constructed of metal, ringers can be fabricated of plastics and ceramics. For this program, it was decided to build and test the ringer shown in Figure 4.2, primarily because it was easier and faster to build, as well as lower risk than the RING horn described previously. The experimental results are described in the following section.

5. EXPERIMENTAL RESULTS

An electronic interface unit (EIU) was constructed to test the three components. Three Optical Information Systems, 20 mW laser diodes were incorporated in the EIU along with their associated signal circuitry and power supplies. The laser diodes were biased at 20 mW for the RING and 10 mW for the TALK and HEAR. The optical telephone side tone feedback signal was generated electronically. A 3000 cm, 4 fiber optical link was used for interconnection in testing the components.

The TALK signal levels were measured as a function of input frequency. The measurement breadboard is shown in Figure 5.1. A helium

neon laser was coupled to the input fiber through a 20X microscope objective. An optical power meter was used to detect the light variations; the output of the meter was fed to an oscilloscope for measurement. An audio oscillator provided the sound frequency input which was normalized to 90 dB at each frequency. Data was taken under three conditions: the cell placed flat on the bench, placed over a 7 cubic inch volume, and finally a mechanical voice filter (a standard telephone mouthpiece) was placed over the membrane. The measured voltage as a function of input sound frequency is shown in Figures 5.2, 5.3, and 5.4 for these three cases. These experimental results are of the same form as the theoretical prediction shown in Figure 2.1. The response, observed when the diaphragm was backed by a reasonable volume, has a series of resonances with the primary peak at about 2375 Hz. Tests were then run in which different people spoke into the mechanism and the resulting light modulation was converted back into sound by the EIU. The response of the cell was such that the individual voices were easily understandable and identifiable. Tonal quality was similar to that of the conventional telephone set.

The HEAR mechanism was fabricated and initially tested by placing the absorption cell near the ear and detecting the output. The laser diode, biased at 10 mW, was 100% modulated by the audio generator and the light signal was applied to the Hear cell. The tone was easily audible. Final HEAR horn testing its continuing.

The Ring mechanism described in Section 4 was fabricated and tested with the EIU. After four seconds of a 16 mW cw light signal, the ring signal began and continued until the light pulse turned off. The ring produced an audio output of 75 dB at a distance of 1 meter from the mechanism, as required.

6. CONCLUSIONS/FUTURE OF THE CONCEPT

The results of the current study indicate that an all optical telephone set is technical feasible. The implementation methods and subsequent designs were chosen after an intensive literature survey of past research and brainstorming sessions for new ideas. The techniques selected were determined primarily on a risk/performance basis where the lowest risk approach having the greatest chance of success was chosen. It is obvious that much work still needs to be done both in optimizing the performance and manufacturing cost parameters of those functions investigated in this study as well as other functions such as hook switch, sidetone and dialing. The associated technologies required already exist with low loss optical fibers and high power laser diodes commercially available. The authors are hopeful that the all optical telephone first envisioned by Alexander Graham Bell over 100 years ago, will soon become a reality.

ACKNOWLEDGEMENT

The authors wish to thank Mr. Rollie McCollum and Mr. Thomas Conroy for their work on the mechanical and electronic interface designs and Mr. Scott Stewart for his assistance in the fabrication and testing. The funding for the program was from the U.S. Army, CECOM at Fort Monmouth, New Jersey.

REFERENCES AND FOOTNOTES:

1. S. Edelman, U.S. Patent Pending.
2. D. Kleinman and D. Nelson, The Photophone - An Optical Telephone Receiver, J. Acoust. Soc. Am., Vol. 59, No. 6., June 1976.
3. S. Edelman, Private Communications, Acoustic-Optic Workshop, Ft. Monmouth, March 31, 1982.
4. D. Nelson, K. Wecht and D. Kleinman, Photophone Performance, J. Acoust. Soc. Am., Vol. 60, No. 1., July 1976.

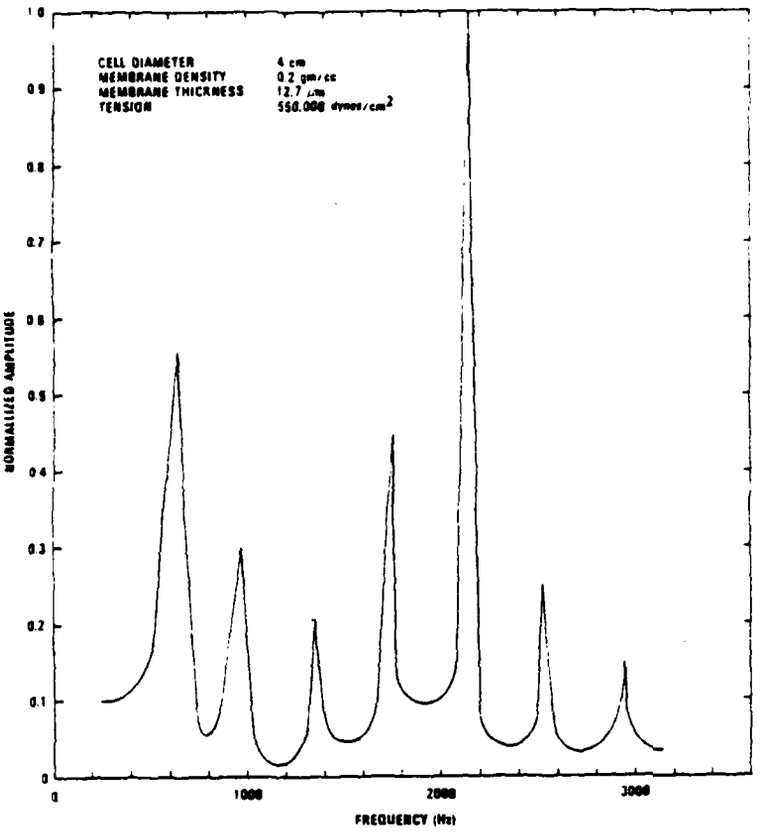

Fig. 2.1. Computer Generated TALK Predictions.

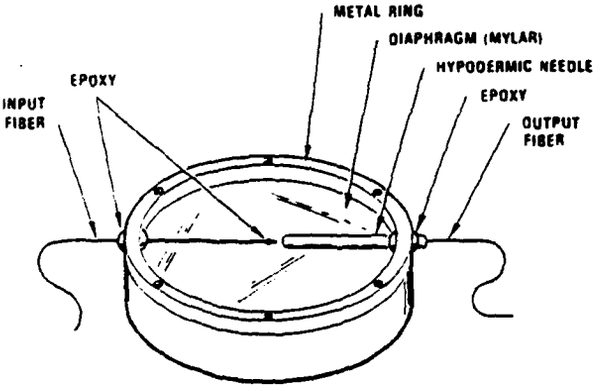

Fig. 2.2. Harris TALK Mechanism.

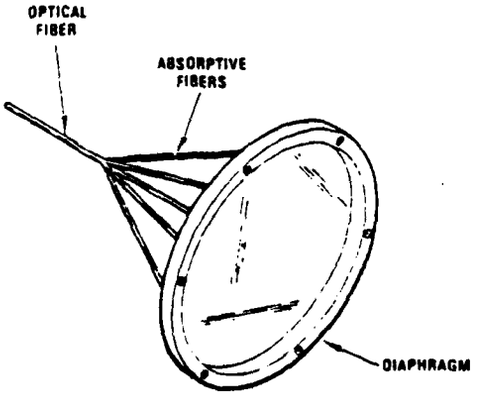

Fig. 3.1. Edelman HEAR Design.

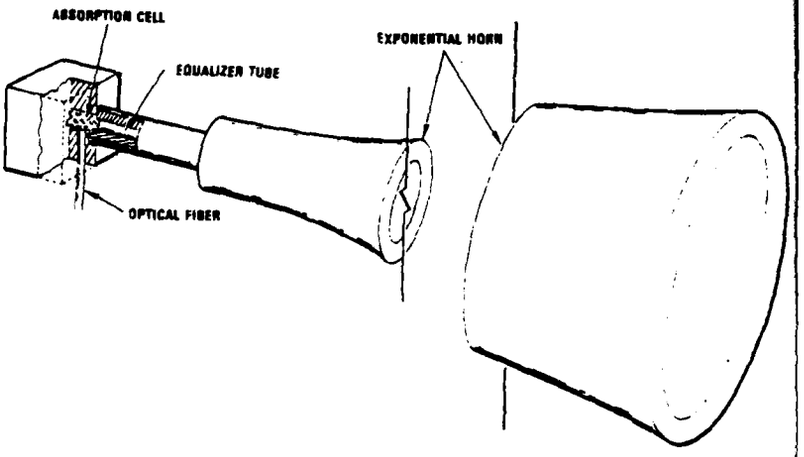

Fig. 3.2. Kleinman-Nelson HEAR Design.

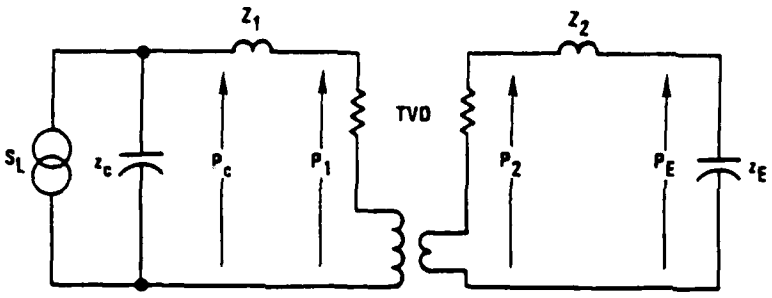

Fig. 3.3. Kleinman-Nelson Equivalent Circuit.

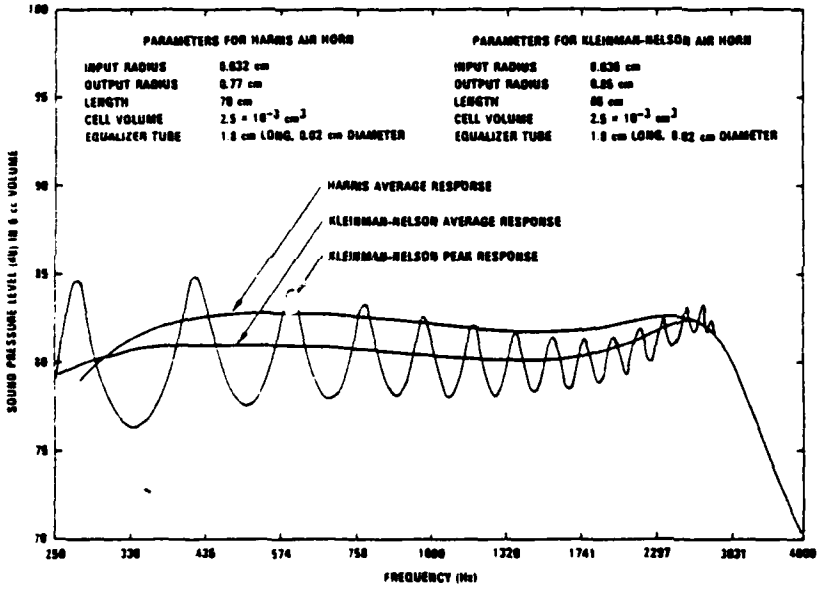

Fig. 3.4. Kleinman-Nelson Versus Harris Predictions.

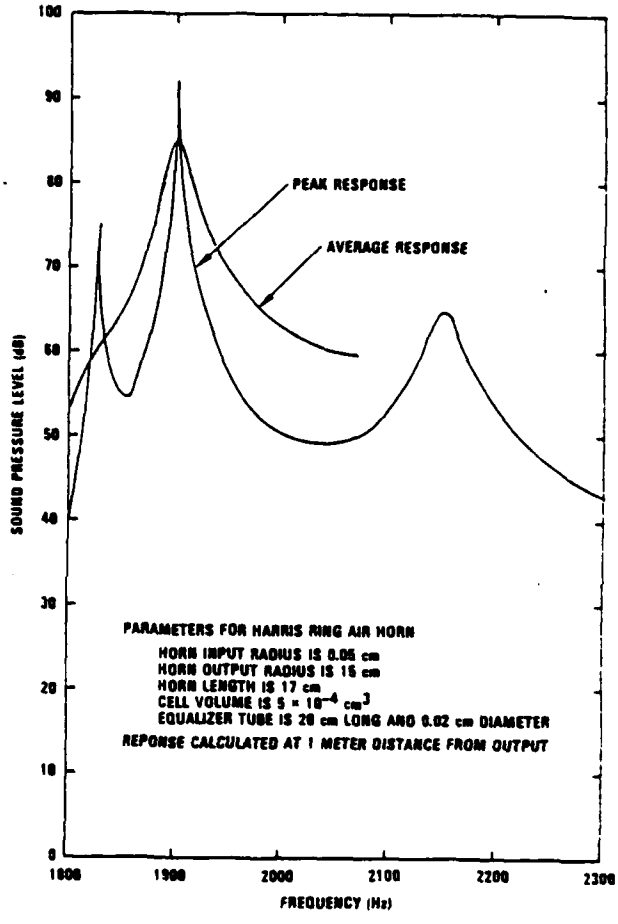

Fig. 4.1. Predicted RING Horn Response.

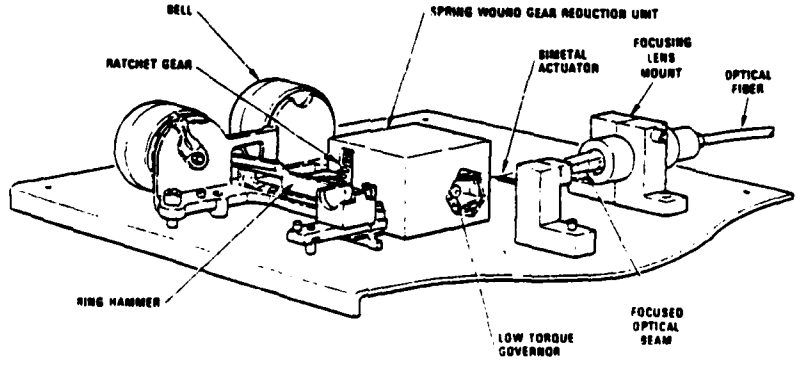

Fig. 4.2. Mechanical RING Design.

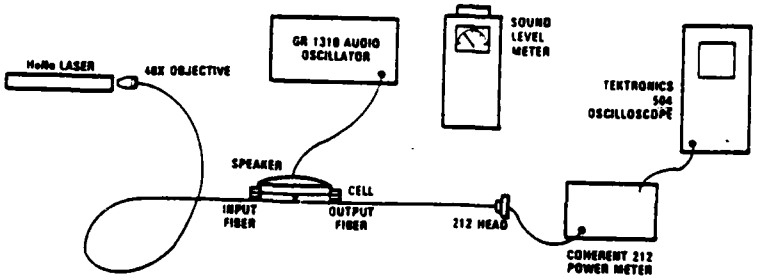

Fig. 5.1. Experimental Breadboard for Frequency Response Measurements.

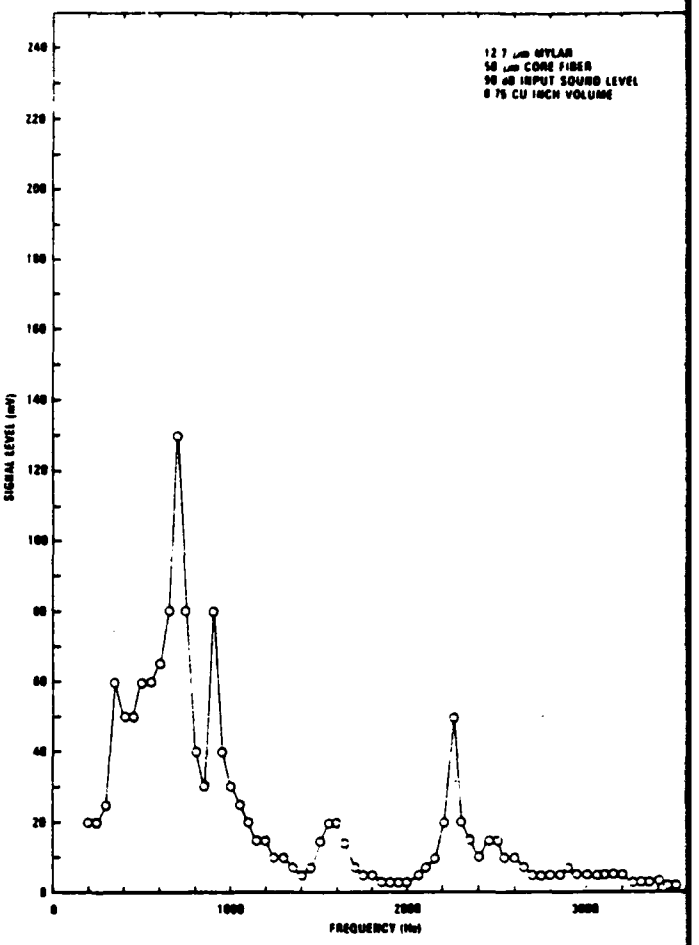

Fig. 5.2. TALK Response with .75 cu. in. Volume

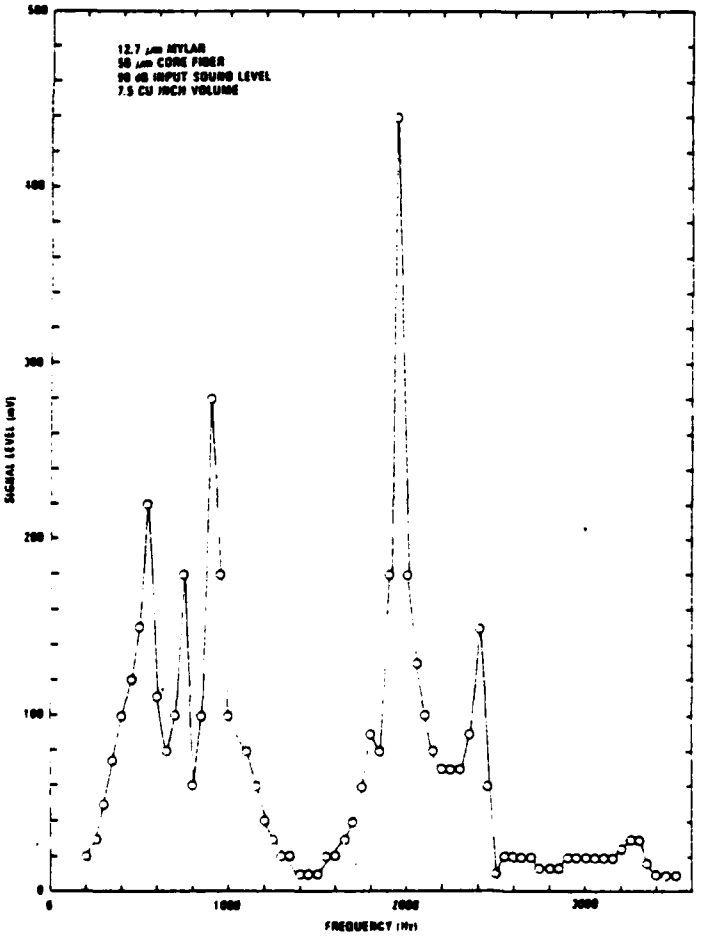

Fig. 5.3. TALK Response with 7.5 cu. in. Volume.

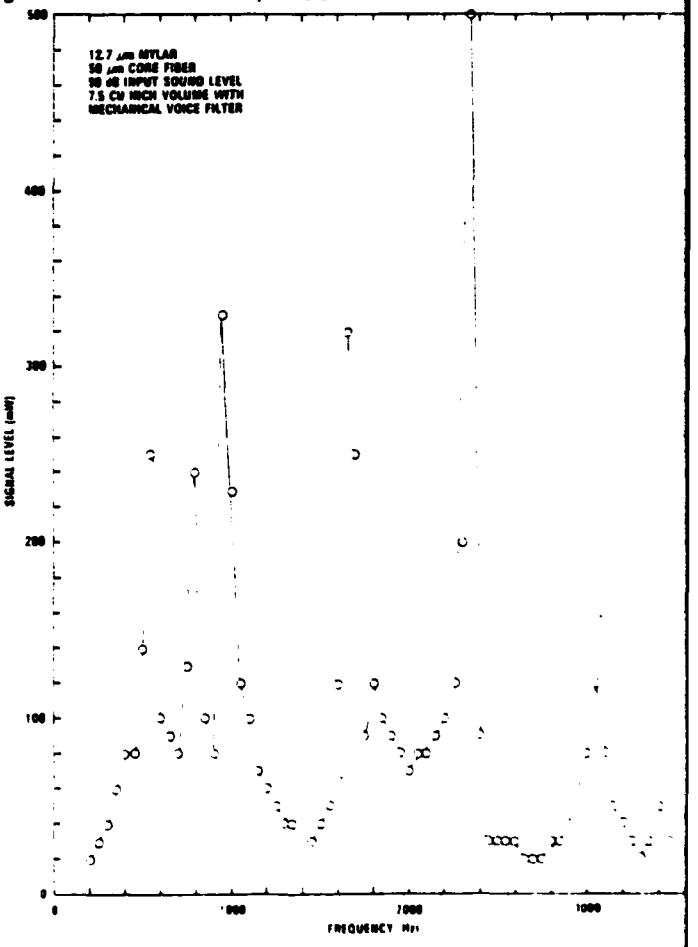

Fig. 5.4. TALK Response with 7.5 cu. in. Volume and Mechanical Voice Filter.

New Wave Communications

Harris-designed all-optical telephones that directly convert acoustic and mechanical energy for telephone functions soon may be streamlining military tactical communications.

In 1880, 4 years after he created the telephone, Alexander Graham Bell invented another amazing device—a phone which could reproduce articulate speech by using beams of light. The concept was intriguing, but in the 19th century, Bell's "photophonic receiver" was hardly practical. The technology of the 1880's limited Bell to sunlight as his radiant energy source and air as the transmission medium for the light beams. As a result, the new phone could only be used on sunny days and over distances no more than several feet. Today, however, with knowledge of fiber optics, Harris experts are proving that a passive optical telephone set is not only practical but may well become the phone of the future.

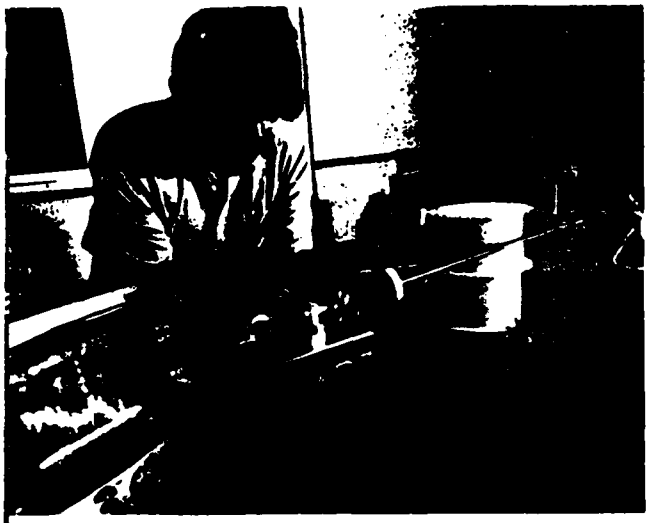

Harris Optical Systems specialists convert light into sound using fiber optics.

A second method, not yet tested, involves a more simplified and reliable process. A tone generated at the switchboard drives a laser diode to produce a frequency-modulated beam of light. The light is transmitted to the phone set by an optical fiber, and, as in the "hear" function, it is absorbed by a small expansion cell. The resulting sound waves are relayed through another exponentially tapered horn and heard as ringing.

Recently, a series of experiments was conducted to test each individual function on the Harris phone. Results demonstrated that the tonal quality from the optical phone is similar to that of conventional phones, that conversation is easily understood on the new phone, and that voices are recognizable. Tests on the mechanical ringing device showed that ringing begins 4 seconds after the light pulse is sent and continues until the pulse is stopped.

For the military, the Harris all-optical telephone will have a number of advantages over a conventional phone. It can supply both the convenience and the security which the military needs in tactical situations. Electrical outlets and generators will no longer be necessary in the battlefield ~~to operate~~ the phones. Attempts at external wiretapping will be easily detectable. And electromagnetic radiation, which does not affect optical fibers, will no longer be a potential hindrance to communications.

In addition, the all-optical phone has commercial advantages which may well lead to its be-

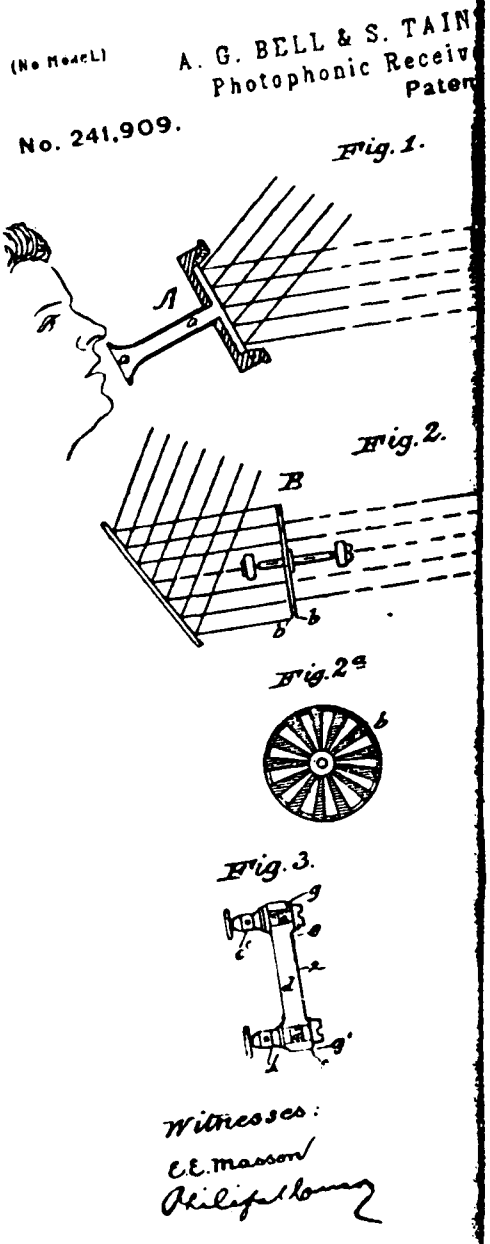

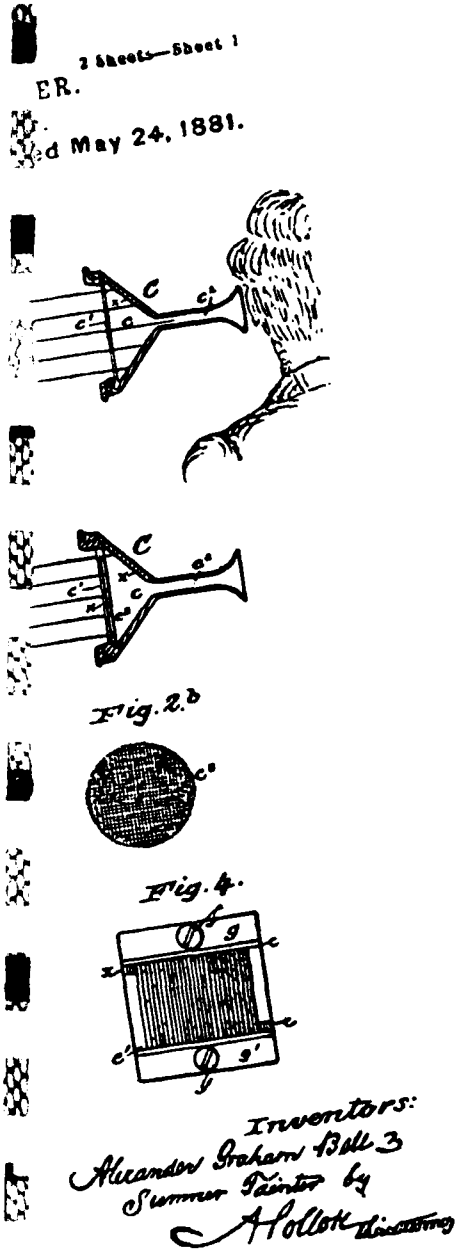

This illustration of Bell's 19th century patent shows the inventor's concept of an optically powered phone. Today, his design is a model for a more feasible phone system.

coming everyone's "phone of the future." The new phone requires no electronic interfaces, and thus has no need for metal—specifically, copper—parts. With the world's supply of copper decreasing and the cost of the metal rising comparably, fiber optics provide a cost-effective alternative. The raw materials from which the fibers are made are inexpensive and abundant. High-powered laser diodes, which supply the light source for the all-optical phone, are already commercially available. In general, the future looks bright for an all-optical phone.

It's been a century since Alexander Graham Bell's photophonic receiver was stored in the Smithsonian Institution for safekeeping. Since then, the technology has been developed to make an optically powered telephone practical, as well as possible. The all-optical phone developed by the Optical Systems Department of the Harris division is an important breakthrough to a whole new way of communication by telephone and has proven the feasibility of this new technology.

The all-optical phone, shown in its breadboard state, will require no metallic parts.

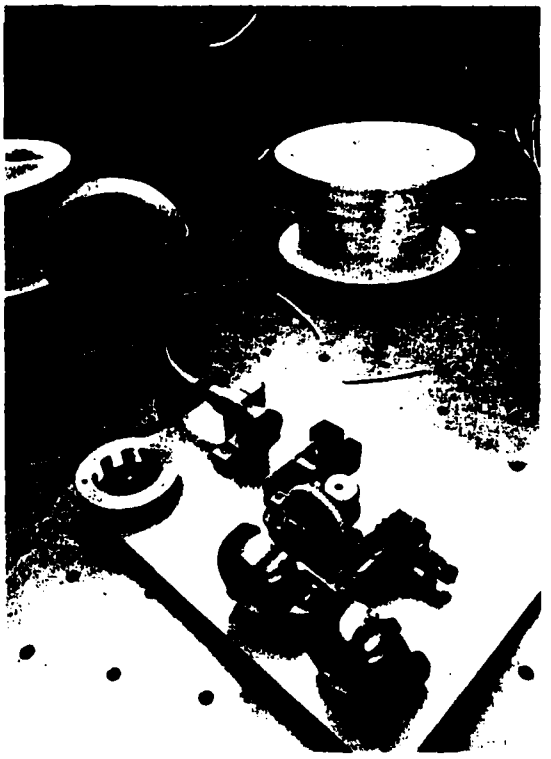

The use of fiber optics in telephone communications systems is not new. Already, optical fibers have been demonstrated as an effective substitute for the metallic cable trunks between switchboards. The fibers are readily available and are capable of handling the large bandwidths needed to accommodate heavy user traffic; however, today's telephone systems still require electrical power and electronic interfaces at the user instrument level. For the military, which uses telephone communications in many tactical situations, this often presents a great inconvenience.

At Harris Government Communications Systems Division, communications specialists in the Optical Systems Department have taken the first major step toward designing a phone which can alleviate this problem. Working with CENCOMS, the U.S. Army Communications Research and Development Command, the division has designed, built, and successfully tested a phone system which uses the direct conversion of optical energy into acoustic and mechanical energy to perform the three basic phone functions: talk, hear, and ring.

To accomplish the talk function in the all-optical phone, the division has designed a small, thin diaphragm with two fibers optically coupled across its center. The fibers—one attached to the diaphragm, the other mounted in a fixed position—become misaligned as sound waves hit the diaphragm and cause it to vibrate. Light passing through the optical fibers is thus modulated and transmitted to the switchboard. Here it is coupled into the "hear" fiber of the receiving phone and into the earphone of the originating telephone for side tone generation.

Hearing in the Harris phone results from direct opto-acoustic conversion. The voice-modulated light signal being sent through the optical fiber is absorbed in a small expansion cell filled with carbonized material. Air within the cell expands and contracts with the varying light intensity, sending out pressure waves. A specially designed, exponentially tapered horn captures the sound waves and relays them to the listener's ear, where they are heard as speech.

Two potential methods have been designed by the division to perform the ring function. The first method, which has actually been built and tested, relies on light from optical fibers to release stored mechanical energy. The action of depressing a hook, like the receiver button on a conventional telephone, sets a spring geared to a low torque governor. Normally, the governor is held fast by a bimetallic strip. But when an incoming call is being received, beams of light from an optical fiber focus onto the strip, causing it to heat up quickly, bend, and release the governor. Once released, the drum rotates, striking bells and producing the ringing sound which alerts the user. When the light pulse stops, the strip cools and returns to its original latching position.

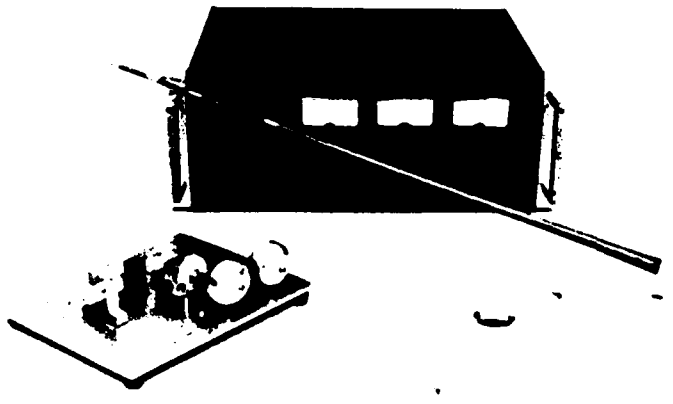

The ring, talk, and hear functions of the all-optical phone were tested by connecting each mechanism to an electronic interface. Results compared favorably in quality and performance with conventional phones.

END

FILMED

3 -86

DTIC